TECHNICAL REPORTS

MATERIALS STUDIES FOR MAGNETIC FUSION ENERGY APPLICATIONS AT LOW TEMPERATURES - I

Edited By

F.R. Fickett and R.P. Reed
Thermophysical Properties Division
National Bureau of Standards
Boulder, CO 80303

April 1978

CONTENTS

SUMMARY

The reports presented here summarize the work of the low temperature materials research project for the first year of the program. The various projects are outlined and the research results are presented. The major thrust of the measurements has been the evaluation of the low temperature properties of stainless steel base metal and welds, with particular emphasis on the nitrogen strengthened stainless steels. Some initial work has also been done on the production and properties of nonmetallics, primarily industrial laminates, for low temperature applications. A handbook of material properties is also planned. A survey of low temperature materials needs and problems related to magnetic fusion energy, performed by NBS as groundwork for the program, is included as is a brief description of the first workshop held in October 1977.

NOTE

The use of trade names of commercial materials is essential to the proper understanding of the work presented. This use in no way implies approval, endorsement or recommendation by the National Bureau of Standards.

ORGANIZATIONAL CONTACTS

Listed here are the people responsible for the various aspects of the program so that those with specific technical questions may contact the individual directly.

Department of Energy, Division of Magnetic Fusion Energy, Washington, D.C. 20545
    Program Monitor   E. N. C. Dalder   (FTS) 233-4964
                                            (301) 353-4964

National Bureau of Standards, Thermophysical Properties Division, Boulder, CO 80302
    Program Manager   R. P. Reed   (303) 499-1000 X3870
    Program Coordinator   F. R. Fickett   (FTS) 323-1000 X3785
    Welding   H. I. McHenry   X3268
    Elastic Properties   H. M. Ledbetter   X3443
    Nonmetallics   M. B. Kasen   X3558

Martin Marietta Aerospace, Denver Division, P.O. Box 31, Denver, CO 80201
    Project Manager   F. R. Schwartzberg   (303) 973-3225
    Fracture, Fatigue   J. A. Shepic

Armco Steel Corp., Research & Technology, Middletown, OH 45043
    Project Manager   R. H. Espy   (513) 425-2490

Arcos Corp., 1500 South 50 Street, Philadelphia, PA 19143
    Project Manager   R. D. Thomas, Jr.   (215) 727-1500

Mechanical Properties Data Center, 13919 West Bay Shore Drive, Traverse City, MI 49684
    Program Manager   R. C. Braden   (616) 947-4500
    Data Evaluation   T. Moore

INTRODUCTION

This report contains results of a research program to produce materials
properties data to facilitate design and development of cryogenic structures,
especially for superconducting magnets, required for magnetic fusion energy
research. The program was conceived and developed jointly by the staffs
of the Cryogenics Division, National Bureau of Standards and the Division
of Magnetic Fusion Energy of the Department of Energy. This program,
sponsored by DOE, is managed by NBS. Research is conducted at NBS and
at various other laboratories, through subcontracts with NBS.

PROGRAM DESCRIPTION

The overall objective of the program is to assist the design, construction and safe operation of low temperature magnetic fusion energy (MFE) systems, especially superconducting magnets, through effective materials research and materials technology transfer. The specific steps taken to achieve this objective are: (1) evaluation of low temperature materials research needs specific to MFE devices; (2) development and monitoring of a research program to acquire the necessary data; and (3) insuring rapid dissemination of the data to potential users through personal contacts, publications and workshops.

The first specific objective was accomplished with the publication of the Survey of Low Temperature Materials for Magnetic Fusion Energy in March 1977. The second objective is described here in Table 1 in the form of an outline of the research projects. The results are contained later in this report. The third objective will be satisfied in part by this report and our handbook project. It has already been accomplished in large part with the holding of the first NBS-ERDA Workshop on Materials at Low Temperatures in October 1977.

Table 1. Outline of the NBS/DOE Program on Materials Studies for Magnetic
Fusion Energy Applications at Low Temperatures

Program Area	Organization	Program Description
A. Nitrogen Strengthened Stainless Steels		
1. Fracture and Fatigue	Martin Marietta	Low cycle, strain controlled, fatigue testing of AISI 304, 316 and 21/6/9 stainless steel. J-integral fracture toughness testing of 21/6/9. All tests at 295, 76 and 4 K.
2. Toughness, Crack Crowth and Tensile Properties	NBS	Measurement of fracture toughness, fatigue crack growth rate and tensile property data for Nitronic 33, Nitronic 50 and AISI 304N stainless steel at temperatures of 295, 76 and 4 K.
B. Stainless Steel Welding		
1.	Armco	Development of a satisfactory filler material for welding of nitrogen strengthened stainless steel for low temperature service. Tensile and impact testing of candidate materials at room temperature and 77 K.
2.	Arcos	Production of test welds with varying ferrite content in austenitic stainless steels. Welds will be evaluated for toughness at NBS later in the program.
3.	NBS	Investigation of metallurgical factors contributing to the toughness (or degradation thereof) of stainless steel weld metals. Later, the program will evaluate the influence of process variables on strength and toughness at 4 K.
C. Physical Properties of Stainless Steels		
1. Elastic Properties	NBS	Measurement of the elastic properties of AISI 304, 304L and 304N stainless steels to determine the effect of temperature to 4 K and to determine the variabilities within and among heats, etc.
D. Nonmetallics	NBS	Acquisition of published formulations of specific G10 and G11 industrial fiberglass-epoxy laminates. Low temperature testing of these materials in later years of the project to determine mechanical and physical properties.
E. Handbook Preparation	MPDC/NBS	Production of a handbook containing low temperature mechanical and physical properties of materials of interest to the MFE community. Presently designated for inclusion: AISI 304, 316 and 21/6/9 stainless steels; 2219, 5083 and 6061 aluminum alloys.

HIGHLIGHTS OF RESULTS

HIGHLIGHTS OF RESULTS

We present a brief description of outstanding results from the project reports which follow in the next section.

Nitrogen Strengthened Stainless Steels

Tensile, fracture toughness and fatigue crack growth rates have been measured on nitrogen strengthened austenitic steels containing Fe-18Cr-13Mn-3Ni (Nitronic 33), Fe-21Cr-5Mn-12Ni (Nitronic 50), and Fe-19Cr-2Mn-9Ni (AISI 304N). AISI 304N is particularly promising for use at 4 K since the yield strength is doubled (60 to 120 ksi), the toughness remains acceptably high, and the cost remains near the cost of AISI 304. Other alloys, including AISI 304LN and AISI 316N, will be measured for comparison.

Smooth-bar strain-controlled fatigue tests have been conducted on AISI 304, 316 and Fe-21Cr-6Ni-9Mn stainless steels at 295, 76, and 4 K. The results indicate reduced fatigue life at 4 K, compared to 76 K. Alloy AISI 316 appears to have the best fatigue life at 4 K.

Fracture toughness tests at 295, 76, and 4 K on a commercial heat of Fe-21Cr-6Ni-9Mn (Nitronic 40) indicates lower toughness than a heat of the same alloy that was electroslag remelted and cross-rolled. Toughness decreases considerably in this alloy between 76 and 4 K.

Stainless Steel Welding

A literature review has indicated that the toughness of stainless steel weld metals is marginal for MFE structural applications, particularly in thick section weldments and in designs where the stresses exceed the ASME allowable, 138 MPa (20 ksi). The best available filler metal appears to be AWS type 330 (18Cr-34Ni); tests on welds prepared by Teledyne-McKay indicate that the Charpy impact toughness at 76 K is 84 J (62 ft lb) and the yield strength is 860 MPa (125 ksi) at 4 K. Armco Steel Corp. evaluated the influence of nitrogen on

7

the strength and toughness of a series of filler metals developed for welding the 21Cr-6Ni-9Mn (Nitronic 40) alloy; nearly matching strengths can be achieved but the decrease in toughness is unacceptable. Arcos Corp. welded a series of test plates to evaluate the influence of ferrite content, ferrite morphology and sensitization on the toughness of 316L weld metal at cryogenic temperatures; the NBS evaluation is in progress.

Physical Properties of Stainless Steels

Elastic properties of 304-type stainless steels were determined accurately between room-temperature and liquid-helium temperature using pulse-echo-superposition ultrasonic techniques. Particular elastic constants of interest were Young's modulus, the shear modulus, the bulk modulus, and Poisson's ratio. The Young's and shear moduli increase up to eight percent during cooling; Poisson's ratio decreases about four percent; and the bulk modulus (reciprocal compressibility) is relatively temperature insensitive. All elastic constants, except perhaps for the bulk modulus, change anomalously and reversibly at about 45 K due to a Neel (paramagnetic-antiferromagnetic) transition. Some samples show anomalies in both the longitudinal modulus and Poisson's ratio at about 16 K, indicating another transition that seems to be reversible. Specimens studied thus far, which include both bar and plate stock, show very little elastic anisotropy.

Nonmetallics

A major problem is posed by the highly proprietary nature of existing NEMA-grade industrial laminates. Discussions with representatives of the industrial laminating industry (Westinghouse and Spaulding Fiber) and with representatives of national laboratories capable of performing the required radiation research (ORNL, ANL) has led to the selection of three laminate systems to be fabricated from published formulations and included in the mechanical, thermal, electrical, and radiation characterization work:

8

1. NEMA G-10/MIL-P-18177, Type GEE

2. NEMA G-11/MIL-P-18177, Type GEB (aromatic amine cure)

3. NEMA G-11/MIL-P-18177, Type GEB (aromatic amine cure, boron-free
    E-glass reinforcement)

Laminates 1 and 2 are to be conventional, state-of-the-art materials dif-
fering from other NEMA laminates only in being defined material systems as
distinct from proprietary formulations. The laminates will be made by the
Micarta Division of Westinghouse, however, information required to fabricate
the laminates will be made available to all industrial laminators. This will
provide the MFE community with access to G-10 and G-11 type laminates having
a known formulation which will become well characterized as part of the FY 78
NBS-ERDA cryogenic materials program. Laminate formulation data should be
available by 1 January 1978.

NITROGEN STRENGTHENED STAINLESS STEELS

Fatigue Testing of Stainless Steels

Martin Marietta

FATIGUE TESTING OF
STAINLESS STEELS

J. A. Shepic
Principal Investigator

F. R. Schwartzberg
Program Manager

MARTIN MARIETTA CORPORATION
Denver Division
Post Office Box 179
Denver, Colorado 80201

15

FOREWORD

This report describes technical activities conducted by the Denver
Division of Martin Marietta from 17 May 1977 through 30 November 1977
under National Bureau of Standards (NBS) contract CST-8426, Item 2.

The views and conclusions contained in this document are those
of the authors and should not be interpreted as necessarily representing
the official policies, either expressed or implied, of the United States
Government.

INTRODUCTION

Superconducting machinery will be subjected to cyclic loading at temperatures down to 4 K. Fatigue data for candidate materials are relatively sparse below 20 K. At 4 K, most of the fatigue data are embodied in three papers (references 1, 2 and 3). This work was undertaken to supplement the data already available, and to demonstrate that a relatively simple testing system for strain-controlled fatigue testing at 4 K could be developed.

Three alloys (21-6-9, 304 and 316 stainless steel)[*] were evaluated. No data were available at 4 K for the 316 alloy. Stress-controlled fatigue data for 21-6-9 were available from a prior program conducted at Martin Marietta. Alloy 304L has been previously evaluated using both stress- and strain-controlled techniques; however, concern for the effect of adiabatic heating due to plastic deformation necessitated confirmation evaluation.

MATERIALS

Stock of each alloy was obtained as plate stock. The 21-6-9 stainless steel was obtained as 3.8 cm (1.5 in.) stock; 304 and 316 stainless steels were obtained as 2.5 cm (1.0 in.) stock. All material was provided by NBS.

The 21-6-9 alloy was received in the hot-rolled, annealed and descaled condition. Data describing annealing and composition are described in the companion Martin Marietta report on fracture testing

---

[*] The designations 21-6-9 and Nitronic 40 are trade names for an alloy with the nominal composition Fe-21Cr-6Ni-9Mn. Throughout the remainder of this report it is described by the first designation. The standard stainless steel alloys AISI 304 and AISI 316 are hereafter referred to as 304 and 316, respectively.

of 21-6-9.

The 304 and 316 stainless steels were from the two LMFBR (Liquid Metal Fast Breeder Reactor) program reference heats received from DOE.

NBS determined the tensile properties of the three materials. Data are summarized in Table 1.

TESTING TECHNIQUE AND APPARATUS

This chapter describes the specimen geometry, testing apparatus and technique used to obtain the fatigue data presented in this report.

The fatigue specimen configuration used for this program was similar to that used by Martin Marietta in previous fatigue studies (references 1 and 4). The design incorporates a smooth gage section with a mild radius and a bearing shoulder at the end of the threaded section for alignment and locking, as opposed to aligning on the threads. This system is advantageous because only two close-tolerance alignment surfaces are required and failure within the prescribed area of the gage is assured. The specimen, when locked with a nut at each end of the threaded bar, can be subjected to a fully reversed loading cycle that is continuous through zero load. Figure 1 gives the specifications for the specimen.

Fatigue specimens were polished after machining using 240 to 320 grit polishing paper (the coarseness of the initial rough polishing paper depended on the alloy hardness and machined surface roughness in the gage section) and then using 320 and 600 grit paper followed by a felt wheel and Tripoli polishing compound. The polishing paper was bonded to a rubber sanding disc mounted in a small Dumore grinding tool.

Table 1 Tensile Properties of Stainless Steel

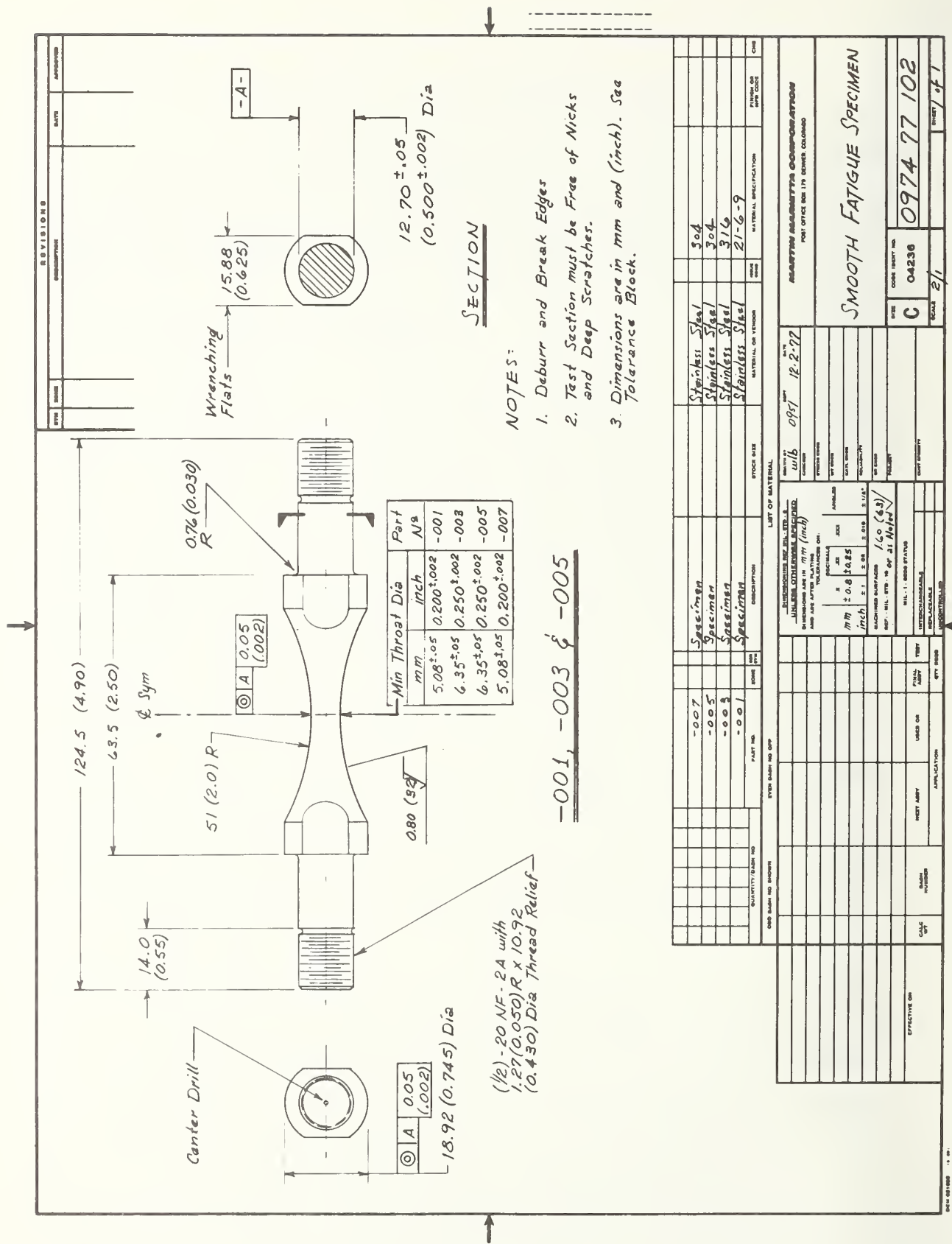| Alloy and Heat No.	Temperature, K	Ultimate Strength, MN/m^2 (ksi)	0.2% Yield Strength, MN/m^2 (ksi)	Elongation, percent	Reduction of Area, percent
21-6-9 [656249-1D]	293	785 (114)	386 (56)	58	76
	77	1488 (216)	916 (133)	34	32
	4	1557 (226)	1399 (203)	11	25
304 [9T-2796]	293	599 (87)	214 (31)	67	67
	77	1433 (208)	262 (38)	42	65
	4	1592 (231)	345 (50)	39	48
316 [8092297]	293	598 (84)	227 (33)	56	73
	77	1240 (180)	606 (88)	62	70

Figure 1 Specifications for Fatigue Specimen

As the specimen is rotated at approximately 350 rpm between lathe centers, the periphery of the spinning (approximately 20,000 rpm) sanding disc contacts the specimen gage section with axial strokes. (The same procedure was used with all grits). The final polish uses a 2 inch diameter felt wheel mounted in a Dumore grinding tool and loaded with Tripoli polishing compound. As the specimen is rotated between lathe centers at approximately 150 rpm, the spinning (approximately 20,000 rpm) impregnated felt wheel contacts the specimen gage section with axial strokes. This polishing technique produces a mirror finish in which any remaining polishing marks are in an axial direction that will have minimal effect on axial fatigue test results.

Because of the non-uniform cross-section area of the specimen, it is necessary to control total strain based on diametral deflection rather than axial deflection. A diametral strain extensometer was designed and built specially for this work. This device is a one-piece aluminum ring with integral strain beams instrumented with nichrome resistance strain gages. The beam ends are machined with knife edges to grip the specimen. The knife edge separation distance is controlled to provide good gripping action on the gage section. The gage grips the specimen sufficiently tight enough that it remains in the horizontal plane during filling of the cryostat and subsequent cyclic loading. Because the aluminum is softer than the stainless steel, no nicks or scratches are imparted to the specimen. Figure 2 gives a closeup view of the extensometer.

The test configuration for 293 K evaluation was quite conventional.

Figure 2   Diametral Strain Extensometer

22

As shown in Figure 3, the specimen is installed in adapters that permit the shoulders to be preloaded; the adapters are then installed in the testing machine.

For 77 K testing, a double-walled, vacuum-insulated cryostat, described in detail elsewhere (reference 5), was used. As shown in Figure 4, the specimen is also installed in adapter plates.

Testing at 4 K was performed in a cryostat system prepared specially for low-cycle fatigue testing. Loading was achieved through two concentric frames, as shown in Figure 5. The smaller frame surrounding the specimen is constructed from titanium alloy. Note that a specimen adapter plate is used at the top of the specimen; at the bottom the specimen shoulder bears against the triangular plate. The remainder of the frame is constructed from aluminum alloy. A glass vacuum dewar is used to provide environmental control. Figure 6 shows the load frame installed in the machine, both without and with the dewar in place.

The liquid helium system is designed so that testing can be achieved with minimum cryogen consumption. The titanium frame and specimen are first precooled to 77 K and placed in a liquid nitrogen filled dewar on the bottom platen. After cooling, the head is raised and a liquid helium filled dewar replaces the liquid nitrogen dewar. A liquid level sensor is used to monitor level, and refilling is performed as required.

Fatigue testing was performed in a 222 kN (50 kip) closed-loop servo-controlled testing machine. Operation was in the strain-control mode. The relationship between total axial strain amplitude and total diametral strain amplitude is as follows:

$$\Delta \lambda_1 = 2 \ \Delta \lambda_d + \frac{\Delta P}{AE} \ (1\text{-}2 \ u)$$

23

Figure 3   Apparatus for 293 K Testing

24
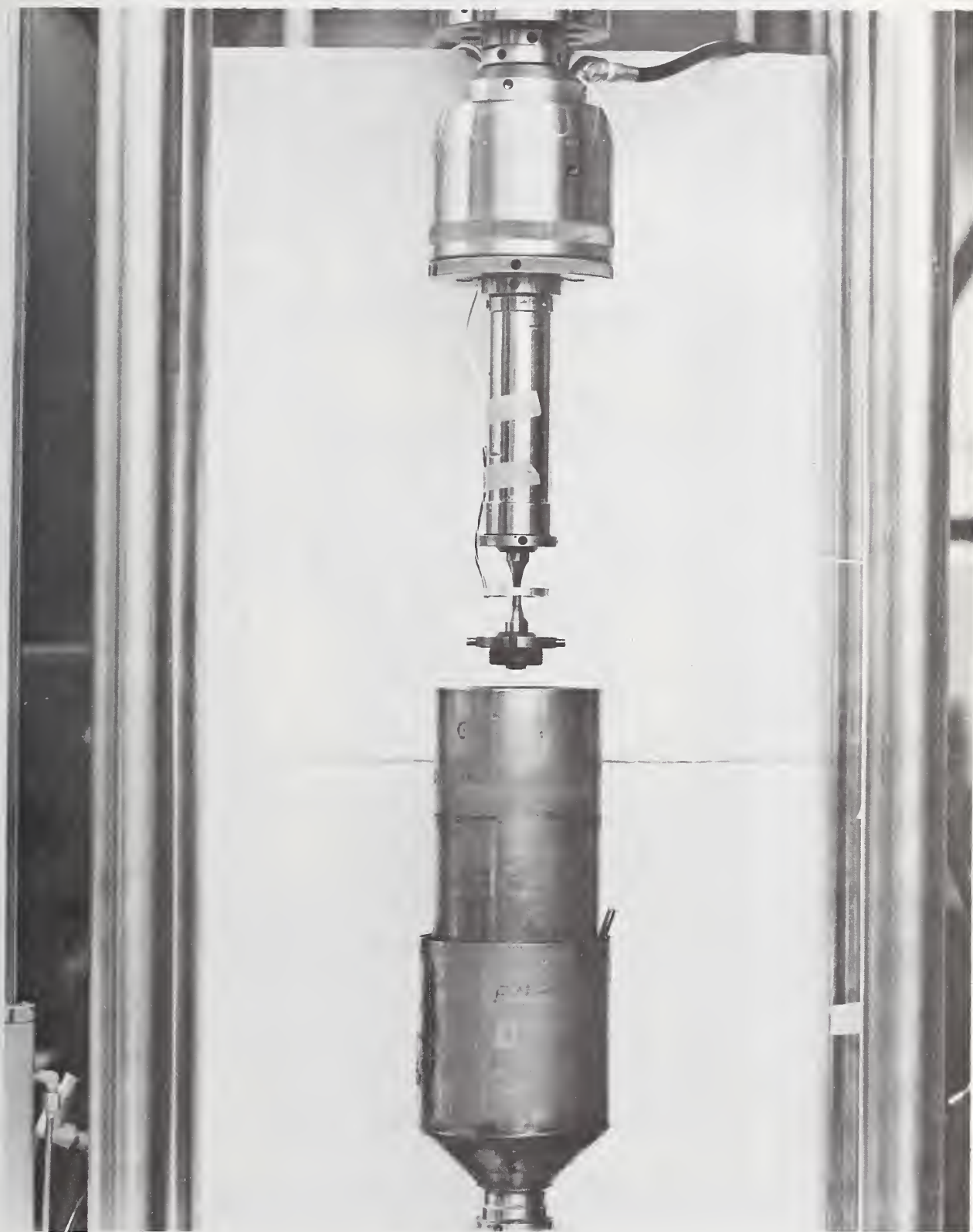
Figure 4 Apparatus for 77 K Testing

25

Figure 5   Load Train for 4 K Testing

26
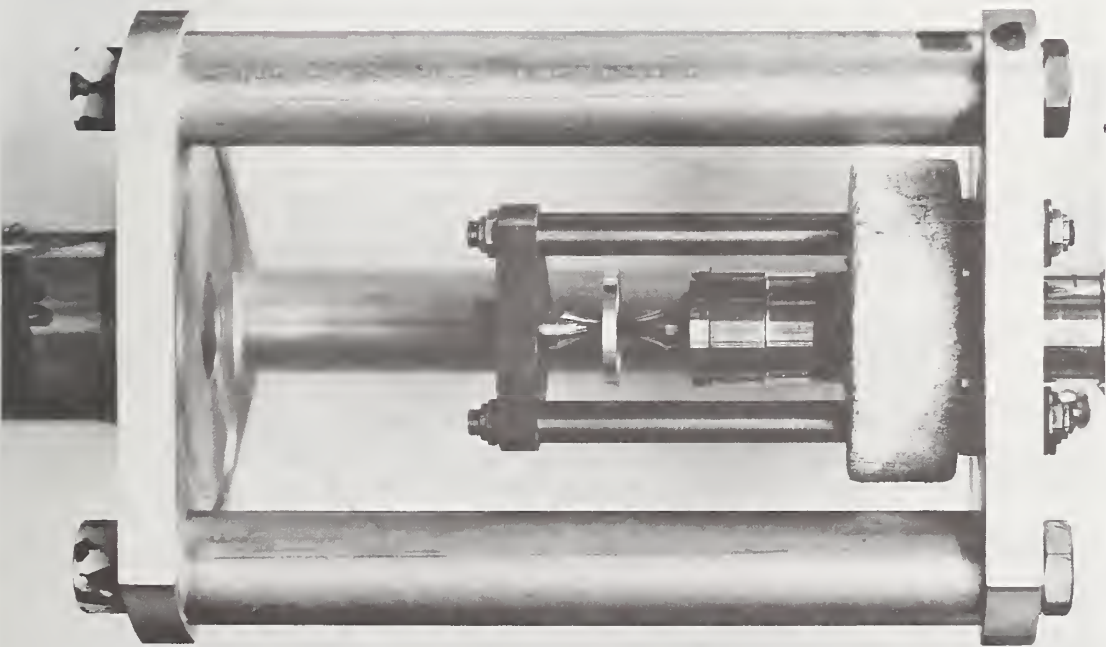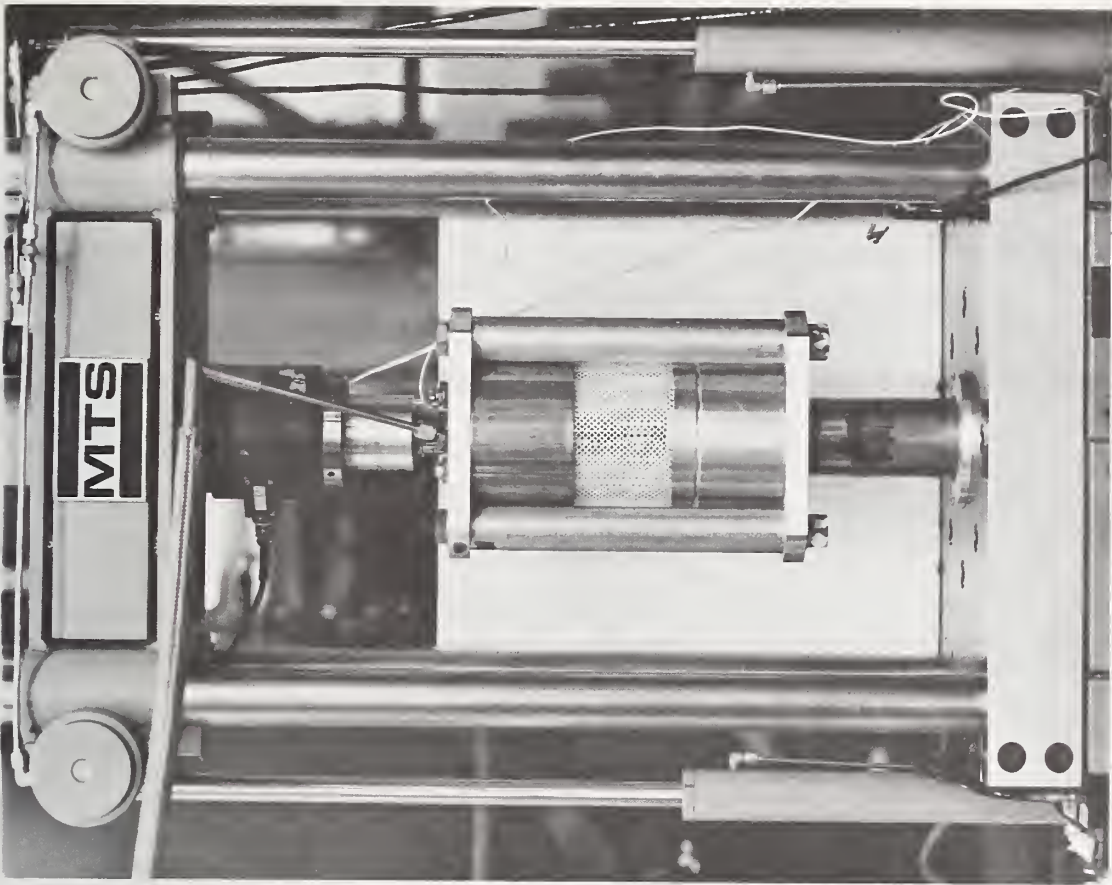
Figure 6 Apparatus for 4 K Testing

where λ_1 = total axial or longitudinal strain amplitude

λ_d = total diametral strain amplitude

ΔP = load amplitude at half-life

A   = cross-sectional area

E   = Young's modulus

u   = Poisson's ratio

To calculate the diametral strain amplitude required to achieve a desired axial strain amplitude, an approximate value for ΔP was selected. Following completion of the test, a more accurate value of ΔP was selected from the load vs strain hysteresis curves and the actual total axial strain amplitude value was recalculated. Accuracy of the $\Delta P$ estimation improved with each succeeding test and, as a result, actual values were quite close to desired values. The elastic component of the total strain was calculated using the ΔP value read from the test record and the appropriate value of Young's modulus. The plastic component of strain was calculated by subtracting the elastic strain from the total strain.

EXPERIMENTAL TEST RESULTS

Fatigue behavior of each of the three alloys was characterized at 293, 77 and 4 K. Because of the extremely high cost of liquid helium and the large quantities required to obtain long-time fatigue data, only a limited number of 4 K tests were conducted beyond 10^3 cycles.

304 Stainless Steel - This alloy exhibits a significant amount of discontinuous yielding at 4 K, as shown by prior tensile test investigations. During cyclic loading it is possible that the heat generated in the plastic range can cause vaporization of the low heat capacity liquid

28

helium and a resultant elevation of the test temperature. This situation

should be rate sensitive and could be eliminated by slower cycling. To

determine whether this was a factor in 4 K testing, a series of tests

were performed at a common strain amplitude and different cyclic fre-

quencies. The data summarized in Figure 7 suggest that fatigue life is

frequency-dependent. For the nominal total strain amplitude of 1.5

percent, it appears that a maximum frequency of 0.1 Hz can be used without

risk of specimen heating.

It was observed that the discontinuous yielding apparent in the

tests performed at or below 0.1 Hz was not noted at 0.3 Hz. This would

suggest that the temperature was greater than 4 K. Without further

extensive testing, it was decided to maintain the test frequency as low

as possible, but consistent with the economics of liquid helium consump-

tion. The frequency for all succeeding liquid helium tests was carefully

selected on the basis of strain level.

Experimental data for the 304 alloy exhibited a temperature depen-

dency of life in the low cycle range in which life decreased with

decreasing temperature. A cross-over occured at approximately $1\frac{1}{4}$ percent

strain in which the order reversed. Below this strain level, life in-

creased with decreasing temperature. Figure 8 graphically depicts the

fatigue life as a function of strain. Table 2 gives detailed information

on the diametral and longitudinal strains, stress amplitude, cyclic rate,

and cycles to failure.

The load vs strain hysteresis curves provide a great quantity of

useful information pertinent to the development of an understanding of

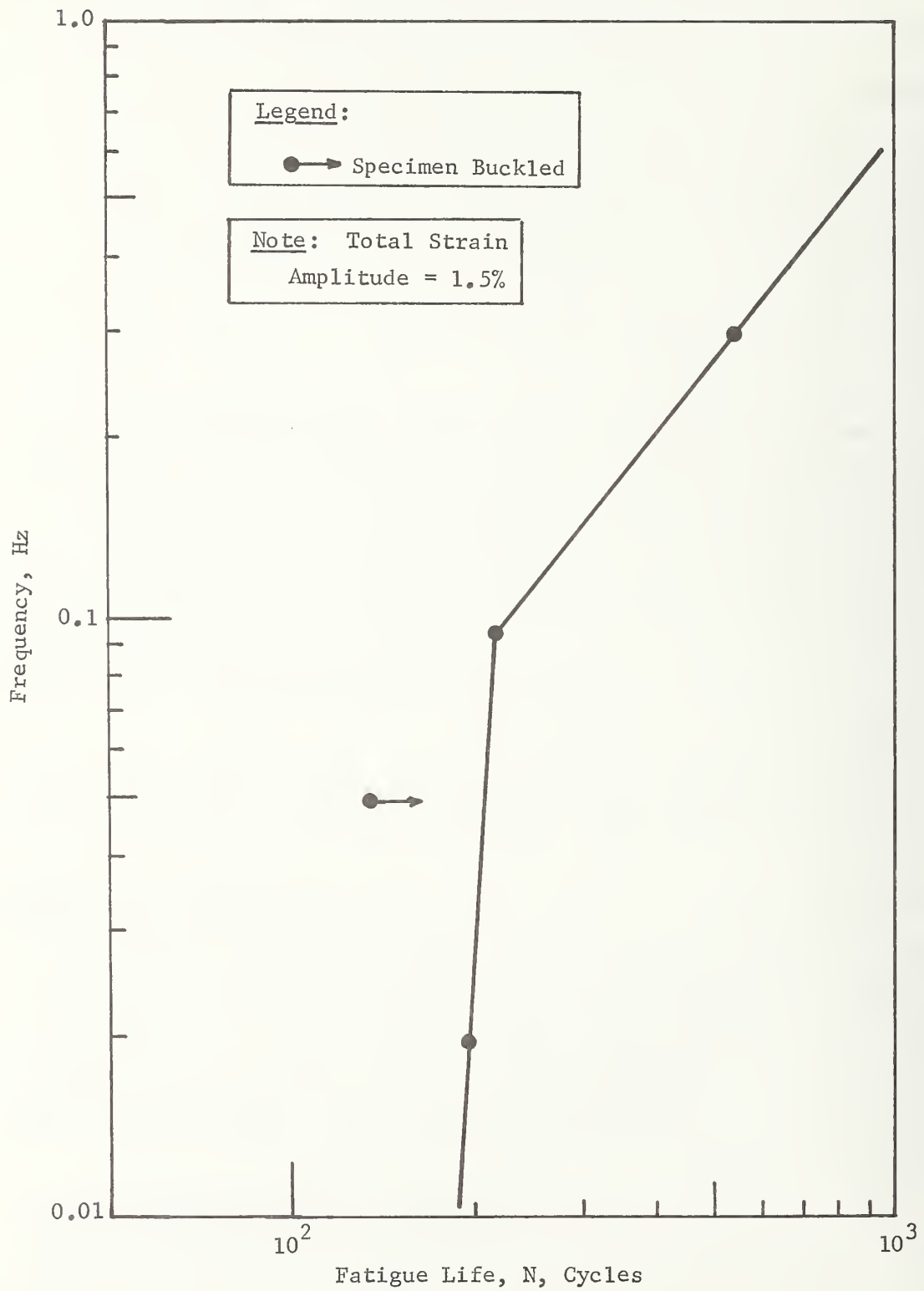cyclic behavior. Figure 9, a typical curve, shows the initial 35 cycles

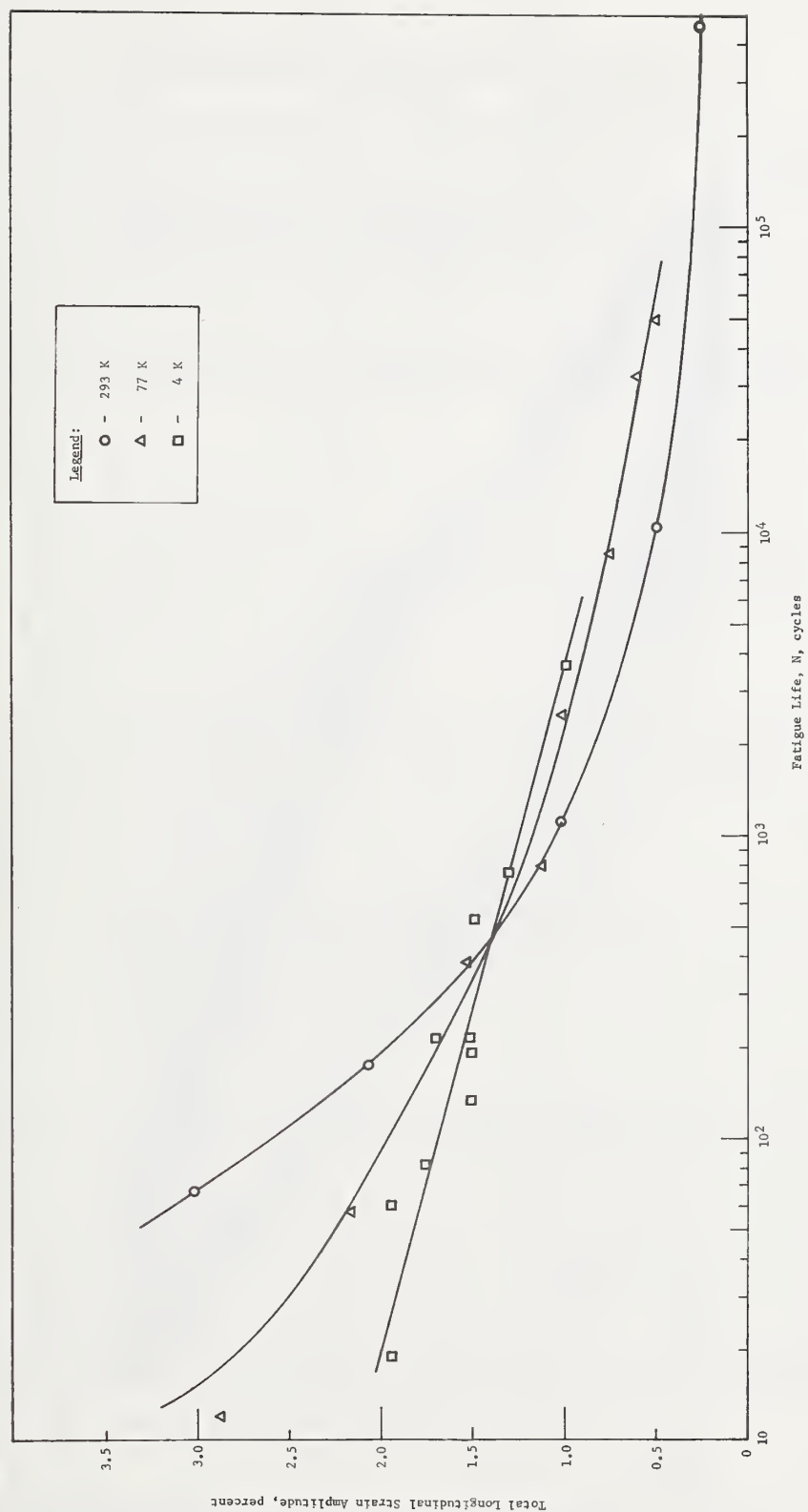*Figure 7   Effect of Frequency on Fatigue Life of 304 at 4 K*

Figure 8 Fatigue Life Curves for 304

Table 2 Fatigue Data for 304 Stainless Steel

Specimen Number	Temperature, K	Diametral Total Strain Amplitude, $\Delta\lambda_d$, Percent	Stress Amplitude at Half-Life, $\Delta\sigma$, MN/m^2 (ksi)	Longitudinal Elastic Strain Amplitude, Δe_1, Percent	Longitudinal Plastic Strain Amplitude, $\Delta\epsilon_1$, Percent	Longitudinal Total Strain Amplitude, $\Delta\lambda_1$, Percent	Cyclic Rate, Hz	Fatigue Life, N Cycles
304-1	293	0.96	655 (95)	0.35	1.72	2.07	0.10	176
-2		0.47	379 (55)	0.20	0.82	1.02	0.60	1,111
-3		1.42	758 (110)	0.41	2.61	3.02	0.10	67
-4		0.22	255 (37)	0.14	0.35	0.49	1.00	10,306
-6		0.10	200 (29)	0.11	0.14	0.25	3.00	457,430
304-7	77	0.94	1517 (220)	0.75	1.42	2.17	0.10	57
-8		0.46	1551 (225)	0.76	0.47	1.23	0.10	795
-9		0.21	814 (118)	0.40	0.19	0.59	1.10	32,077
-10		0.16	793 (115)	0.39	0.10	0.49	3.00	49,470
-11		0.61	1517 (220)	0.75	0.78	1.53	0.30	382
-12		0.28	965 (140)	0.47	0.28	0.75	0.60	8,480
-13		1.30	1517 (220)	0.75	2.12	2.87	0.10	12*
-14		0.37	1310 (190)	0.64	0.37	1.01	0.50	2,535
304-16	4	0.56	1793 (260)	0.88	0.61	1.49	0.30	531
-17		0.57	1793 (260)	0.88	0.63	1.51	0.10	216
-18		0.57	1793 (260)	0.88	0.62	1.50	0.05	134+
-19		0.57	1793 (260)	0.88	0.62	1.50	0.02	192
-20		0.80	1724 (250)	0.85	1.09	1.94	0.05	19
-21		0.67	1724 (250)	0.85	0.85	1.70	0.05	216
-22		0.49	1586 (230)	0.78	0.52	1.30	0.10	755
-23		0.79	1793 (260)	0.88	1.06	1.94	0.02	60
-24		0.36	1310 (190)	0.64	0.35	0.99	0.20	3,647

+ Specimen Buckled

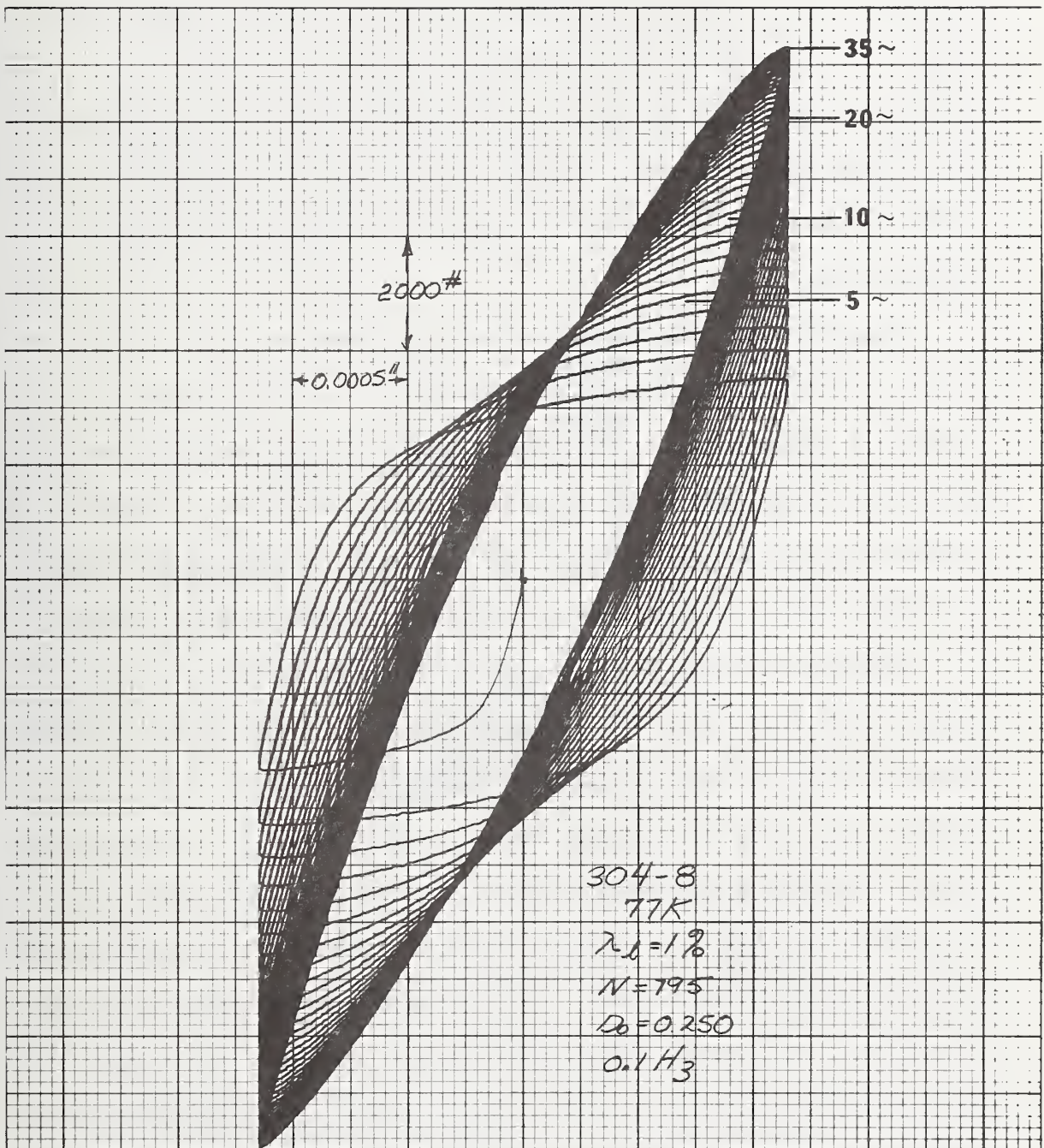|			
Temperature, K	293	77	4
Modulus, GN/m^2 (10^6 psi)	189 (27)	204 (29.5)	204 (29.5)
Poisson's Ratio	0.29	0.28	0.27

Figure 9   Load–Deflection Curve for Specimen 304–8

33

for a nominal 1.0 percent total longitudinal strain test at 77 K. Note the first cycle starting from the center of the loop. Loading was initiated in compression to eliminate the possibility of developing a local necked region during the first tensile loading application of materials prone to strain softening. The curve shows excellent control of strain in both tension and compression. Strain hardening in each cycle is clearly shown.

Figure 10 illustrates strain softening behavior. In this test (0.5 percent strain at 293 K), the highest load is achieved during the first cycle. At the conclusion of 10,000 cycles, significant strain softening is obvious. The figure also illustrates the irregularity (arrow) in the compression portion of the cycle indicative of cracking in the specimen. Note the significant decrease in load associated with the cracking.

The liquid helium tests are particularly interesting. Figure 11 presents the loop for the 1.5 percent strain amplitude specimen (304-16) tested at 0.3 Hz. Note the general similarity to the 77 K data of Figure 9 with respect to strain hardening and degree of strain control. Data shown for the specimen evaluated at the same strain level, but lower frequency (0.02 Hz), are markedly different. Figure 12 illustrates the first two cycles of this test. The discontinuous yielding is extremely pronounced. By careful study of this curve, the first two cycles can be followed. Note the initiation in compression with the initial elastic portion followed by yielding and then with increased straining the initiation of small discontinuous yield jogs. Further straining results in increased size of the discontinuities. The loading in tension at the end of the first half-cycle is characterized by a relatively smooth curve
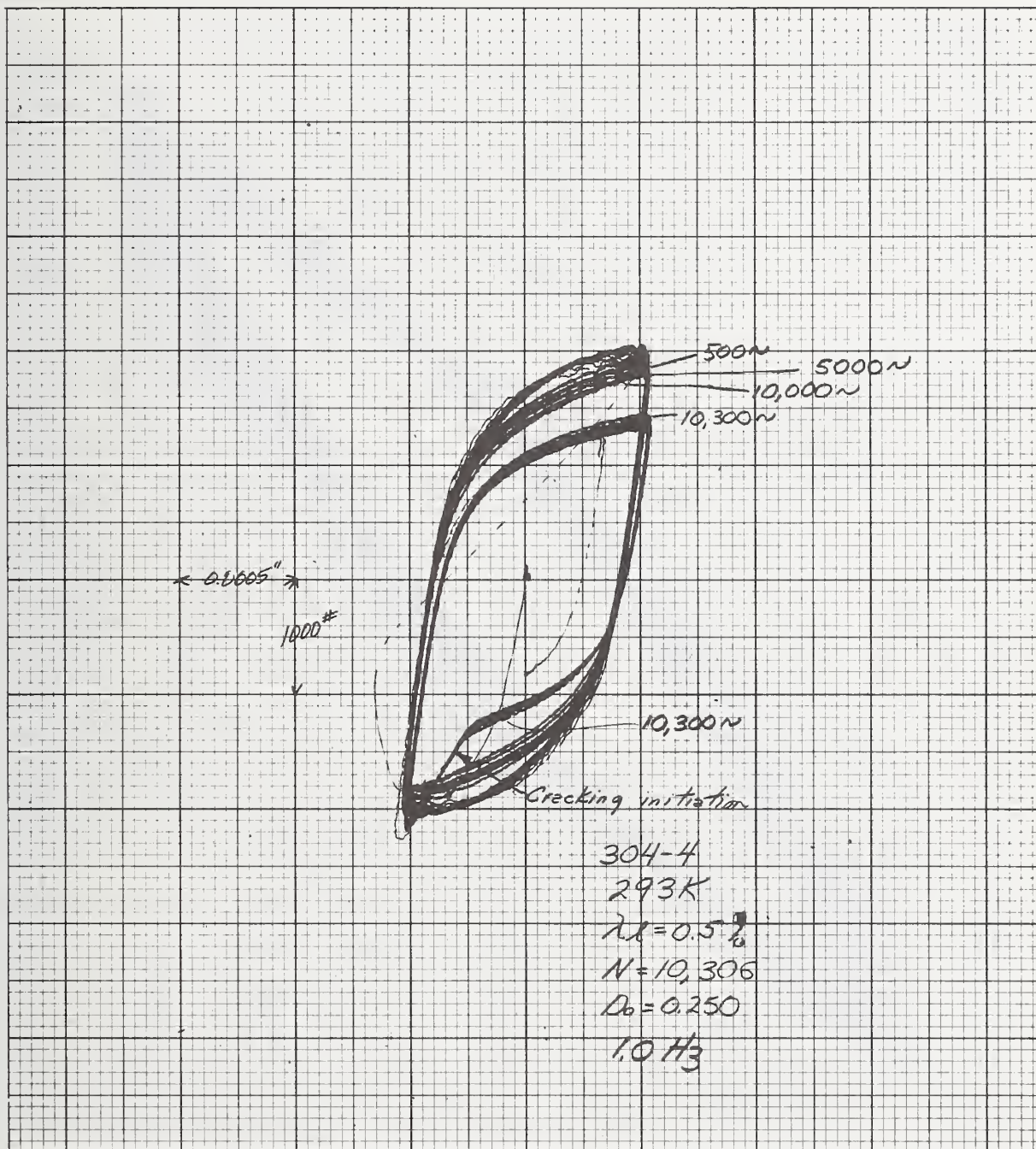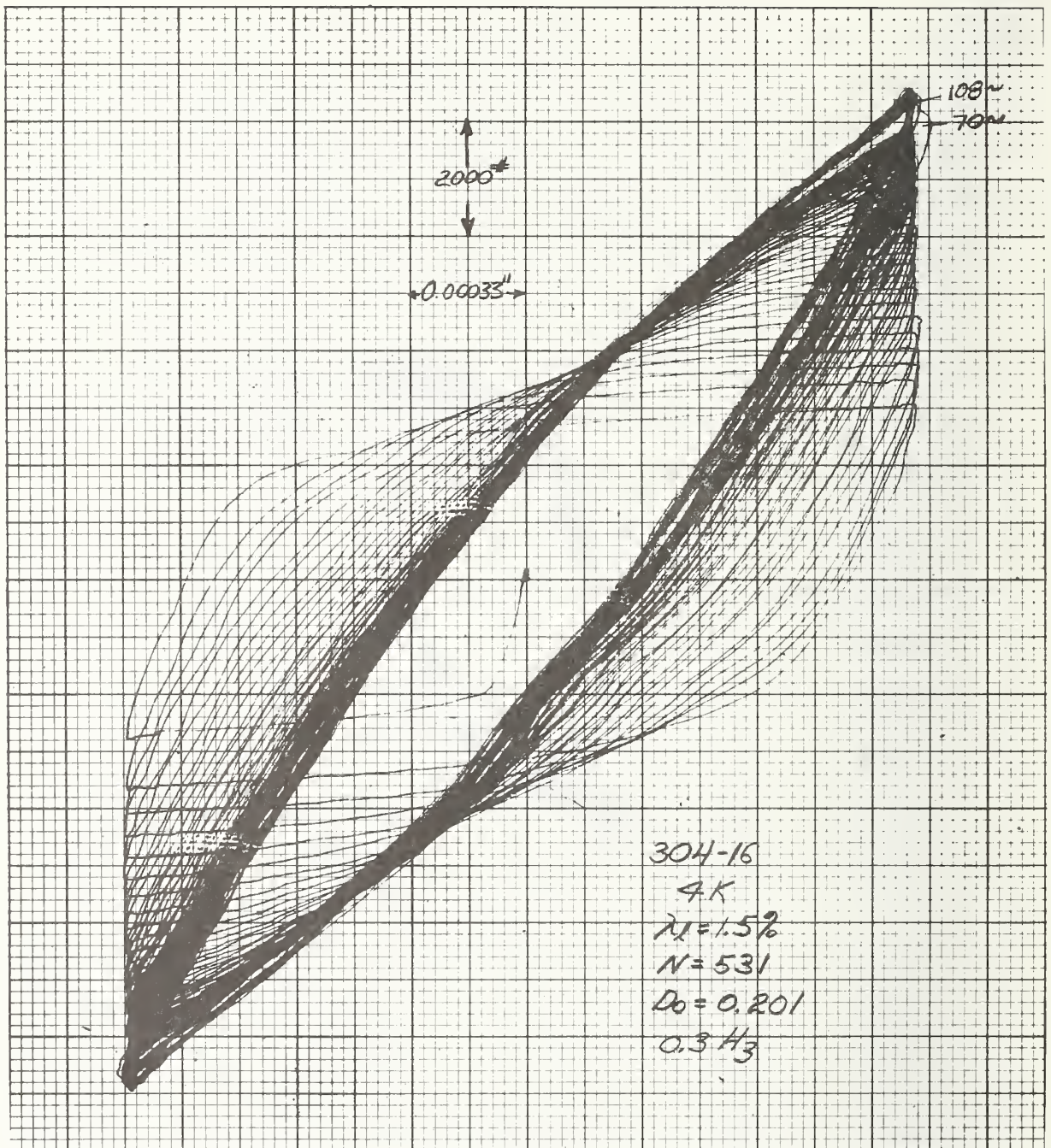
Figure 10 Load-Deflection Curve for Specimen 304-4

35

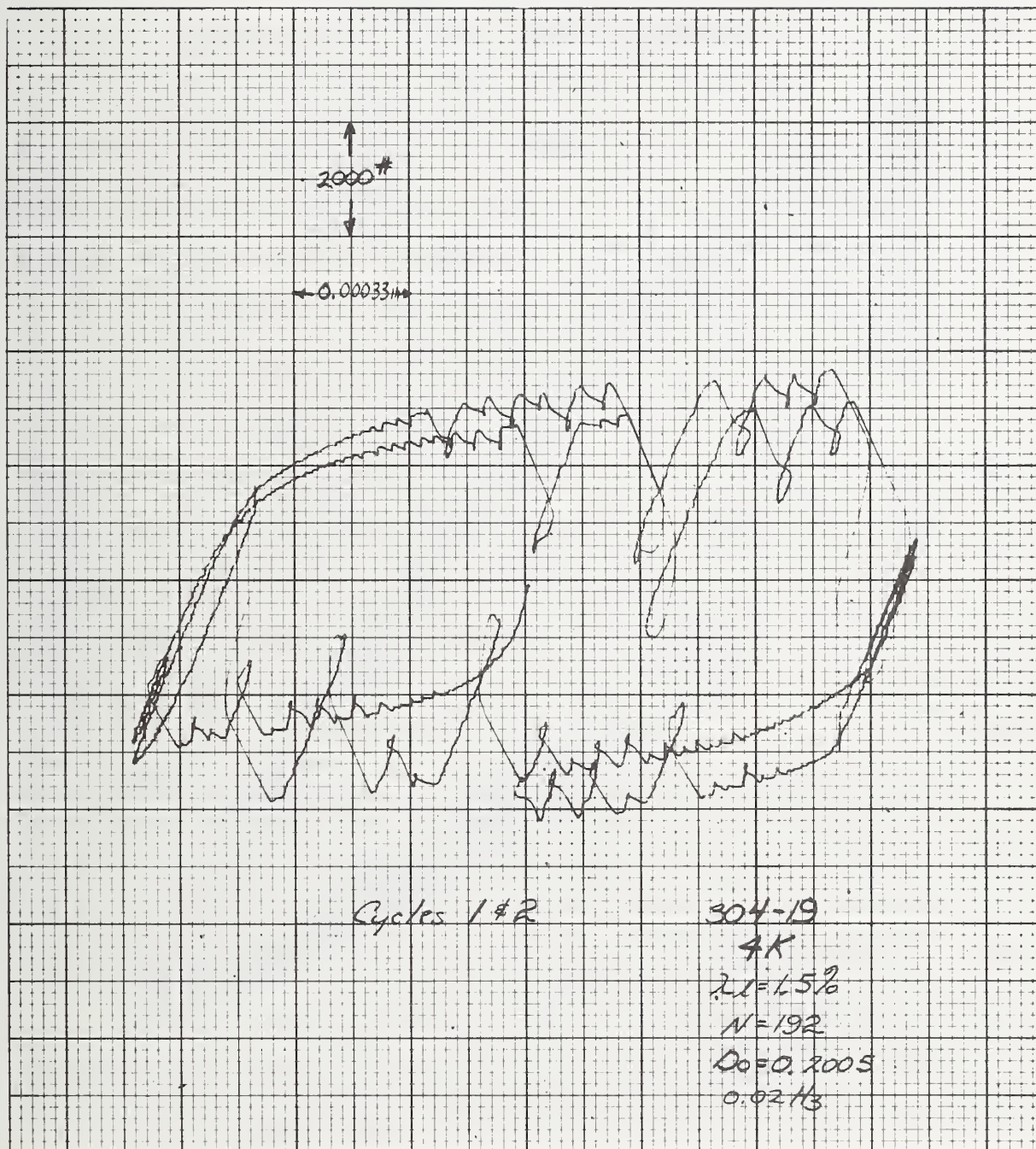Figure 11   Load-Deflection Curve for Specimen 304-16

Figure 12   Load-Deflection Curve for Specimen 304-19 (Cycles 1 and 2)

37

until yielding starts and then an increase in discontinuity activity with increasing strain. The second cycle is much like the first, with the discontinuities occurring at similar locations on the curve.

Figure 13 presents the next 18 cycles. Although hard to follow, the curve does show strain hardening with increased cycling. Despite the abruptness of the discontinuities, the strain control limits are relatively well maintained. During the next 20 cycles, the severity of the yielding discontinuities decreases and the amount of strain hardening with each succeeding cycle becomes small, as illustrated in Figure 14.

Figure 15 illustrates the behavior at a lower strain level than the preceeding test. At a level of 1.0 percent strain, the magnitude of the yielding discontinuities becomes significantly smaller than observed for the 1.5 percent strain level. It should also be noted that the degree of strain hardening compared to the comparable test at 77 K (Figure 9) is significantly reduced and, as a result, an approximate fourfold increase in life is achieved.

21-6-9 Stainless Steel - Figure 16 summarizes the strain vs life data and shows a significant temperature dependency of life at strain levels greater than 1 percent. Below 1 percent strain, a reversal occurs and an indication of increasing life with decreasing temperature becomes apparent. A presentation of the data is given in Table 3.

Figure 17 presents a typical hysteresis loop at 77 K. This specimen, evaluated at 1 percent nominal longitudinal strain, exhibits some strain softening in the initial cycling and relatively little softening after 1000 cycles; total life was 2443 cycles. The curve is smooth and well defined, and exhibits good strain control. The corresponding curve

38

Figure 13   Load-Deflection Curve for Specimen 304-19 (Cycles 3 through 20)

39

2000#
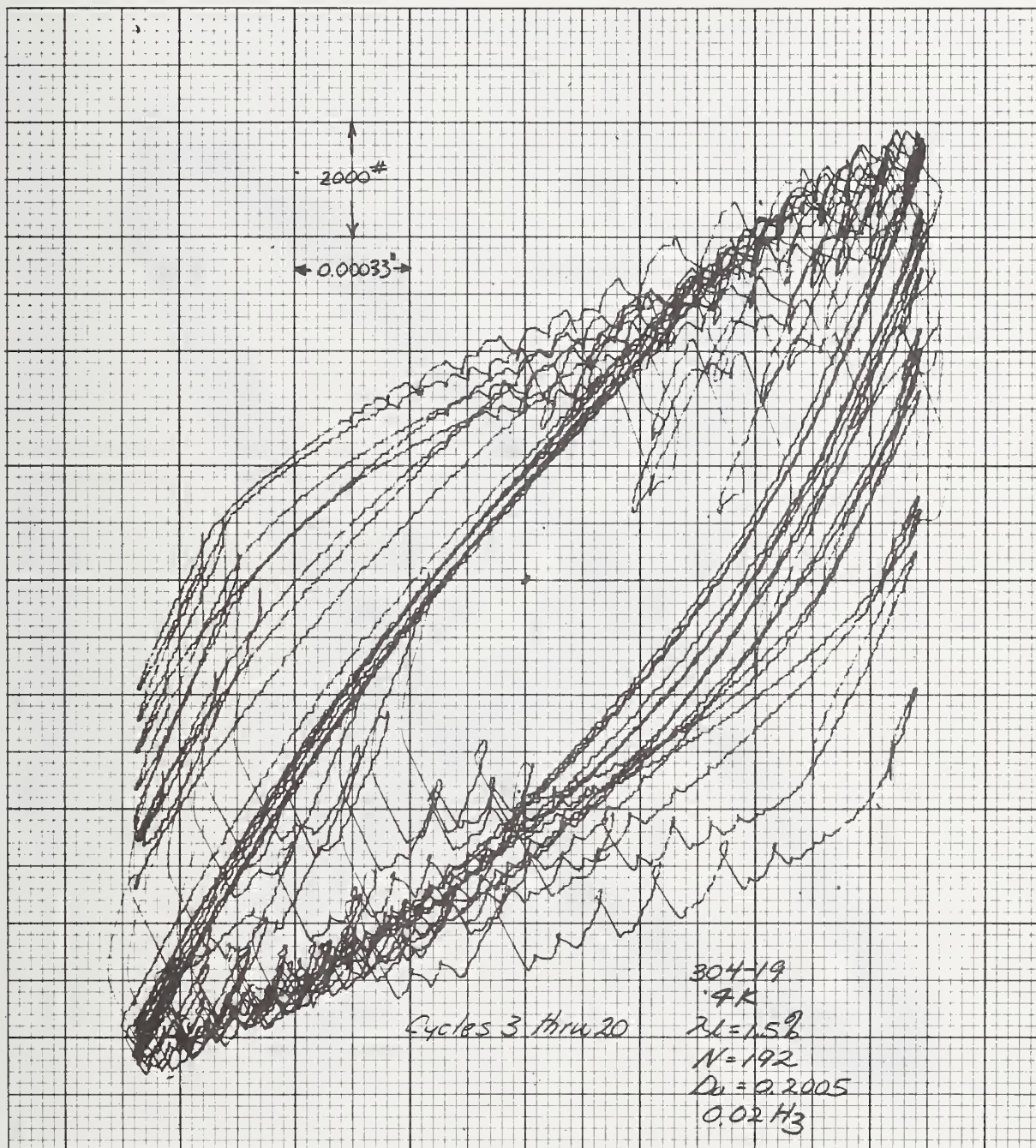
0.00033"

304-19
4K
$2_I = 1.5\%$
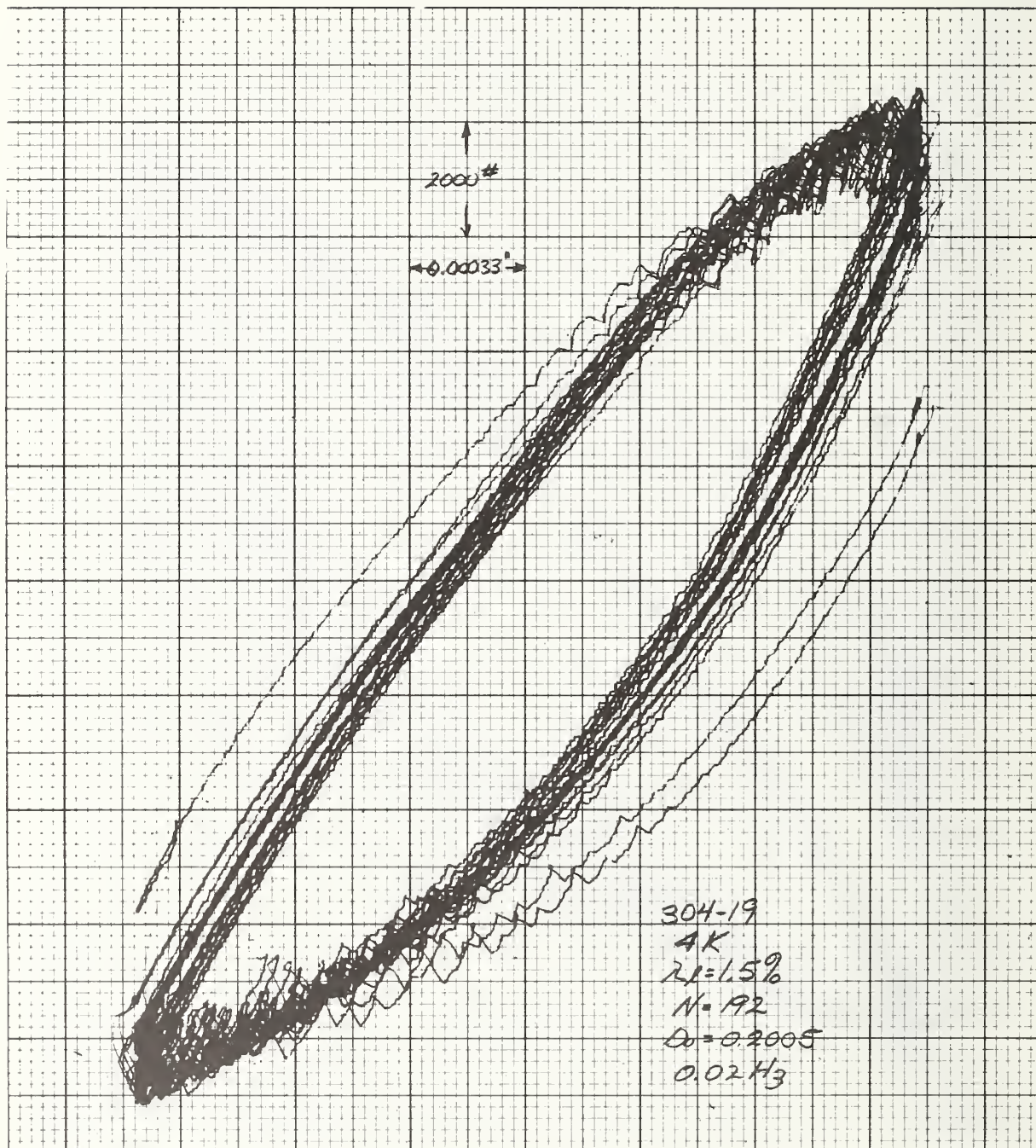$N = 192$
$D_0 = 0.2005$
$0.02 \, H_3$

Figure 14 Load–Deflection Curve for Specimen 304-19 (Cycles 21 through 40)
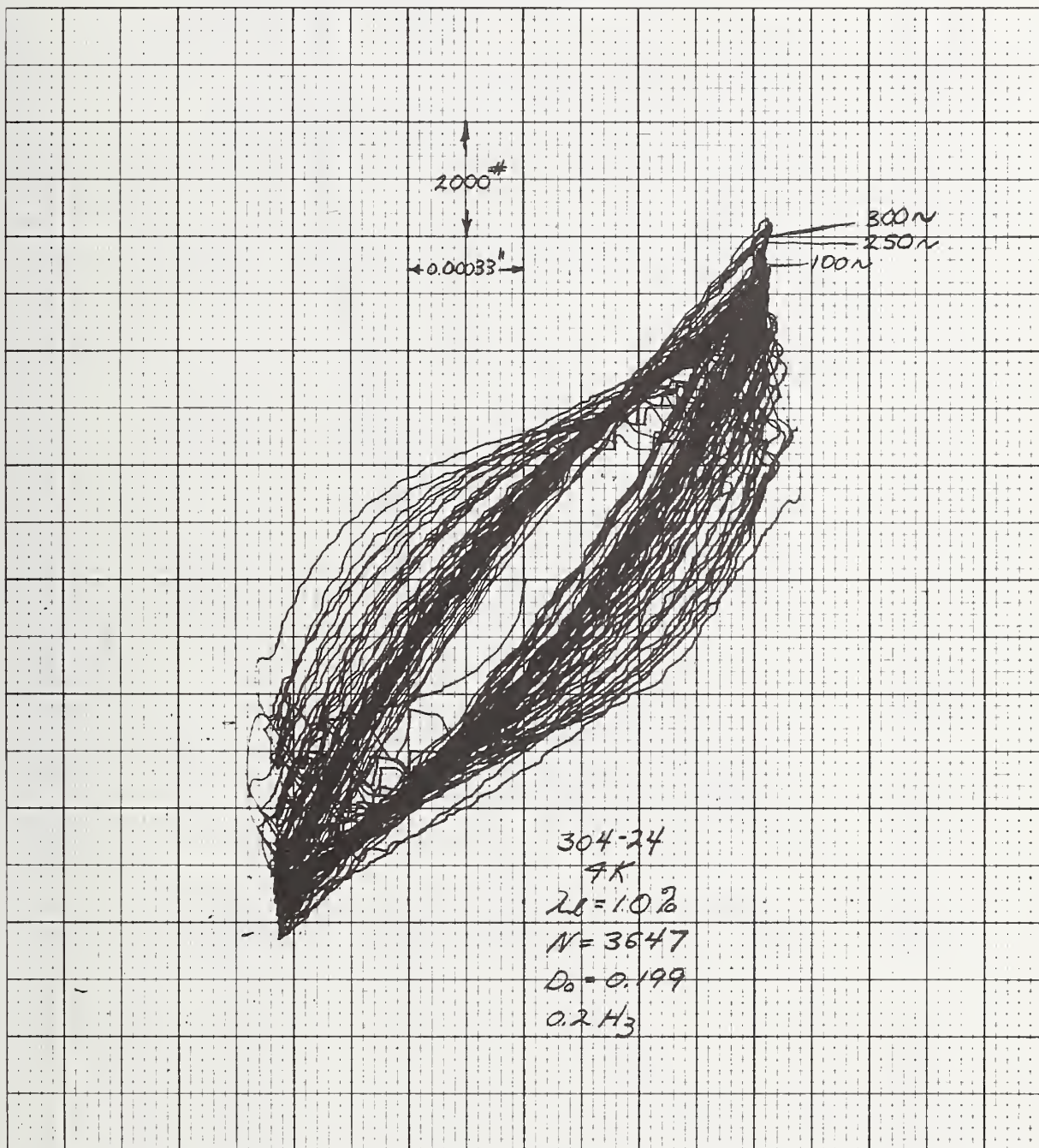
Figure 15 Load-Deflection Curve for Specimen 304-24
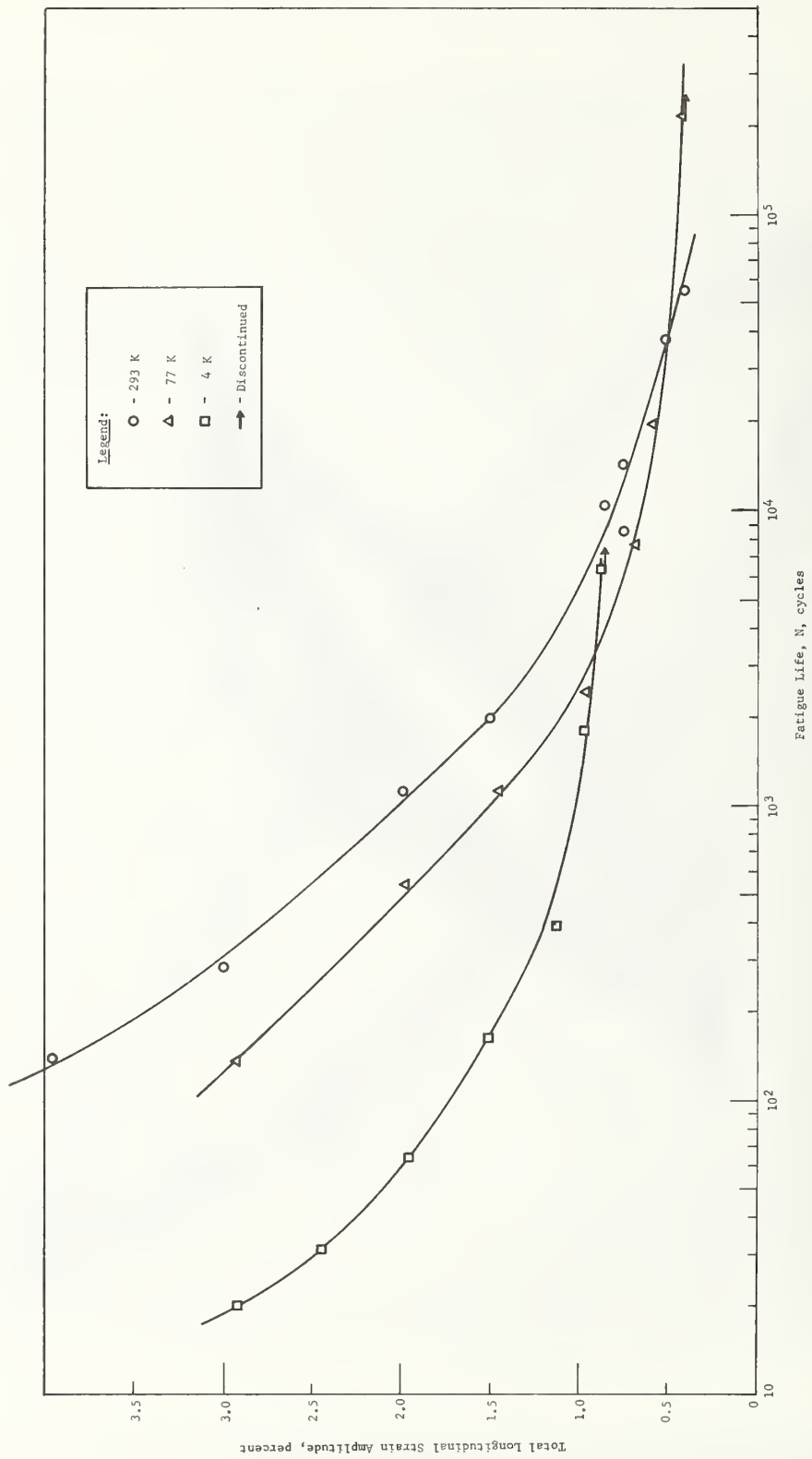
Figure 16 Fatigue Life Curves for 21-6-9

42

Table 3 Fatigue Data for 21-6-9 Stainless Steel

Specimen Number	Temperature, K	Diametral Total Strain Amplitude, $\Delta\lambda_d$, Percent	Stress Amplitude at Half-Life, $\Delta\sigma$, MN/m² (ksi)	Longitudinal Elastic Strain Amplitude, Δe_l, Percent	Longitudinal Plastic Strain Amplitude, Δc_l, Percent	Longitudinal Total Strain Amplitude, $\Delta\lambda_l$, Percent	Cyclic Rate, Hz	Fatigue Life, N Cycles
2169-1	293	0.93	552 (80)	0.29	1.70	1.99	0.20	1,111
-2		0.39	345 (50)	0.18	0.67	0.85	0.90	10,236
-3		1.42	690 (100)	0.36	2.63	2.99	0.20	281
-4		0.70	448 (65)	0.23	1.27	1.50	0.70	1,995
-5		0.34	345 (50)	0.18	0.57	0.75	1.50	8,530
-6		0.34	345 (50)	0.18	0.57	0.75	1.50	14,160
-7a		0.22	310 (45)	0.16	0.35	0.51	1.50	37,640
-7b		0.17	310 (45)	0.16	0.26	0.42	3.00	56,430
-8		1.90	724 (105)	0.38	3.58	3.96	0.20	139
2169-9	77	0.89	1103 (160)	0.55	1.43	1.98	0.20	535
-10		0.39	896 (130)	0.45	0.51	0.96	1.00	2,443
-11		0.29	621 (90)	0.31	0.05	0.36	3.00	216,000
-12		0.63	965 (140)	0.48	0.96	1.44	1.00	1,117
-13		0.27	690 (100)	0.34	0.34	0.68	0.90	7,700
-14		1.36	1241 (180)	0.62	2.31	2.93	0.10	137
-15		0.23	655 (95)	0.33	0.26	0.59	2.00	19,470
2169-16	4	0.84	1448 (210)	0.72	1.23	1.95	0.10	64
-17		0.62	1379 (200)	0.69	0.81	1.50	0.10	163
-18		0.28	931 (135)	0.47	0.28	0.75	0.30	6,353*
-19		1.08	1586 (230)	0.79	1.65	2.44	0.05	31
-20		1.32	1586 (230)	0.79	2.13	2.92	0.02	20
-21		0.37	1103 (160)	0.55	0.42	0.97	0.10	1,786
-22		0.49	1310 (190)	0.66	0.59	1.25	0.10	389

* Test discontinued

Temperature, K	293	77	4
Modulus, GN/m² (10⁶ psi)	195 (28)	203 (29)	203 (29)
Poisson's Ratio	0.29	0.28	0.28

43

Figure 17   Load-Deflection Curve for Specimen 2169-10

44

obtained at 4 K is presented in figure 18. The curve is not quite as smooth as observed at 77 K, probably as a result of localized heating due to strain gage excitation, but does not exhibit discontinuous yielding.

By comparison, the 4 K curve obtained at a high strain level (2.5 percent) exhibits significant discontinuities (Figure 19). The repetitive trace clearly shows an increase in the magnitude of the discontinuities with increasing strain level. Although masked by the multiple traces, the degree of strain hardening observed was relatively small compared to that exhibited by the 304.

An anomaly noted at 293 K for several tests was a combination of strain hardening and strain softening occurring at intermediate strain levels. Although the magnitude of the change was small, it was deemed unusual. Figure 20 shows this behavior. Strain hardening occurs during the first 20 cycles, followed by continuous softening until failure occurs.

316 Stainless Steel - The 316 stainless steel exhibits a decrease in fatigue strength with decrease in temperature from 293 to 77 K for strain levels greater than 1 percent. At 4 K, the fatigue life is greater than at 77 K for all but the highest strain level evaluated. At 293 K, the crossover with the 4 K data occurs at approximately 2 percent strain. Figure 21 presents the data. Table 4 gives detailed test information.

The hysteresis loops obtained at 293 and 77 K are similar to that observed for 304 except that much less strain hardening occurred. Figure 22 presents a typical 77 K curve (1.5 percent strain).

At 4 K, discontinuous yielding was found, but the magnitude was much less than observed for the 304. Figures 23 and 24 present data

45

Figure 18   Load-Deflection Curve for Specimen 2169-21

The handwritten annotations on the figure read:

2169-19
4K
$\lambda_1 = 2.5\%$
$N = 31$
$D_o = 0.201$
$0.05 Hz$

2000 # ← .000325" →

Figure 19   Load-Deflection Curve for Specimen 2169-19

*Figure 20   Load-Deflection Curve for Specimen 2169-4*

48
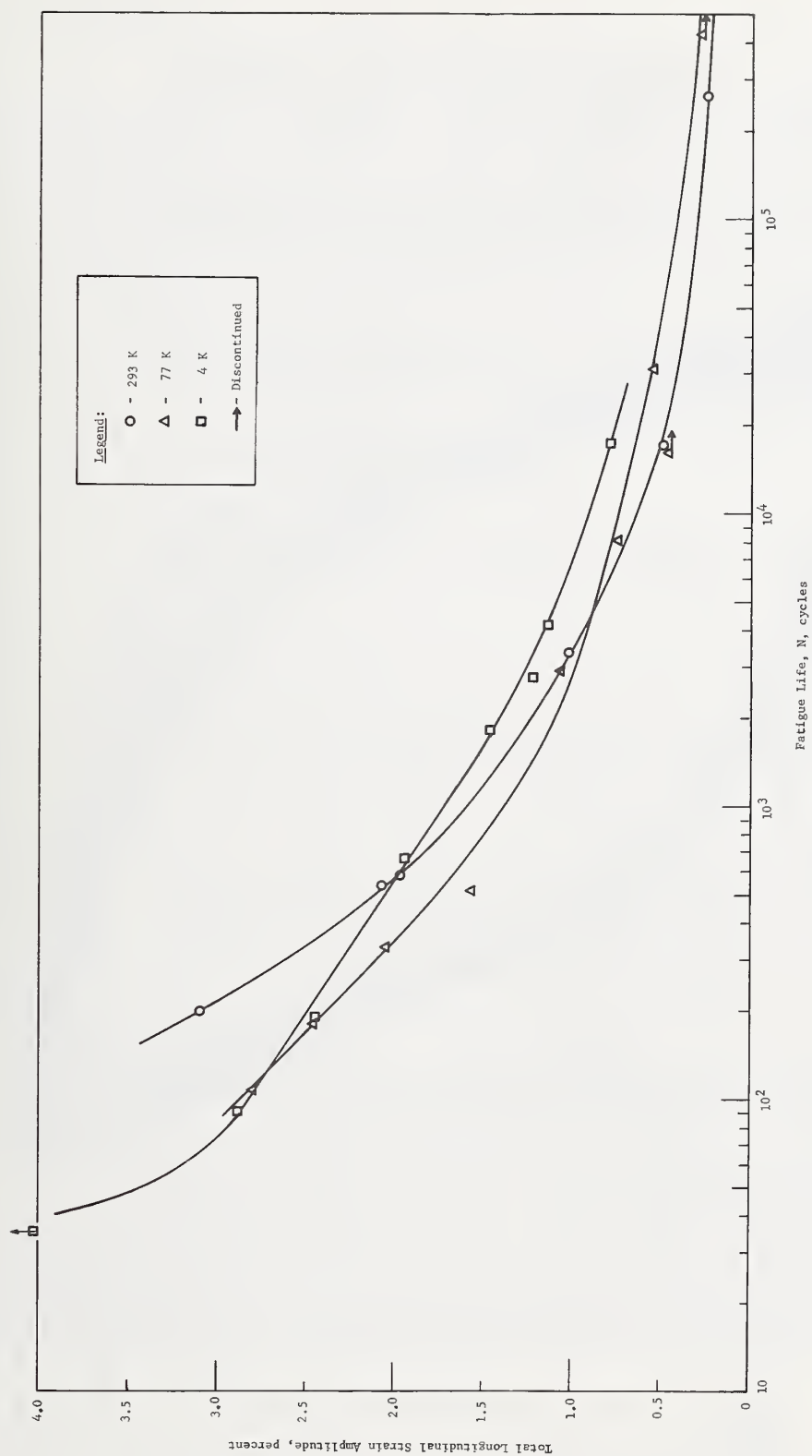
Figure 21 Fatigue Life Curves for 316

Table 4 Fatigue Data for 316 Stainless Steel

Specimen Number	Temperature, K	Diametral Total Strain Amplitude, $\Delta\lambda_d$, Percent	Stress Amplitude at Half-Life, $\Delta\sigma$, MN/m² (ksi)	Longitudinal Elastic Strain Amplitude, Δe_1, Percent	Longitudinal Plastic Strain Amplitude, $\Delta\epsilon_1$, Percent	Longitudinal Total Strain Amplitude, $\Delta\lambda_1$, Percent	Cyclic Rate, Hz	Fatigue Life, N Cycles
316-1	293	0.96	621 (90)	0.29	1.78	2.07	0.10	527
-2		0.47	379 (55)	0.18	0.84	1.02	0.80	3,328
-3		1.48	552 (80)	0.26	2.83	3.09	0.10	198
-4		0.93	517 (75)	0.24	1.73	1.97	0.40	579
-5		0.22	276 (40)	0.13	0.36	0.49	3.00	17,131
-6		0.10	193 (28)	0.09	0.16	0.25	3.00	259,459
-7		2.38	758 (110)	0.35	4.58	4.93	0.05	36
316-8	77	0.94	1000 (145)	0.43	1.62	2.05	0.40	329
-9		0.46	758 (110)	0.32	0.75	1.07	0.40	2,898
-10		0.21	586 (85)	0.25	0.30	0.55	1.10	31,300
-11		0.10	414 (60)	0.18	0.09	0.27	3.00	426,000*
-11a		1.36	828 (120)	0.35	2.45	2.80	0.10	107
-12		0.69	965 (140)	0.41	1.16	1.57	0.40	510
-13		1.86	965 (140)	0.41	3.45	3.86	0.10	30+
-14		1.14	1034 (150)	0.44	2.02	2.46	0.20	179
-16		0.18	483 (70)	0.21	0.25	0.46	3.00	164,567*
-17		0.31	621 (90)	0.26	0.49	0.75	1.10	8,157
316-18	4	0.64	965 (140)	0.41	1.06	1.47	0.05	1,815
-19		0.89	1123 (163)	0.48	1.46	1.94	0.07	661
-20		1.35	1337 (194)	0.41	2.47	2.88	0.05	90
-21		.55	882 (128)	0.38	0.85	1.23	0.05	2,751
-23		1.42	1468 (213)	0.63	2.40	2.45	0.05	188
-24		0.50	868 (126)	0.37	0.76	1.13	0.02	4,130
-25		0.33	785 (114)	0.34	0.44	0.78	0.03	17,100

* Discontinued
+ Specimen buckled

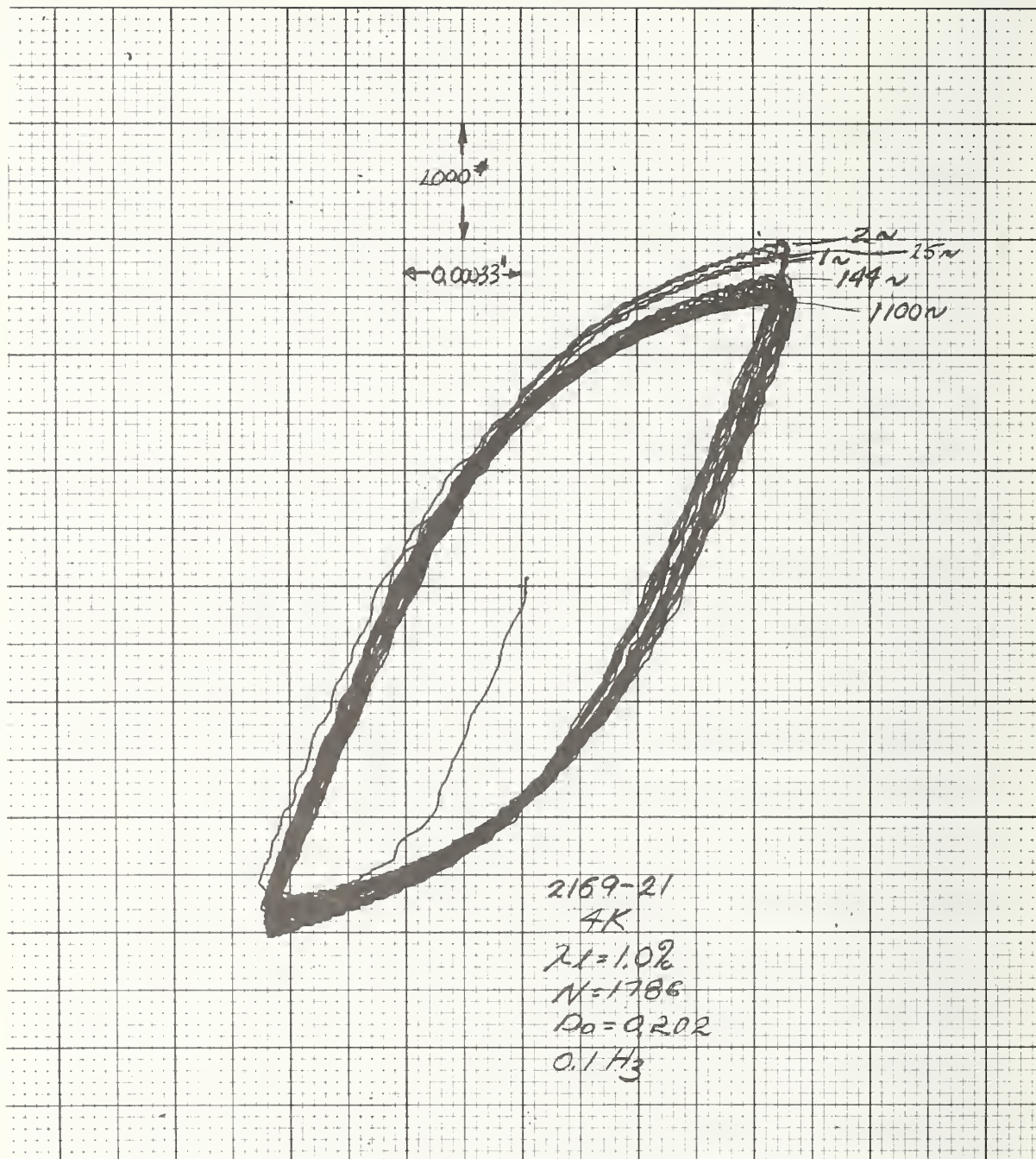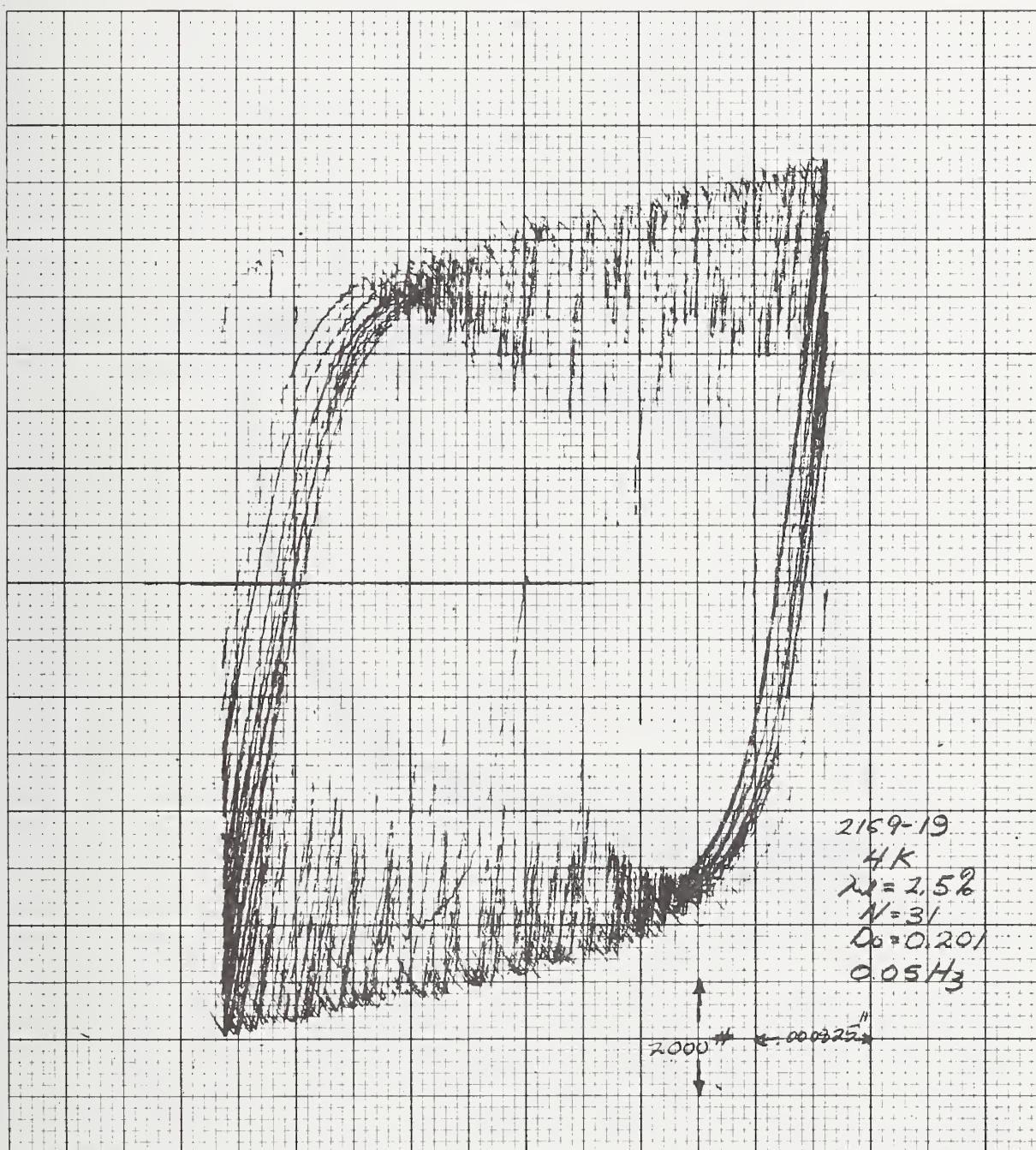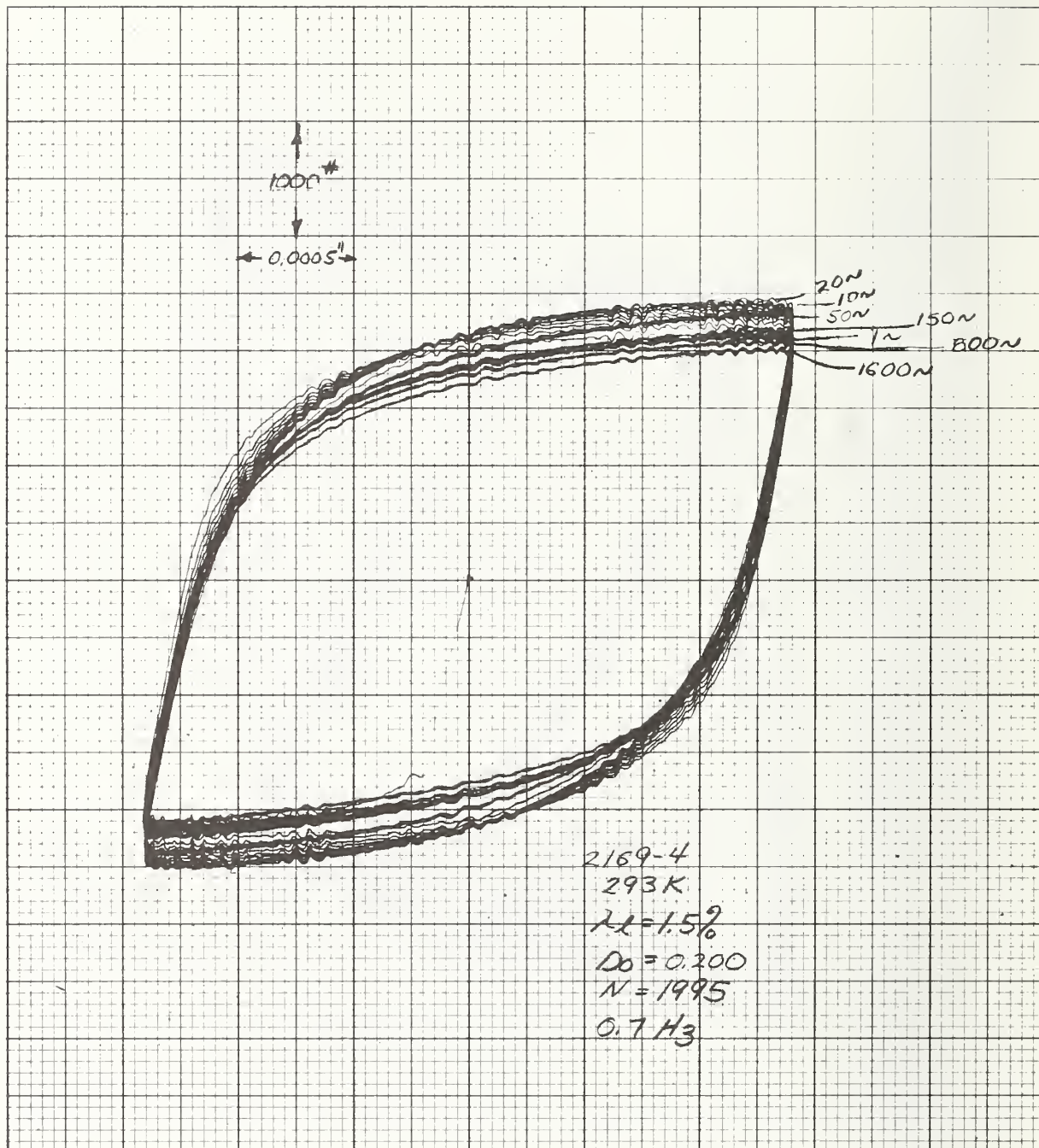|			
Temperature, K	293	77	4
Modulus, GN/m² (10⁶ psi)	216 (31)	234 (34)	234 (34)
Poisson's Ratio	0.30	0.28	0.28

50
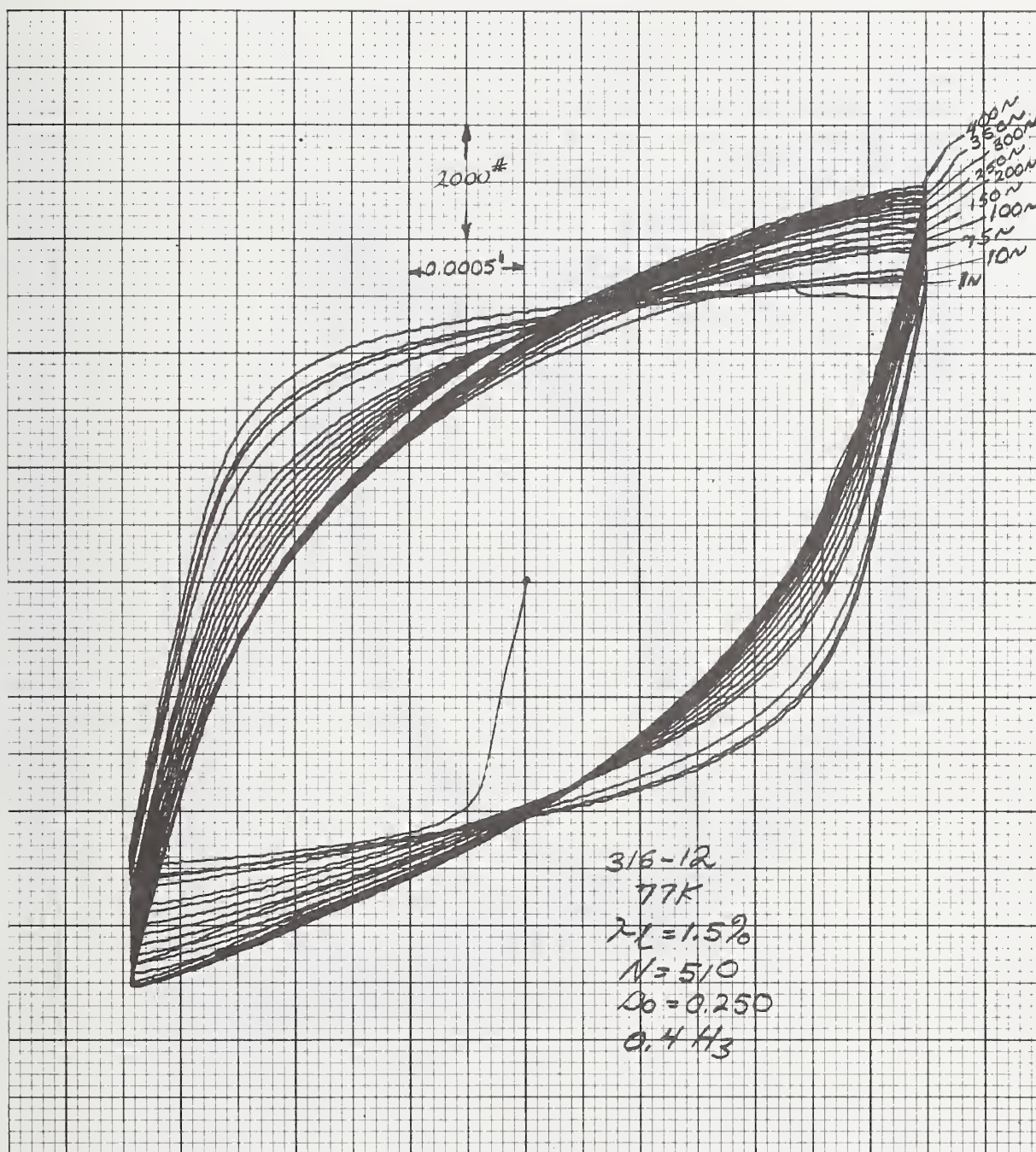
Figure 22   Load-Deflection Curves for Specimen 316-12

51
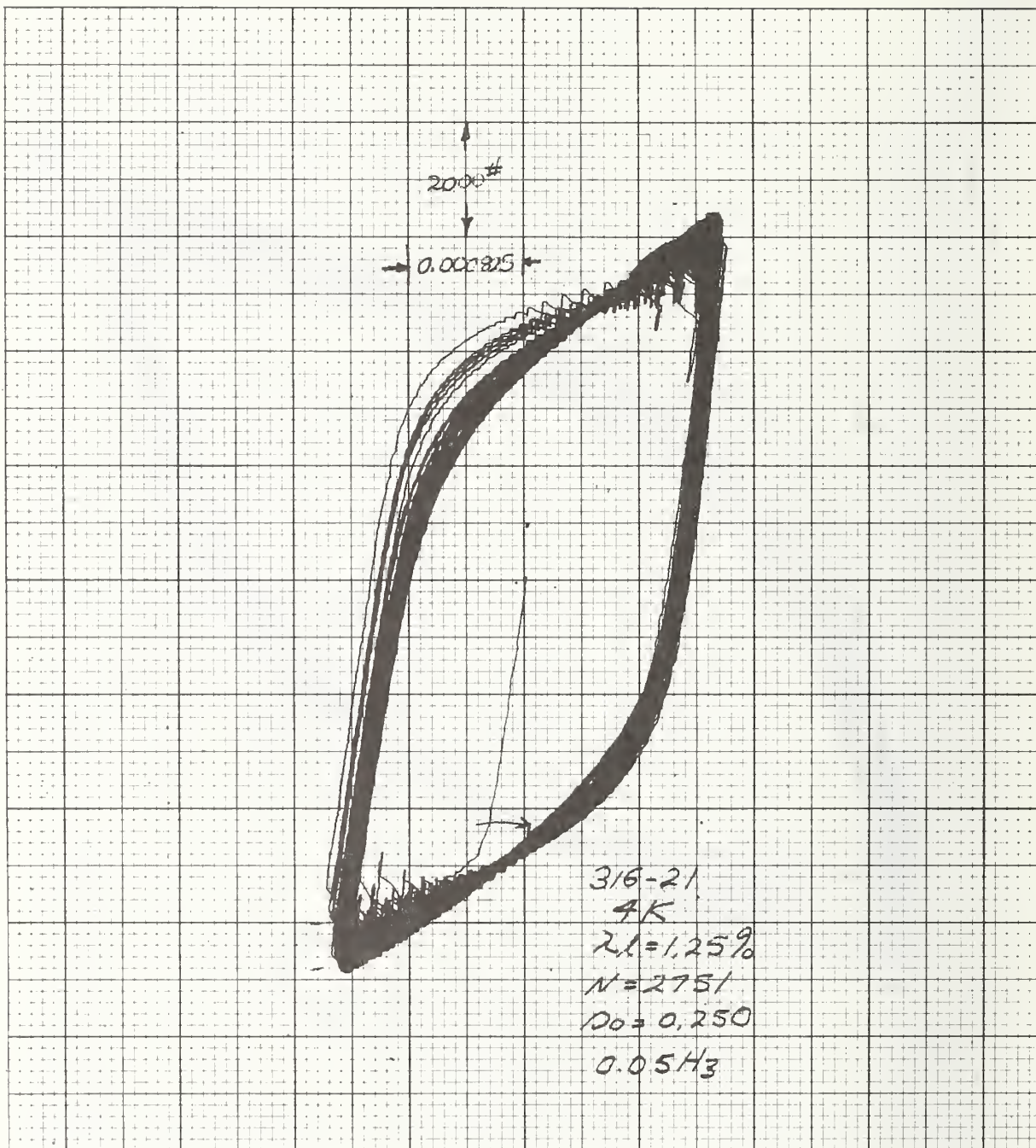
Figure 23   Load-Deflection Curves for Specimen 316-21
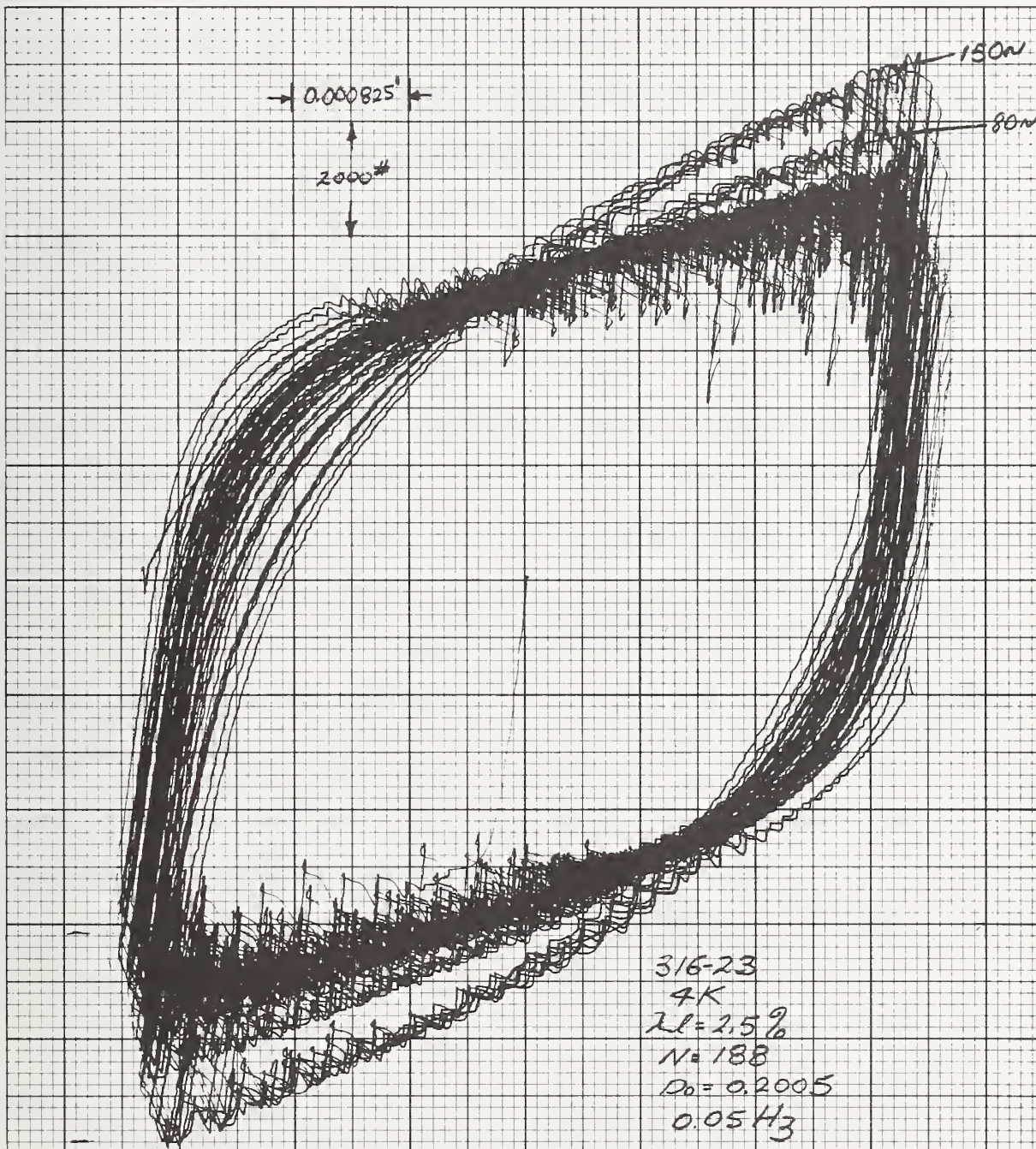
Figure 24   Load-Deflection Curves for Specimen 316-23

at 1.25 and 2.5 percent strain levels as evidence of the reduction in yield jogs. The degree of strain hardening was also much lower.

Strain Hardening - A comparison of the strain hardening behavior of the three alloys at each temperature reveals certain interesting trends. Figure 25 plots the change in stress amplitude from the first to final cycle as a function of total axial strain amplitude. The changes in stress amplitude for the 304 stainless steel at 77 and 4 K is extremely high. This alloy displays no evidence of strain softening at cryogenic temperatures. The 316 alloy at all three temperatures and the 304 at 293 K exhibit a modest change in strength; the change is only a fraction of that observed for the latter alloy at cryogenic temperatures. At low strain levels, types 304 and 316 exhibit slight strain softening. The 21-6-9 exhibits even less strain hardening than the 316. At 77 K, the magnitude of strain softening at low strain levels is similar to that of strain hardening. The 4 K data for 21-6-9 show strain hardening similar to that observed at 77 K; however, little strain softening is evident.

Transformation - Preliminary attempts to determine the degree of transformation on the fracture surfaces using a Magne-Gage was unsuccessful. Differences in surface roughness and variations in magnetic attraction associated with local deformation (shear lips) made measurements difficult. Specimens will be retained for future study using alternative techniques and methods.

With the use of a hand-held magnet, qualitative estimates of magnetic susceptibility were made. Data are summarized below:
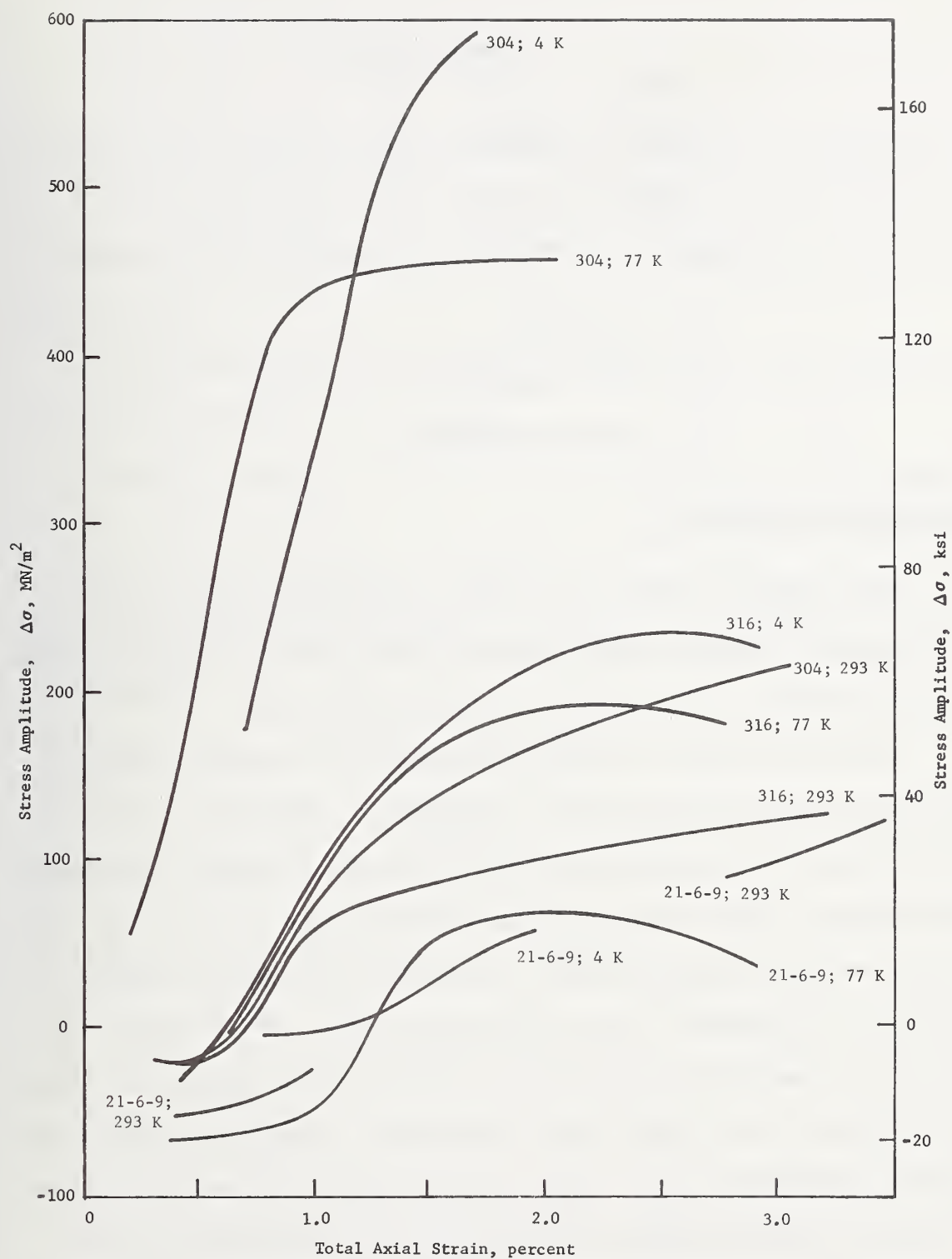
Figure 25 Effect of Strain Amplitude on Change in Stress Amplitude

	Temperature (K)		
Alloy	293	77	4
304	N to W	M	M
21-6-9	N	N	N
316	N to W	M	M

N = nonmagnetic

W = weakly magnetic

M = moderately magnetic

DISCUSSION OF RESULTS

Data obtained from this work were compared with other available information to obtain fatigue life curves that provide the best possible characterization of the behavior of the various alloys.

For the 304 alloy, the strain-controlled data obtained from this work, the strain-controlled data of Nachtigall (reference 2), and the stress-controlled data from a prior Martin Marietta program (reference 1) were combined to give composite strain versus fatigue life curves. The stress controlled data from tests conducted in the elastic range were converted to equivalent total longitudinal strain. The plots for 293, 77 and 4 K show excellent agreement between the three sources and permit a smooth curve to be drawn at each temperature. Figures 26, 27 and 28 present the fatigue plots. These strain-contolled fatigue data may be plotted as stress-amplitude-to-failure data by converting the strain amplitude λ_1 to a stress amplitude S_a using the relation $S_a = E \lambda_1$ where E is Young's modulus. This form is appropriate for comparison to data

as used in the A.S.M.E. Boiler and Pressure Vessel Code (reference 6).

The resulting stresses are, of course, much larger than would occur in

a stress-controlled fatigue tests. No safety or adjustment factors have

been included.

The calculated stress amplitudes are shown on the right-hand ordinate

of the plots in Figs. 26, 27 and 28.

Similarly, data for the 21-6-9 from this work and the prior Martin

Marietta study (reference 1) were combined and give a smooth curve extend-

ing into the 10^6 cycle range. Figures 29, 30 and 31 present these curves.

Again, calculated stress amplitudes are shown on the right-hand ordinate

of the graphs.
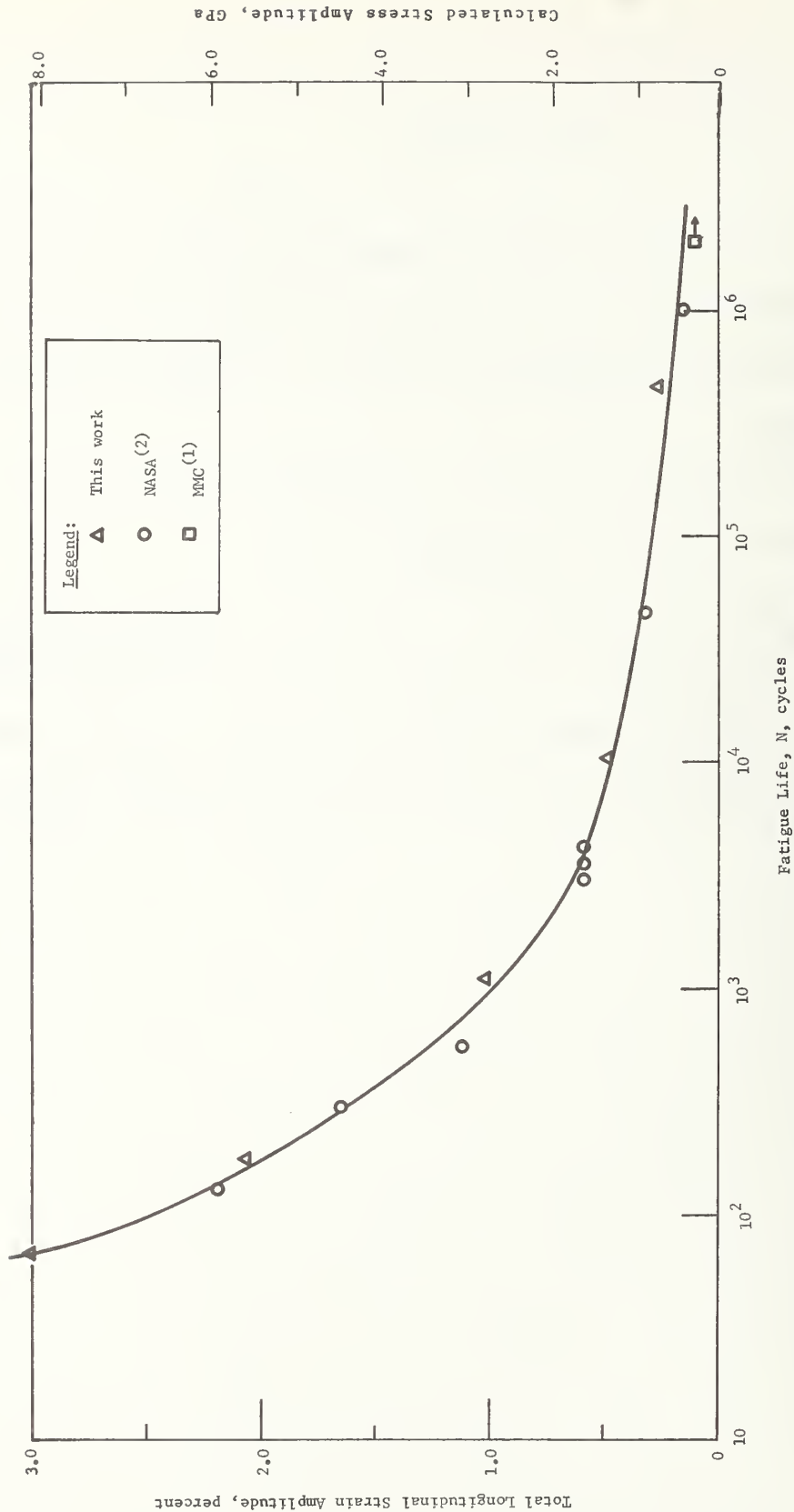
Figure 26   Fatigue Life Curve for 304 at 293 K
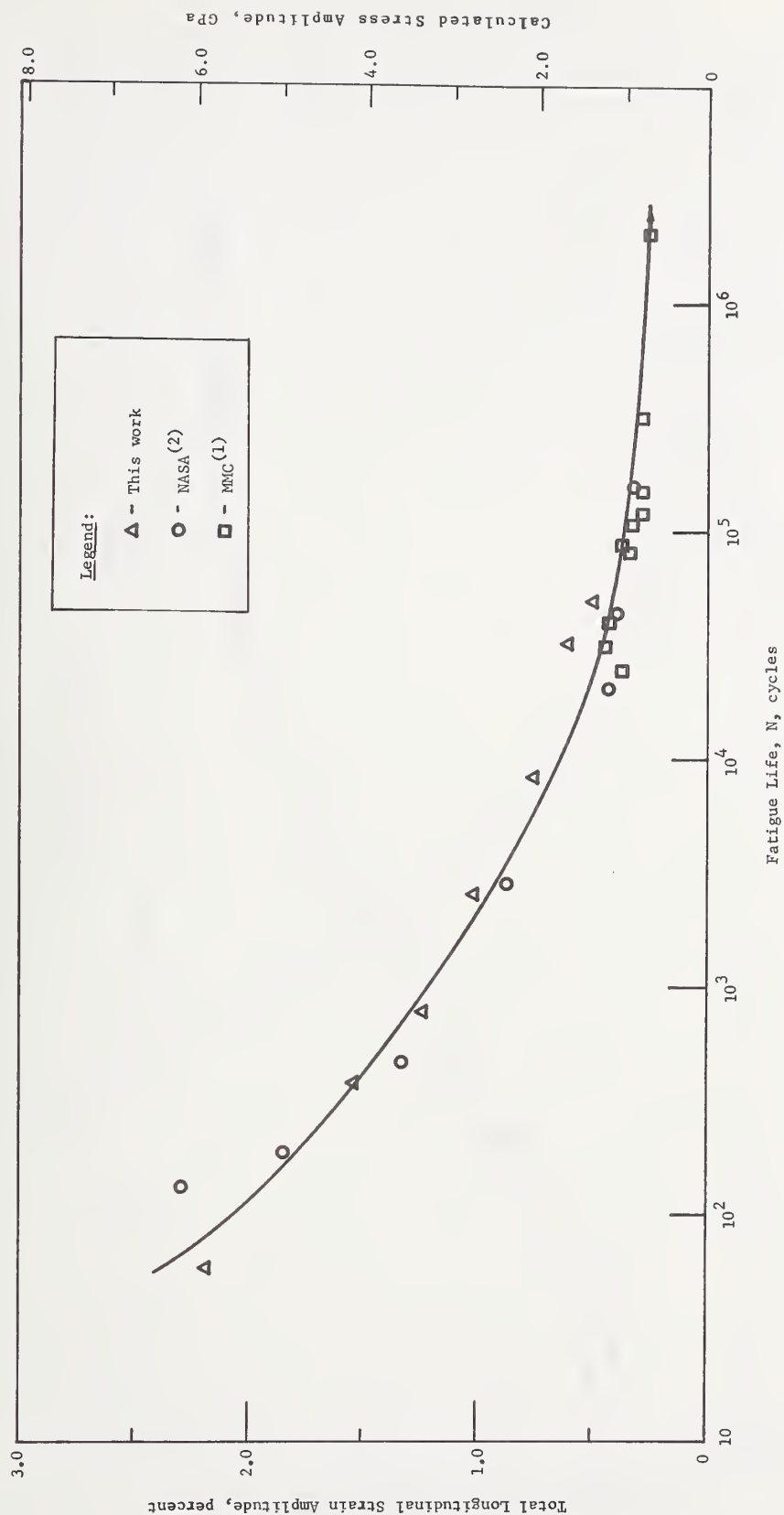
Figure 27 Fatigue Life Curve for 304 at 77 K
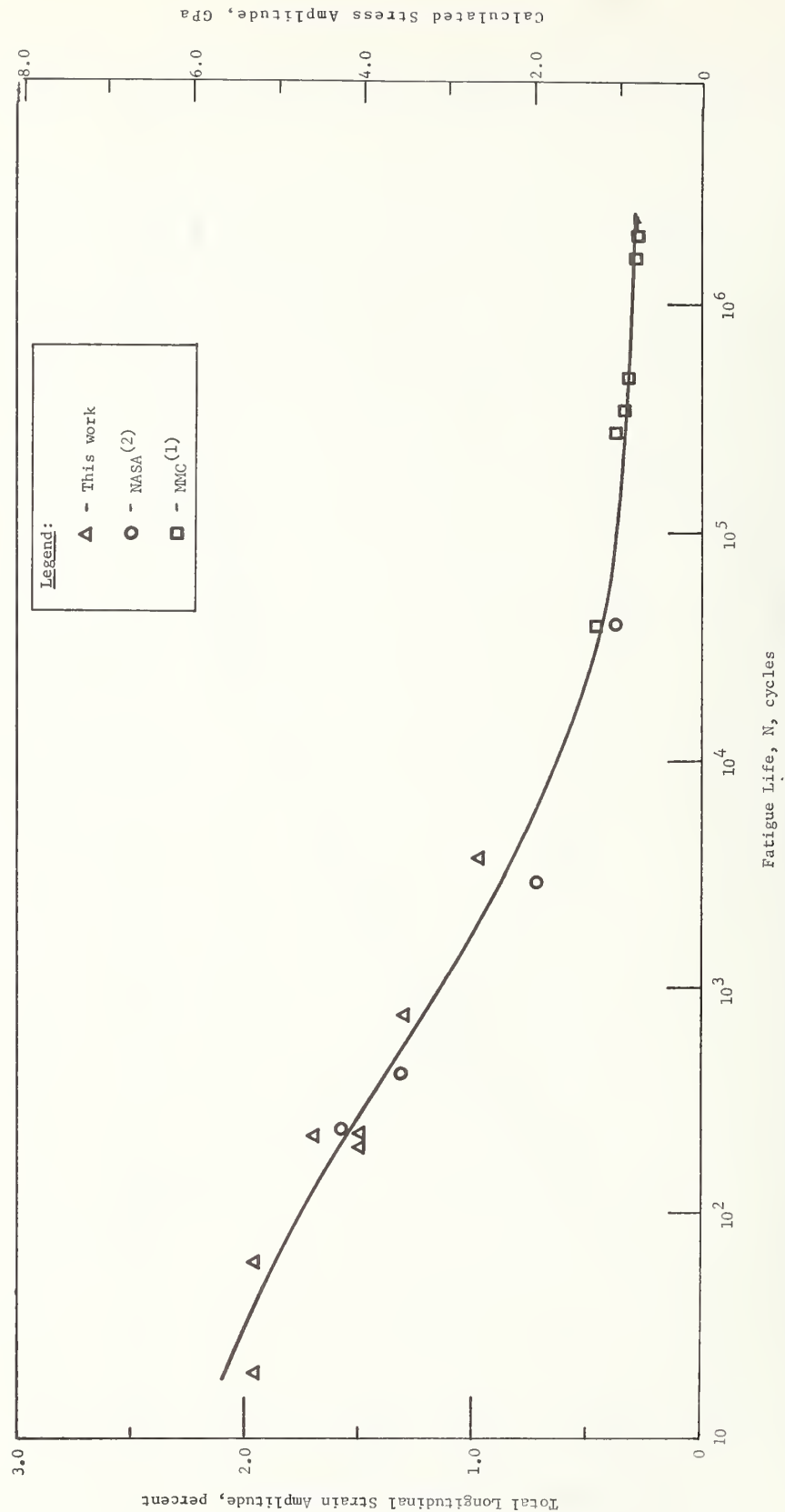
Figure 28 Fatigue Life Curve for 304 at 4 K

60
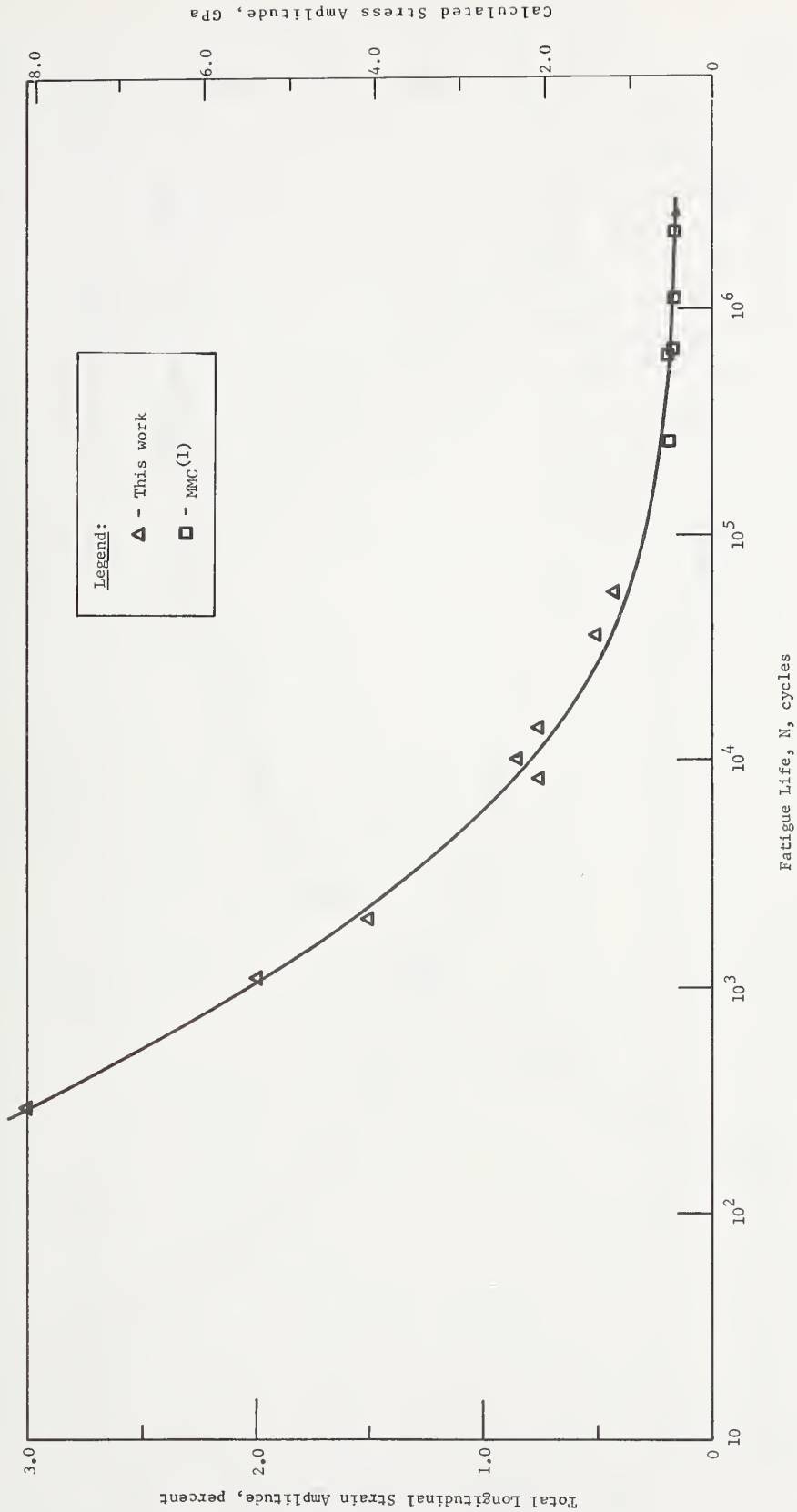
Figure 29 Fatigue Life Curve for 21-6-9 at 293 K
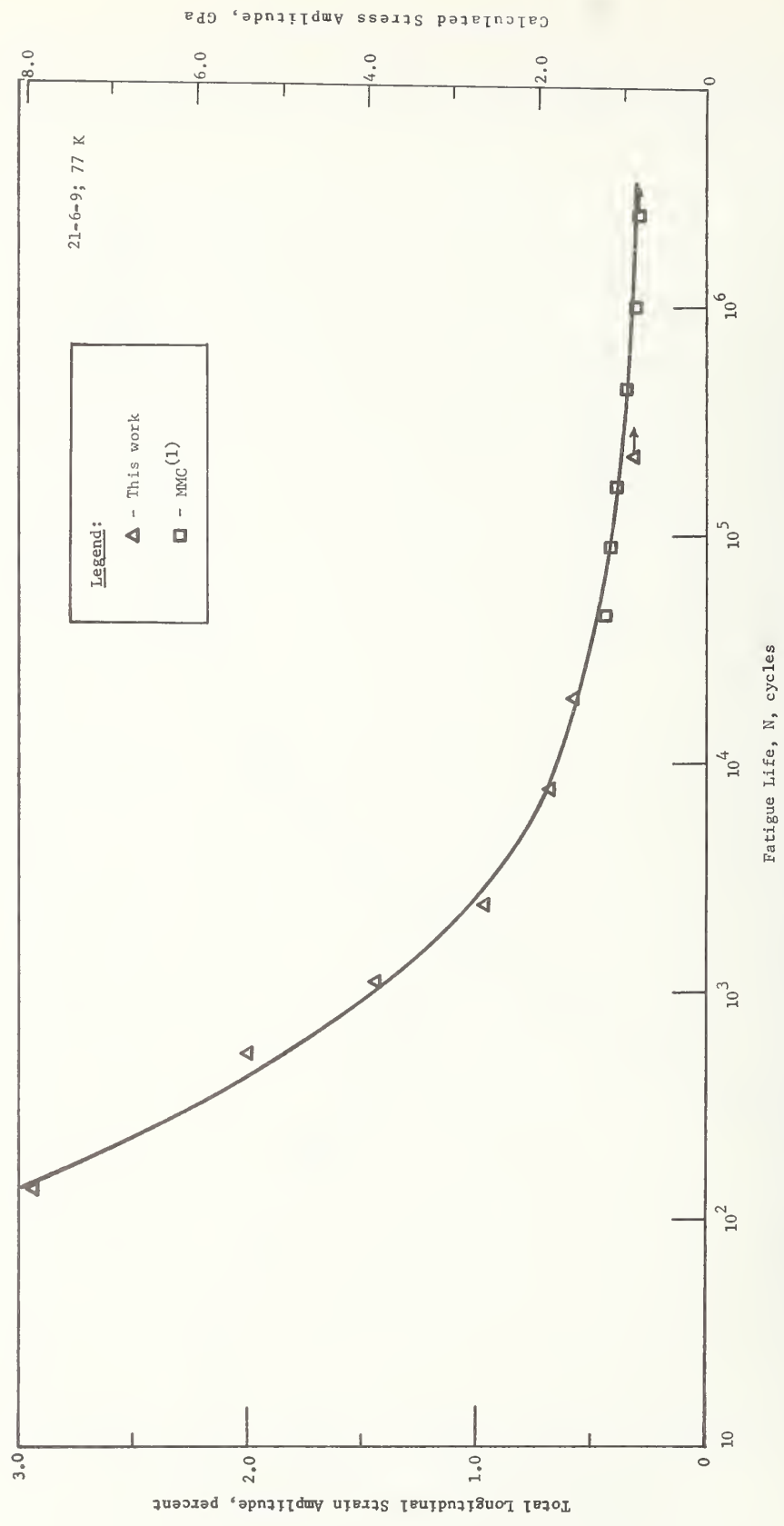
Figure 30 Fatigue Life Curve for 21-6-9 at 77 K

62
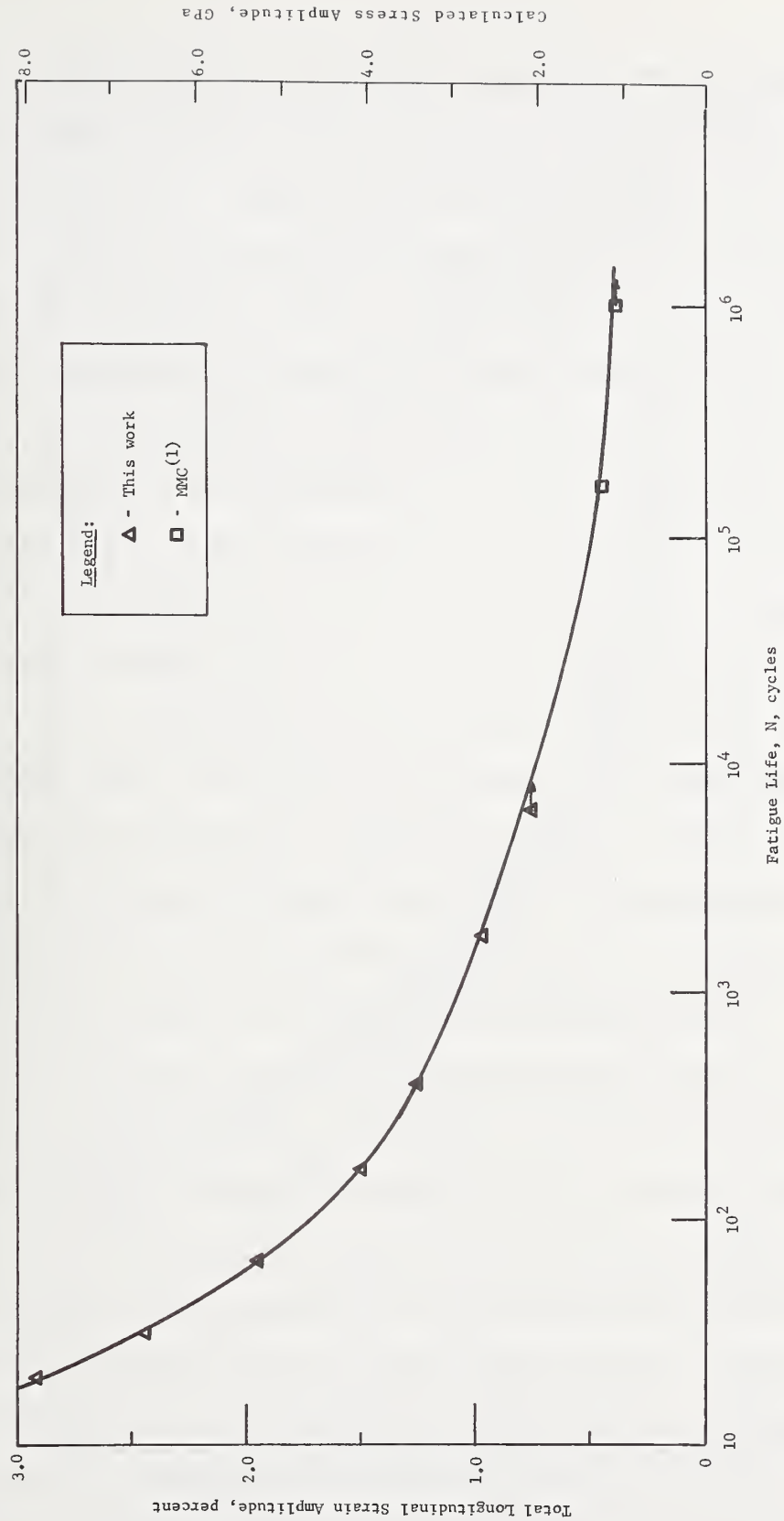
Figure 31 Fatigue Life Curve for 21-6-9 at 4 K

63

A comparison of the fatigue strength of the three alloys at each test temperature was performed. At 293 K, the 21-6-9 alloy exhibits the highest fatigue strain capability in the low cycle range. 316 exhibits slightly lower properties. The 304 stainless has significantly poorer low-cycle properties. In the high-cycle range ($> 10^4$), 316 exhibits the highest endurance limit. Figure 32 shows the comparative properties of the three alloys at 293 K. Approximate stress levels calculated as before are indicated on the right-hand ordinate. The stress levels are approximate because of a difference of about 4% among the Young's moduli of the three materials. The average of the three moduli was used for the stress calculation.

A similar comparison made for the 77 K data shows the 21-6-9 alloy to be superior in fatigue behavior for the low-cycle range. 316 is slightly lower in performance, but crosses the 21-6-9 curve at about 1000 cycles and exhibits the highest long-term properties. 304 exhibits the poorest fatigue properties throughout the test range. Figure 32 presents the composite curve. Again, approximate stress amplitude levels are indicated on the right-hand ordinate. At this temperature, the spread of the Young's moduli is about 8%.

At 4 K, 316 is clearly superior to the 21-6-9 and 304 in the low-cycle range. Insufficient data are available to confirm retention of superiority in the high-cycle range, but that trend is apparent. The 304 exhibits behavior generally equivalent to the 21-6-9 (Figure 34). In Fig. 34, as before, calculated stress amplitude levels are indicated on the right-hand ordinate, and the spread in Young's moduli among the three materials is about 8%.

A comparison of the effect of temperature for each alloy shows that the behavior of 304 is relatively independent of temperature. In the low-cycle range, the 4 and 293 K data are almost identical, and the 77 K results are quite similar to the other temperatures. Likewise, the 316 exhibits little
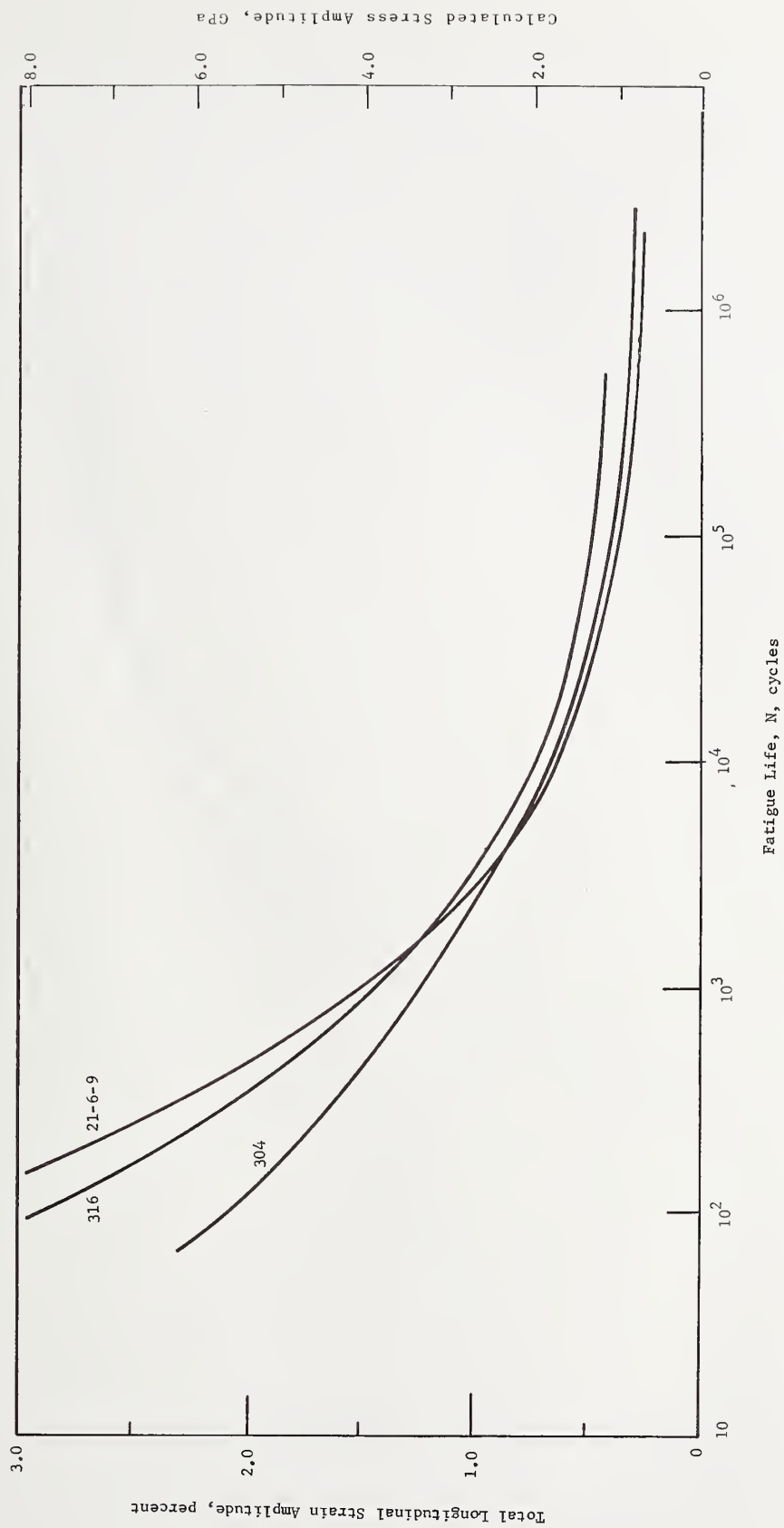
Figure 32 Comparison of Fatigue Behavior at 293 K

65
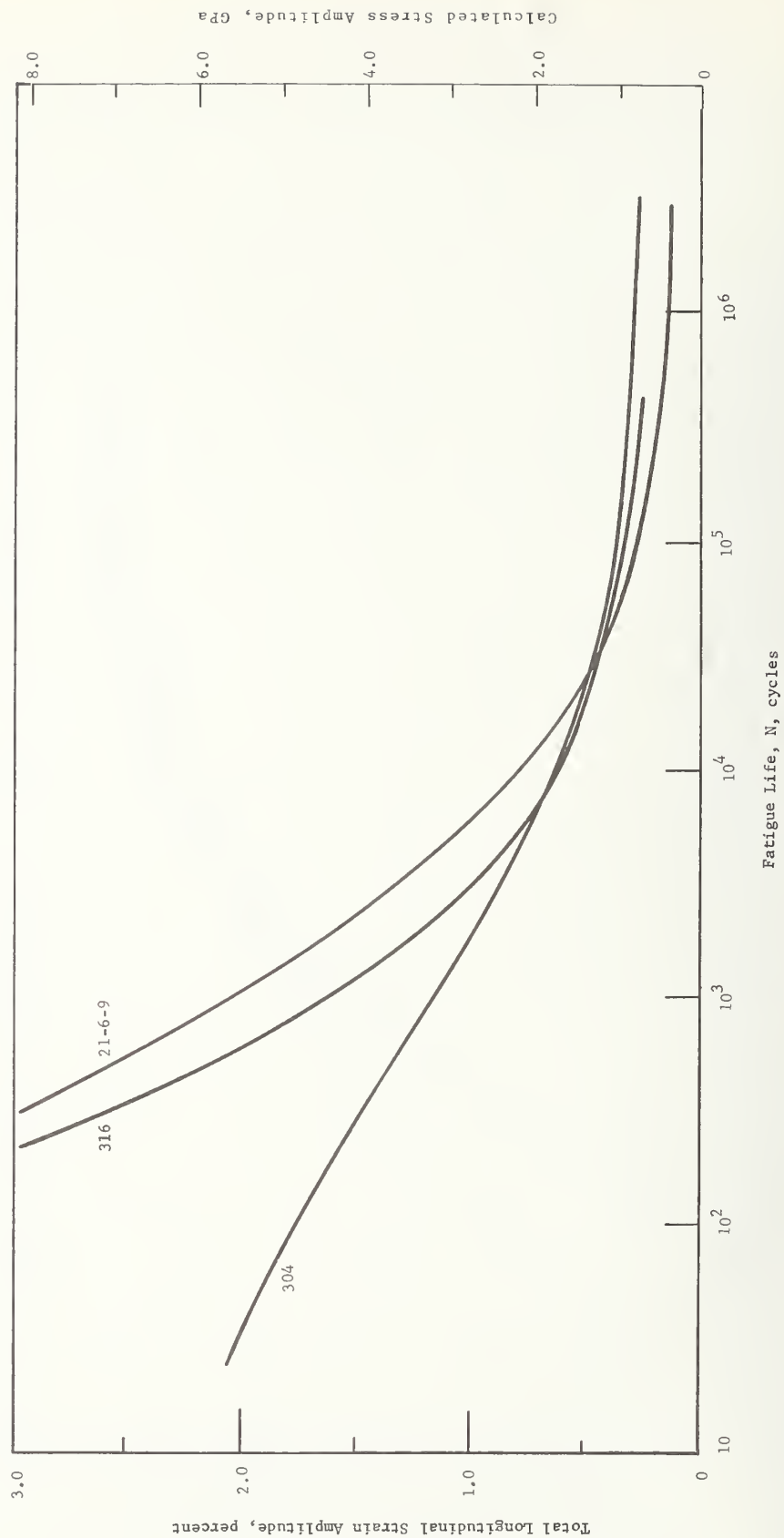
Figure 33 Comparison of Fatigue Behavior at 77 K
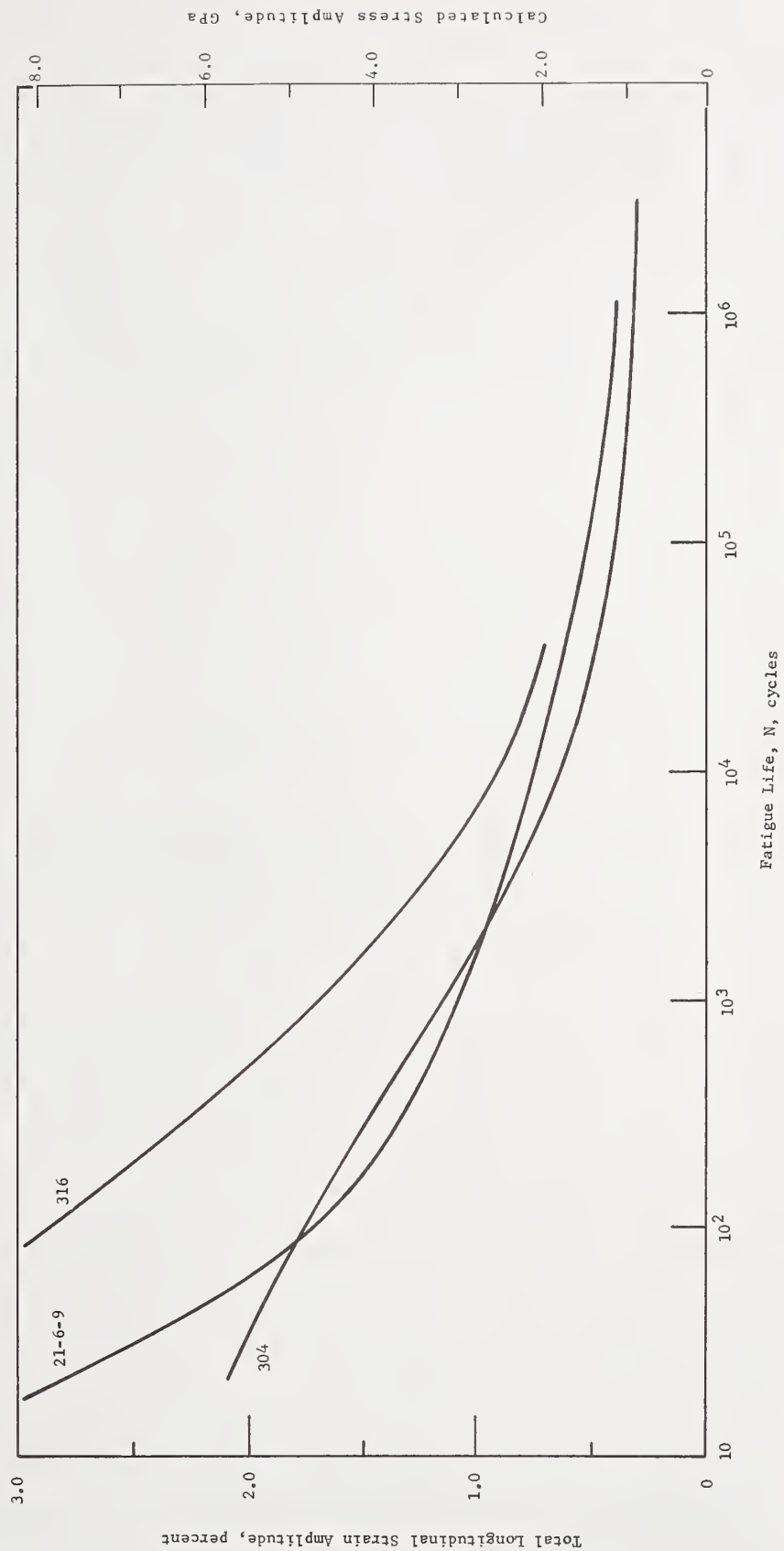
Figure 34 Comparison of Fatigue Behavior at 4 K

67

effect of temperature on behavior. The 21-6-9 exhibits the greatest effect of temperature on behavior. The low-cycle like is decreased slightly with reduction in temperature to 77 K, and quite significantly with reduction to 4 K.

Although differences in fatigue behavior of the three alloys are apparent, none displays qualities that should affect its candidacy for service down to 4 K.

REFERENCES

1. F. R. Schwartzberg and T. F. Kiefer, "Study of Fracture Behavior of Metals for Superconducting Applications", Materials Research for Superconducting Machinery, Semi-Annual Technical Report IV, October 1975, National Bureau of Standards, Boulder, Colorado.

2. A. J. Nachtigall, "Strain-Cycling Fatigue Behavior of Ten Structural Metals Tested in Liquid Helium, in Liquid Nitrogen, and in Ambient Air", NASA TN D-7532, February 1974.

3. A. J. Nachtigall, S. J. Klima, and J. C. Freche, "Fatigue of Liquid Rocket Engine Metals at Cryogenic Temperatures to -452F", NASA TN D-4274, December 1967.

4. E. J. Beck, "Effect of Beta Processing and Fabrication on Axial Loading Fatigue Behavior of Titanium", AFFDL-TR-69-108, Martin Marietta Corporation, June, 1969.

5. R. D. Keys and F. R. Schwartzberg, "Axial Fatigue Testing of Sheet Materials Down to -423F", Materials Research and Standards, May, 1964.

6. "A.S.M.E. Boiler and Pressure Vessel Code, Section VIII, Division 2," American Society of Mechanical Engineers, 1977, p. 399-404.

Fracture Testing of 21-6-9 Stainless Steel

Martin Marietta

Final
Report   December 1977

FRACTURE TESTING
OF 21-6-9 (Nitronic 40)
STAINLESS STEEL

J. A. Shepic
Principal Investigator

F. R. Schwartzberg
Program Manager

FOREWORD

This report describes technical activities conducted by the Denver Division of Martin Marietta Corporation during the period 17 May 1977 through 30 November 1977 under National Bureau of Standards (NBS) contract CST-8426, Item 1.

The views and conclusions contained in this document are those of the authors and should not be interpreted as necessarily representing the official policies, either expressed or implied, of the United States Government.

INTRODUCTION

Austenitic stainless steel alloy, 21-6-9 (Fe-21Cr-6Ni-9Mn-0.3N), (Nitronic 40), is of great interest for cryogenic machinery, particularly in superconducting magnets, because of its excellent combination of strength and toughness.

A preliminary evaluation of the fracture toughness of this alloy was reported by Tobler and Reed[1] using laboratory processed material. The objective of this work is to further characterize the same gage, 3.8 cm (1.5 in.) of commercially produced plate material.

MATERIAL

The 21-6-9 stainless steel evaluated in this program was provided by National Bureau of Standards (NBS) in the form of 3.8 cm (1.5 in.) plate. The material had been procured from G.O. Carlson and was iden- tified as heat number 656249. The plate was received in the hot rolled, annealed, and descaled condition. Final annealing temperature was re- ported to be 1366-1394K (2000-2050F) for ½ hour per 2.5 cm (1 in.) of thickness, followed by water quenching.

Vendor's analysis showed the following composition for the plate:

        Cr = 20.11 w/o
        Ni = 6.34 w/o
        Mn = 8.97 w/o
        C = 0.033 w/o
        P = 0.013 w/o
        S = 0.005 w/o
        Si = 0.56 w/o
        N = 0.29 w/o
        Fe = balance

73

NBS determined the tensile properties of the material at three temperatures. Data are as follows:

| | Temperature, K | | |
	293	77	4
Ultimate strength, MN/m^2 (ksi)	785 (114)	1488 (216)	1832 (266)
Yield strength, 0.2% offset MN/m^2 (ksi)	386 (56)	916 (133)	1399 (203)
Elongation, percent	58	34	11
Reduction of area, percent	76	32	25

TESTING TECHNIQUE AND APPARATUS

This chapter describes the specimen geometry, testing apparatus, and technique used to obtain the fracture data presented in this report.

The J-integral specimen configuration used for this program was a 3.8 cm (1.5 in.) thick compact specimen of the basic geometry described in ASTM E-399-74[2]. The specimen was modified, as shown in Figure 1, to permit loadline compliance measurements to be obtained. Specimens were machined so that the notch was oriented parallel to the rolling direction (TL orientation).

Precracking of 293K test specimens was performed at the test temperature. Cryogenic test specimens were precracked at 77K. Specimens were precracked in closed-loop servo-hydraulic testing machine at a frequency of 10 Hz and a load of 22-27 kN (5-6 kips). The maximum stress intensity (K_f) at the conclusion of precracking to an a/W ratio

Figure 1   Specifications for J-Integral Test Specimen

75

of 0.65 was a maximum of 42 $MN/m^{3/2}$ (38 $ksi\sqrt{in.}$). Extension of the crack during cycling was approximately 0.25 cm (0.1 in.). Crack front curvature was significantly less than the minimum of 90% of average crack length specified by ASTM E-399-74; typical values were 96 to 98%.

Compliance measurements at 293 and 77K were obtained with a Martin Marietta built clip gage that permitted loadline displacement of approximately 1.2 cm (0.5 in.) to be measured. Figure 2 shows the gage installed at the loadline on a specimen. At 4K, a commercial clip-gage designed to measure opening up to 0.5 cm (0.2 in.), was used.

Fracture testing was performed in a 448 kN (100 kip) testing machine. At 77K, a simple foam insulated container attached to the lower loading rod was used to provide environmental control. For evaluation at 4K, a more sophisticated cryostat was used. The system consists of an internal load frame fabricated from filament wound glass-epoxy rods, a titanium base plate, and a liquid nitrogen jacketed vacuum dewar.

Figure 3 shows a closeup view of the load train with a specimen installed. An overall view of the sealed cryostat installed in the testing machine is given in Figure 4. The cryostat is equipped with level sensors so that economical use of liquid helium can be assured. The system is precooled with liquid nitrogen; following cooling, the liquid nitrogen is removed from the system by pressurizing the cryostat. Care is taken to ensure that all liquid nitrogen is removed from the system, because of the deleterious effect on helium resulting from residual liquid nitrogen. Typical liquid helium consumption for the system is approximately 40 liters per fill and test of moderate duration.

76
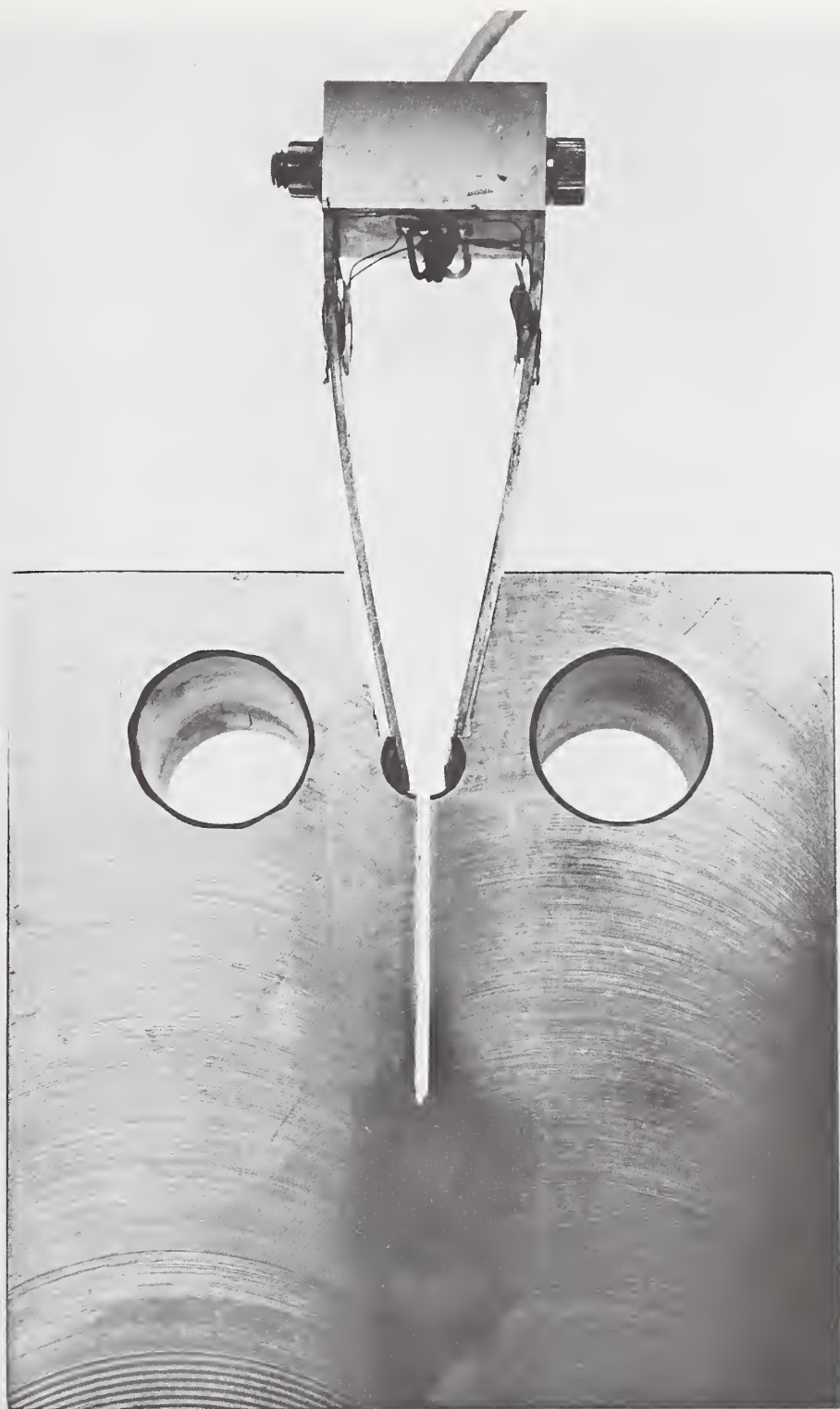
Figure 2   Clip Gage Installed at the Loadline
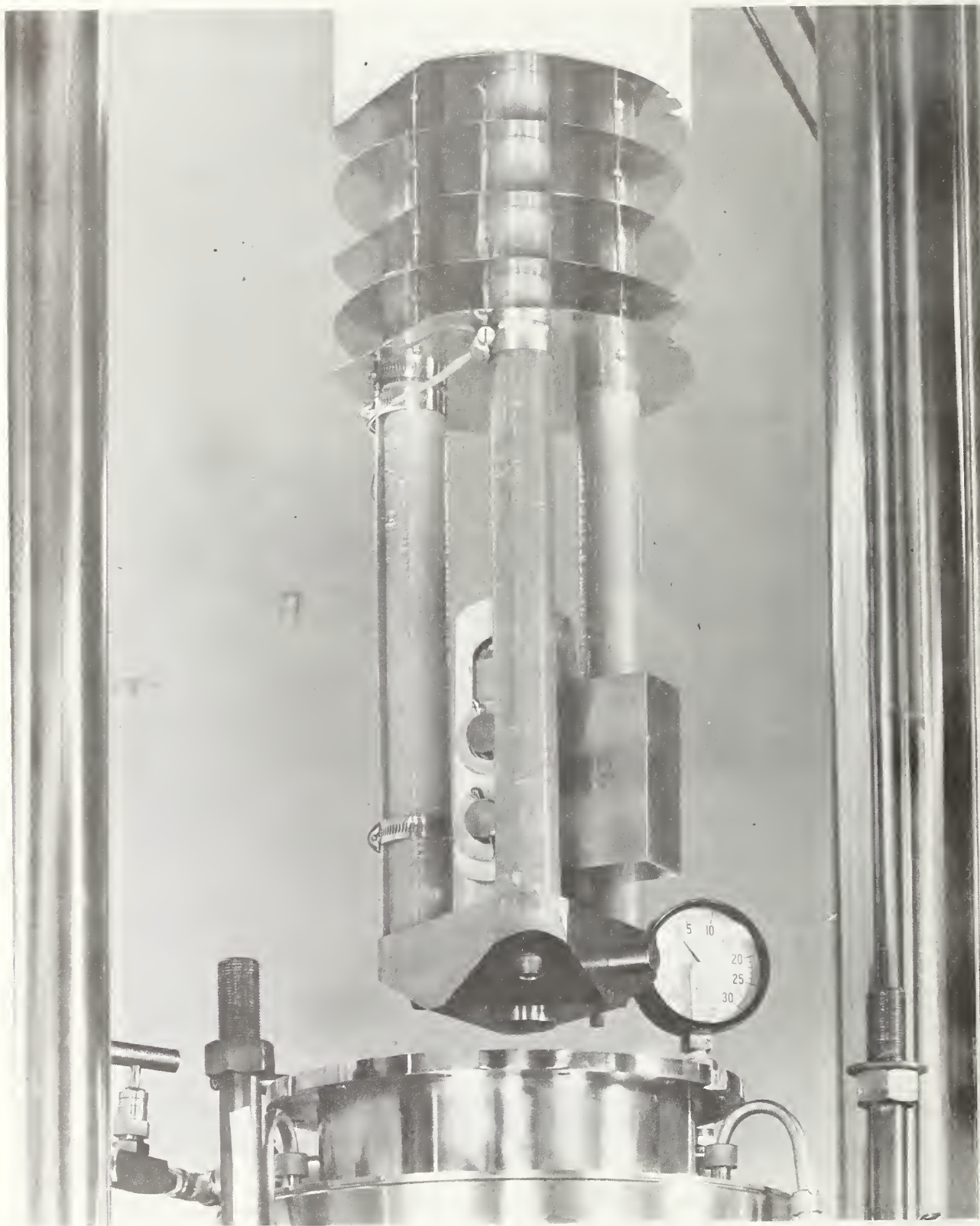
Figure 3   Close-Up View of Load Train for Liquid Helium Testing System
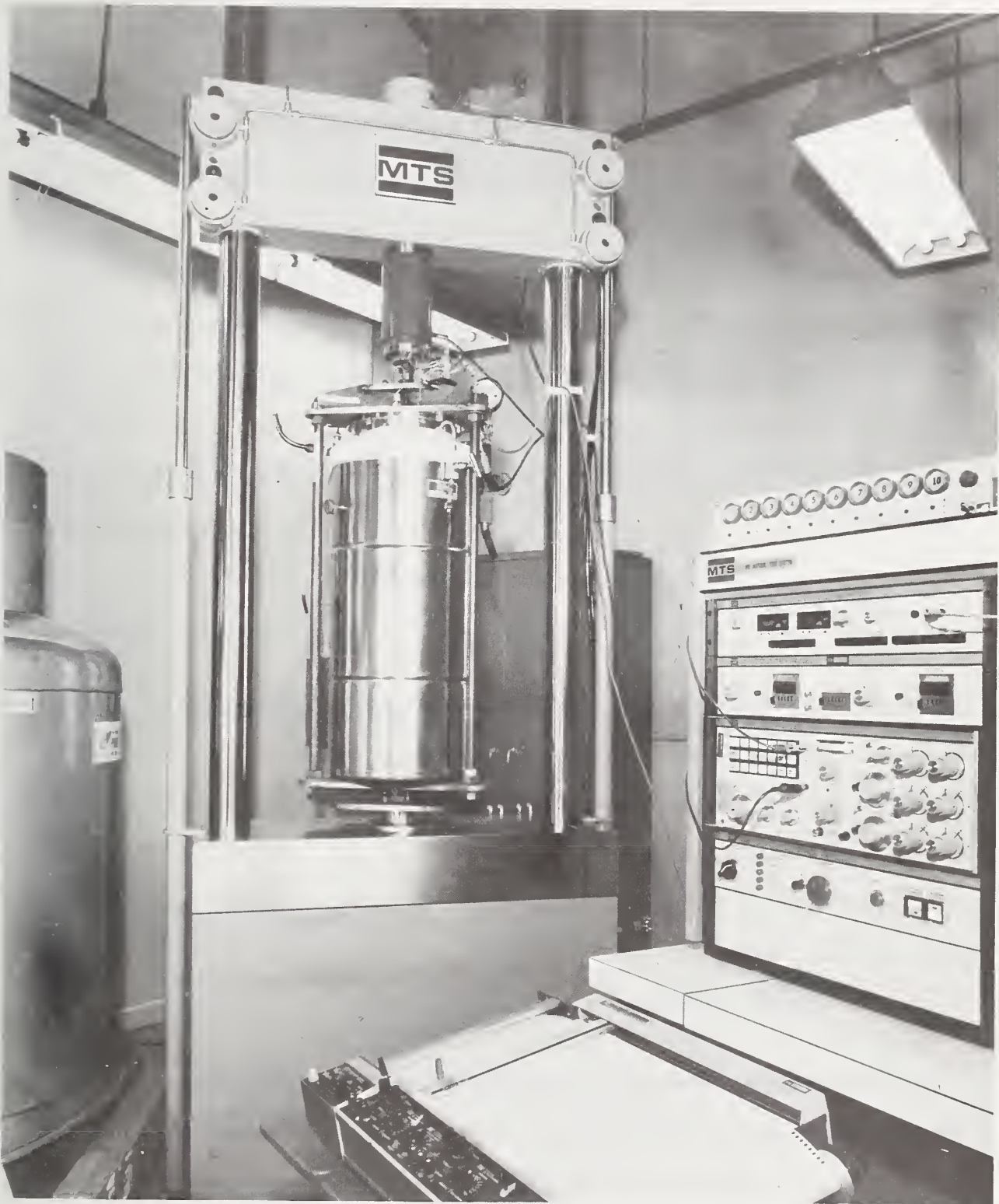
Figure 4   Overall View of Liquid Helium Testing System

Testing was performed in accordance with the ASTM recommended procedure for J_{Ic} determination, dated 3/1/77[3]. The initial specimen evaluated at each temperature was loaded to maximum load. Succeeding specimens were loaded to varying levels of displacement less than that found at maximum load.

After unloading, each specimen was heat tinted at approximately 800K and then fatigue extended before fracturing. Crack extension was measured at nine (9) points across the crack front to establish Δa, the amount of quasistatic crack-growth.

J was calculated from the load displacement record according to the following:

$$J = \alpha_1 \ \frac{2A}{Bb} \ + \ \alpha_2 \ \frac{2P\delta}{Bb}$$

where α_1 and α_2 are the Merkle-Corten coefficients (Reference 2) to account for the tension component of loading

A = area under the load vs displacement curve;

B = specimen thickness;

b = remaining ligament (W - a);

P = final load; and

δ = final displacement.

The J-Δa resistance curve was developed in accordance with the recommended procedure (Reference 3) with respect to establishment of the blunting line (J = 2 σ_y Δa), number of data points, and size requirements.

EXPERIMENTAL RESULTS

A total of thirteen (13) J integral tests were conducted. Four each were performed at 293 and 4K; five were conducted at 77K.

The load vs loadline deflection curves are reproduced on a single sheet for each test temperature and presented in Figures 5 through 7. A tabular presentation of the data is given in Table 1.

Evaluation of the test result validity, in accordance with the recommended guidelines, showed that the room temperature specimens were significantly below the thickness and ligament criteria required to establish validity. Tests conducted at 77 and 4K satisfy the thickness and ligament criteria.

Figures 8 and 9 present the J vs Δa data in the prescribed manner for determining J_{Ic}. Results were as follows:

Temperature, K	J_{Ic}, kN/m	(kip/in.)
77	280	(1.60)
4	86	(0.49)

DISCUSSION OF RESULTS

The results clearly show a decrease in fracture toughness of 21-6-9 stainless steel with decreasing temperature from 293 to 4K. At room temperature, the toughness, in terms of J-integral, would be at least 875 kN/m (5 kip/in.). In terms of K_{Ic} this would represent a value of approximately 500 MN/m$^{3/2}$ (450 ksi $\sqrt{in.}$). The J_{Ic} value at 77K is only 280 kN/m (1.6 kip/in.), or less than a third of the minimum toughness anticipated. Converting this value to K_{Ic} gives a toughness of
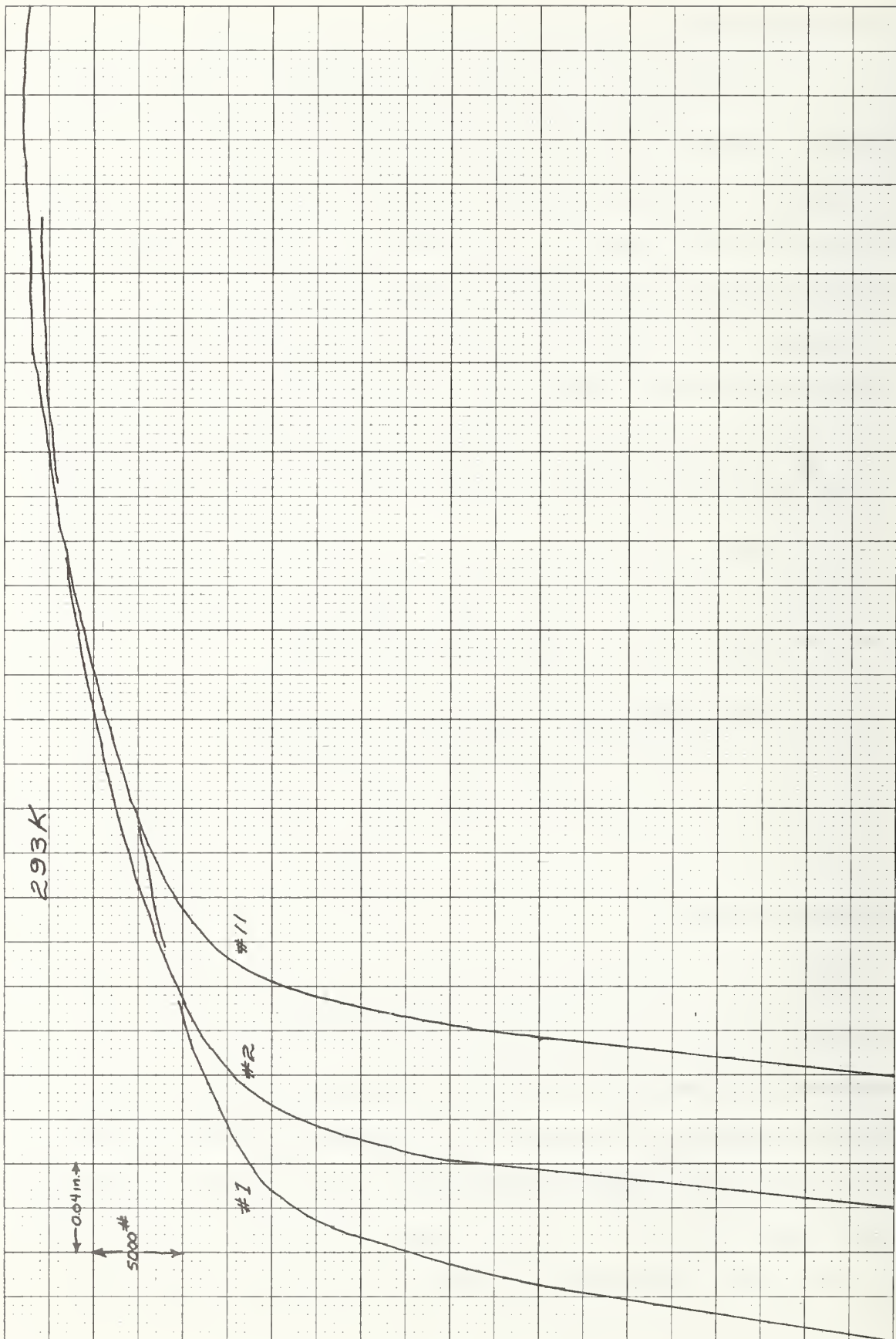
Figure 5 Load vs Loadline Deflection Data at 293 K
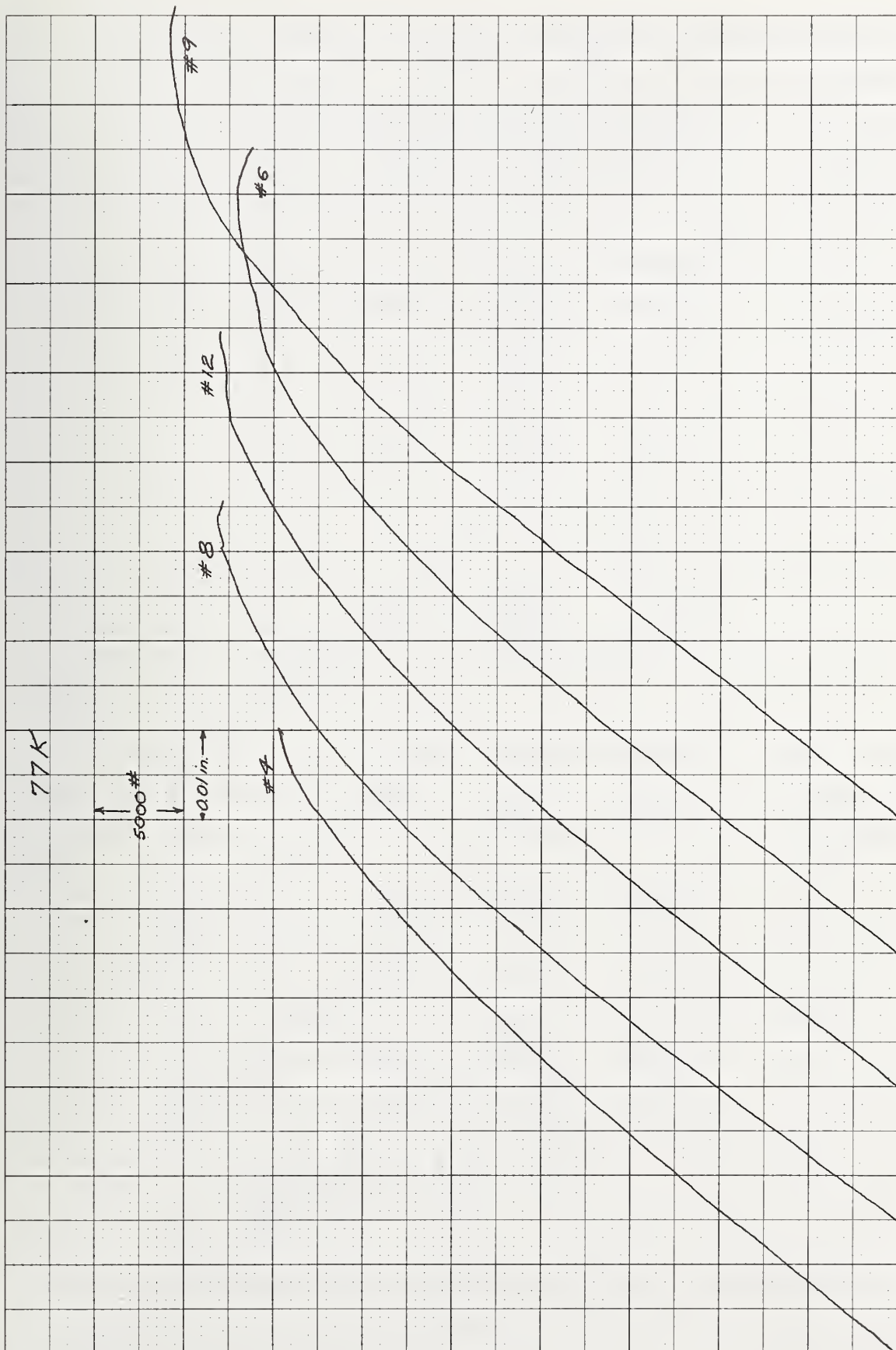
Figure 6 Load vs Loadline Deflection Data at 77 K
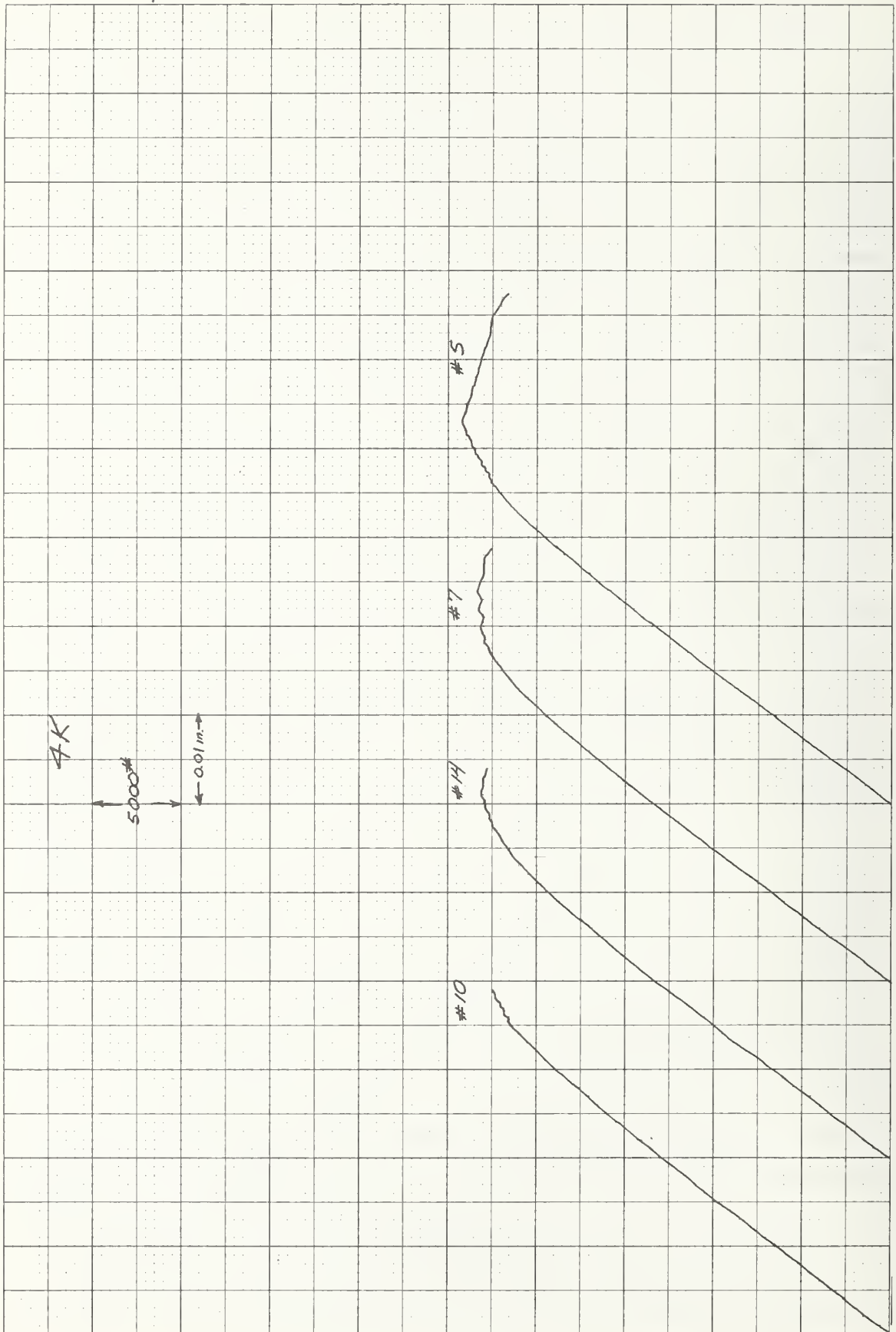
Figure 7 Load vs Loadline Deflection Data at 4 K

84

Table 1 J-Integral Test Results for 21-6-9 Stainless Steel

Specimen Number	$a,$[+] cm (in.)	$\Delta a,$ cm (in.)	$b,$ cm (in.)	Area, $A,$ cm-kN (in.-kip)	$P_f,$ kN (kips)	Deflection, $\delta,$ cm (in.)	$J,$ kN/m (kip/in.)
				293K			
1	4.65 (1.83)	0	—	31.4 (2.78)	94.3 (21.2)	0.380 (0.15)	—
2	4.62 (1.82)	0.170 (0.067)	2.82 (1.11)	108 (9.56)	107 (24.0)	1.14 (0.45)	2113 (12.1)
3	4.60 (1.81)	0.239 (0.094)	2.95 (1.16)	72.7 (6.44)	111 (25.0)	0.76 (0.30)	1343 (7.7)
11	4.65 (1.83)	0.091 (0.036)	2.74 (1.08)	124 (10.98)	108 (24.3)	1.27 (0.50)	2557 (14.6)
				77K			
4	4.75 (1.87)	0.053 (0.021)	2.82 (1.11)	15.6 (1.38)	154 (34.7)	0.178 (0.070)	335 (1.91)
6	4.72 (1.86)	0.221 (0.087)	2.67 (1.05)	24.6 (2.18)	162 (36.5)	0.229 (0.090)	515 (2.94)
8	4.62 (1.82)	0.114 (0.045)	2.87 (1.13)	21.2 (1.88)	168 (37.8)	0.203 (0.080)	439 (2.51)
9	4.70 (1.85)	0.196 (0.077)	2.72 (1.07)	26.9 (2.38)	187 (42.0)	0.234 (0.092)	526 (3.01)
12	4.70 (1.85)	0.112 (0.044)	2.82 (1.11)	22.5 (1.99)	169 (38.0)	0.213 (0.084)	438 (2.50)
				4K			
5	4.72 (1.86)	0.617 (0.242)	2.29 (0.90)	10.4 (0.92)	95.6 (21.5)	0.145 (0.057)	213 (1.22)
7	4.72 (1.86)	0.414 (0.163)	2.49 (0.98)	8.14 (0.72)	100 (22.5)	0.124 (0.049)	171 (0.98)
10	4.65 (1.83)	0.122 (0.048)	2.84 (1.12)	5.42 (0.48)	100 (22.5)	0.099 (0.039)	112 (0.64)
14	4.65 (1.83)	0.239 (0.094)	2.74 (1.08)	6.78 (0.60)	101 (22.6)	0.112 (0.044)	139 (0.79)

+ $a/w = 0.61 - 0.62$; $\alpha_1' = 1.02$; $\alpha_2 = 0.088$
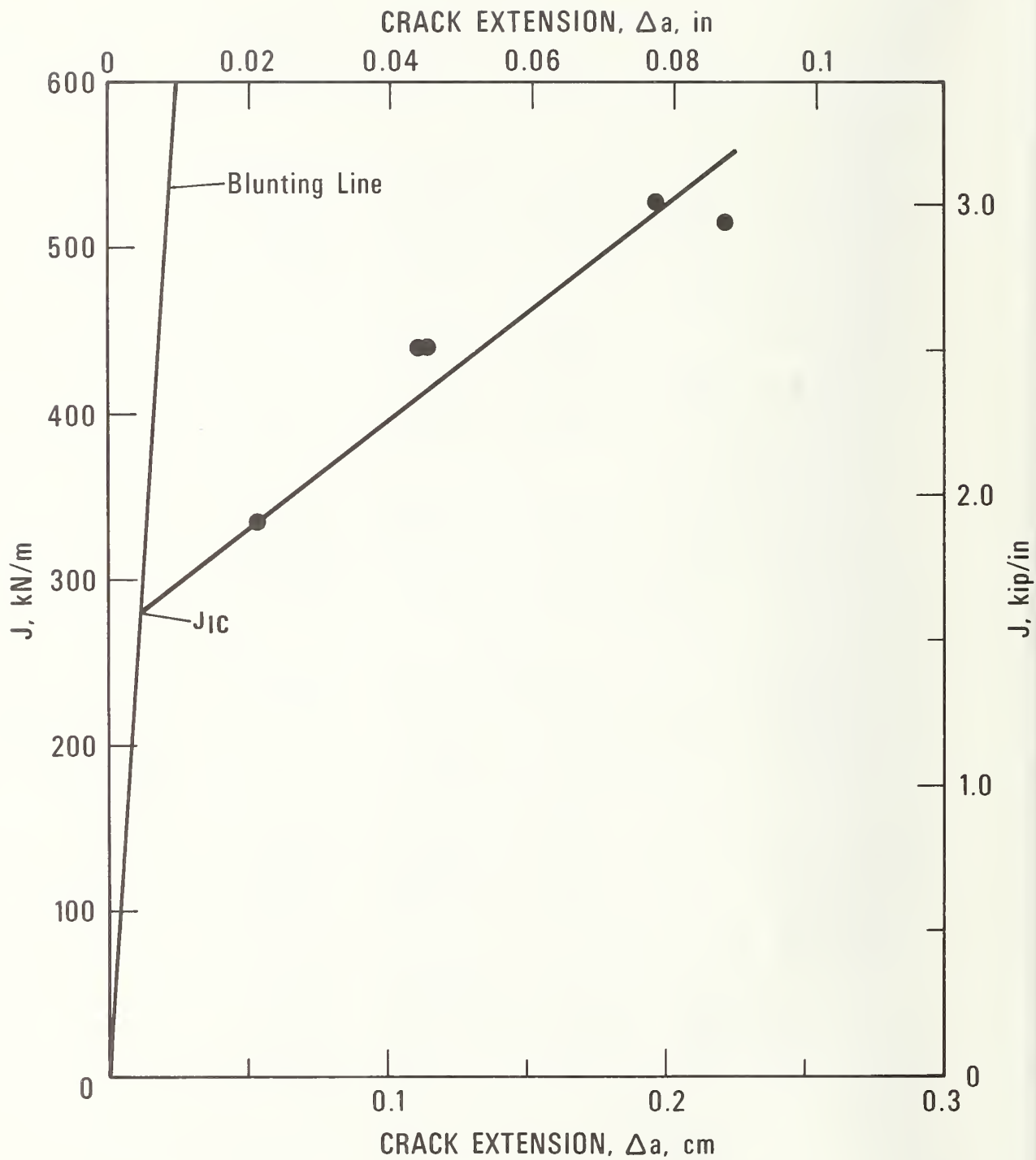
Figure 8   J-Integral Data at 77 K

CRACK EXTENSION, Δa, in

Blunting Line

J, kN/m

J, kip/in

J$_{IC}$

CRACK EXTENSION, Δa, cm
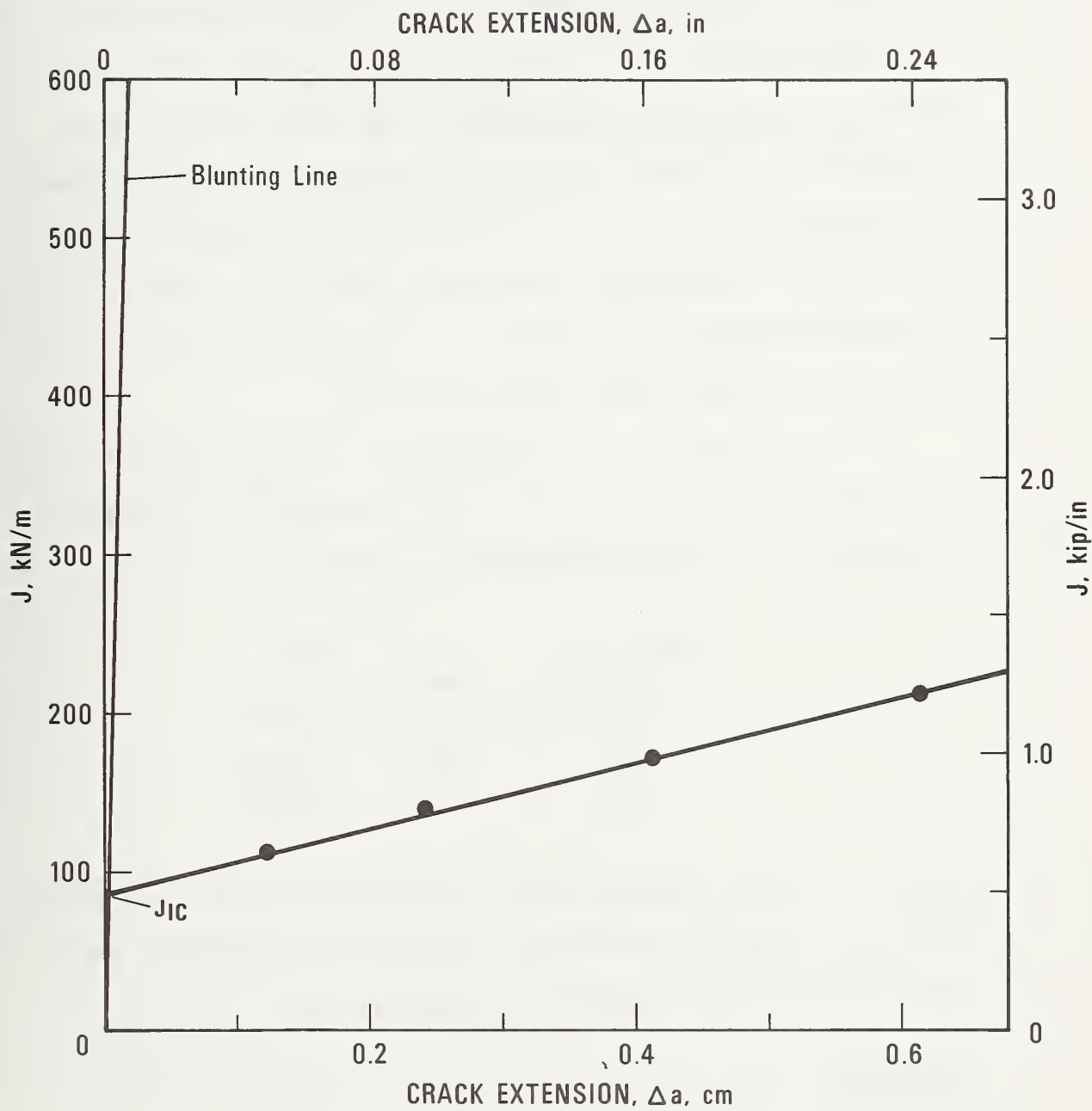
Figure 9   J-Integral Data at 4 K

approximately 280 MN/m^2 (255 ksi $\sqrt{\text{in.}}$), which is still a relatively high toughness value.

The 4K data show a further decrease in toughness to less than one-third of that found at 77K. The J_{Ic} value of 86 kN/m (490 lb/in.) represents a K_{Ic} level of approximately 150 MN/m^2 (140 ksi $\sqrt{\text{in.}}$). Although this is a small fraction of the extremely high room temperature toughness, this level nevertheless represents tough behavior. For example, a semicircular surface flaw defect in a component stressed to 690 MN/m^2 (100 ksi) would have to be approximately 3 cm (1.2 in.) deep to cause failure under these conditions.

The data obtained in this program are in general agreement with the results previously reported by Tobler and Reed[1]. A comparison of results of the two investigations is given below:

Temperature, K	J_{Ic}, kN/m	
	MMC	NBS
293	>875	~1400
77	280	310-350
4	86	~150

Ignoring the room temperature data, for which the results are invalid and merely estimates of level, we find that the 77K data are quite close. The 4K results are of similar relative magnitude.

REFERENCES

1. R. L. Tobler and R. P. Reed: "Tensile and Fracture Behavior of a Nitrogen-Strengthened, Chromium-Nickel-Manganese Stainless Steel at Cryogenic Temperatures," Materials Research for Superconducting

1. (continued) - Machinery, Semiannual Technical Report IV, October 1975, National Bureau of Standards, Boulder, Colorado.

2. ASTM Standards, E399-74, Part 10, American Society for Testing and Materials, Philadelphia, PA, 1974.

3. Recommended Procedure for J_{Ic} Determination, ASTM Committee E24-01-09, March 1, 1977.

Toughness, Fatigue Crack Growth, and Tensile Properties
of Three Nitrogen-Strengthened Stainless Steels
at Cryogenic Temperatures

National Bureau of Standards

TOUGHNESS, FATIGUE CRACK GROWTH, AND TENSILE PROPERTIES OF THREE
NITROGEN-STRENGTHENED STAINLESS STEELS AT CRYOGENIC TEMPERATURES*

D. T. Read and R. P. Reed

Cryogenics Division
Institute for Basic Standards
National Bureau of Standards
Boulder, Colorado   80302

ABSTRACT

Fracture toughness, fatigue crack growth rate, and tensile property data for three nitrogen-strengthened stainless steels at 295, 76, and 4 K have been obtained. These materials were tested to determine their acceptability as candidate structural materials for cryogenic service. The materials tested were Fe-18Cr-3Ni-13Mn (Nitronic 33)*, Fe-21Cr-12Ni-5Mn (Nitronic 50), and Fe-19Cr-9Ni-2Mn (304N). The nitrogen-strengthened alloy Fe-21Cr-6Ni-9Mn (Nitronic 40) has been tested previously in our laboratory.

Toughness measurements employed J-integral, plane strain critical stress intensity, and crack-opening-displacement tests. It was found that the nitrogen-strengthened austenitic stainless steels generally exhibit lower toughness at 4 K than the widely used 300-series stainless steels AISI 304, AISI 310, and AISI 316. Of the nitrogen-strengthened steels tested to date, Fe-18Cr-3Ni-13Mn is the strongest and least tough, and Fe-19Cr-9Ni-2Mn is the toughnest with lowest strength. Fatigue crack growth rates at 4 K in the nitrogen-strengthened stainless steels were found to be generally higher than or comparable to rates for previously tested stainless steels. Fe-18Cr-3Ni-13Mn had rates significantly above previously tested materials, especially at high stress intensity range levels. Crack growth rates for Fe-19Cr-9Ni-2Mn for an austenitic stainless steel at 4 K and the rates for Fe-21Cr-12Ni-5Mn fell approximately in the mid-range of previous data.

All studied materials exhibited high strengths at cryogenic temperatures. After being strained to failure at 4 and 76 K, Fe-18Cr-3Ni-13Mn and Fe-19Cr-9Ni-2Mn exhibited some ferromagnetism, indicating that body-centered-cubic strain-induced martensitic transformations had occurred during straining; Fe-21Cr-12Ni-5Mn exhibited no ferromagnetism within experimental uncertainty.

---

*Use of trade names is for clarity only, and does not imply acceptance or endorsement of a particular material by NBS.

INTRODUCTION

Nitrogen-strengthened austenitic stainless steels have attracted interest as possible cryogenic structural materials because of their superior strength;[1-4] but data on their toughness at cryogenic temperatures is generally lacking, except for a few studies.[5,6] The availability of high-strength, high-toughness alloys for cryogenic service would contribute to increased structural safety, and economy in structural material bulk in devices such as magnetic-fusion-energy systems.[7] Cost savings allowed by reduced nickel content without loss of low temperature toughness or austenite stability also would be welcome. Therefore fracture toughness, fatigue crack growth rate, and tensile property data for three nitrogen-strengthened stainless steels have been obtained at 4, 76, and 295 K to determine their acceptability as candidate structural materials for cryogenic service. The specific goal of the test program reported here was to obtain 4 K mechanical property behavior of the three tested alloys for comparison to the previously tested alloy Fe-21Cr-6Ni-9Mn.[5]

MATERIALS

Two of the alloys tested are sold under the trade names Nitronic 33 and Nitronic 50. The third is usually sold as stainless steel AISI 304N. The alloys will be denoted in the text by approximate weight percent of iron, chromium, nickel, and manganese, their major constituents, as follows*:

Nitronic 33	Fe-18Cr-3Ni-13Mn
Nitronic 50	Fe-21Cr-12Ni-5Mn
AISI 304N	Fe-19Cr-9Ni-2Mn
Nitronic 40	Fe-21Cr-6Ni-9Mn

---

*Use of trade names is for clarity only, and does not imply acceptance or endorsement of a particular material by NBS.

The chemical compositions of the nitrogen-strengthened steels used in the present study as supplied by the manufacturers are listed in Table 1. Also included in Table 1 for reference is the chemical composition of another nitrogen-strengthened alloy, Fe-21Cr-6Ni-9Mn. Fracture and tensile data for that material have been reported separately,[5] but are repeated here where appropriate for comparison with present results. These alloys have no familiar designations except trade names, and so will be denoted in the text by the approximate weight percent of their major constituents: iron, chromium, nickel, and manganese. Approximate major constituent content, ASTM designation, relevant ASTM specifications, and trade names are listed in Table 2. Fe-18Cr-3Ni-13Cr was obtained as a 2.5 cm thick plate, Fe-21Cr-12Ni-5Mn as a 5 cm thick plate, and Fe-19Cr-9Ni-2Mn as a short section of extruded tube about 1 m in diameter by 5 cm wall thickness. Each material was tested as received, in a commercially-annealed condition. A portion of one of the materials, Fe-21Cr-12Ni-5Mn, was given an additional heat treatment, a 1.5 hr anneal in an 1177°C furnace followed by a water quench. This material is designated Fe-21Cr-12Ni-5Mn-X below. Final heat treatments, grain sizes and hardnesses of the materials are listed in Table 3, and representative microstructures are given in Figs. 1-4. It can be seen that the additional heat treatment applied to the Fe-21Cr-12Ni-5Mn-X alloy brought its grain size and microstructural appearance close to those of the other alloys.

SPECIMENS

Fracture toughness and fatigue crack growth data were obtained using compact specimens of the shape shown in Fig. 5a in the TL orientation. Specimens of Fe-18Cr-3Ni-13Mn were 2.5 cm thick; all others were 3.8 cm thick. Tensile property data were obtained using the miniature

96

round tensile specimen geometry shown in Fig. 5b, oriented transverse to the rolling direction. The orientation of fracture toughness and tensile specimens relative to the original plates is shown in Fig. 5c. The rolling direction of the large tube section was considered to be the direction of the tube axis, and the transverse direction the circumferential direction.

TECHNIQUES

Toughness data were obtained using J-integral techniques[8] for all materials at 295 and 76 K and for Fe-19Cr-9Ni-2Mn at 4 K. A conventional critical stress intensity measurement technique (the K_{Ic} test[9]) was used for the other materials at 4 K. In the J-integral technique several specimens are precracked in tension-tension fatigue approximately to a predetermined crack length. Each specimen is then loaded quasistatically (load line displacement 50 microns/sec or less) under displacement control until crack extension is produced. Load is recorded graphically as a function of load-line displacement during the test. After unloading, the specimens are heat-tinted to mark the crack extension Δa on the fracture surface. The specimen is then broken in two and the crack extension is measured. Reduction of the data consists of analyzing each test record to determine the area under the load versus load-line-displacement curve and its complement, calculating the J-integral value, plotting the several J-Δa data, and determining the critical J value J_{Ic}. The approximation often used in previous studies[8] to calculate the J-integral value from the test data is:

$$J = \frac{2A}{Bb} \tag{1}$$

where A is the area under the load-displacement curve, B is specimen thickness, W is the width of the specimen from load line to face side, a is crack depth after precracking measured from the load line, and b = W-a. A more elaborate formulation was given by Merkle and Corten[10]

$$J = \frac{1}{Bb} \left[\eta A + \eta_c A_c \right] \qquad (2)$$

where A_c is the complement of the area A, η is a numerical factor of about 2.2 which depends on the value of a/W, η_c is a similar numerical factor of about .1, and the other symbols have the same meanings as before. Values of η and η_c calculated by Merkle and Corten[10] are listed in Table 4. This procedure has been recommended by the steering committee of the ASTM E24-01-09 task group on elastic-plastic fracture.[11] It results in J values slightly higher than those obtained using Eq. (1) and is considered to be more accurate. The critical value of J is its value at the intersection of the J-Δa curve with the line given by

$$J = 2\Delta a \bar{\sigma} \qquad (3)$$

where $\bar{\sigma}$ is the flow strength, taken as the average of the yield and ultimate strengths. This graphical procedure is illustrated in Fig. 6 for Fe-18Cr-3Ni-13Mn at 76 K. The critical stress intensity factor K_{Ic} is inferred from the critical J-integral value using the equation:[12]

$$K_{Ic} = \sqrt{\frac{E J_{Ic}}{1 - \nu^2}} \qquad (4)$$

where E is Young's modulus and ν is Poisson's ratio for the material tested. Values of E, ν, and E' = $E/(1-\nu^2)$ used[13,14] are listed in Table 5.

The load-displacement records were also analyzed to obtain crack-opening-displacement (COD) data. The COD value δ for a given value of load line displacement V is inferred using:[15]

$$\delta = \frac{.45(W - a)}{.45W + .55a} \left[V - \frac{\gamma\sigma_y W}{E} \right], \quad V \geq \frac{2\gamma\sigma_y W}{E'} \qquad (5a)$$

$$\delta = \frac{.45(W - a)}{.45W + .55a} \frac{V^2 E'}{4\gamma\sigma_y W}, \quad V < \frac{2\gamma\sigma_y W}{E'} \qquad (5b)$$

where σ_y is the yield strength, and γ is a numerical factor depending on a/W, approximately 2.5 for the a/W values obtained here, and $E' = E/(1-\nu^2)$. Values of γ given by Wells[15] are listed in Table 4. COD is extensively used by the British in elastic-plastic fracture mechanics and in fact a Draft British Standard exists for design using COD. The fracture resistance of a material is characterized by its critical COD value. British practice is to choose the critical value at maximum load or at "pop-in", a peak in the load-displacement curve followed by a drop and subsequent rise in load which signifies a sudden but small crack extension. Note that the critical point on a test record analyzed for critical COD need not coincide with the critical point determined in a J_{Ic} test.

Conventional K_{Ic} tests are performed by precracking compact specimens, then loading them until fracture. A procedure detailed in ASTM standard test method E 399 is used to determine a candidate K_{Ic} value and to determine whether a successful measurement of K_{Ic} has been achieved.

Fatigue crack growth rates were also measured using compact specimens. The specimen is loaded repeatedly (at a frequency of 20 Hz in this test program) and the compliance, that is, the reciprocal slope of a plot of load against load-line-displacement, is recorded periodically, at intervals

ranging from 100 to 20,000 cycles depending on the rate of crack growth. The compliance data are converted to crack lengths using the formula[16]

$$a = W[-.9505 + .3447(EBC)^{1/6} + .5654(EBC)^{1/3} - .1748(EBC)^{1/2}] \quad (6)$$

where C = displacement/load and E and B have been previously defined. From these, crack growth rates are easily obtained. The crack length is also used in calculating the applied stress intensity factor range using the formula[9]

$$\Delta K = (P_{max} - P_{min})\frac{a^{1/2}}{BW} [29.6 - 185.5(\tfrac{a}{W}) + 655.7(\tfrac{a}{W})^2 - 1017(\tfrac{a}{W})^3 + 638.9(\tfrac{a}{W})^4] \quad (7)$$

where P_{max} and P_{min} are the maximum and minimum loads. The end product of the analysis is a plot of crack growth rate, da/dN, against stress intensity factor range.

Conventional tensile testing techniques were used to obtain tensile property data. Yield strength values at 0.2% offset are reported. The flow strength is taken as the average of the yield and ultimate strengths. After tensile testing, specimens of each material and test temperature were checked for ferromagnetism, and thus for bcc martensite content, with a bar-magnet, torsion-balance apparatus.[17]

For all tests, temperature control was achieved by immersing the specimen in liquid helium or liquid nitrogen at local atmospheric pressure* or by testing in laboratory air.

RESULTS

The J-Δa, J_{Ic}, and K_{Ic} values obtained are listed in Tables 6-9. Toughness values are listed in Table 10 and plotted against temperature in Fig. 7. From this figure it can be seen that the toughnesses of all materials

---

*Typically 620 mm Hg. At this pressure, helium boils at 4 K and nitrogen at 76 K.

decrease with decreasing temperature, as expected. The 4 K toughness of two of the tested materials, Fe-18Cr-3Ni-13Mn and Fe-21Cr-12Ni-5Mn (commercial heat treatment) were found to be definitely lower than the value previously obtained for Fe-21Cr-6Ni-9Mn. Fe-19Cr-9Ni-2Mn was found to have a higher toughness than Fe-21Cr-6Ni-9Mn, and Fe-21Cr-12Ni-5Mn-X (special heat treatment) was found to have a toughness value approximately equal (within a rather large experimental uncertainty) to that of Fe-21Cr-6Ni-9Mn. The large uncertainty reported for the Fe-21Cr-12Ni-5Mn-X alloy is due to the large difference between the toughness values obtained for the two specimens tested, the significant deviation of one of those from the requirements of ASTM Method E 399, and the fact that the heat treatment was applied in a small laboratory furnace to machined specimens rather than plate stock. Measured critical COD values are given in Table 11.

Fatigue crack growth data obtained are plotted in Figs. 8-10. Such data is commonly represented by a Paris law of the form:

$$\frac{da}{dN} = C(\Delta K)^n \tag{8}$$

Best fit (by least squares) Paris law lines are shown on the logarithmic fatigue-data plots. The parameters of these best-fit lines are given in Table 12. The fatigue crack growth rate for Fe-18Cr-3Ni-13Mn increased strongly with decreasing temperature, and at 4 K was significantly higher than any of the other materials tested and also higher than any other austenitic stainless steel previously tested in this laboratory. Fe-19Cr-9Ni-2Mn had the second highest fatigue crack growth rate at 4 K, with values about the same as the highest observed for austenitic stainless steels previously tested in this laboratory. Fe-21Cr-12Ni-5Mn had the lowest 4 K fatigue crack growth rates of the three measured, in the mid-range of pre-

viously observed values. The fatigue crack growth rate for Fe-21Cr-12Ni-5Mn-X was not measured.

Tensile data obtained are plotted in Figs. 11 and 12 and listed in Table 13. Figure 11 shows that the strong increases of yield and ultimate strengths expected for these nitrogen-strengthened materials were indeed obtained. The order of yield strength values correlated inversely with toughness, for each material as temperature was varied and among materials at 4 K. The Fe-18Cr-3Ni-13Mn had the highest strength, Fe-21Cr-12Ni-5Mn (commercial anneal) was next, followed by this same alloy with the special anneal at a value slightly higher than that observed previously for Fe-21Cr-6Ni-9Mn. Fe-19Cr-9Ni-2Mn had the lowest 4 K yield strength of the materials tested.

Results of the magnetic measurements on fractured tensile specimens are listed in Table 14. Fe-19Cr-9Ni-2Mn fractured in tension at 76 K was most magnetic (approximately 100% ferromagnetic martensite); the specimen of this alloy fractured at 4 K was somewhat less ferromagnetic. The Fe-18Cr-3Ni-13Mn alloy specimens fractured at 76 and 4 K were also slightly magnetic. However Fe-21Cr-12Ni-5Mn specimens in commercial and special heat treatments fractured at 4 K and commercially treated material fractured at 76 K were not ferromagnetic within experimental uncertainty.

Photomicrographs of the fracture surfaces of the toughness specimens tested at 4 K taken using scanning electron microscopy, Figs. 22a-d, revealed differences in surface morphology among the specimen materials. None appeared fully ductile, rather, relatively flat, brittle-appearing areas were always present. Areas of apparent microvoid coalescence were present to a significant degree in the Fe-19Cr-9Ni-2Mn specimen, to a lesser degree in the Fe-21Cr-12Ni-5Mn-X and even less in the Fe-21Cr-12Ni-5Mn and Fe-18Cr-3Ni-13Mn. The Fe-21Cr-12Ni-5Mn in its commercial heat

treatment contained noticeably more intergranular fracture than did the same material in the special heat treatment.

Tensile specimens fractured at 4 K were sectioned, and examined using optical microscopy. All 4 K specimens showed dark bands apparently along $\{111\}$ planes. These are interpreted as due to the stress-induced martensite ε' (hcp) and are illustrated in Fig. 23a for the case of Fe-18Cr-3Ni-13Mn. The Fe-19Cr-9Ni-2Mn revealed, in addition, very small lath-shaped martensitic phases associated with the α' (bcc) ferromagnetic phase. The general appearance of these laths was the same as previously observed for other stainless steels of approximate composition Fe-18Cr-8Ni. No differences were found between Fe-19Cr-9Ni-2Mn specimens fractured at 76 and at 4 K.

Experimental Uncertainties

Uncertainties in toughness data are of three kinds: first, those associated with the quantities directly measured, such as load, crack length, displacement, and so on; second, those associated with the procedure used to infer toughness values from the measured quantities; and third, those which arise from specimen to specimen and heat to heat material variability. Errors of measurement are readily assessed by repeated measurement, measurement of standard loads or dimensions, calibration, and so on. Errors associated with inferring a toughness value can be formally eliminated by adoption of a standard practice. But questions about the applicability of a value determined according to a standard practice may persist. Errors associated with variability are the most severe. Evaluation of material properties for structural design requires careful consideration of uncertainties due to material variability, through understanding of its causes and extensive data on its magnitude.

Detailed assessment of uncertainties associated with inferring toughness from measured quantities and with material variability are beyond the scope of this paper. Briefly, where comparisons have been made, values of toughness inferred using Eq. 4 have usually been found less than or approximately the same as those measured by the standard method (ASTM E 399). Values of critical COD determined using Eqs. 5 can be considered to be correct by definition, because while the meaning of the actual crack-opening-displacement is not well-defined, in practice, values obtained using these equations are commonly taken as correct. Measurements of plane strain critical stress intensity K_{Ic} conducted according to ASTM E 399 are considered correct by definition. Measurements reported here as not in strict compliance with E 399 are considered to be of value comparable to those with no deviations, because the deviations from compliance were generally considered minor.

Measurement uncertainties in individual J values are considered to be of the order of 5% or less, from accumulated uncertainties in load cell and displacement gauge calibrations and measurements of the area under the load-displacement record. Uncertainties in crack extension measurements are larger, on the order of ten percent at large values and up to .05 mm at low values due to difficulty in locating exactly the boundaries of the region of crack extension on the fractured specimens. The cumulative uncertainty in J_{Ic} values is estimated to be 10% or less, so the measurement uncertainty in K_{Ic} values inferred using Eq. 4 is 5% or less. Errors in fracture toughness associated with material variability are generally larger than this, and often much larger. Therefore, data reported here are in general not applicable to materials with different chemical composition or thermomechanical processing.

Uncertainties associated with inferring property values from measured quantities are not a problem in fatigue and tensile property measurements, because standard test procedures are widely accepted. However uncertainties

of measurement and material variability remian. The scatter visible in the fatigue crack growth rate data presented in Figs. 8-10 is indicative of the measurement uncertainties involved. Standard deviations of 20 to 40% from the average value were typical. Fatigue data is not considered to be as sensitive to material variability as toughness data, and in fact each data set in Figs. 8-10 consists of points from two or three specimens, and all sets appear consistent. However, heat to heat variations may be larger.

Measurement uncertainties in tensile properties are estimated to be 3 % or less; these are due to uncertainties in specimen dimensions, load values as read from analog recorder traces, and (for the yield strength) specimen strains from the calibrated extensometer.

The uncertainties discussed here for fracture toughness, fatigue crack growth, and tensile properties are considered usual for such measurements. The fact that many tests were conducted at cryogenic temperatures did not contribute significantly to the experimental uncertainties.

DISCUSSION

An indication of the effectiveness of nitrogen-strengthening is given in Fig. 13, which shows the yield strengths of AISI 304[18] and AISI 304N as a function of temperature. A nitrogen content of 0.12 wt % is seen to increase the 4 K yield strength by approximately a factor of two, with lesser effects at higher temperatures.

Only a small amount of previous data on the nitrogen-strengthened austenitic stainless steels used in the present study is available. Montano[2] reported the tensile properties of Fe-18Cr-3Ni-13Mn between room and liquid hydrogen temperatures. Figures 14 and 15 allow comparison of his results to those of the present study. Agreement of strength properties is good. Agreement of the elongation is poor. A possible reason for the

105

discrepancies is the difference in the specimen geometries used in the two studies; Montano used a flat specimen with a ratio of width to thickness of about 6 to 1. Spaeder and Domis[3] have reported tensile properties of Fe-19Cr-9Ni-2Mn. Figures 16 and 17 allow comparison of their results to those of the present study. Again, agreement among the strength property values is good. The elongation and reduction of area data agree at 77 K but differ somewhat at room temperature. The reason for the disagreement is unknown.

Figure 18 shows for comparison three sets of toughness results for Fe-21Cr-12Ni-5Mn: results of the present study for commercially-annealed and specially annealed materials, and previous results by Dessau.[6] A significant increase in 4 K toughness due to higher annealing temperature is apparent in this figure. This increase is believed to be due to dissolution of precipitates and enhancement of grain size promoted by higher annealing temperature, because large brittle precipitates at grain boundaries are associated with intergranular fracture at low stress intensity values and small grain sizes raise the yield strength, decreasing crack tip plasticity. The influence of higher-temperature annealing on microstructure can be seen clearly in Figs. 2 and 4 and the grain-size data of Table 3.

4 K toughness data presented in Fig. 19 allow comparison between nitrogen-strengthened and conventional stainless steels. As a group, the nitrogen-strengthened steels are stronger but less tough than the conventional alloys. Fracture toughness data is used in design to guide material selection for prevention of brittle failure. For a material of a given toughness, resistance to brittle behavior depends on section thickness stress concentrations. Large thicknesses and large stress concentrations promote brittle behavior. No exact calculation of the

maximum safe section thickness is available at present. A simple approximation is that section thicknesses greater than t, where

$$t = \left(\frac{K_{Ic}}{\sigma_y} \right)^2 \qquad (9)$$

may be susceptible to brittle fracture. This relation may be used to determine approximately the fracture toughness necessary to prevent brittle failure in a material of given thickness and yield strength. In Fig. 19, lines relating fracture toughness and yield strength according to Eq. 9 for various values of section thickness t are shown. A material for which the yield-strength, fracture toughness point lies above the line given by Eq. 9 with the chosen section thickness should be used. Figure 19 thus may be used to determine which materials should be considered for use in sections of various thicknesses.

Figure 20 shows 4 K fatigue crack growth rate data for three nitrogen-strengthened stainless steels and a band which includes all 4 K crack growth rate data obtained to date in our laboratory for conventional stainless steels. 4 K fatigue crack growth rates for the nitrogen-strengthened stainless steels tend to be higher than for conventional stainless steels, although Fe-21Cr-12Ni-5Mn is an exception, its rates falling below the center of the band which includes the conventional austenitic steels.

Crack-opening-displacements (COD) values are usually related to J-integral values by an equation of the form[15]

$$J = m\sigma_y \delta \qquad (10)$$

where δ is the crack opening displacement, σ_y is the material yield strength, and m is a numerical factor with a value between 1 and 2.5 which varies with

107

material, temperature, and other factors. Equation (10) was tested using each set of J-integral data obtained by plotting the J values against COD values obtained from the same test records for each material and temperature. A typical example of these plots is shown in Fig. 21. From these plots it appeared that the data fit the generally accepted linear relationship between J-integral and COD values although some scatter was usually found. Values of the factor m obtained in the present study ranged from 1.42 to 2.12; no systematic dependence of m on any other measured parameters was discovered.

Note that even given the value of m, critical values of COD δ_c cannot generally be obtained from Eq. (9) and the critical value J_{Ic} because the critical point for COD measurement is defined differently from the critical point for J_{Ic} measurement. The critical COD value occurs at maximum load or pop-in,[20] while the critical J-integral value occurs at crack extension Δa equal to $J/2\bar{\sigma}$. Thus, care must be exercised in converting J-integral results to COD values.

SUMMARY AND CONCLUSIONS

1. Fracture toughness, fatigue crack growth and tensile property data at 4, 76, and 295 K for nitrogen-strengthened austenitic stainless steels Fe-12Cr-3Ni-9Mn, Fe-21Cr-12Ni-5Mn, and Fe-19Cr-9Ni-2Mn have been obtained and compared with previous data for another nitrogen-strengthened stainless steel, Fe-21Cr-6Ni-9Mn.

2. Nitrogen-strengthened Fe-19Cr-9Ni-2Mn is tougher at 4 K than nitrogen strengthened Fe-21Cr-6Ni-9Mn alloy. Nitrogen-strengthened Fe-18Cr-3Ni-13Mn and Fe-21Cr-12Ni-5Mn, both in the commercially-annealed condition are less tough at 4 K than Fe-21Cr-6Ni-9Mn. Fe-21Cr-12Ni-5Mn with an additional heat treatment has approximately the same toughness as Fe-21Cr-6Ni-9Mn, within a rather large experimental uncertainty.

3. The 4 K fatigue crack growth resistance ranking of these alloys, in descending order of resistance, is Fe-21Cr-12Ni-5Mn, Fe-19Cr-9Ni-2Mn, Fe-18Cr-3Ni-13Mn. Fe-21Cr-6Ni-9Mn ranks between Fe-21Cr-12Ni-5Mn and Fe-19Cr-9Ni-2Mn.

4. The 4 K strength ranking of these alloys is inverse to their toughness ranking. The order of decreasing strength is: Fe-18Cr-3Ni-13Mn, Fe-21Cr-12Ni-5Mn (commercial anneal), Fe-21Cr-12Ni-5Mn (special anneal) and Fe-19Cr-9Ni-2Mn. Previously tested Fe-21Cr-6Ni-9Mn has slightly lower 4 K yield strength than Fe-21Cr-12Ni-5Mn with the special heat treatment.

REFERENCES

1. D. C. Larbalestier and D. Evans, "High Strength Austenitic Stainless
    Steels for Cryogenic Use," Sixth International Cryogenic Engineering
    Conference, Grenoble, France, 1976, p. 345-347. IPC Science and
    Technology Press Ltd., Surrey.

2. J. W. Montano, "Stress Corrosion Resistance and Cryogenic Temperature
    Mechanical Behavior of 18-3Mn (Nitronic 33) Stainless Steel Parent and
    Welded Material," NASA TM X-73309, Marshall Space Flight Center, Alabama.

3. C. E. Spaeder, Jr., and W. F. Domis, "Cryogenic and Elevated-Temperature
    Mechanical Properties of a High-Nitrogen Type 304 Stainless Steel," Report
    No. 44012-062-2, United States Steel Corporation, Pittsburgh.

4. R. B. Gunia and G. R. Woodrow, "Nitrogen Improves Engineering Proper-
    ties of Chromium-Nickel Stainless Steels," Journal of Materials, JMLSA,
    Vol. 5, No. 2, June 1970, p. 413-430.

5. R. L. Tobler and R. P. Reed, "Tensile and Fracture Behavior of a
    Nitrogen-Strengthened, Chromium-Nickel-Manganese Stainless Steel at
    Cryogenic Temperatures," Symposium on Elastic-Plastic Fracture,
    American Society for Testing and Materials, Atlanta, November 1977.

6. P. P. Dessau, "LN_2 and LH_2 Fracture Toughness of Armco Alloy 22-13-5,"
    Report No. TID/SNA-2083, Aerojet Nuclear Systems Co., 1971.

7. R. P. Reed, F. R. Fickett, M. B. Kasen, and H. I. McHenry, "Magnetic
    Fusion Energy Low Temperature Materials Program: A Survey," 1977, p. 28.

8. J. D. Landes and J. A. Begley, "Test Results from J-Integral Studies:
    An Attempt to Establish a J_{Ic} Testing Procedure," Fracture Analysis,
    ASTM STP 560, American Society for Testing and Materials, 1974, p. 170-186.

9. Standard Method of Test for Plane-Strain Fracture Toughness of Metallic
    Materials (Designation E 399-74), 1974 Annual Book of ASTM Standards,
    Part 10 (1974), p. 432-451.

10. J. G. Merkle and H. T. Corten, "A J-Integral Analysis for the
    Compact Specimen, Considering Axial Force as Well as Bending Effects,"
    J. Pressure Vessel Tech., Trans ASME No-6, 1974, P. 1-7.

11. Recommended Procedure for J_{Ic} Determination, Steering Committee,
    ASTM Task Group E24-01-09, March 1, 1977.

12. J. A. Begley and J. D. Landes, "The J-Integral as a Fracture Criterion",
    in Fracture Toughness, ASTM STP 514, American Society for Testing
    and Materials, 1972, p. 1-20.

13. H. M. Ledbetter, W. F. Weston, and E. R. Naimon, "Low-temperature Elastic Properties of Four Austenitic Stainless Steels," J. App. Phys. 46, (1975), p. 3855-3860.

14. H. M. Ledbetter, private communication.

15. A. A. Wells, "The Status of COD in Fracture Mechanics," Proceedings of the Third Canadian Congress of Applied Mechanics, Calgary, 1971, p. 59-77.

16. H. I. McHenry, private communication.

17. R. P. Reed and R. P. Mikesell, "The Stability of Austenitic Stainless Steels at Low Temperatures as Determined by Magnetic Measurements," Adv. Cry. Eng. 4, (1960), p. 84-100.

18. R. P. Reed and C. J. Guntner, "Stress-Induced Martensitic Transformations in 18Cr-8Ni Steel", Trans. Met. Soc. AIMI 230, 1713-1720 (1964).

19. Handbook on Materials for Superconducting Machinery, Metals and Ceramics Information Center, Battelle, Columbus, OH, Table 8.1.2-ME4.

20. Materials Research for Superconducting Machinery I-VI, edited by R. P. Reed, A. F. Clark, E. C. van Reuth and H. M. Ledbetter. NTIS Order Numbers AD780596, ADA004586, ADA012365, ADA019230, ADA030170, and ADA036919.

21. British Standards Institution, "Draft for Development on Crack Opening Displacement (COD) Testing," DD 19 (1972).

LIST OF TABLES

Table 1. Chemical composition by weight percent of the studied alloys and a pre-
viously studied alloy.

Designation	Fe	Cr	Ni	Mn	N	C	Mo	Si	S	P	Nb	V	Cu	Co
Fe-18Cr-3Ni-13Mn	bal	18.09	3.26	13.22	.37	.038	.12	.52	.005	.028	---	---	---	---
Fe-21Cr-12Ni-5Mn	bal	21.15	12.37	4.96	.31	.041	2.17	.49	.015	.026	18	.15		...
Fe-19Cr-9Ni-2Mn	bal	18.65	9.49	1.88	.12	.048	.52	.38	.024	.019	---	.03	.07	.06
Fe-21Cr-6Ni-9Mn	bal[a]	19.75	7.16	9.49	.28	.019	---	.15	.003	.004	---	---	---	---

[a]Reported in Reference 5.

Table 2. Major alloy content, ASTM designations, relevant ASTM plate speci-
           fications, trade names for the alloys studied, and a previously
           studied alloy.

Fe-18Cr-3Ni-13Mn	XM29	A240, A412	Nitronic 33	18-3Mn
Fe-21Cr-12Ni-5Mn	XM19	A240, A412	Nitronic 50	22-13-5
Fe-19Cr-9Ni-2Mn	AISI 304N	A240	----	---
Fe-21Cr-6Ni-9Mn	XM11	A412	Nitronic 40	21-6-9

Table 3. Final anneal durations, grain sizes, Rockwell B hardnesses of the tested materials and Fe-21Cr-6Ni-9Mn.[a]

Alloy	Nominal Grain Diameter μm	ASTM Grain Size Number	Rockwell-B Hardness	T (°C)	Final heat treatment Duration hr/cm	hr	Quench
Fe-18Cr-3Ni-13Mn	48	6.0	93	1080	.4	1	water
Fe-21Cr-12Ni-5Mn	34	7.0	98	1120	.4	2	water
Fe-19Cr-9Ni-2Mn	120	3.0	79	1052	~.4	2.5	water
Fe-21Cr-12Ni-5Mn-X	120	3.0	93	1177	.4	1.5	water
Fe-21Cr-6Ni-9Mn[a]	160	2.5	92	1093	~.4	1.5	water

[a]Time in furnace is 1 1/2 hours. Time-at-temperature was somewhat less.

[b]Non-standard heat treatment for this alloy.

115

Table 4. Elastic-plastic fracture mechanics parameters [15]
used in calculating J-integral and COD values.

a/W	η	η_c	γ
.3	2.352	0.194	1.62
.35	2.336	0.202	--
.4	2.318	0.206	2.04
.45	2.284	0.206	--
.5	2.262	0.198	2.34
.55	2.238	0.188	--
.6	2.206	0.174	2.50
.65	2.178	0.156	--
.7	2.164	0.144	2.50

Table 5. Values of Young's modulus E, Poisson's ratio ν, and plane strain modulus $E' = E/(1 - \nu^2)$ used in calculations.[13,14]

	T (K)	E GPa	ν	$E' = E/(1 - \nu^2)$ GPa
Fe-18Cr-3Ni-13Mn	295	1.97	.280	2.13
	76	1.97	.277	2.13
	4	1.98	.277	2.14
Fe-21Cr-12Ni-5Mn	295	1.94	.295	2.13
	76	2.08	.284	2.26
	4	2.09	.283	2.27
Fe-19Cr-9Ni-2Mn	295	1.90	.290	2.07
	76	2.05	.278	2.22
	4	2.04	.271	2.20

Table 6. J-Δa, J_{Ic} and K_{Ic} values for Fe-18Cr-3Ni-13Mn.

T (K)	J (kJ/m^2)	Δa (mm)	K_{Ic} MPa$\sqrt{m}$	J_{Ic} (kJ/m^2)	Calculated or average measured K_{Ic} MPa$\sqrt{m}$
295	658	.66			
295	752	.91		665[a]	377[c]
295	1140	2.06			
295	1520	3.94			
76	71.8	.036			
76	86.3	.28			
76	112	1.14		77	129[c]
76	120	1.85			
76	120	1.75			
4			70		
4			70		71[b]
4			73		

[a] Invalid according to the proposed standard test method because specimens too small.

[b] Invalid according to ASTM E 399 due to slightly excessive crack front curvature. This deviation is considered insignificant.

[c] Using Eq. 4

118

Table 7. J-Δa, J_{Ic} and K_{Ic} values for Fe-21Cr-12Ni-5Mn (commercial heat treatment).

T (K)	J (KJ/m^2)	Δa (mm)	K_{Ic} MPA$\sqrt{m}$	J_{Ic} (KJ/m^2)	Calculated or average measured K_{Ic} MPA$\sqrt{m}$
295	313	1.32			
295	443	3.56			
295	749	6.60		228	221
295	1211	14.0			
76	98.9	.51			
76	116	NA[a]	142[b]	87.5[c]	141
76	172	NA[a]			
4	NA	NA	108		106
4	NA	NA	104[d]		

[a]Fractured before unloading

[b]Invalid according to ASTM E 399, because maximum load occured too far above deviation of load-displacement curve from linear.

[c]Estimate

[d]Invalid according to ASTM E 399, due to excessive crack-front curvature.

Table 8. J-Δa, J_{Ic} and calculated K_{Ic} values for Fe-19Cr-9Ni-2Mn.

T (K)	J (k J/m^2)	Δa (mm)	J_{Ic} (k J/m^2)	Calculated K_{Ic}[a] MPa$\sqrt{m}$
295	472	.33		
295	562	.46	553[b]	338
295	625	.74		
295	794	1.17		
295	1015	1.57		
76	448	.38		
76	481	.43		
76	698	.94	486	329
76	906	2.6		
76	1010	3.8		
76	1230	4.9		
4	224	.41		
4	269	.41		
4	354	.46		
4	362	1.78	208	214
4	494	2.06		
4	723	3.43		

[a]Calculated from Eq. 4.

[b]Invalid according to the specimen size criterion of Ref. 11.

Table 9 K_{Ic} values for Fe-21Cr-12Ni-5Mn-X
          (special heat treatment).

T (K)	K_{Ic} (MPa√m̄)	Average K_{Ic} (MPa√m̄)
4	152	
		176
4	199[a]	

[a]Invalid according to ASTM E 399 because $B < 2.5\left(\dfrac{K_{Ic}}{\sigma_y}\right)^2$.

121

Table 10. Summary of measured and calculated critical stress intensity values, in MPa√m.

	4 K	76 K	295 K
Fe-18Cr-3Ni-13Mn	71	131	377
Fe-21Cr-12Ni-5Mn	111	141	221
Fe-19Cr-9Ni-2Mn	214	329	338
Fe-21Cr-12Ni-5Mn-X	176 ± 24	--·-	---
Fe-21Cr-6Ni-9Mn[a]	182	272	489

[a]Data taken from Reference 5

Table 11. Average inferred critical (maximum load or pop-in) crack-opening-displacement values, in mm.

	4 K	76 K	295 K
Fe-18Cr-3Ni-13Mn	.009	.044	.76
Fe-21Cr-12Ni-5Mn	.025	.07	.33
Fe-19Cr-9Ni-2Mn	.30	.49	1.01
Fe-21Cr-12Ni-9Mn-X	.05	--	--

Table 12. Paris law fatigue crack growth parameters C and n for the studied materials, for ΔK in MPa$\sqrt{m}$ and da/dN in mm/cycle.

| | 4 K | | 76 K | | 295 K | |
	C	n	C	n	C	n
Fe-18Cr-3Ni-13Mn	1.35×10^{-11}	5.32	3.15×10^{-10}	3.98	9.7×10^{-11}	3.82
Fe-21Cr-12Ni-5Mn	3.81×10^{-12}	4.66	3.86×10^{-11}	3.94	9.8×10^{-11}	3.80
Fe-19Cr-9Ni-2Mn	1.71×10^{-9}	3.46	4.23×10^{-9}	3.02	3.05×10^{-9}	3.0
Fe-21Cr-6Ni-9Mn[a]	3.6×10^{-11}	4.4	1.9×10^{-10}	3.7	1.9×10^{-10}	3.7

[a]Reference 5.

124

Table 13. Tensile properties of the nitrogen-strengthened stainless steels used in the present study and a previously tested material.

	Temperature (K)	Yield Strength 0.2% offset MPa	Tensile Strength MPa	Flow Strength[a] MPa	Elongation 2.5 cm gage length (%)	Reduction of Area (%)
Fe-18Cr-3Ni-13Mn	295	421 / 459 / 440	787 / 803 / 796	604 / 632 / 618	54 / 58 / 56	53 / 53 / 53
	76	1154 / 1134 / 1144	1522 / 1516 / 1519	1338 / 1325 / 1331	19 / 18 / 18	23 / 25 / 24
	4	1572 / 1509 / 1540	1807 / 1815 / 1811	1689 / 1662 / 1676	5 / 4 / 4	23 / 29 / 26
Fe-21Cr-12Ni-5Mn	295	534 / 522 / 528	845 / 840 / 842	690 / 681 / 685	35 / 35 / 35	64 / 58 / 61
	76	1164 / 1178 / 1171	1584 / 1591 / 1587	1373 / 1384 / 1379	28 / 29 / 28	36 / 31 / 34
	4	1472 / 1422 / 1446	1898 / 1889 / 1893	1685 / 1655 / 1670	9 / 9 / 9	34 / 32 / 33
-19Cr-9Ni-2Mn	295	310 / 290 / 300	654 / 644 / 649	4?2 / 467 / 474	61 / 60 / 60	70 / 69 / 70
	76	633 / 676 / 655	1512 / 1502 / 1507	1073 / 1089 / 1081	48 / 48 / 48	66 / 67 / 66
	4	846 / 743 / 794	1663 / 1647 / 1655	1255 / 1195 / 1225	37 / 32 / 34	42 / 47 / 44
-21Cr-12Ni-5Mn-X (special anneal)	4	1307 / 1353 / 1330	1842 / 1853 / 1848	1575 / 1604 / 1589	16 / 15 / 16	36 / 41 / 38
-21Cr-6Ni-9Mn[b]	295	350 / 357 / 353	696 / 705 / 701	523 / 531 / 527	61 / 61 / 61	79 / 78 / 78
	76	0.913 / 0.886 / 0.899	1462 / 1485 / 1474	1188 / 1186 / 1187	42 / 43 / 43	32 / 41 / 37
	4	1258 / 1224 / 1241	1633 / 1634 / 1634	1446 / 1429 / 1438	16 / -- / 16	40 / -- / 40

ow strength is taken as the average of the tensile and yield strengths.

ta from Reference 5.

125

Table 14. Normalized magnetization of the studied materials, given as (percent bcc martensite)/(percent elongation) from specimens fractured in tension.

	T(K)	Normalized magnetization
Fe-18Cr-3Ni-13Mn	295	< .002
	76	.05
	4	.3
Fe-21Cr-12Ni-5Mn	295	< .003
	76	< .005
	4	< .012
Fe-21Cr-12Ni-5Mn-X	4	< .005
Fe-19Cr-9Ni-2Mn	295	.006
	76	2.1
	4	2.6
Fe-21Cr-6Ni-9Mn[a]	76	.6
	4	.3

[a]Data taken from Reference 5.

LIST OF FIGURES

Fe-18Cr-3Ni-13Mn

L - Longitudinal or rolling direction
T - Long transverse or width direction
S - Short transverse or plate thickness direction

Figure 1. Composite Photomicrograph of Fe-18Cr-3Ni-13Mn.

Fe-21Cr-12Ni-5Mn
(commercial heat treatment)

L - Longitudinal or rolling direction
T - Long transverse or width direction
S - Short transverse or plate thickness direction

Figure 2. Composite Photomicrograph of Fe-21Cr-12Ni-5Mn.

Fe-19Cr-9Ni-2Mn
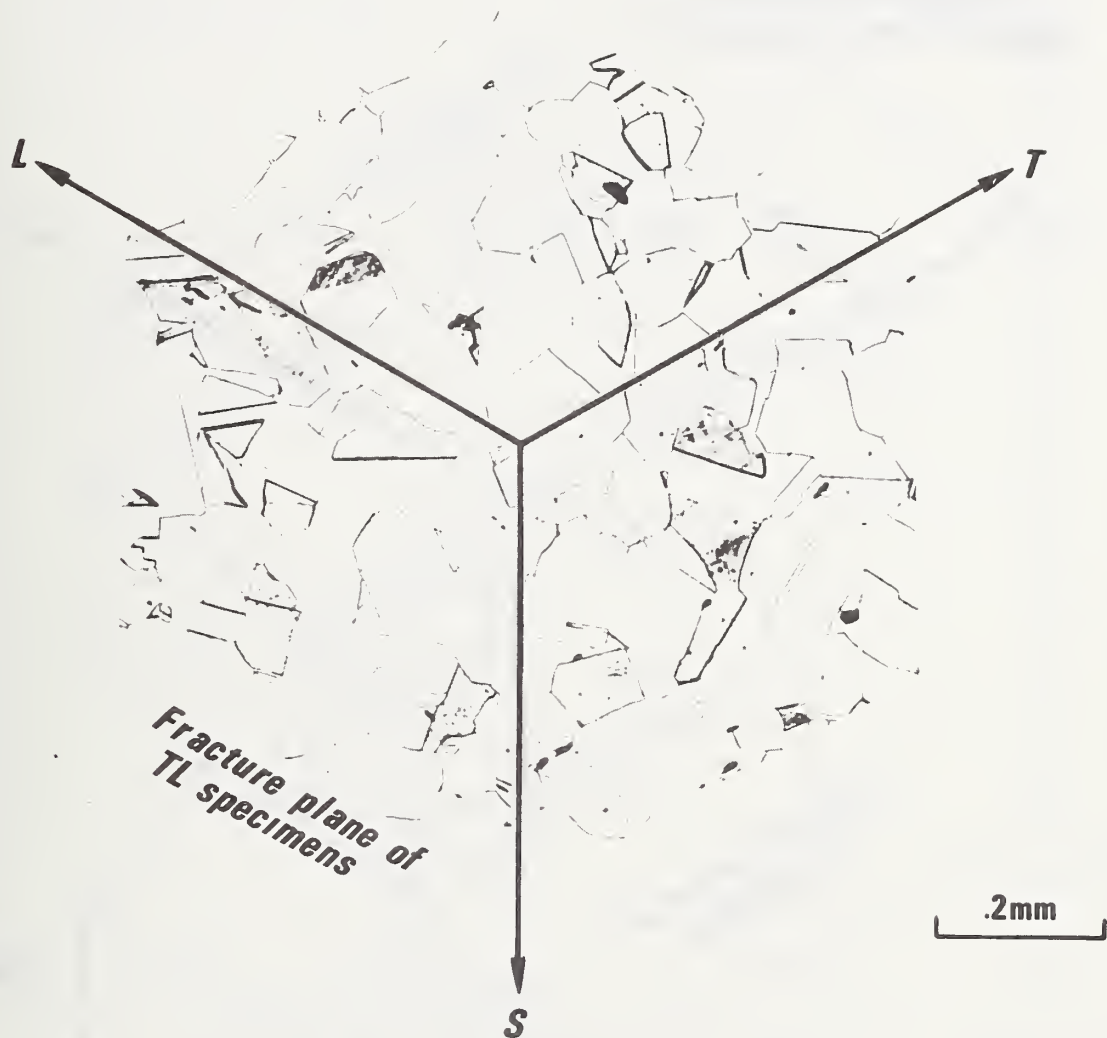
L - Longitudinal or rolling direction

T - Long transverse or width direction

S - Short transverse or plate thickness direction

Figure 3. Composite Photomicrograph of Fe-19Cr-9Ni-2Mn.

Fe-21Cr-12Ni-5Mn-X
(special heat treatment)
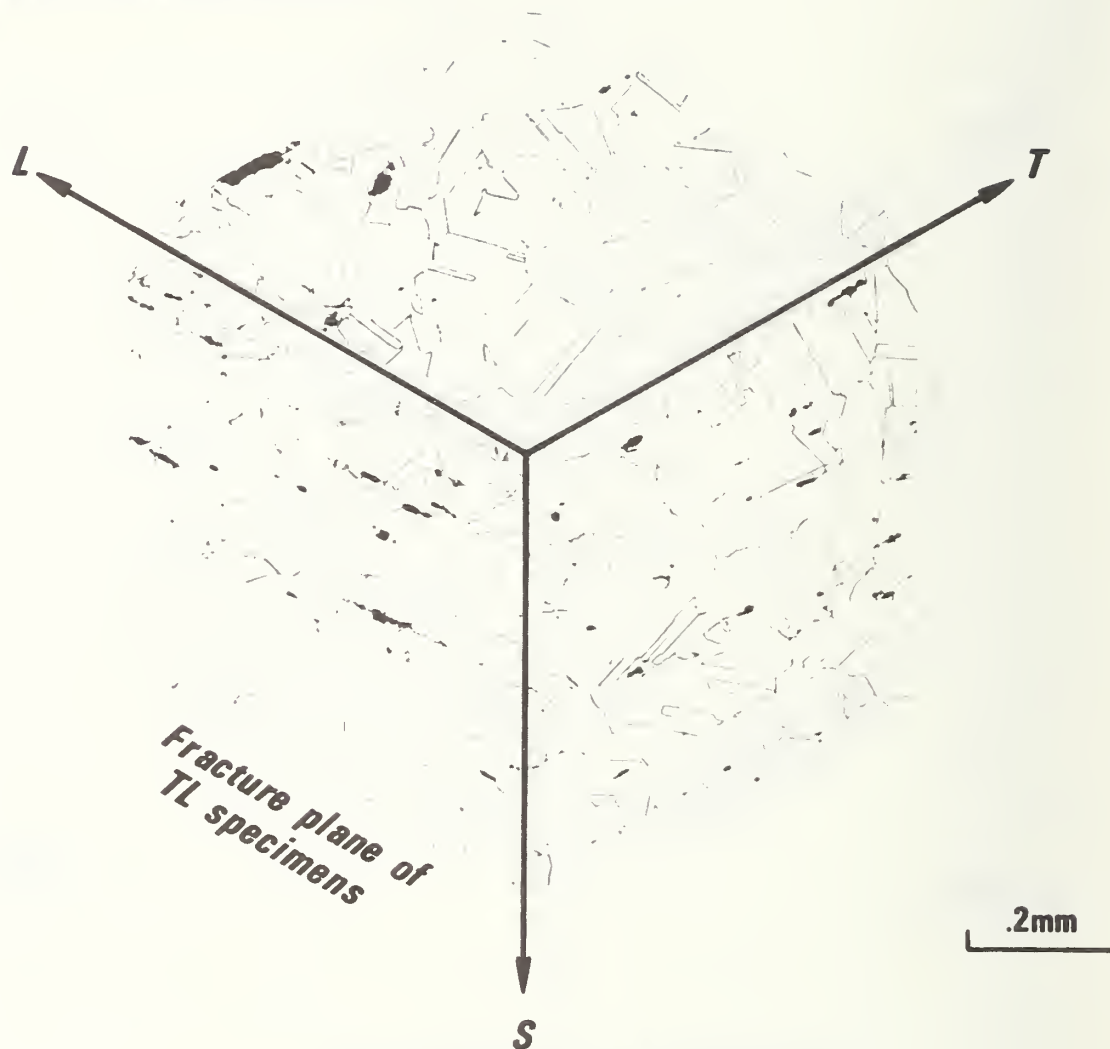
L

T

Fracture plane of
TL specimens

S

.2mm

L - Longitudinal or rolling direction
T - Long transverse or width direction
S - Short transverse or plate thickness direction

Figure 4. Composite Photomicrograph of Fe-21Cr-12Ni-5Mn-X (special anneal).

132
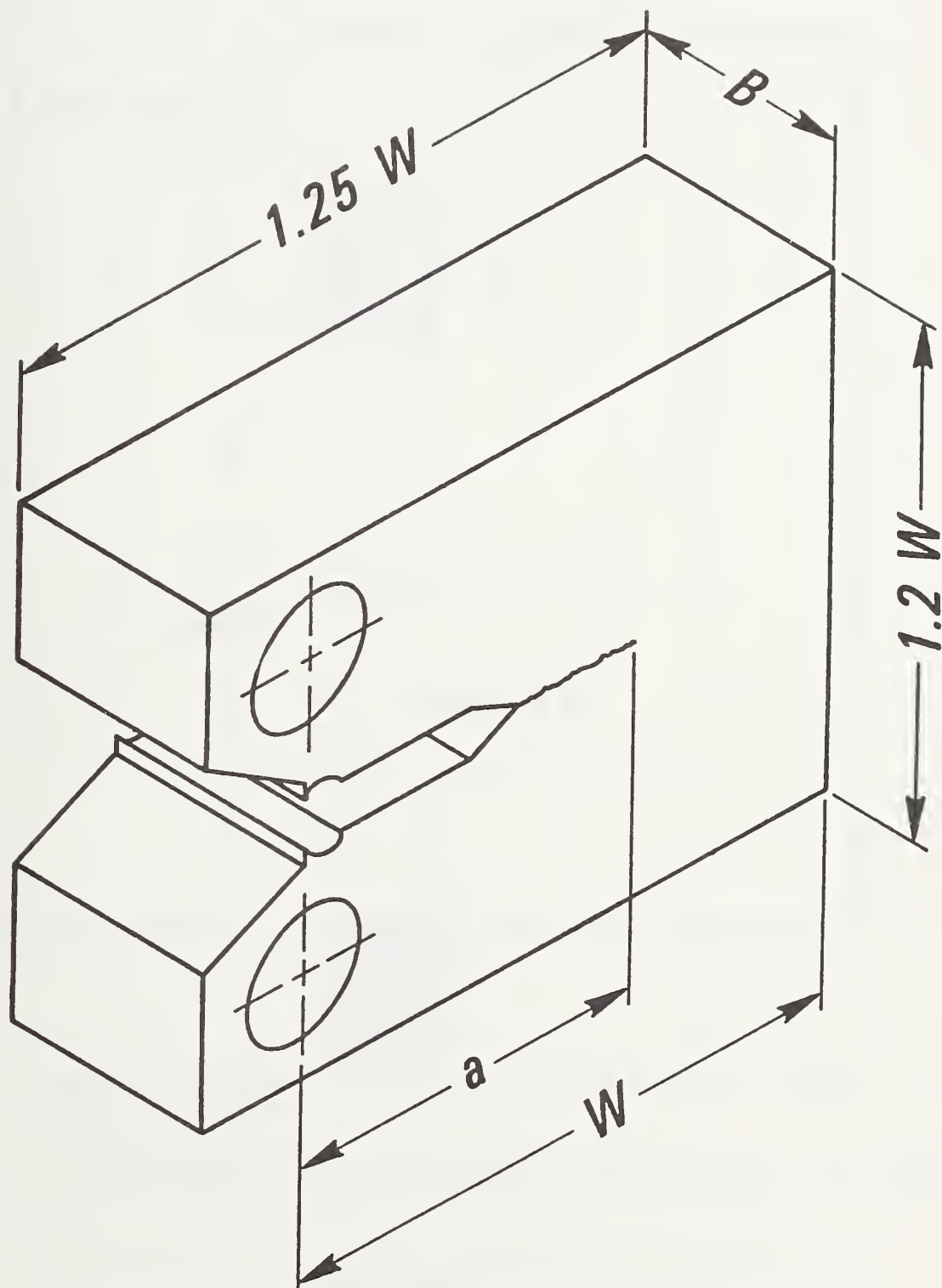
Figure 5. a. Fracture toughness specimen geometry used in the present study (compact).

133
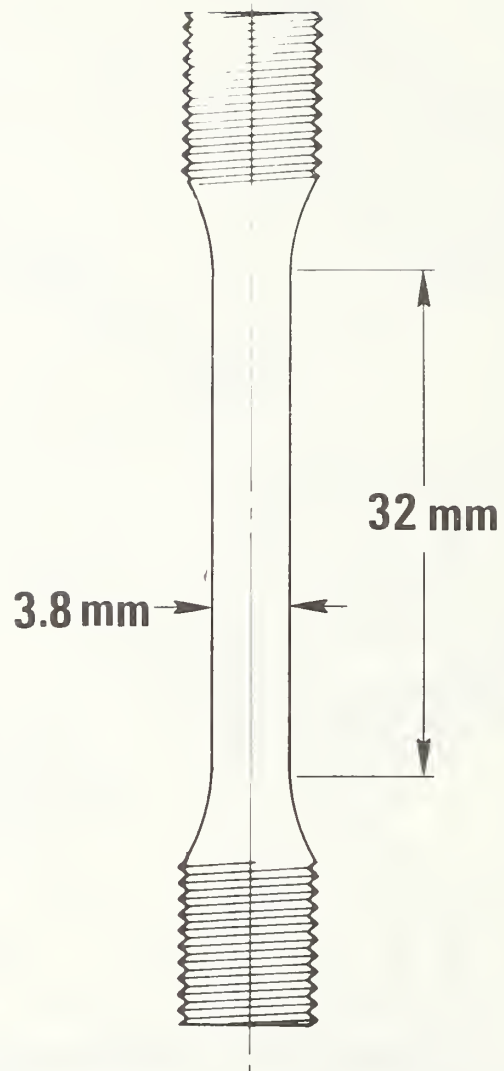
Figure 5. b. Tensile specimen geometry used in the present study.
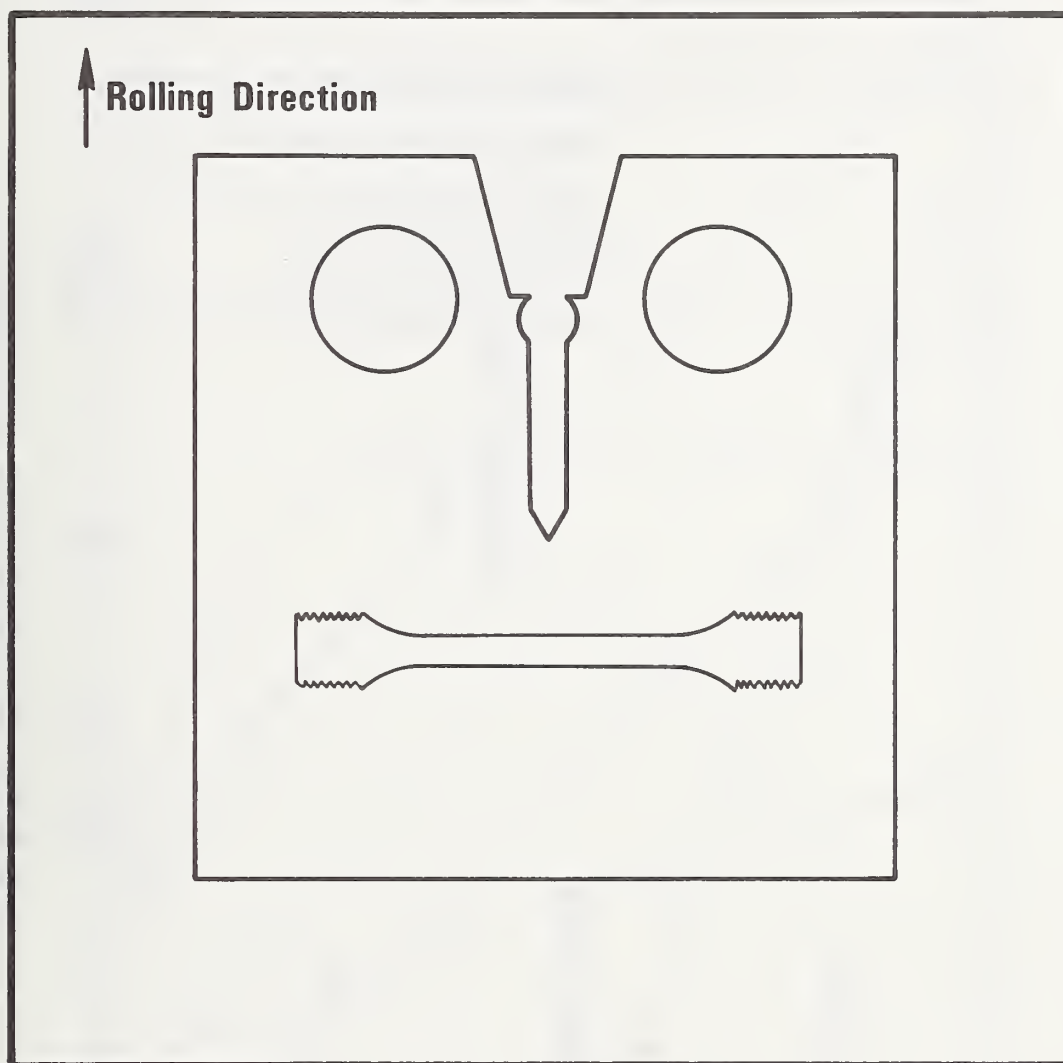
Figure 5. c. Relative orientation of fracture toughness and tensile specimens and plate stock.
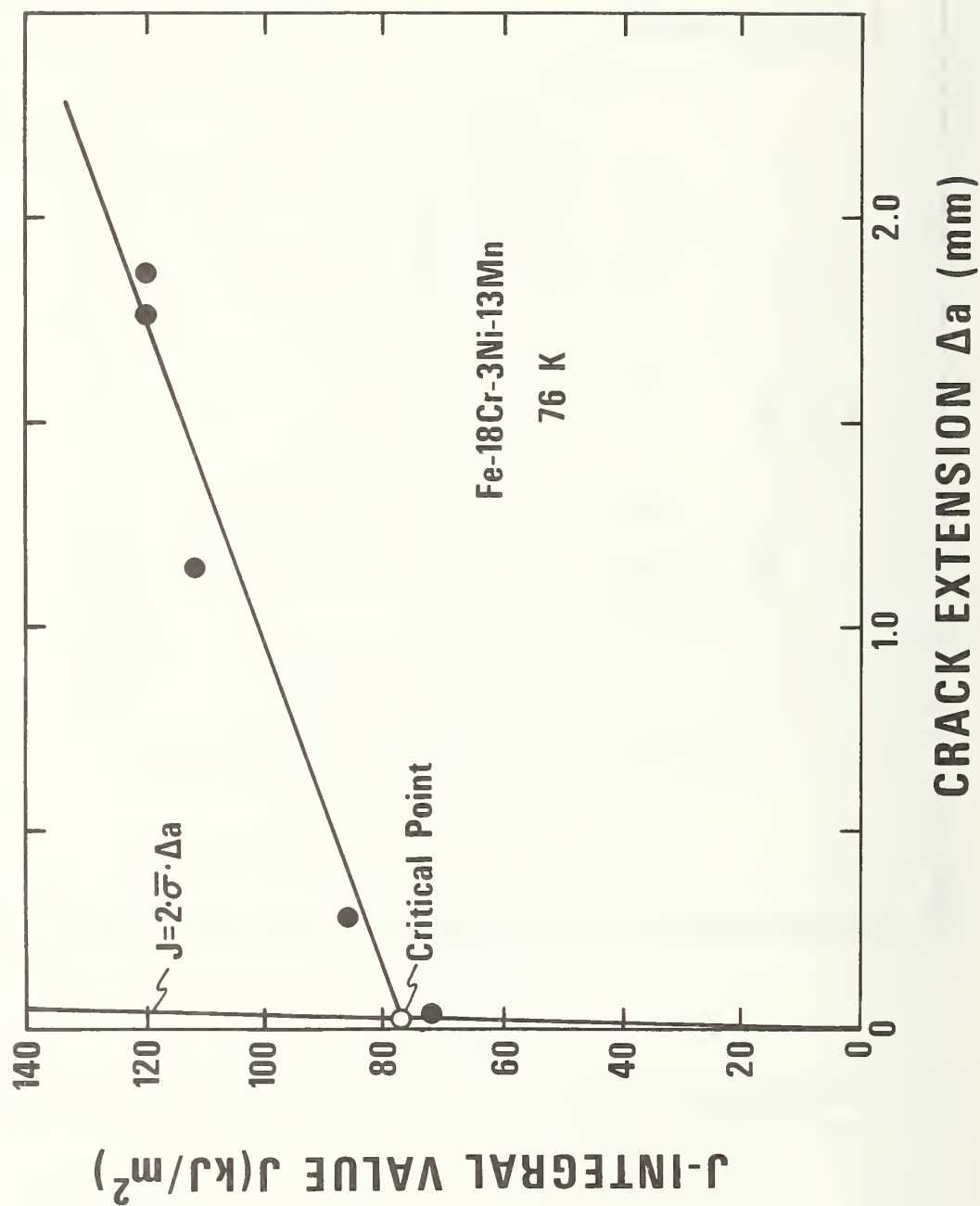
Figure 6. J-Δa curve for Fe-18Cr-3Ni-13Mn at 76 K.

136
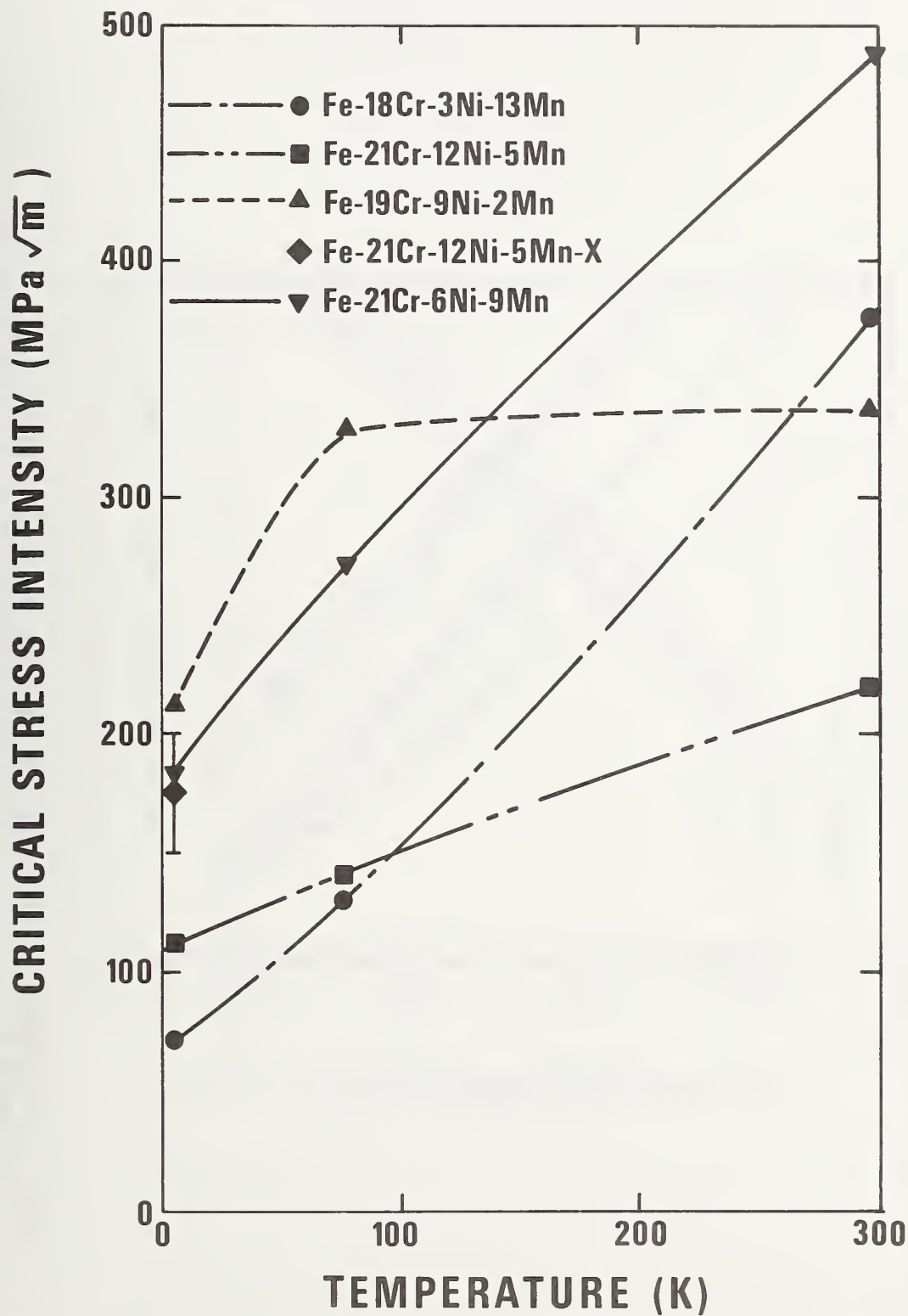
Figure 7. Fracture toughness results at 4, 76, and 295 K for nitrogen-strengthened stainless steels used in the present study.
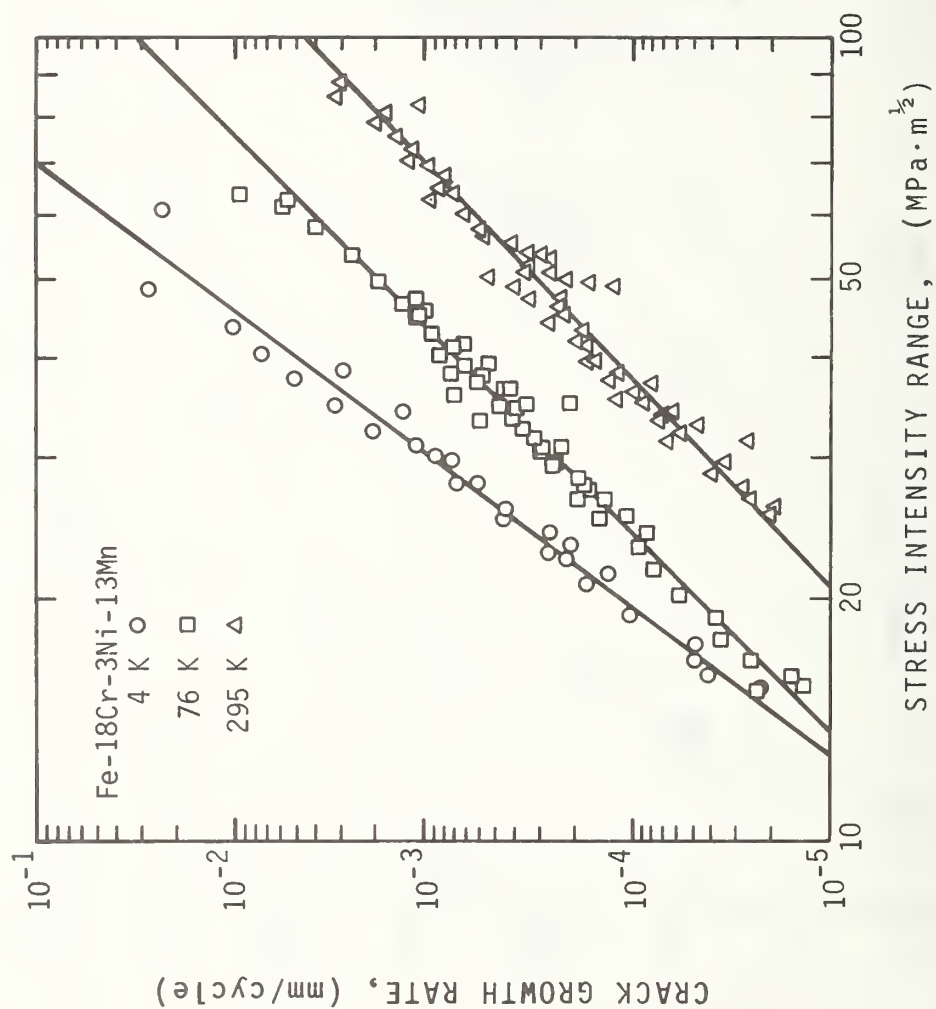
Figure 8. Fatigue crack growth rate results for Fe-18Cr-3Ni-13Mn at 295, 76, and 4 K.
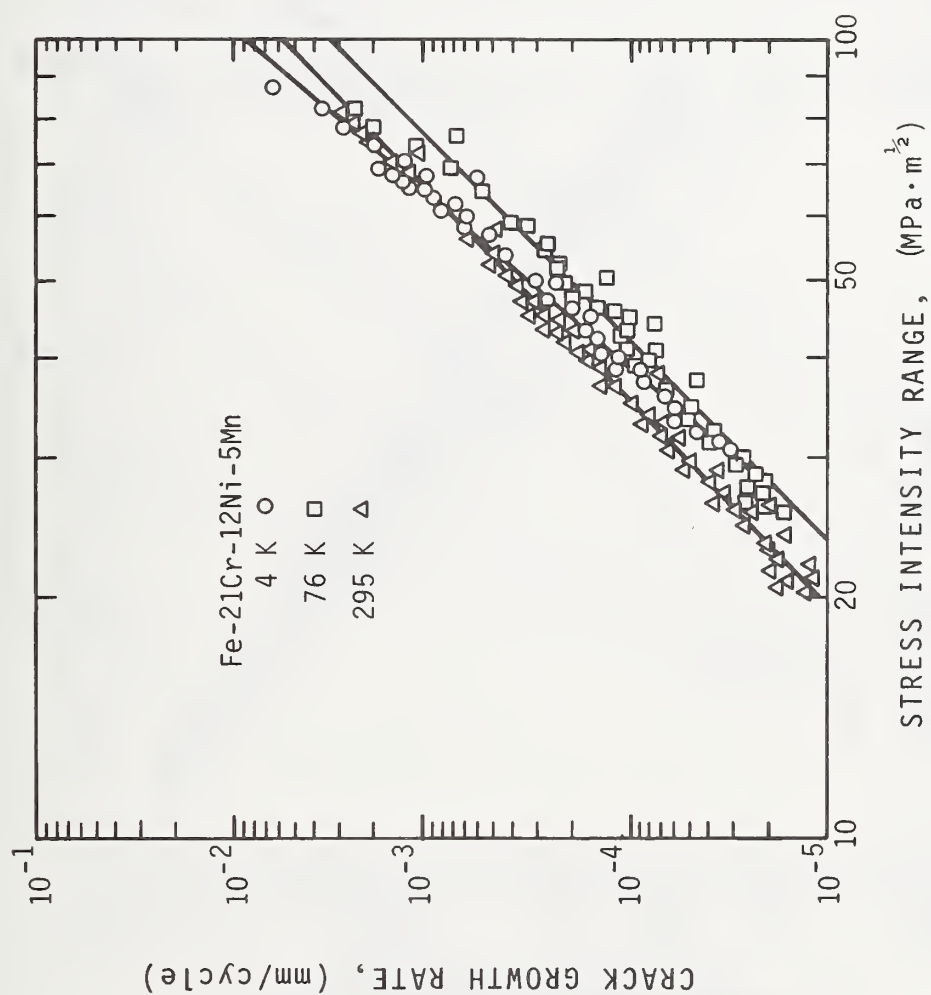
Figure 9. Fatigue crack growth rate results for Fe-21Cr-12Ni-5Mn at 295, 76, and 4 K.
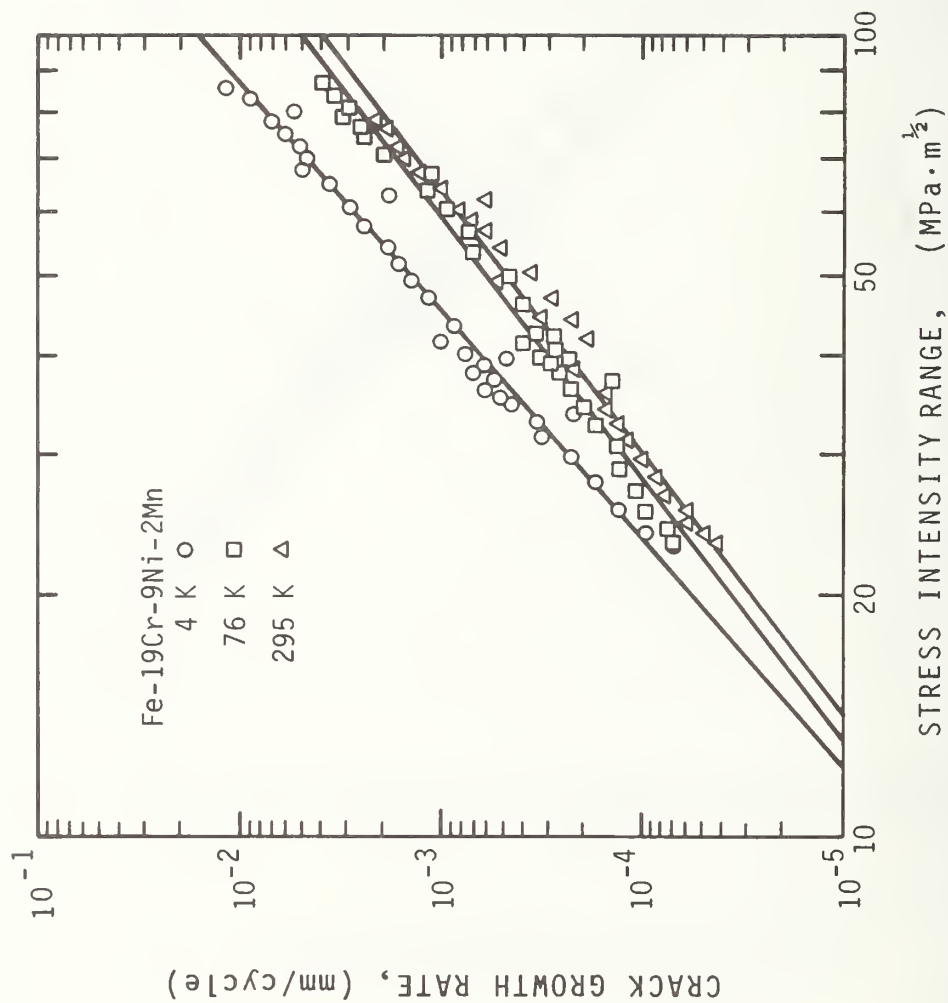
Figure 10. Fatigue crack growth rate results for Fe-19Cr-9Ni-2Mn at 295, 76, and 4 K.
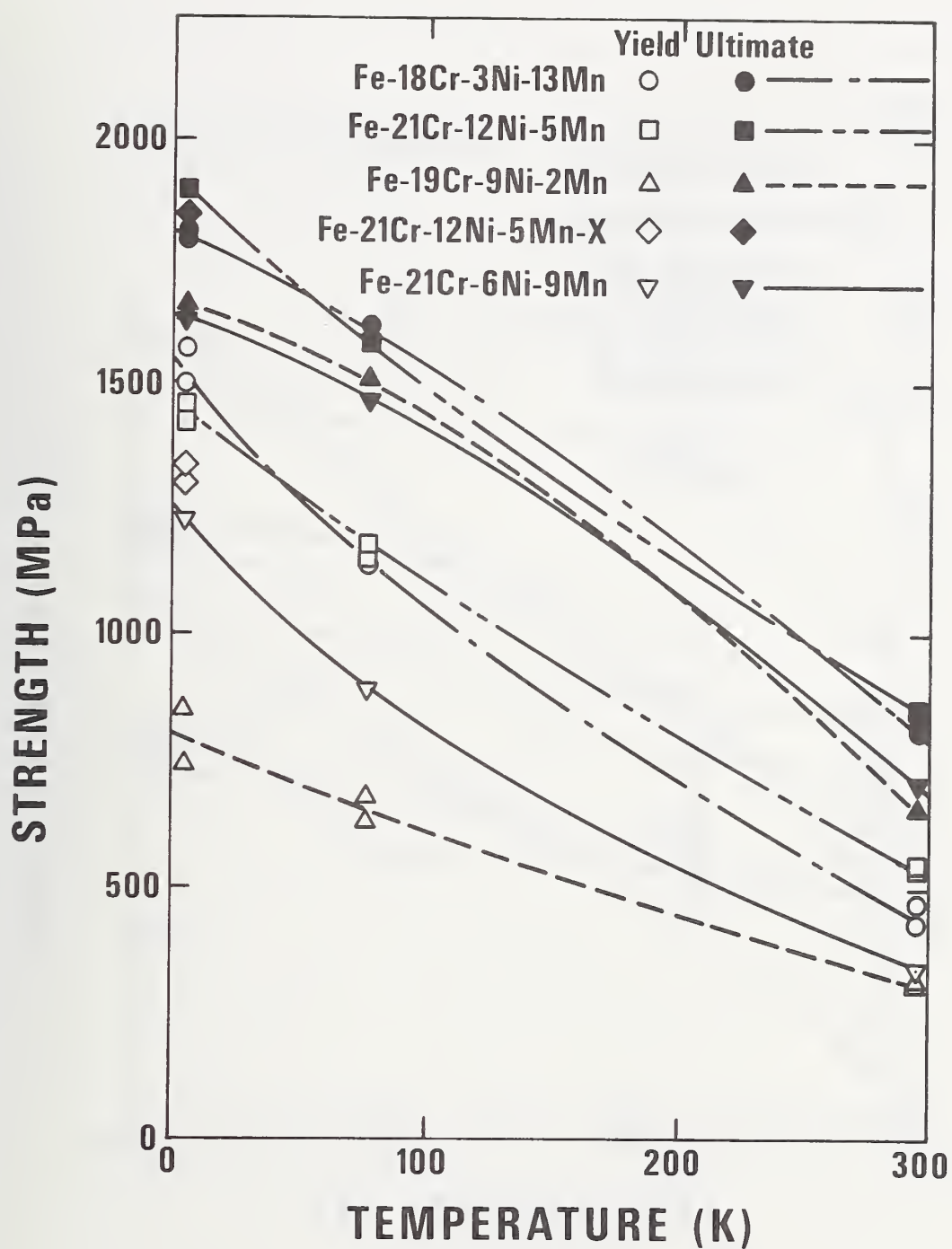
Figure 11. Yield and ultimate strengths of materials used in the present study.
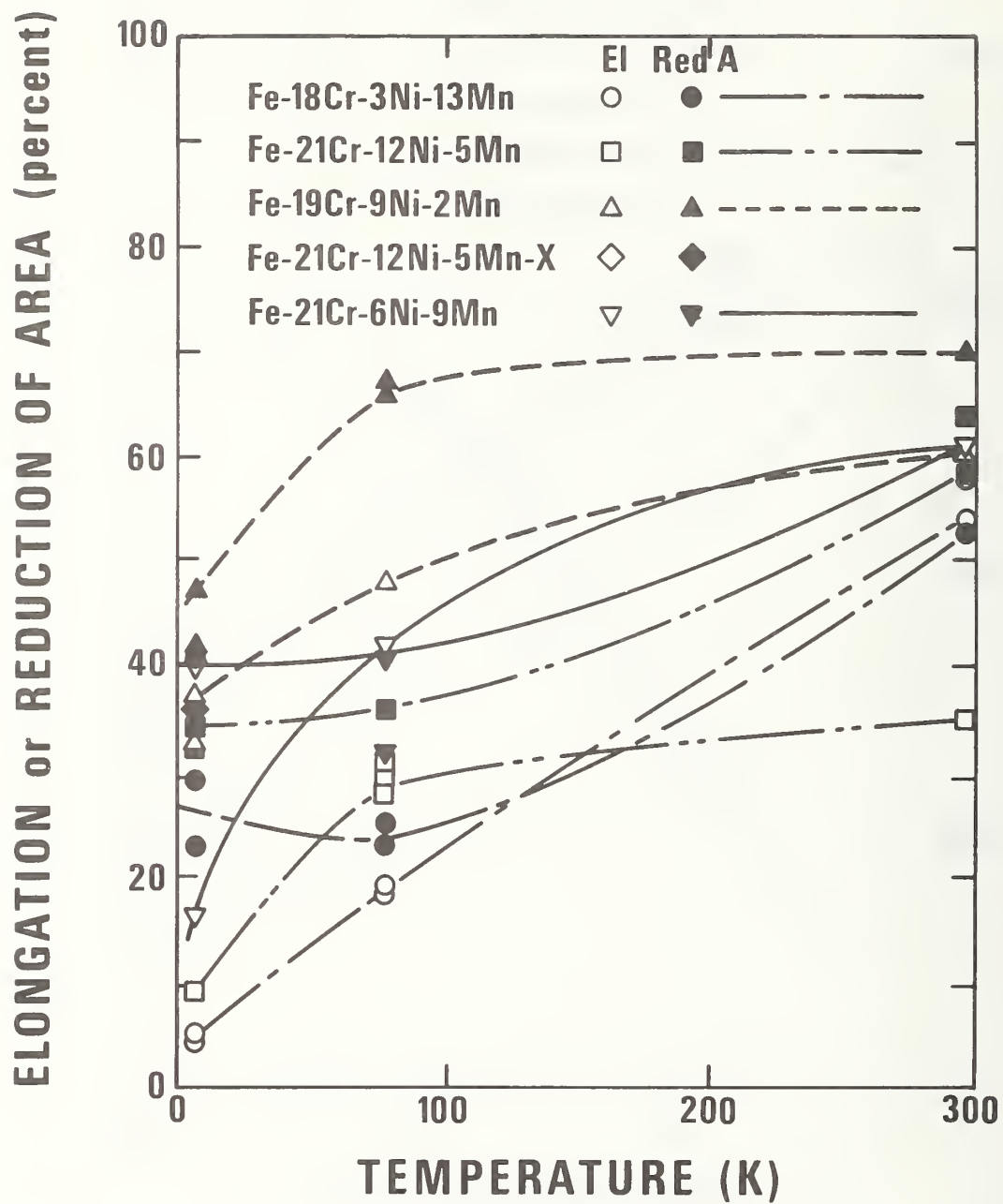
Figure 12. Elongations and reduction of areas of the materials used in the present study.
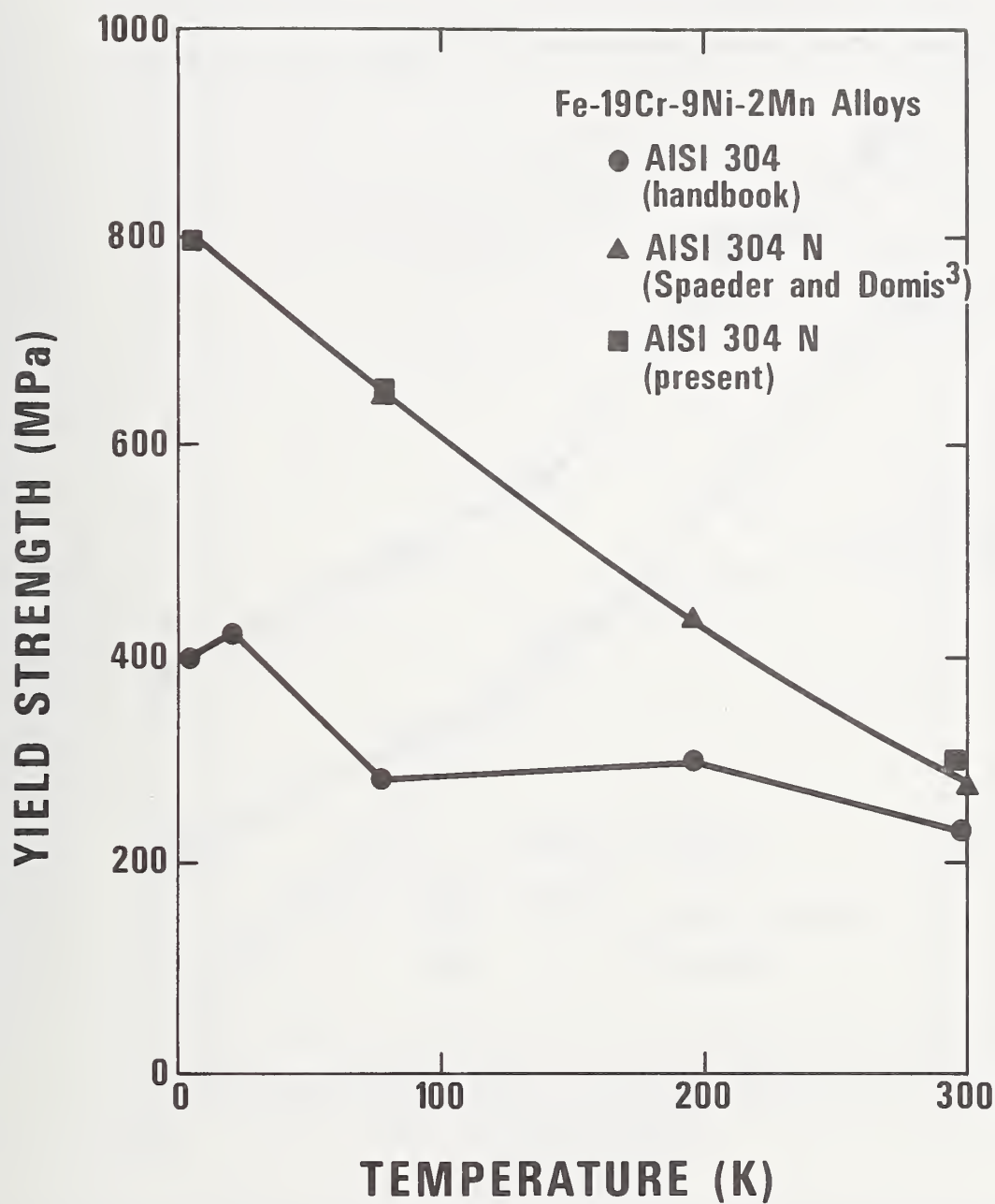
Figure 13.Yield strengths of AISI 304 and AISI 304N (Fe-19Cr-9Ni-2Mn) between 4 and 300 K..
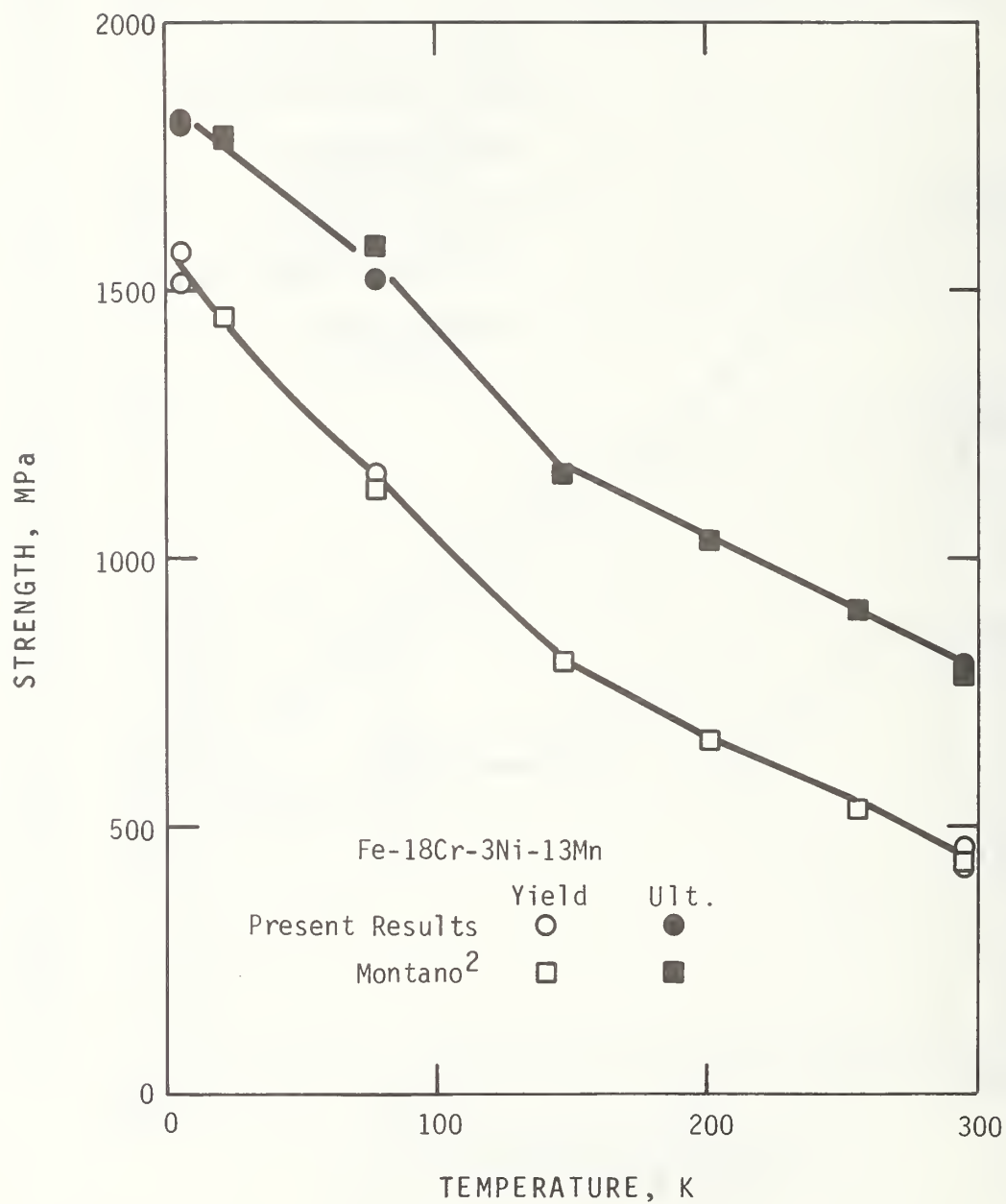
Figure 14. Strength property data for Fe-18Cr-3Ni-13Mn from the present study and from Montano.[2]
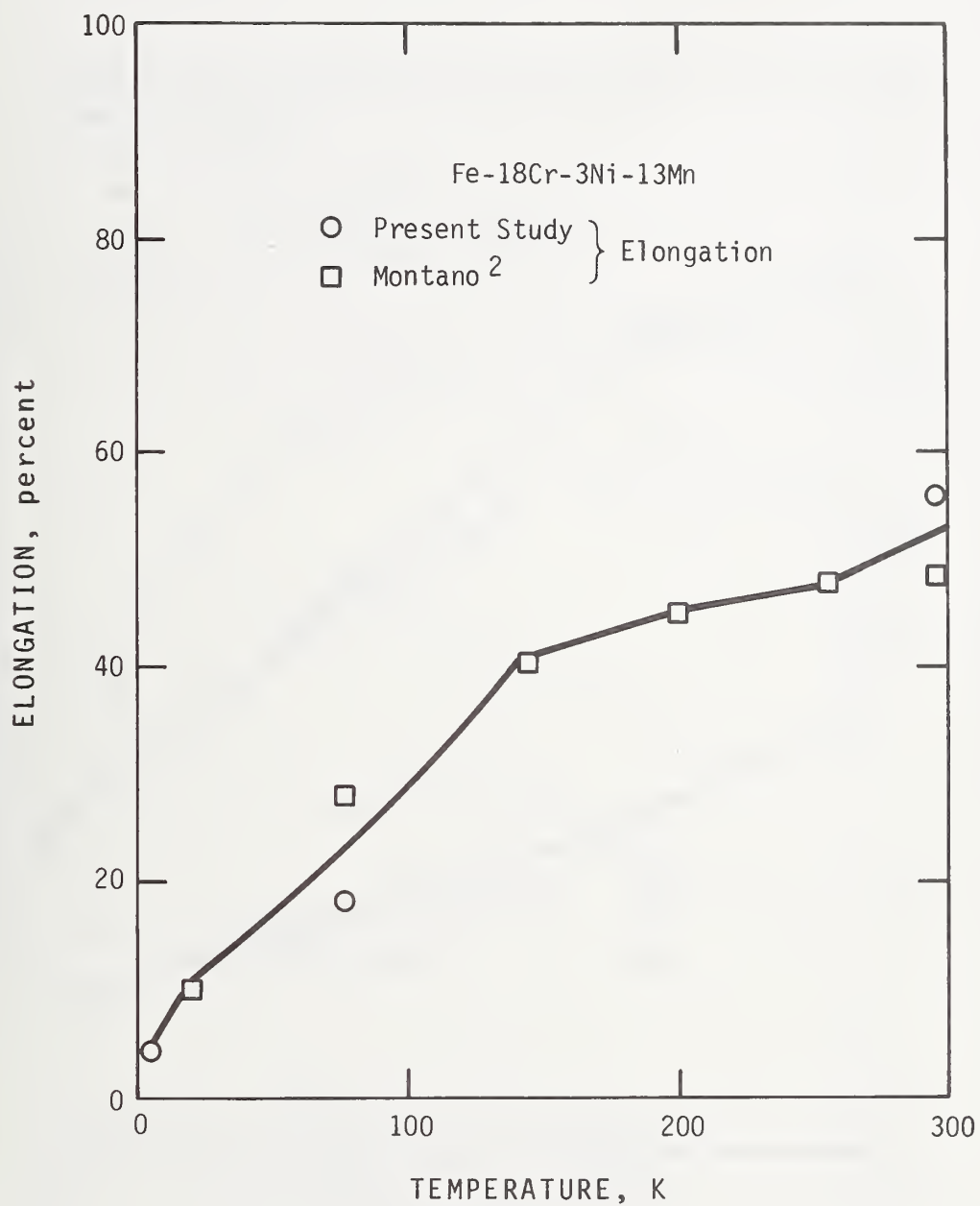
Figure 15. Elongation data for Fe-18Cr-3Ni-13Mn from the present study and from Montano.[2]

145
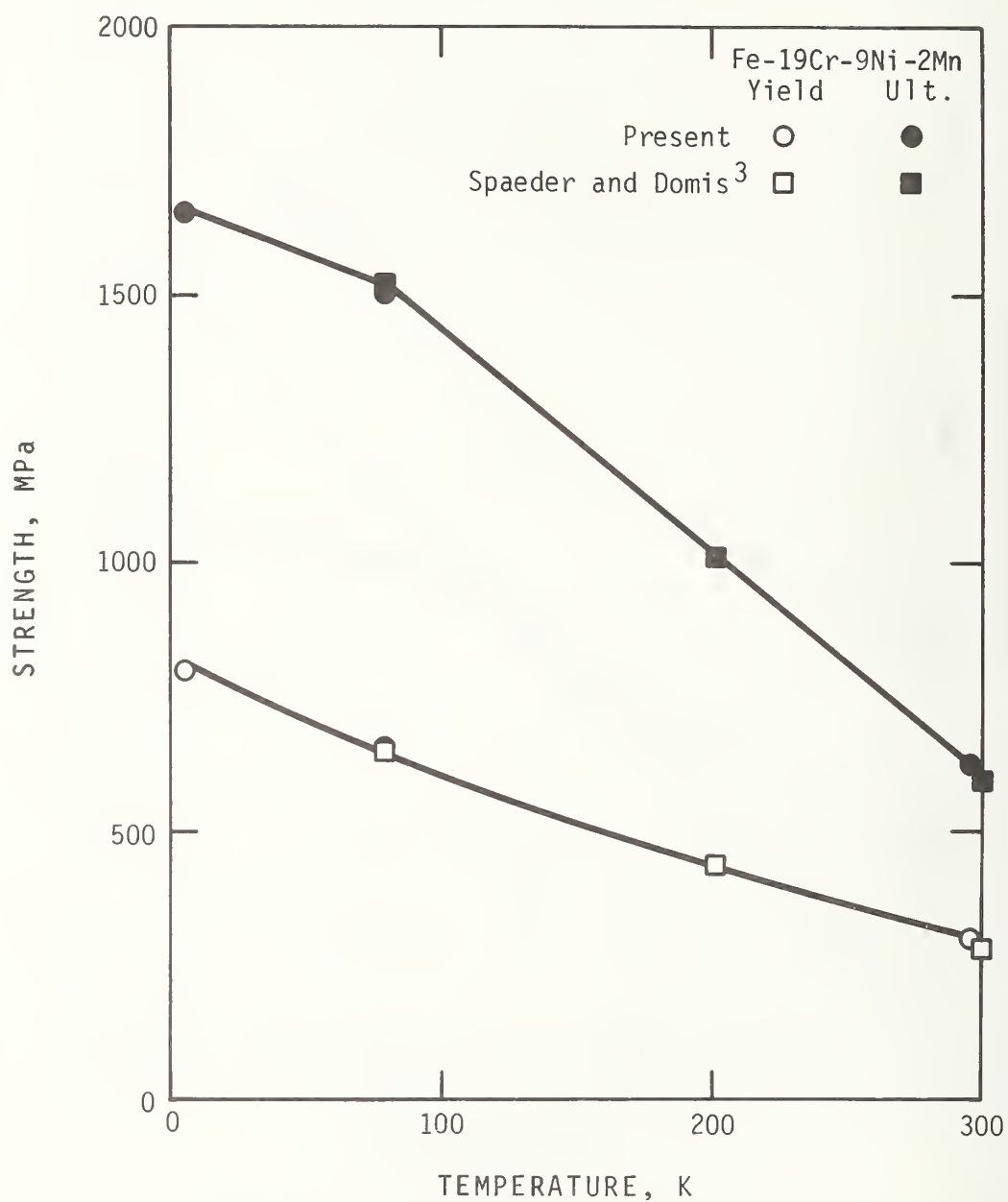
Figure 16. Strength property data for Fe-19Cr-9Ni-2Mn from the present study and from Spaeder and Domis.[3]

146
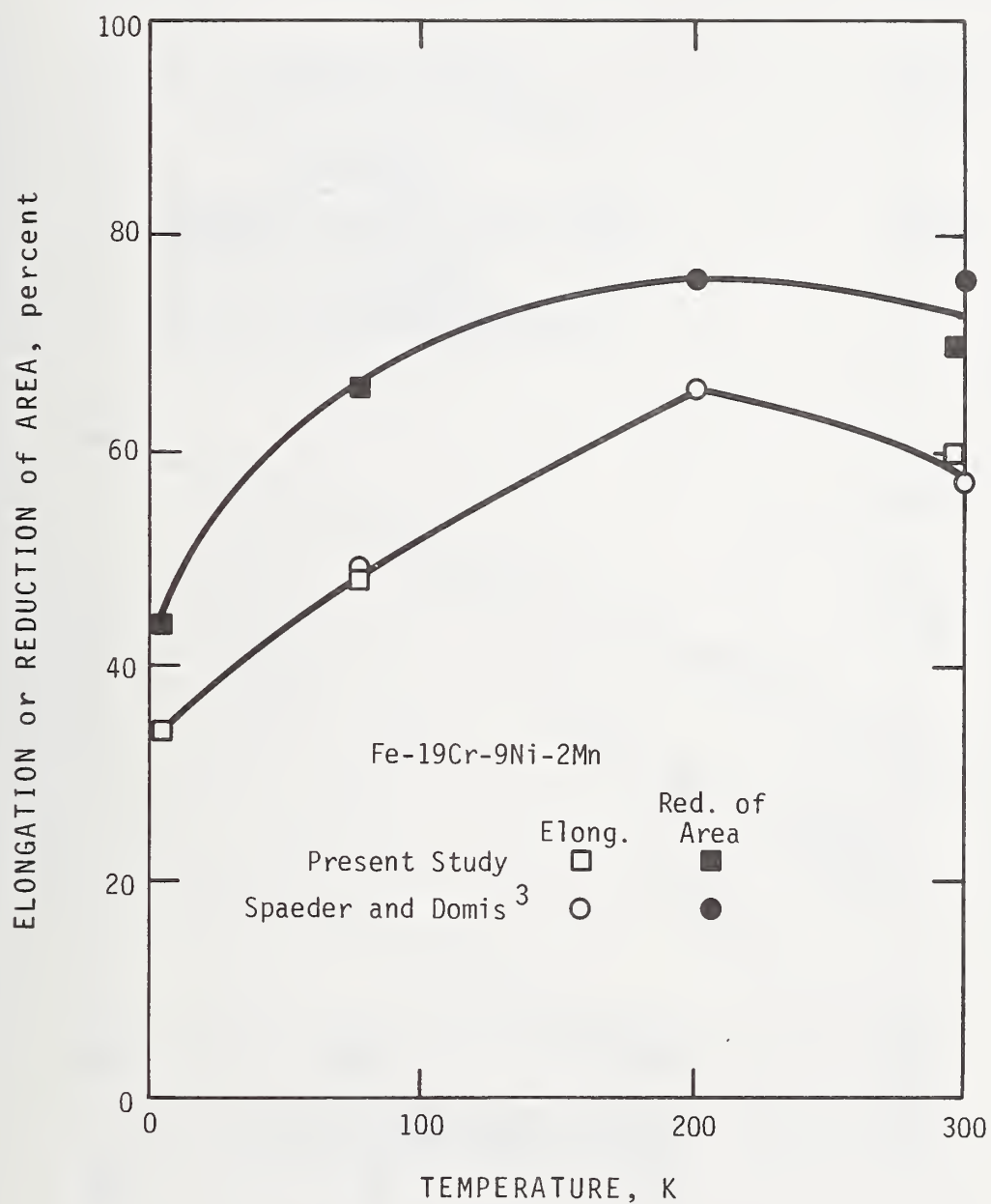
Figure 17.Elongation and reduction of area data for Fe-19Cr-9Ni-2Mn from the present study and from Spaeder and Domis.[3]

147
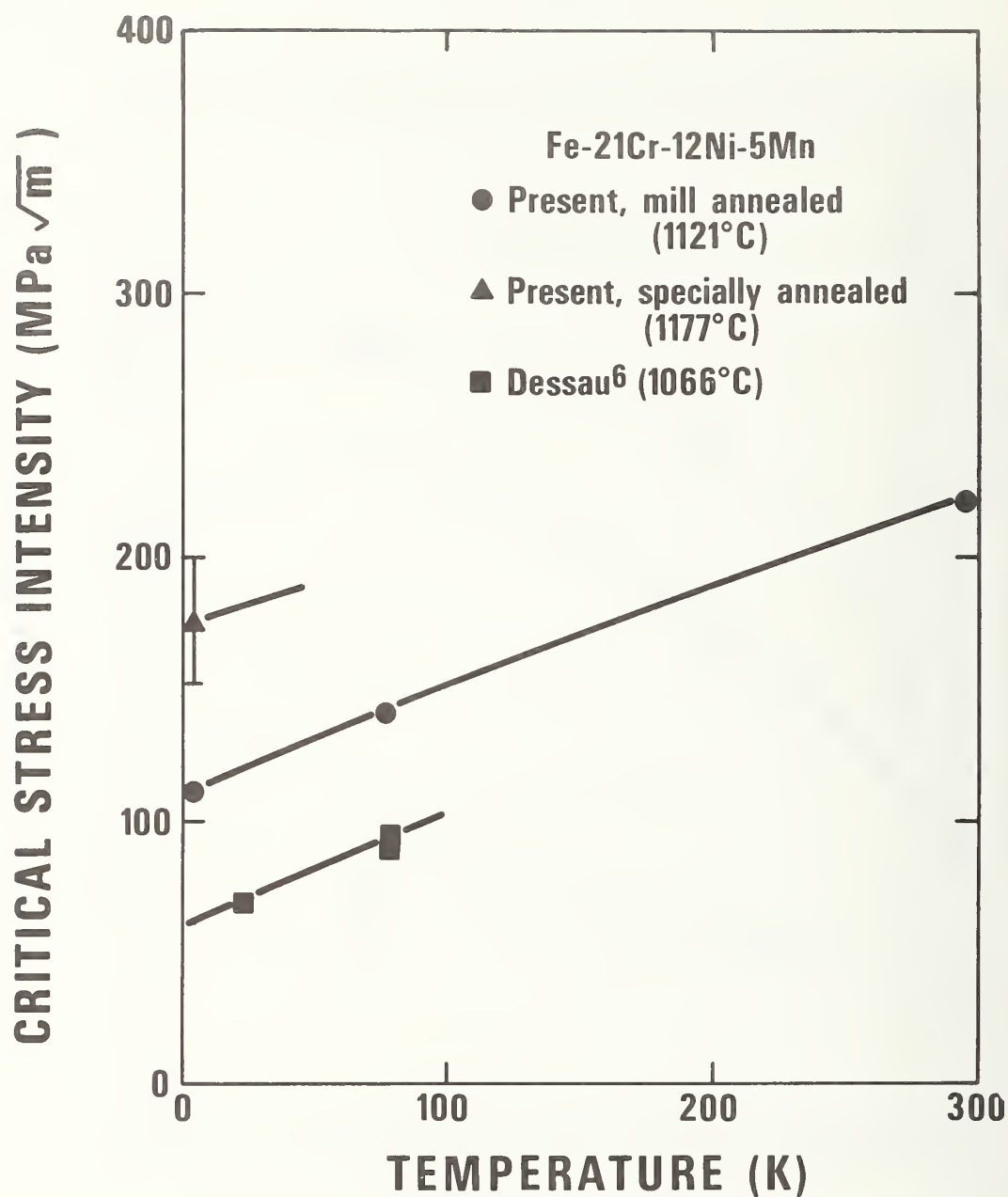
Figure 18. Three sets of toughness results for Fe-21Cr-12Ni-5Mn; two from the present study and one by Dessau.[6]
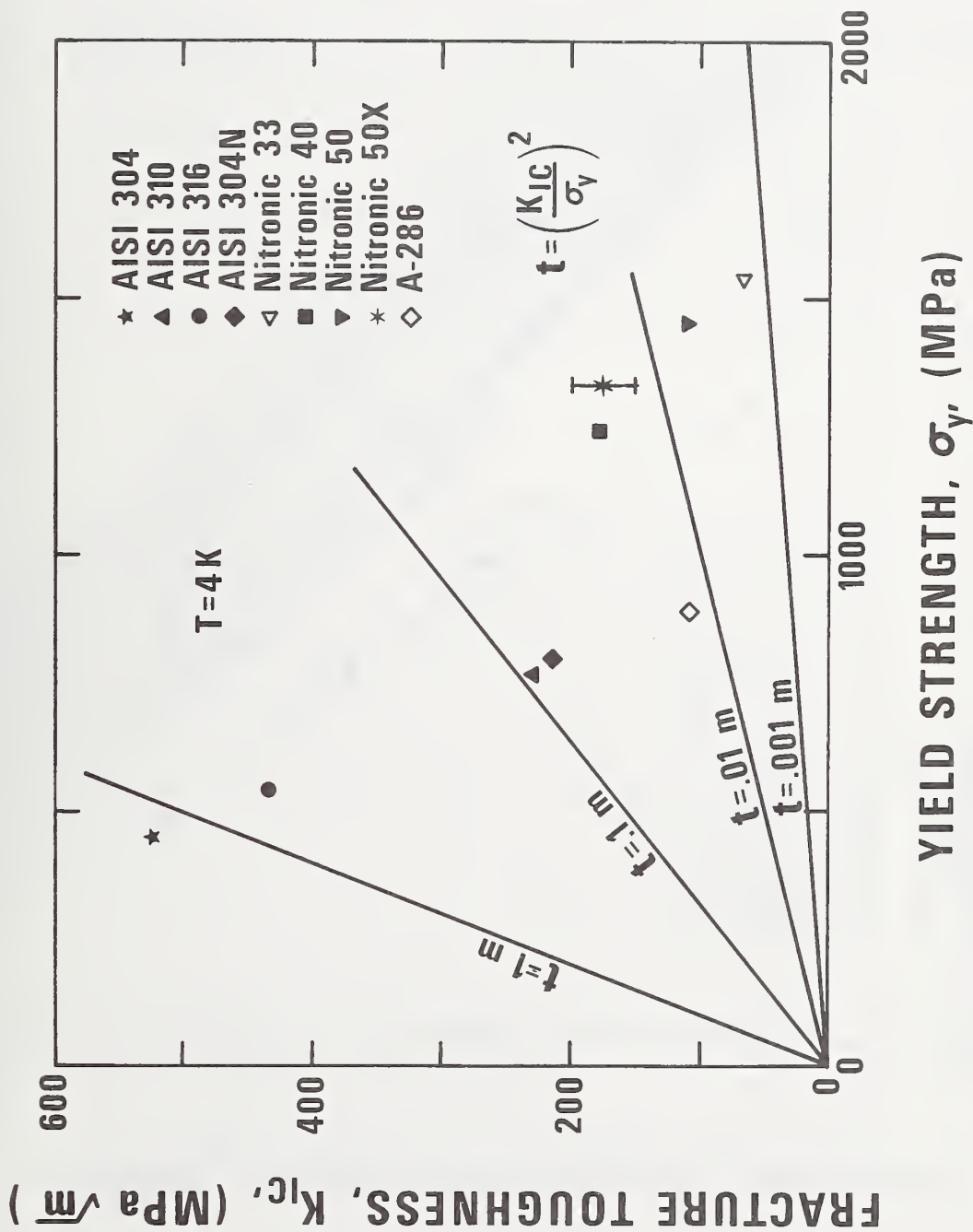
Figure 19. Fracture toughness plotted against yield strength at 4 K for conventional and nitrogen-strengthened austenitic stainless steels.

Figure 20.4 K Fatigue-crack-growth rate data for nitrogen-strengthened stainless steels obtained in the present study, for comparison with the range of data previously obtained for conventional austenitic stainless steels.
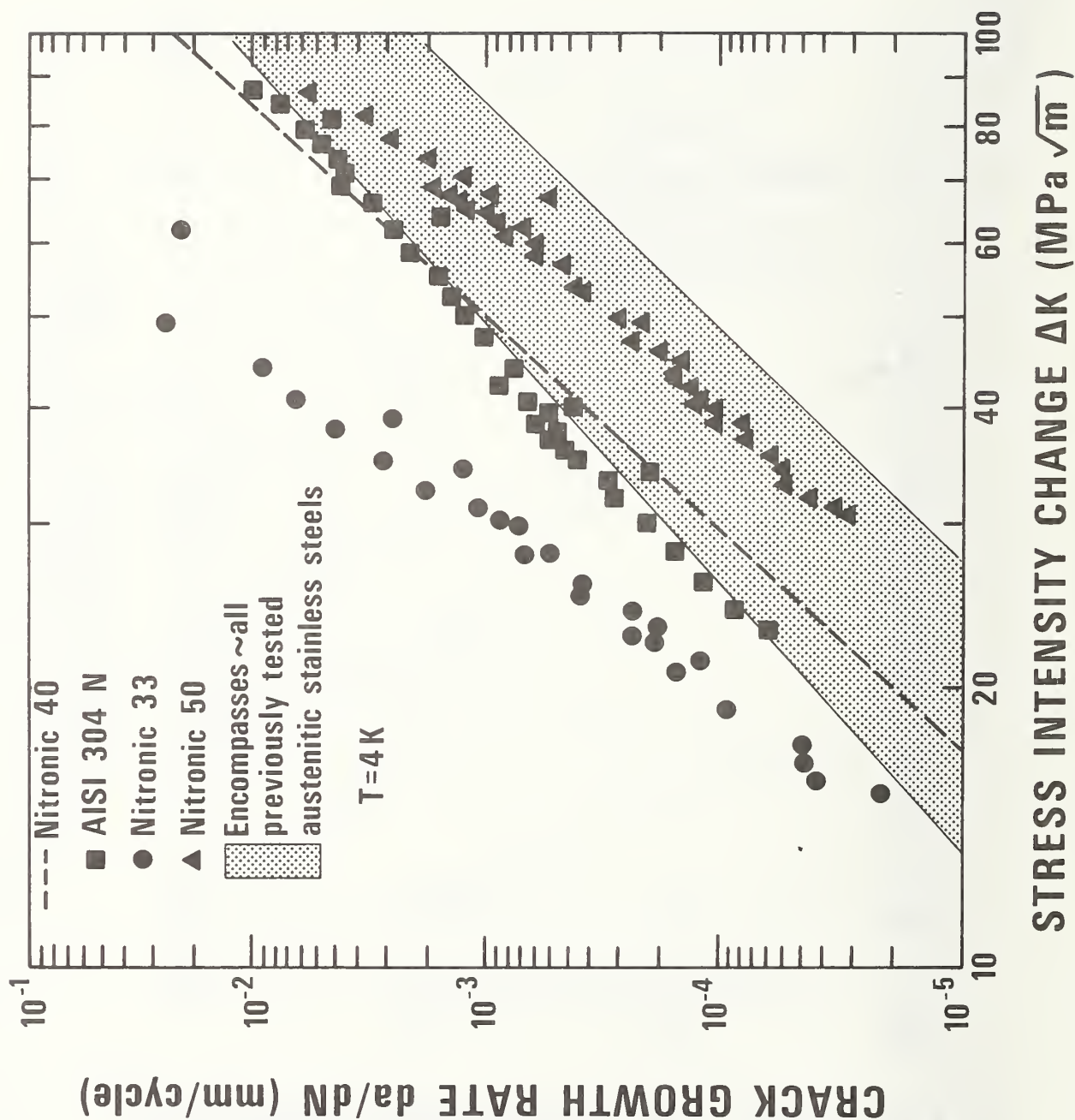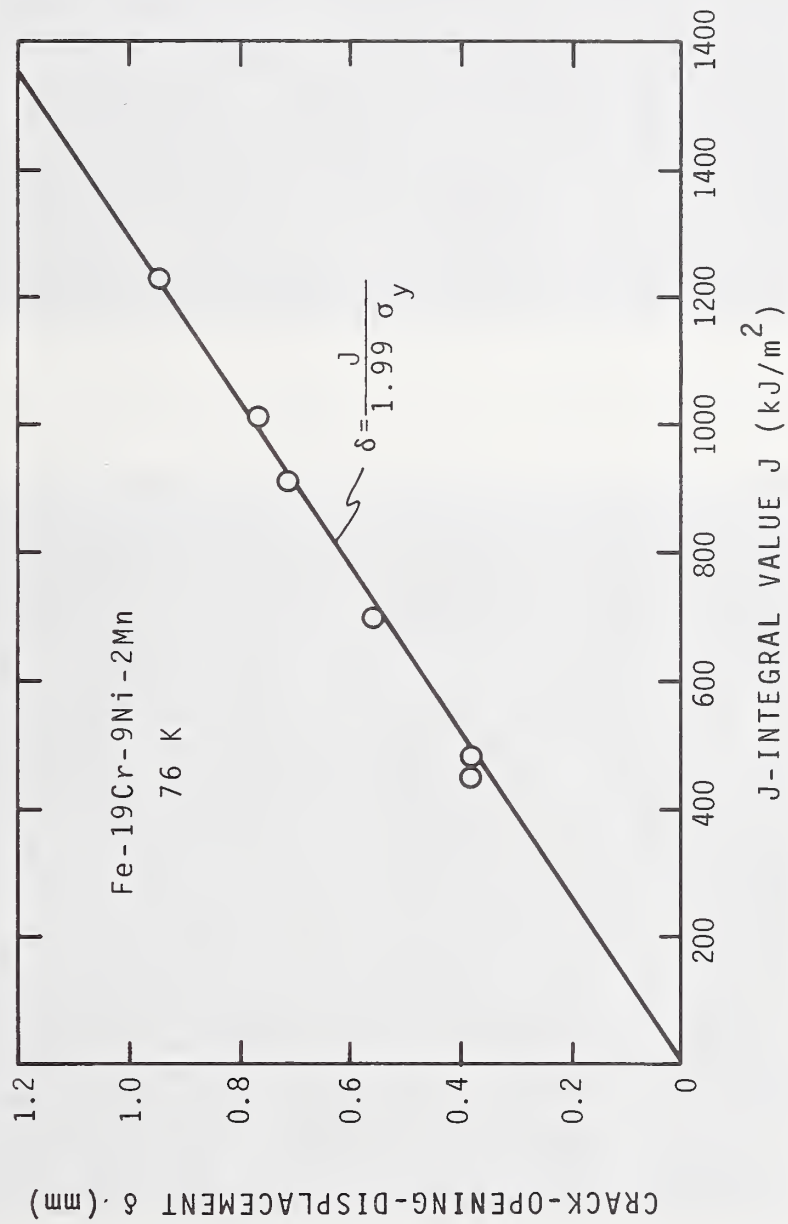
Figure 21. Crack-opening-displacement plotted against J-integral values for Fe-19Cr-9Ni-2Mn at 76 K.
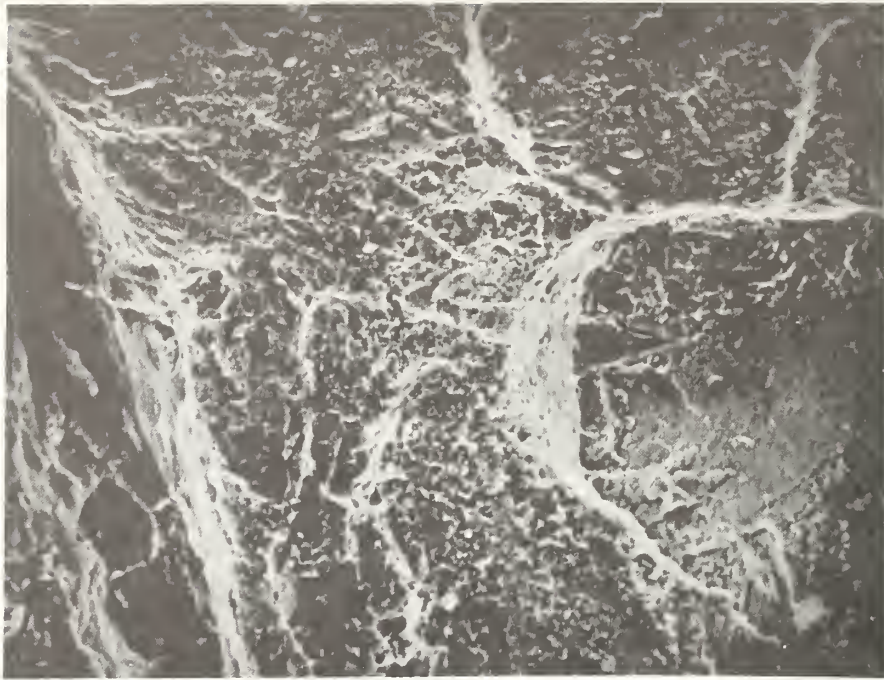
a. Fracture surface of Fe-19Cr-9Ni-2Mn tested at 4 K. 1000X.
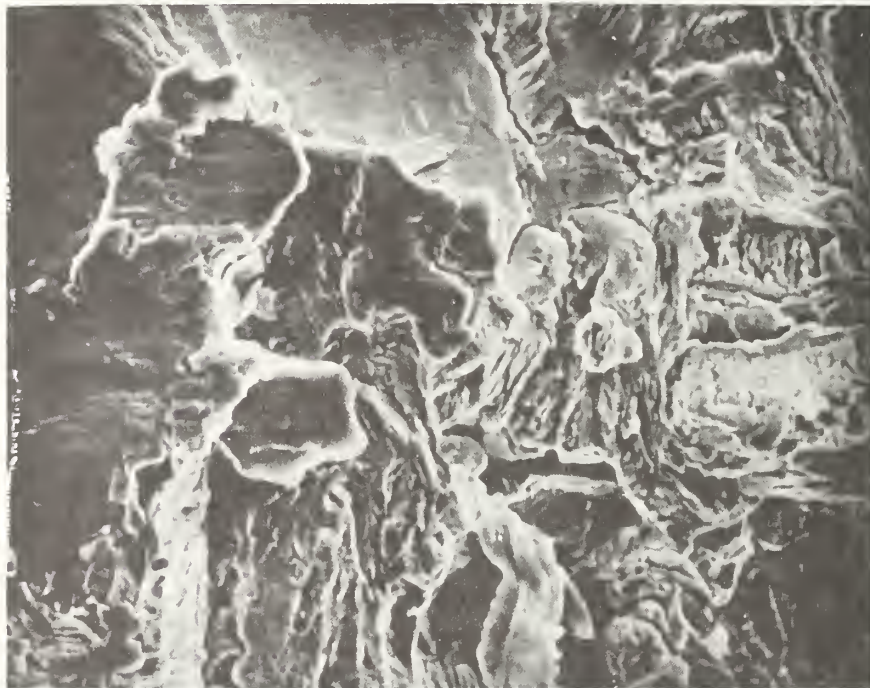
b. Fracture surface of Fe-18Cr-3Ni-13Mn tested at 4 K. 1000X.

Figure 22. SEM micrographs of fracture surfaces of toughness specimens fractured at 4 K.

c. Fracture surface of Fe-21Cr-12Ni-5Mn tested at 4 K. 1000X.
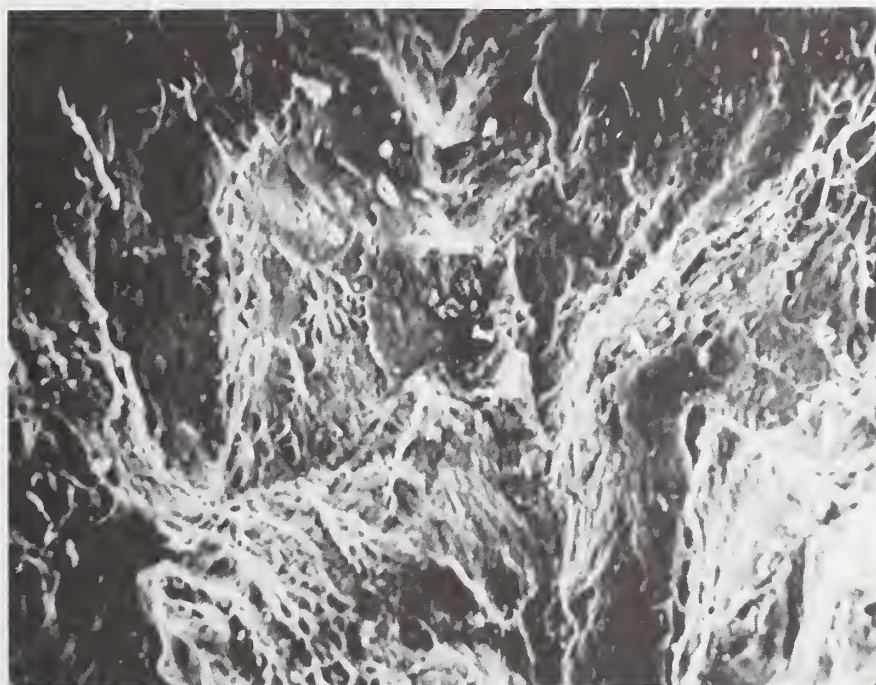
d. Fracture surface of Fe-21Cr-12Ni-5Mn-X tested at 4 K. 500X.

Figure 22 (continued). SEM micrographs of fracture surfaces of toughness
specimens fractured at 4 K.

153
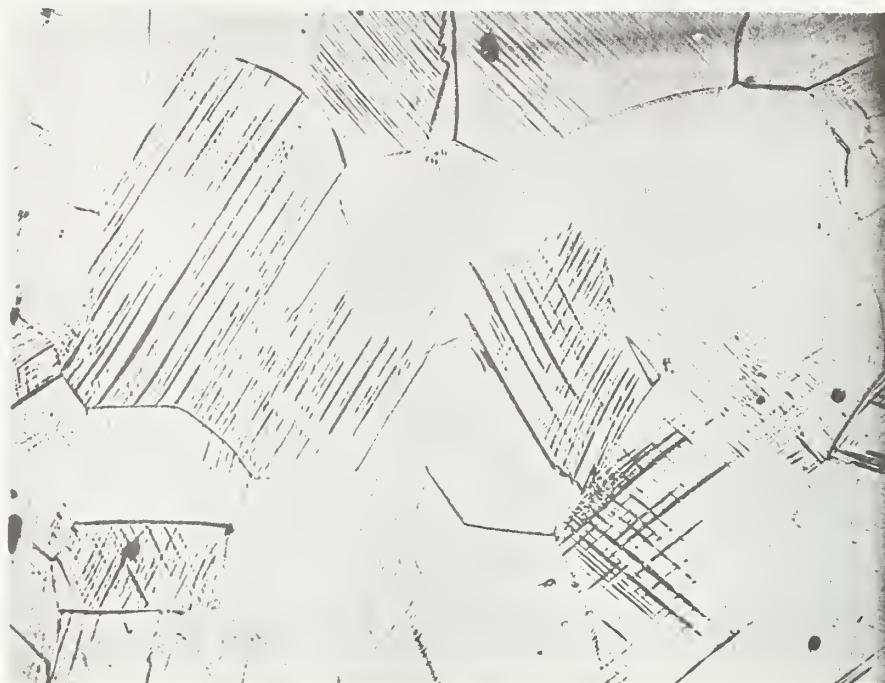
a. Fe-18Cr-3Ni-13Mn 450X.
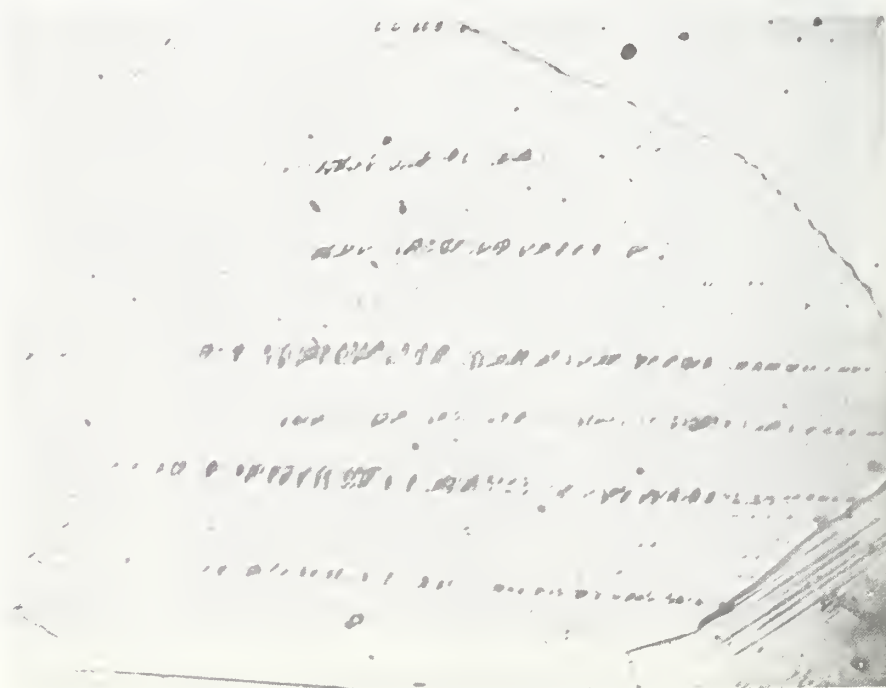
b. Fe-19Cr-9Ni-2Mn 850X.

Figure 23.Photomicrographs of sectioned tensile specimens fractured at 4 K.

STAINLESS STEEL WELDING

Evaluation of Stainless Steel Weld Metals
at Cryogenic Temperatures

National Bureau of Standards

EVALUATION OF STAINLESS STEEL WELD
METALS AT CRYOGENIC TEMPERATURES

Harry I. McHenry
Cryogenics Division
National Bureau of Standards
Boulder, CO   80302

Austenitic stainless steels such as AISI types 304 and 316 and the nitrogen strengthened 21Cr-6Ni-9Mn alloy (Nitronic 40) are readily weldable by all common welding processes, providing the appropriate consummables and procedures are used. The service experience with welded assemblies of these alloys has been satisfactory at cryogenic temperatures. A contributing factor to this success has been low design stresses; generally the stresses have been limited to about 140 MPa (20 ksi), the ASME allowable stress for AISI 304 and 316 stainless steels at room temperature. For large superconducting magnets, the enormous forces that must be contained and the limited space available for structure may necessitate operating at significantly higher stresses, stresses based on the strength of the alloy at the operating temperature. Many of the unwelded austenitic stainless steels exhibit excellent fracture toughness at temperatures down to 4 K in the base metal. However, weld metal fracture toughness has not yet been determined at 4 K. Charpy impact results at 76 and 20 K suggest that the toughness may be marginal at 4 K, particularly if the stress levels in the magnets are higher than current practice.

A program is being conducted to evaluate stainless steel welds at cryogenic temperatures. The objectives of the initial phase of investigation are:

1. To investigate the metallurgical factors contributing to the toughness, or degradation thereof, of stainless steel weld metals.

2. To develop a high strength, high fracture toughness, filler wire for welding nitrogen-strengthened stainless steels such as the 21Cr-6Ni-9Mn alloy.

3. To evaluate the fracture toughness of stainless steel welds at 4 K. The approach has been to draw on the experience and expertise of filler metal suppliers to develop the high strength, high fracture toughness, filler wire and to provide welds for the metallurgical and fracture mechanics evaluations conducted by NBS. The shielded metal arc process is being used to produce the test weldments because this process permits control of the weld deposit chemistry by modifying the chemistry of the electrode coating. Upon completion of the initial phase of the investigation, the most promising weld metals will be used to evaluate the influence of other welding processes and process variables on strength and toughness at 4 K. The test weldments will be supplied to NBS by an industrial firm with experience in fabricating cryogenic structures.

At the present time, three contracts with industry have been awarded and the work on each contract has been completed: (1) Armco Steel Corp., for the development of a high strength filler metal; (2) Arcos Corp., for the preparation of test weldments designed to study the effect of ferrite content, ferrite morphology and sensitization effects; and (3) Teledyne-McKay to prepare test weldments with AWS 330 filler metal. This report summarizes the work done on these contracts plus the related work done by NBS.

Metallurgical Effects on Toughness

A joint program is being conducted by NBS and the Arcos Corp. to investigate the effects of ferrite content, ferrite morphology and sensitization on toughness at cryogenic temperatures. The investigation is being conducted on AISI 316 base plate (25 mm thick) welded with AWS 316L electrodes.

The Arcos program consisted of manufacturing controlled chemistry (within AWS 316L chemistry limits) electrodes, welding a series of test plates and evaluating the influence of process variables on ferrite content. The chemistries and ferrite contents of the five electrodes and the test plate design are given here in the Arcos report. Electrodes 1 through 4 were formulated to systematically vary ferrite content from 0 to 12%. Electrode 5

was nominally the same as electrode 2 in chemistry except the carbon content was 0.059% which is typical of AWS 316 weld metal. Since carbon is an austenite stabilizer, the ferrite content of electrode 5 was essentially zero, i.e. comparable to electrode 1.

Arcos welded a series of ten test plates using the parameters summarized in Table 1. Test plates 1 through 4 were welded used electrodes 1 through 4, respectively, to systematically vary the ferrite content between 0 and 12%. Test plates 5, 9 and 10 were welded to evaluate the effect of carbon content and cooling rate on the degree of sensitization. Plate 5 (C = 0.059%) was welded using the same procedures used to weld Plate 1 (C = 0.031%), i.e. procedures that result in normal cooling rates. Plate 9 (C = 0.031%) and plate 10 (C = 0.059%) were welded using slow-cooling-rate welding parameters, i.e. high preheat and interpass temperatures, high current and low travel speed. Plates 6, 7 and 8 were welded using electrode 3 (9% ferrite) and welding parameters designed to significantly alter the cooling rate in order to vary the ferrite morphology.

Arcos also conducted a study of ferrite in 316L weld metal. Ferrite content was measured for a variety of welding conditions resulting in differing cooling rates. The results are reported in the Arcos report.

The ten test plates have been delivered to NBS and machining of test specimens is in progress. NBS will conduct tensile, Charpy impact and fracture toughness tests and a metallurgical evaluation on each of the weldments. The metallurgical evaluation of the weldments will consist of x-ray diffraction measurement of ferrite content, metallographic examination of ferrite morphology and sensitization tests on the weld metal and the HAZ.

High Strength Filler Wire Development

Armco Steel Corp. conducted a program to develop a high strength filler wire for welding nitrogen strengthened stainless steels such as the 21Cr-6Ni-9Mn

alloy (Nitronic 40). The results of their program are summarized here in the Armco report. As part of this contract, Armco will supply NBS with a test plate (25 mm thick, .46 m of weld length) from each of the three chemistries evaluated. Since nitrogen has an adverse effect on toughness, the three test plates will all be welded with the minimum nitrogen level, to permit comparison of the experimental alloys with the data on AWS 300-series weld metals.

Evaluation of AWS 330

Teledyne-McKay Corp. furnished NBS with two test plates welded with a modified version of AWS 330 filler metal. The principal modification is in Mn content, the modified 330 has nominally 4.5% Mn instead of the 2.5% Max specified in AWS 330. Two joint configurations were evaluated. An open joint having the AWS specification A5.4 weld pad configuration was used to give undiluted weld metal in the test section. A double-Vee joint with a 2.4 mm land typical of commercial practice was used to give a diluted weld joint. The base metal was 25 mm thick plate of AISI 304L stainless steel in the annealed condition.

Teledyne-McKay also evaluated welded test pads of the same batch of electrodes used for the test plates. The test pads were prepared in accordance with AWS specification A5.4 using 19 mm thick mild steel plates buttered with the test electrodes. Tests were conducted to determine the weld metal composition, tensile properties at room temperature and Charpy impact toughness at 76 K. The results are summarized in Table 2.

The test plates have been machined into tensile and fracture toughness specimens for evaluation by NBS. The tensile properties were determined at room temperature, 76 K and 4 K. The results, summarized in Table 3, indicate that dilution with the base metal causes a slight decrease in strength. The strength at 4 K, 860 MPa (125 ksi) yield and 1090 MPa (158 ksi) ultimate, of the

diluted weld joint is higher than the strengths of AISI 304 and 316 base metals at 4 K. Fracture toughness tests are in progress.

Future Work

During FY 78, the evaluation of the test plates furnished by Arcos, Armco and Teledyne-McKay will be completed. On the basis of the test results, filler metals will be selected for further evaluation using the gas metal arc, gas tungsten arc and the submerged arc processes.

Table 1. AISI 316 stainless steel test plates welded with AWS 316 electrodes by Arcos Corp.

NBS Plate No.	Arcos Plate No.	Electrode No.	Welding Parameters Current amps	Volts	Travel ipm	Interpass Temp. °F	No. of Passes	Ferrite % Ave.*	Ferrite No. FN Ave.*
1	T12,005R	1	130	24	6- 8	200-250	31	0.13	0.12
2	T12,006R	2	130	24	6- 8	200-250	25	4.1	4.5
3	T12,007R	3	130	24	6- 8	200-250	29	8.5	9.2
4	T12,008R	4	130	24	6- 8	200-250	33	10.1	11.0
5	T12,009R	5	130	24	6- 8	200-250	33	1.2	1.3
6	T12,007R-II	3	100	24	8-10	200-250	39	6.5	7.1
7	T12,007R-III	3	160	24	4- 6	200-250	26	9.7	10.5
8	T12,007R-IV	3	160	26	4- 6	550-650	17	7.3	7.9
9	T12,005R-IV	1	160	26	4- 6	550-650	22	0.67+	0.73+
10	T12,009R-IV	5	160	26	4- 6	550-650	23	2.2	2.4

*12 Readings
+Fissures observed on surface

164

Table 2. Properties of AWS 330 modified test pads measured by Teledyne-McKay.

Weld Metal Composition:

	%C	%Mn	%Si	%P	%S	%Cr	%Ni	%Mo	%N
AWS 330	.25 max	2.5 max	0.6 max	.04 max	.03 max	14 to 17	33 to 37	---	----
Pad 1	.147	4.47	.51	.019	.007	17.80	34.40	.25	----
Pad 2	.136	4.70	.45	---	.006	17.82	34.36	---	.044

Tensile Properties at Room Temperature (.503 inch diameter specimen)

Ultimate MPa/ksi	Yield MPa/ksi	% Elong. m2"	% RA
585/84.8	382/55.4	45	56

Charpy Impact at 77 K

Energy		Lateral Expansion	
J	Ft-Lbs	mm	mils
91.0	66.9	1.45	57
90.0	66.2	1.17	46
80.6	59.3	1.30	51
80.0	58.5	1.37	54
87.4	64.3	1.35	53
Average: 84.3	62.2	1.33	52.2

Table 3. Tensile properties of AWS 330 weld metal.

Sample	Temperature	σ_y (ksi)	σ_{uts} (ksi)	ε_f %
		UNDILUTED		
A1	RT	66	83	29
B4	RT	58	85	32
A2	76 K	107	142	38
B2	76 K	104	141	42
A4	4 K	128	169	30
B3	4 K	135	174	31
		DILUTED		
B1	RT	59.9	84.9	34
A2	RT	55.5	83.1	35
A3	76 K	91.5	131	47
B3	76 K	88.9	133	49
A4	4 K	124	157	42
B4	4 K	125	159	44

Weldability of 21-6-9 Stainless Steel

Armco

WELDABILITY OF 21-6-9 STAINLESS STEEL
(ARMCO NITRONIC 40 STAINLESS STEEL)

R. Harry Espy
Armco Steel Corporation
Middletown, OH 45043

INTRODUCTION

The 21-6-9 stainless steel is a nitrogen strengthened austenitic
alloy having good mechanical properties over a wide range of tem-
peratures. Its .2% yield strength at room temperature is about
two times that of Type 304 stainless steel. The alloy is readily
joined by welding using any of the standard processes in use today.
When a matching weld filler is employed (NITRONIC 40W), sound welds
in all thicknesses having good toughness at temperatures to -100°F
are readily obtained. In welds where thicknesses are less than a
1/4", satisfactory toughness has been obtained when tested at
-320°F. Where thicknesses of the weld are 1/4" or greater, tough-
ness at -320°F as measured by the CVN test average about 10 ft. lbs.
Such a value when compared to Type 304 stainless steel (Type 308
weld metal - 26 ft. lbs. at -320°F) is not favorable, espe-
cially when acceptable limits of 15 to 20 ft. lbs. are used. At
room temperature, the impact strengths of heavy weldments in Type
304 (308 weld metal) and 21-6-9 (NITRONIC 40W - weld metal) are
about the same - 40 to 45 ft. lbs., even though the yield strength
of 21-6-9 weld metal (NITRONIC 40W) is 20,000 psi higher than the
308 weld metal. The loss in impact strength at -320°F for 21-6-9
weld metal is related to the fact that the yield strength at -320°F
is increased more than that of the 308 weld metal as shown in the
table.

	Room Temperature		-320°F	
	.2% Yld. Str.	CVN Toughness	.2% Yld. Str.	CVN Toughness
308 Weld Metal SMA Process	62,000	43 ft. lbs.	78,000 psi	26 ft. lbs.
21-6-9 Weld Metal (NITRONIC 40W) SMA Process	82,000	40 ft. lbs.	160,000 psi	10 ft. lbs.

Development work under this contract aimed at producing a weld
having improved toughness and a reasonable strength at -320°F
was divided into 3 areas as shown.

Cr Ni Mn (weight percent)

(1) 13-20-9 + Cb (Ferrite free) N & Si Varied

(2) 20-10-9 (Ferrite containing) N Varied

(3) 18-16-9 (Ferrite free) N Varied

TEST PROCEDURE

Prepare a total of eleven lots of covered welding electrodes using 3 base core wire chemistries as shown. Each lot designed to produce the aim weld deposit composition listed.

Type 13-20-9+Cb (N&Si Varied) Ferrite-Free

		C	Mn	P	S	Si	Cr	Ni	N	Cb
Core Wire Chemistry Aim		.04	9.0	.015	.015	.40	14.0	20.0	low	1.8
SMA Weld Deposit Aim	(A)	"	"	"	"	.30	"	"	.08	"
	(B)	"	"	"	"	"	"	"	.14	"
	(C)	"	"	"	"	"	"	"	.20	"
	(D)	"	"	"	"	.60	"	"	.08	"
	(E)	"	"	"	"	"	"	"	.20	"

Type 20-10-9 (N Varied) Ferrite Containing

		C	Mn	P	S	Si	Cr	Ni	N
Core Wire Chemistry Aim		.04	9.0	.015	.015	.40	19.5	9.0	.04
SMA Weld Deposit Aim	(F)	"	"	"	"	"	20.0	"	.08
	(G)	"	"	"	"	"	20.5	"	.14
	(H)	"	"	"	"	"	21.0	"	.20

Type 18-16-9 (N Varied) Ferrite-Free

		C	Mn	P	S	Si	Cr	Ni	N
Core Wire Chemistry Aim		.04	9.0	.015	.015	.40	18.0	16.0	.04
SMA Weld Deposit Aim	(I)	"	"	"	"	"	"	"	.08
	(J)	"	"	"	"	"	"	"	.14
	(K)	"	"	"	"	"	"	"	.20

Examine the SMA weld deposits obtained with each of the eleven lots of covered electrodes for:

(1) Tensile Strength at 300°K (Room Temperature)

(2) Tensile Strength at 77°K (-320°F)

(3) CVN Toughness at 300°K (Room Temperature)

(4) CVN Toughness at 77°K (-320°F)

(5) FN (Ferrite Number) at 300°K (Room Temperature)

(6) Metallurgical Structure

The welds from which the above specimens were obtained were made according to AWS 5.4-69. The tensile specimens for test at 300°K (room temperature) were .505" diameter and for test at 77°K were .357" diameter. The CVN specimens were 10 mm as per ASTM E23. The metallographic specimens were sectioned transverse to weld direction and examined optically up to 500X. Analysis for composition was by X-ray, emission and Leco combustion methods calibrated with acceptable standards. Magnetic attraction of test piece fracture faces was measured by magnetized needle and rated for change as an indicator of austenite stability during plastic deformation at test temperature.

TEST RESULTS

The test results using the eleven groups (A to K) of coated electrodes for deposition of welds are shown in Tables I to IV. Weldability of the coated electrode lots appeared normal, each performing in a uniform manner when good stainless steel welding practice was employed.

DISCUSSION OF TEST RESULTS

In comparing properties of the several alloy systems examined in this project the unwelded 21-6-9 (Armco NITRONIC 40) base metal and matching 21-6-9 (Armco NITRONIC 40W) all-weld metal are used as shown below.

21-6-9 BASE METAL PROPERTIES (TESTED UP TO 5" THICK)

Composition Typical	C	Mn	P	S	Si	Cr	Ni	N
	.03	9.0	.025	.015	.60	20.5	6.75	.30

Tensile	Room Temperature					-320°F				
	U	Y	E	R	Mag.	U	Y	E	R	Mag.
	103	58	–	70%	–	203	150	–	24%	–

Toughness	205'#s CVN	65'#s CVN
Structure	Austenite	Austenite

171

21-6-9 SMA ALL-WELD METAL PROPERTIES (1" THICK)

Composition Typical	C .03	Mn 9.0	P .020	S .017	Si .40	Cr 20.5	Ni 0.5	N .25	FN 5

Tensile			Room Temperature						-320°F				
	U	Y	E	R	Mag.	Defects	U	Y	E	R	Mag.	Defects
	109	82	31%	46%	No Change	None	205	160	29%	26%	No Change	None

Toughness	40'#s CVN		No	None	10'#s CVN		No	None

Structure   1 to 5% Ferrite in a Matrix of Austenite

U — Ultimate Tensile Strength KSI   Y — .2% Yld. Str. KSI
E — Elongation 2"   R — Reduction of Area   Mag. — Magnetism

The lesser toughness of welds when compared to unwelded base metal (wrought) is related to the cast structure of the weld plus the fact that the weld is also higher in strength. This phenomena is similar to that seen when Type 304 base metal is compared to Type 308, its matching weld metal.

13-20-9+Cb (With N Varied) Ferrite-Free

The use of Cb in this ferrite-free weld deposit system resulted in sound defect free welds in all cases with the exception of a few points of porosity noted in the higher N containing welds. From the results tabulated below it appears that at -320°F yields of approximately 100 KSI with toughnesses greater than 15'#s can be obtained with N contents of approximately .10. The effect of Si in this Cb containing system was not clear with variations in the range examined being of no significance.

Effect of N on Properties of
Cb Containing Ferrite-Free Weld Deposits

Code	N	Si	Room Temp.		-320°F	
			Y	CVN	Y	CVN
A	.05	.30	65	46'#s	91	28'#s
D	.09	.53	65	39'#s	94	22'#s
B	.11	.30	66	35'#s	103	15'#s
E	.16	.44	69	37'#s	98	19'#s
C	.18	.23	75	27'#s	117	12'#s

Y — .2% Yld. Str. KSI

20-10-9 (N Varied) Ferrite Containing

The ferrite levels, obtained with this alloy balance, of 1.4 to
4.2 FN were sufficient in all cases to produce sound defect-free
welds. While strengths were good even at the lowest level of N
used, none of the toughness values at -320°F were satisfactory.
Tabulated below is a summation of results related to N contents.

Effect of N on Properties
of Welds Containing Ferrite

		Room Temp.		77°K (-320°F)	
Code	N	Y	CVN	Y	CVN
F	.09	74	47'#s	115	9'#s
G	.14	73	51'#s	137	10'#s
H	.19	80	49'#s	153	9'#s

Y - .2% Yld. Str. KSI

18-16-9 (N Varied) Ferrite-Free

In selecting this chemistry it was known that varying degrees of
grain foundary defects would occur. To determine at what strength
such grain boundary weaknesses would become a problem three levels
of N were examined. Good toughness-strength relationships appear
possible at approximately .15 N with yields at -320°F of approxi-
mately 126 KSI and toughnesses of approximately 18'#s.

CONCLUSIONS AND FUTURE WORK

In this project to develop a weld metal for joining heavy sections
of 21-6-9 stainless steel (Armco NITRONIC 40) three basic alloy
systems were examined and can be commented on as follows. The
ferrite-free 18-16-9 with N at approximately .15 offered the best
combination of toughness (18'#s CVN) and strength (126 KSI .2 Yield)
at -320°F. The grain boundary problem which had little effect on
CVN toughness is deserving of further evaluation. The ferrite-free
13-20-9+Cb with N at approximately .10 gave sound defect-free welds
with an acceptable toughness (15'#s CVN) at a lower level of
strength (100 KSI .2 Yield) at -320°F. The ferrite containing
20-10-9 welds were all sound and free of defects but did not ex-
hibit any acceptable levels of toughness.

Weld joints in 1" thick 21-6-9 plate will be made using one
chemistry from each of the three weld deposit groups and for-
warded to the NBS lab at Boulder for J-integral testing.

TABLE I – EFFECT OF N ON PROPERTIES OF LOW Si-Cb CONTAINING FERRITE-FREE WELD DEPOSITS

13-20-9+Cb (LOW Si WITH N VARIED) – (FERRITE-FREE) SMA WELD METAL 1" AS WELDED

A

Composition	C	Mn	P	S	Si	Cr	Ni	N	Cb	FN
Aim	.04	9.0	.015	.015	.30	14.0	20.0	.08	1.8	
Actual	.06	8.9	.013	.007	.30	14.4	19.6	.05	1.6	0

Tensile

	U	Y	E	R	Mag.	Defects
Room Temperature	81	65	29%	52%	None	None
-320°F	140	91	33%	38%	None	None

Toughness: 46'#s CVN   28'#s CVN

Structure: 0 to 4% Columbium Carbides (Not Interconnected) in a Matrix of Austenite

---

B

Composition	C	Mn	P	S	Si	Cr	Ni	N	Cb	FN
Aim	.04	9.0	.015	.015	.30	14.0	20.0	.14	1.8	
Actual	.06	9.5	.007	.009	.30	14.7	20.0	.11	1.6	0

Tensile

	U	Y	E	R	Mag.	Defects
Room Temperature	87	66	26%	43%	None	None
-320°F	146	103	25%	27%	None	None

Toughness: 35'#s CVN   15'#s CVN   2 porosity pts.

Structure: 0 to 7% Columbium Carbides (Not Interconnected) in a Matrix of Austenite

---

C

Composition	C	Mn	P	S	Si	Cr	Ni	N	Cb	FN
Aim	.04	9.0	.015	.015	.30	14.0	20.0	.20	1.8	
Actual	.06	10.8	.004	.006	.23	14.7	19.8	.18	1.5	0

Tensile

	U	Y	E	R	Mag.	Defects
Room Temperature	94	75	24%	47%	None	None
-320°F	154	117	20%	21%	None	None

Toughness: 27'#s CVN   12'#s CVN   3 porosity pts.   1 porosity pt.

Structure: 0 to 6% Columbium Carbides (Not Interconnected) in a Matrix of Austenite

---

U – Ultimate Tensile Strength KSI   Y – .2% Yield Strength KSI
E – Elongation 2"   R – Reduction of Area   Mag. – Magnetism

TABLE II - EFFECT OF N ON PROPERTIES OF HIGH Si-Cb CONTAINING FERRITE-FREE WELD DEPOSITS

13-20-9+Cb (HIGH Si WITH N VARIED) - (FERRITE-FREE) SMA WELD METAL 1" AS WELDED

Composition	C	Mn	P	S	Si	Cr	Ni	N	Cb	FN
Aim	.04	9.0	.015	.015	.60	14.0	20.0	.08	1.8	
D Actual	.07	9.1	.007	.007	.53	14.8	20.1	.09	1.9	0

Tensile — Room Temperature

U	Y	E	R	Mag.	Defects
82	65	29%	52%	None	None

Toughness   39'#s CVN

Structure   0 to 5% Columbium Carbide (Not Interconnected) in a Matrix of Austenite

Tensile — -320°F

U	Y	E	R	Mag.	Defects
127	94	13%	22%	None	None

Toughness   22'#s CVN

Composition	C	Mn	P	S	Si	Cr	Ni	N	Cb	FN
Aim	.04	9.0	.015	.015	.60	14.0	20.0	.20	1.8	
E Actual	.06	10.4	.004	.005	.44	14.4	20.0	.16	1.8	0

Tensile — Room Temperature

U	Y	E	R	Mag.	Defects
86	69	29%	43%	None	None

Toughness   37'#s CVN

Structure   2 to 7% Columbium Carbides (Not Interconnected) in a Matrix of Austenite

Tensile — -320°F

U	Y	E	R	Mag.	Defects
140	98	22%	20%	None	None

Toughness   19'#s CVN

U - Ultimate Tensile Strength KSI   Y - .2% Yield Str. KSI

E - Elongation 2"   R - Reduction of Area   Mag. - Magnetism

TABLE III – EFFECT OF N ON PROPERTIES OF FERRITE CONTAINING WELD DEPOSITS

20-10-9 (FERRITE CONTAINING) SMA WELD METAL 1" AS WELDED

Composition

	C	Mn	P	S	Si	Cr	Ni	N	FN
Aim	.04	9.0	.015	.015	.40	20.0	9.0	.08	
F Actual	.07	9.1	.006	.010	.22	20.2	9.1	.09	4.2

Tensile

	Room Temperature						-320°F					
	U	Y	E	R	Mag.	Defects	U	Y	E	R	Mag.	Defects
	93	74	34%	34%	No Change	None	171	115	17%	17%	Mod. Incr.	None

Toughness: 47'#s CVN — No Change | 9'#s CVN — No Change

Structure: 2 to 8% Ferrite in a Matrix of Austenite

Composition

	C	Mn	P	S	Si	Cr	Ni	N	FN
Aim	.04	9.0	.015	.015	.40	20.5	9.0	.14	
G Actual	.07	8.9	.006	.011	.23	20.3	9.0	.14	2.4

Tensile

	Room Temperature						-320°F					
	U	Y	E	R	Mag.	Defects	U	Y	E	R	Mag.	Defects
	95	73	37%	47%	No Change	None	185	137	15%	15%	Mod. Incr.	None

Toughness: 51'#s CVN — No Change | 10'#s CVN — No Change

Structure: 0 to 5% Ferrite in a Matrix of Austenite

Composition

	C	Mn	P	S	Si	Cr	Ni	N	FN
Aim	.04	9.0	.015	.015	.40	21.0	9.0	.20	
H Actual	.07	8.9	.006	.012	.20	20.3	9.0	.19	1.4

Tensile

	Room Temperature						-320°F					
	U	Y	E	R	Mag.	Defects	U	Y	E	R	Mag.	Defects
	101	80	33%	45%	No Change	None	208	153	29%	24%	M to L Incr.	None

Toughness: 49'#s CVN — No Change | 9'#s CVN — 1 porosity pt.

Structure: 0 to 3% Ferrite in a Matrix of Austenite

U – Ultimate Tensile Strength KSI   Y – .2% Yld. Strength KSI
E – Elongation 2"   R – Reduction of Area   Mag. – Magnetism

TABLE IV - EFFECT OF N ON PROPERTIES OF FERRITE-FREE WELD DEPOSITS

18-16-9 (FERRITE-FREE) SMA WELD METAL 1" AS WELDED

Specimen I

Composition	C	Mn	P	S	Si	Cr	Ni	N	FN
Aim	.04	9.0	.015	.015	.40	18.0	16.0	.08	
I Actual	.06	9.0	.006	.008	.19	18.1	16.1	.09	0

Tensile	U	Y	E	R	Mag.	Defects
Room Temperature	83	64	19%	20%	None	10% M.C.
−320°F	160	110	23%	18%	None	30% M.C.

Toughness		Mag.	Defects
Room Temperature	53 #s CVN	None	60% M.C.
−320°F	27 #s CVN	None	40% M.C.

Structure: Fully Austenitic With a Varied Distribution of a Grain Boundary Participate Plus a Few Grain Boundary Separations

Specimen J

Composition	C	Mn	P	S	Si	Cr	Ni	N	FN
Aim	.04	9.0	.015	.015	.40	18.0	16.0	.14	
J Actual	.06	8.9	.006	.009	.22	18.1	16.2	.14	0

Tensile	U	Y	E	R	Mag.	Defects
Room Temperature	88	66	21%	24%	None	15% M.C.
−320°F	156	124	15%	10%	None	15% M.C.

Toughness		Mag.	Defects
Room Temperature	49 #s CVN	None	75% M.C.
−320°F	20 #s CVN	None	50% M.C.

Structure: Fully Austenitic With a Varied Distribution of a Grain Boundary Participate Plus a Few Grain Boundary Separations

Specimen K

Composition	C	Mn	P	S	Si	Cr	Ni	N	FN
Aim	.04	9.0	.015	.015	.40	18.0	16.0	.20	
K Actual	.05	9.0	.007	.009	.22	18.0	16.2	.18	0

Tensile	U	Y	E	R	Mag.	Defects
Room Temperature	93	71	25%	26%	None	25% M.C.
−320°F	162	134	10%	12%	None	10% M.C.

Toughness		Mag.	Defects
Room Temperature	44 #s CVN	None	75% M.C.
−320°F	13 #s CVN	None	50% M.C.

Structure: Fully Austenitic With a Varied Distribution of a Grain Boundary Participate Plus a Moderate Number of Grain Boundary Separations

---

U – Ultimate Tensile Strength Y – .2% Yield Strength KSI
E – Elongation 2" R – Reduction of Area Mag. – Magnetism
M.C. – Micro Condition

Ferrite in Type 316L Weld Metal

Arcos

FERRITE IN TYPE 316L WELD METAL

R. David Thomas, Jr.
Arcos Corporation
1500 South 50th Street
Philadelphia, PA 19143

BACKGROUND

For the Magnetic Fusion Energy program, the Department of Energy has authorized an investigation of the materials, including weldments, to be used in the construction of large superconducting magnets. Involved in the study is the notch toughness of the materials when operating at liquid helium temperatures. The structures will involve thick weldments; hence, welding processes may require large welding energy input. Besides shielded metal arc, the processes will probably involve submerged-arc and electroslag.

The location of welds may be such that magnetic permeability should be at a minimum. Most austenite chromium-nickel stainless steel weld metals are designed to have small amounts of ferrite in order to avoid cracks and fissures, especially in heavy weldments and with high welding energy input. Control of the amount of ferrite may become critical in order to minimize the magnetic permeability and minimize the hazard of weld metal cracks and fissures.

Many development projects have been conducted, and considerable documentation has appeared, particularly in the past ten years, on the reliability of measurements of ferrite in weld metals. The effect of compositional changes and the effect of dilution are reasonably well known. The reliability of measurements under standard welding conditions has been greatly improved. The effect of welding variables on the reproducibility of the measurements has not been adequately studied. This area was studied in a preliminary way and the results reported herein.

ARCOS PROGRAM

Five weld metal compositions were obtained using a single composition of core wire and adjusting the ingredients in the electrode coverings to give the compositions shown in Table 1. Electrodes were all of the AC-DC titania type, classified under the AWS system as "E316L-16" except one with higher carbon would be classified "E316-16".

The location of compositions with respect to ferrite number is shown in Figure 1. Actual measured ferrite under controlled conditions specified in the AWS-WRC procedure (Ref. 1) appears in Table 1.

The ferrite variation in Type 316L is represented by electrode numbers 1 through 4. Believing that the low carbon grades are more sensitive to fissures than normal carbon grades when the ferrite is low, one additional electrode, No. 5, was prepared with essentially no ferrite but with a higher carbon level. This test will help to verify whether the low carbon is essential for fracture toughness.

As directed by the National Bureau of Standards, weldments are being prepared in accordance with Figure 2, using welding parameters appearing in Table 5. All electrodes use the welding parameters which are typical of arc welding with this size (5/32") electrode. Electrode No. 3, having an intermediate amount of ferrite, is used with parameters giving considerably less and considerably greater weld energy input. Three of the electrodes, Nos. 1, 3, and 5, are also being used with high energy input and a high preheat and interpass temperature. These ten weldments are identified in the contract as Tasks A and C.

Before deciding on the conditions to be used in Tasks A and C, Task B was carried out to assess the effect of welding variables on ferrite measurements. Weld beads were deposited under conditions where compositional changes due to dilution would not be a factor, all using the intermediate ferrite electrode No. 3. An outline of the types of weld beads being examined is shown in Figure 3.

All testing of the large weldments is to be done by the National Bureau of Standards, using fracture mechanics type specimens at cryogenic temperatures.

PURPOSE OF TASK B

One object of the task is to determine the reproducibility of the ferrite readings, using the Magne-Gage testing procedure recommended by AWS-WRC. Whereas much of the literature indicates wide variations, many of the reports involve multi-pass welds wherein several welding cycles are involved. All of the tests in

Task B were conducted on single-pass welds. Where discrepancies in the data occur, an attempt was made to determine the cause by considering the factors which may account for the scatter.

Another object was to consider the effect of wide differences in welding parameters. In the 5/32" diameter welding electrode, it is possible to vary the current from 100 amps to 160 amps and still have reasonable stable welding conditions. It was also possible to vary the welding speed from nominally 3 inches per minute (actually 3-1/2) up to 12 inches per minute (actually 11-1/2). This caused the welding energy input to vary from a minimum of 11.7 kJ/in to 71.3 kJ/in.

The simplicity of bead-on-plate deposition allowed us to make a number of tests with a limited budget. Such welds, however, would not be typical of that which would be encountered in heavy weldments. Consequently, a few tests were made with beads deposited in a pre-machined weld groove.

Cooling rate is known to be affected by the ambient temperature of the metal surrounding the weld bead. By dramatically changing the preheat within limits which might be encountered in ordinary welding (from room temperature to 600 F), the effect of ambient temperature on ferrite measurements was evaluated.

As the data were assembled, it was possible to test theories of the solidification mechanism of stainless weld metal against results obtained. By this means, it was hoped that a better understanding of the role of ferrite in welding might be obtained, possibly to lead to design of welding filler metals and/or welding procedures which will permit greater control of ferrite level.

DATA SCATTER

The ferrite readings obtained in each of the various tests are given in Tables 2, 3, and 4. In the first series of tests five readings were taken along the length of the weld. Subsequently, ten readings were used in order to obtain a more

183

precise average and standard deviation of the readings. When the averages and standard deviations were plotted against welding energy (Figure 4), a trend was indicated; however, a relatively wide scatter in the data was seen. Some of the scatter appeared to be a consistent change in ferrite readings from the beginning to the end of the weld bead, as shown in the average of the four to six figures in a given location. Thus part of the data scatter would seem to be accounted for by progressive changes that occur during the welding operation. The WRC-AWS method calls for a light mechanical dressing of the top of the weld surface before making the readings. (Note: The standard procedure calls for the use of a file; we chose to use a coarse grinding wheel.) It has been reported that this has the effect of raising the average ferrite reading, and we confirmed that finding. One explanation has been that the ferrite measuring magnet can more uniformly contact the surface of the weld when its ripples are removed. If this were the case, one would expect more uniform data from the ground welds than from the unground welds. The standard deviation calculated on the ground specimens, however, generally scatter as widely as the unground specimens, raising doubt as to whether greater reliability is actually obtained by this mechanical dressing of the weld.

In order to get meaningful data to illustrate progressive changes during the welding operation, all of the readings within a given area were averaged. Thus the data points appearing in Figure 5 include the significant differences arising from the mechanical grinding of the second weld bead.

EFFECT OF WELDING PARAMETERS

It is evident (Figure 5) that ferrite readings increase as the current is raised. In Figure 5 are plotted the data from Table 2, using all of the bead-on-plate welds made without preheat. At constant current level, there is higher ferrite reading with low speed than with high speed. This trend becomes more noticeable with increasing current.

184

Realizing that welding energy is a major factor in cooling rate, the relation-ship set forth in pioneering work by D. Rosenthal (Ref. 2) on the theory of heat flow with a moving heat source (in this case, the arc), the simplest form of relationship is

$$\frac{dT}{dt} = K \frac{s(T-To)^2}{60\ I\ V}$$

where

$\frac{dT}{dt}$ = cooling rate

K = constant depending primarily on thermal conductivity

s = travel speed, inches per minute

T-To = temperature differential between solidifying metal and adjacent parent plate

I = welding current

V = welding voltage

60 = conversion of speed from inches per minute to inches per second

Note: $\frac{s}{60\ I\ V} = \frac{1}{J}$ where J is the Joules per inch welding energy input

In figure 6 it is shown that, as welding progresses, the temperature of the plate rises. An attempt was made to estimate the temperature (by Tempilstiks) immediately after the end of the weld. It·was assumed that the temperature increased uniformly from the original temperature (room temperature) to the final temperature. The effect of the changing temperature could then be put into the Rosenthal equation, and the points shown in Figure 6 illustrate the change in average ferrite readings from the initial reading to the reading at location 8. The final readings were felt to be unreliable due to non-uniform conditions at the end of the weld. Figure 6 shows that cooling rate has a major influence in the ferrite reading and supports the view that the increase in ferrite reading is caused by the change in ambient temperature as the weld is made.

185

Examination of the bead-on-plate welds made with a 600 F preheat showed that the ferrite-content decreased with increasing preheat temperatures in contrast to what was shown in Figure 6.

Figure 7 shows the average of all readings under comparable welding conditions for three bead-on-plate welds and one groove weld with and without preheat. The data in Table 3 and illustrated in Figure 8 indicate that the increase in ferrite-content in welds made with a 600 F preheat remains, as was seen in the room temperature bead-on-plate tests. The amount of heat build-up in the high energy tests (80 KJ/in.) is considerably greater than in the low energy tests (20 KJ/in.). The unexpected results from the preheat test specimens suggest that the ferrite-level increase along the length of the weld is caused by more than one factor.

When the results of the groove welds are examined, little increase in ferrite-content along the weld is seen. The data from Table 4 are plotted in Figures 9 and 10, wherein the dotted lines show a comparison with bead-on-plate tests. These results indicate that the changes in ferrite-level along the weld that appeared in the bead-on-plate welds is caused more by chemical reactions in the welding arc, than by temperature conditions which are independent of weld-configuration (i.e., groove versus bead-on-plate).

SOLIDIFICATION MECHANISM

The constitution diagrams for the chromium-nickel-iron system have been well known for over forty years. Much of the welding literature, however, fails to make use of these constitution diagrams. It is helpful, therefore, to review the solidification mechanism in the light of the information that is known about the chromium-nickel-iron system.

The first crystals to form from the melt are delta ferrite. The liquid
composition shifts until it reaches a temperature at which a eutectic mixture
of ferrite and austenite form. As the temperature decreases below the solidus,
ferrite transforms to austenite. In compositions where the primary delta ferrite
is sufficiently rich in ferrite-stabilizers a network of delta ferrite remains;
as is illustrated schematically in Figure 11.

In Figure 12, an attempt has been made to represent a section of the
chromium-nickel-iron system with a constant iron-content of 62% and chromium and
nickel expressed as their "equivalents," as was done in Figure 1. The five
electrode compositions are located on this diagram to indicate how delta ferrite
may form. In the solidification of a weld from electrode No. 3 (Task B), the
composition of the primary delta ferrite is illustrated, as well as the trans-
formation of that primary delta-ferrite into austenite at temperatures below the
solidus. The eutectic delta-ferrite crystals are shown as a composition which
readily transforms to austenite. Thus the phase transformations which occur
during cooling of a single weld-pass (from liquid to room temperature) are:

<div style="text-align:center">

Cooling

$L \rightarrow \delta$ (primary)

$L \rightarrow \delta + \gamma$ (eutectic)

$\delta \rightarrow \gamma$

</div>

Another schematic diagram (Figure 13) is an attempt to present a relation-
ship between temperature and time during solidification and subsequent ferrite-to-
austenite transformation. In this diagram, the right-hand dotted line shows a slow
cooling situation representative of that seen in the consitution diagrams. This
may be compared with the left-hand dotted lines which depict rapid cooling situations
representative of that seen during most welding processes. With a high energy input
resulting in slow cooling, a greater amount of primary delta ferrite forms than
when a low energy input resulting in a fast cooling rate occurs. As indicated
in Figure 12, the greater the amount of primary ferrite that forms, especially if

it is rich in ferrite-stabilizing elements, the less likely the delta-ferrite is to convert to austenite. This helps to explain the initial results in Figures 4,5, and 6. The high preheat resulting in a lower ferrite content is explained by the longer time that the metal remains in the ferrite-to-austenite transformation region. The slight difference in cooling rate in the freezing area, due to higher preheat, is overshadowed by the much longer times existing at the temperature below freezing.

Consider the chemical reactions which may occur during welding and influence the variation in ferrite-level along the length of bead-on-plate welds. This variation was not seen in groove welds. The following reactions were considered:

	Effects on Ferrite Reading
O_2 (atmosphere) $+ C \rightarrow CO \uparrow$	Higher
N_2 (atmosphere) $\rightarrow N_2$ weld metal	Lower
CO (coatings) $\rightarrow$ increases C	Lower
CO (coatings) improves shielding $\rightarrow$ decreases N_2	Higher

The extent to which each of these reactions occurs is not known. At the high welding energy input in the bead-on-plate welds, which have less shielding from the atmosphere, the start of the weld might have more nitrogen contamination than the end. Because of self-resistance heating of the electrode-core, a deeper arc crucible is formed at the end of the electrode and the rate of flow of metal across the arc is greater at the end of the weld than at the beginning. Both of these effects lower the amount of nitrogen in the weld metal and increase the ferrite level. When welding in a groove, convection currents in the weld-atmosphere do not permit entrainment of as much atmospheric nitrogen. Hence, lesser variations in ferrite-level along the length of the groove-weld, relative to the bead-on-plate welds, are expected.

The chemical reaction effects described above are offered as a hypotheses, and are subject to verification by accurate analysis for both carbon and nitrogen.

STRAIN HARDENING EFFECTS

Austenite will transform on plastic straining to martensite at room temperature. Weld beads cooling under severe restraint may experience enough plastic deformation to increase the magnetic response of the ferrite-measuring instruments. The magnetic measurements taken on most of the groove welds were noticeably higher than those on the less restrained bead-on-plate welds made under the same conditions indicating a higher content of ferromagnetic phase(s) in the former series of welds. The lower level of nitrogen, a strong austenite-stabilizer, in the groove welds would explain this observation.

The expectation of a higher cooling rate, because of a larger fusion surface and a greater volume of metal to conduct away the heat, is not borne out by the results. The ferrite readings were higher in the groove welds than in the bead-on plate welds, which is the opposite of what the cooling-rate considerations would predict.

The remaining possibility is that there is enough plastic strain during cooling below the austenite-to-martensite transformation temperature to cause a noticeable increase in formation of strain-induced martensite and in magnetic response. This appears to be the remaining explanation, as groove welds are subject to greater restraint than bead-on-plate welds. Also, it should be noted that magnetic readings measure both delta ferrite and strain-induced martensite. Also a significant consideration when measuring the magnetic response of weld surfaces which have been mechanically worked, is the possibility of strain-induced martensite formation, as was observed in the higher readings on the ground surfaces.

SUMMARY

The data available in this study and the conclusions drawn from them are tentative. The program was relatively small; more work would be necessary to support quantitative conclusions. A summary of the observations follows:

Accuracy of Readings

a. Standard deviation for 5 - 11 readings generally lies between .2 to 1.0 percentage of ferrite.

b. Ground surfaces generally read 0.5 - 1.0 percent higher than as-welded surfaces.

c. The above generally confirms WRC and IIW round-robin experience.

Effect of Welding Heat Input

a. Higher current and lower travel rate consistently caused higher ferrite readings.

b. Increasing energy input (hence decreasing cooling rate) gives higher ferrite readings (presumably by allowing greater amounts of δ ferrite to form on cooling).

Effect of Preheat

a. A 600 F preheat consistently caused a drop in ferrite readings.

b. Preheat decreases cooling rate which presumably promotes the formation of greater amounts of δ-ferrite in solidification, but a longer time for transformation of δ-ferrite to austenite in cooling from solidification to room temperature.

c. The increase in ferrite readings from start to finish of a single weld bead cannot be accounted for by decreased cooling rates, because the same trend is shown by the 600 F preheat tests whose overall average shows a distinct drop in ferrite as compared with room temperature tests. Latent energy released during solidification may have to be considered in the cooling model. Compositional changes, i.e., ingress of lesser amounts of nitrogen, an austenite-stabilizer may explain the observed increase in ferrite content.

Effect of Weld Shape (Bead-on-Plate vs. Groove)

a. Groove welds had higher ferrite-levels than bead-on-plate welds.

b. Cooling rate is expected to be higher than bead-on-plate welds. On this basis, ferrite content results are contrary to expectation. A possible explanation is greater shrinkage strains which cause austenite to transform to martensite, increasing the overall magnetic-response of the groove-welds.

190

  c. Groove welds show little or no ferrite changes from start to finish of weld.

  d. Observations a. and c. are explainable by the lower level of a potent austenite-stabilizer, nitrogen, anticipated in groove welds, as compared with bead-on-plate welds.

  The Task B test program was designed to examine welds which underwent one heating cycle. Most heavy-section welding involves multi-pass welding, wherein several welding cycles are observed by any one weld bead. The following phase changes may be expected to occur in multi-pass welds:

Effect of Reheating Weld Metals (as in Multi-pass Welds)

  a. Ferrite will reform close to the fusion line but probably will not be retained on cooling within any normal weld-temperature sequence.

  b. Ferrite will transform to austenite in a narrow band below fusion line.

  c. Martensite probably redissolves on each reheating cycle only to reform during cooling, due to shrinkage-induced strains.

REFERENCES

1. AWS Specification A5.4-7x, WRC recommended weld pad technique, to be published by the American Welding Society, Miami, FL.

2. Rozenthal, D., Theory of moving sources of heat and its application to metal treatment, Trans ASME, 68, 618-866 (1946).

Table 1:   Composition of the Test Electrodes

Electrode No.	WRC Ferrite No.		Composition, Weight Percent									
	Diagram	Measured	C	Mn	Si	S	P	Cr	Ni	Mo	Cb	N
1	2	0.5	.031	1.72	.58	.011	.033	18.47	13.97	2.25	.14	.042
2	4.5	3.5	.030	1.72	.56	.012	.034	18.64	12.97	2.29	.14	.046
3	10	9.0	.034	1.70	.57	.009	.034	19.20	12.01	2.32	.15	.042
4	12.5	12.0	.028	1.76	.59	.008	.029	19.66	11.06	2.18	.15	.067
5	3	0.6	.059	1.75	.56	.009	.033	18.69	12.85	2.25	.15	.044

Table 2:   Ferrite Readings for Bead-on-Plate Welds – No Preheat

Weld	Ferrite Readings										Ave.	Std. Dev.
100 amp – 3 ipm kJ = 41.1												
1st pass	7.3		8.2		8.4		9.2		9.8		8.58	.86
2nd pass	7.8		7.6		7.6		7.8		7.8		7.72	.10
2nd pass, grd.	7.3	6.5	7.6	8.2	8.2	8.2	7.8	8.6	7.6	7.8	7.78	.56
Ave. 4	7.23		7.90		8.10		8.35		8.25		7.966	.674
160 amp – 3 ipm kJ = 71.3												
1st pass	9.6		9.4		9.2		9.4		9.4		9.40	.13
2nd pass	7.8		9.6		9.6		10.6		8.4		9.2	.99
2nd pass, grd.	8.9	9.6	10.0	10.0	9.8	11.1	11.1	9.6	10.0	9.6	9.97	.64
Ave. 4	8.98		9.75		9.93		10.18		9.35		9.638	.717
130 amp – 6 ipm kJ = 31.2												
1st pass	8.9		8.6		9.2		8.9		9.4		9.00	.28
2nd pass	7.8		7.8		7.8		8.2		6.8		7.68	.47
2nd pass, grd.	8.2	7.8	8.2	8.9	8.4	8.4	9.2	9.6	9.2	8.0	8.59	.57
Ave. 4	8.18		8.38		8.45		8.98		8.35		8.503	1.09
100 amp – 12 ipm kJ = 11.7												
1st pass	7.3	6.8	6.8	7.6	7.3	8.0	8.4	6.5	8.0	6.5	7.32	.64
2nd pass	8.4	6.5	6.8	7.3	7.0	8.0	7.6	7.0	7.6	7.8	7.40	.56
2nd pass, grd.	8.9	6.5	8.0	8.4	8.4	8.9	9.6	7.8	8.6	8.2	8.33	.78
Ave. 3	8.2	6.6	7.2	7.7	7.6	8.3	8.5	7.1	8.1	7.5		
Ave. 6	7.40		7.48		7.93		7.81		7.78		7.683	.812
160 amp – 12 ipm kJ = 20.3												
1st pass	8.4	8.4	8.4	8.4	9.4	9.4	8.9	7.8	9.8	9.6	8.85	.63
2nd pass	7.8	8.4	8.9	7.8	9.6	7.0	9.4	9.6	10.0	11.6	9.01	1.26
2nd pass, grd.	8.6	9.2	8.9	9.2	9.4	9.2	10.2	10.0	10.6	11.8	9.71	.91
Ave. 3	8.3	8.7	8.7	8.5	9.5	8.5	9.5	9.1	10.1	11.0		
Ave. 6	8.46		8.60		9.0		9.32		10.57		9.190	1.038

193

Table 3: Ferrite Readings for Bead-on-Plate Welds - 600 F Preheat

Ferrite Readings

Weld											Ave.	Std Dev
100 amp - 12 ipm	kJ = 41.4											
1 pass	5.7	5.5	5.5	6.5	5.5*	5.1*	6.8	5.7	6.8	5.3	5.98	.53
1 pass, grd.	6.8	6.3	6.8	6.8	6.8	5.3*	7.3	8.0	7.8	6.5	7.01	.55
Ave. 4		6.08		6.40		6.8*		6.95		6.60	6.53	.70
130 amp 6 ipm	kJ = 31.2											
1 pass	6.3	7.8	7.3	8.0	7.0	7.8	7.8	7.8	7.0	9.6	7.62	.46
1 pass, grd.	7.6	8.0	8.0	8.6	8.6	8.6	8.6	9.2	8.4	9.2	8.48	.48
Ave. 4		7.43		7.98		8.00		8.35		8.55	8.05	.89
160 amp - 3 ipm	kJ = 71.3											
1 pass	7.3	8.6	8.2	7.8	8.4	8.9	9.4	10.4	9.6	10.0	8.86	.94
1 pass, grd.	6.5	8.9	8.6	8.4	9.8	9.6	9.6	10.9	10.9	10.6	9.38	1.77
Ave. 4		7.83		8.25		9.18		10.08		10.28	9.12	1.15

*Erratic arc-outage -- ignored in averages and standard deviation

194

Table 4: Ferrite Readings for Groove Welds

Ferrite Readings

Weld											Ave.	Std. Dev.
100 amp - 6 ipm - RT												
Unground	8.4	7.6	8.9	8.4	8.4	8.2	8.2	8.9	8.4	8.4	8.35	.79
Ave. 2		8.0		8.6		8.3		8.5		8.4		
			(Compare Bead-on-Plate Welds--Ave. of 3 and 12 ipm								7.84	.61)
100 amp - 6 ipm - 600F												
Unground	6.3	7.6	8.0	7.8	7.6	7.3	8.4	7.8	8.2	7.8	7.68	.55
Ave. 2		7.0		7.9		7.4		8.1		8.0		
130 amp - 6 ipm - RT												
Unground	9.2	10.4	9.2	10.0	8.4	9.2	10.4	8.9	8.9	9.2	9.38	.63
Ave. 2		9.8		9.6		8.8		9.1		9.1		
(Compare Bead-on-Plate Welds - 130 amp - 6 ipm - RT)												
1st pass unground	8.9		8.6		9.2		8.9		9.4		9.0	.28
130 amp - 6 ipm - 600 F												
Unground	8.2	8.6	8.6	8.2	7.6	8.9	8.2	8.4	8.2	7.8	8.27	.36
Ave. 2		8.4		8.4		8.2		8.3		8.0		
(Compare Bead-on-Plate Welds)												
1st pass unground	7.0		7.6		7.4		7.8		8.3		7.62	.46
160 amp - 6 ipm - RT												
Unground	9.6	9.4	10.0	9.4	9.8	9.8	10.0	9.2	10.0	9.2	9.64	.31
Ave. 2		9.5		9.7		9.8		9.6		9.6		
			(Compare Bead-on-Plate Welds--Ave. of 3 and 12 ipm								9.02	.33)
160 amp - 6 ipm - 600 F												
Unground	8.0	8.0	7.8	8.4	7.6	7.8	8.4	7.0	8.6	6.8	7.84	.56
Ave. 2		8.0		8.1		7.7		7.7		7.7		

195

Table 5: Welding Parameters for the NBS Weldments

	I	II	III	IV
Current, Amperes	130	100	160	160
Voltage, Volts	24	24	26	26
Speed, ipm	6-8	8-10	4-6	4-6
kJ/in	23-32	14-18	41-62	41-62
Interpass Temp., F	200-250	200-250	200-250	550-650

Table 6

Electrode	1	2	3	4	5
Task					
A	I	I	I	I	I
A			II		
A			III		
C	IV		IV		IV

196
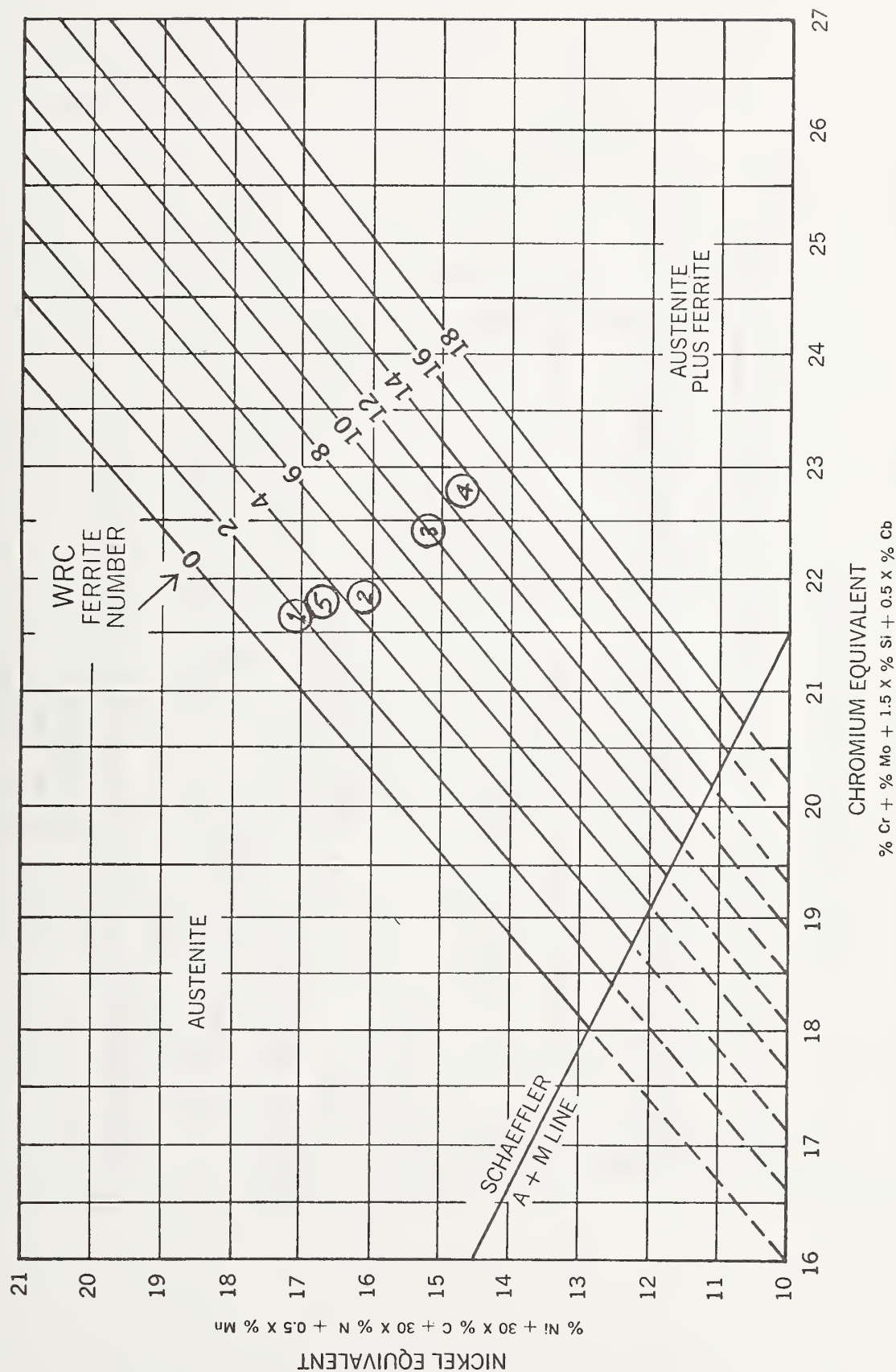
FIGURE 1. Section of Schaeffler Diagram showing Ferrite Number (FN) in accordance with procedures established by the Welding Research Council and the American Welding Society

197
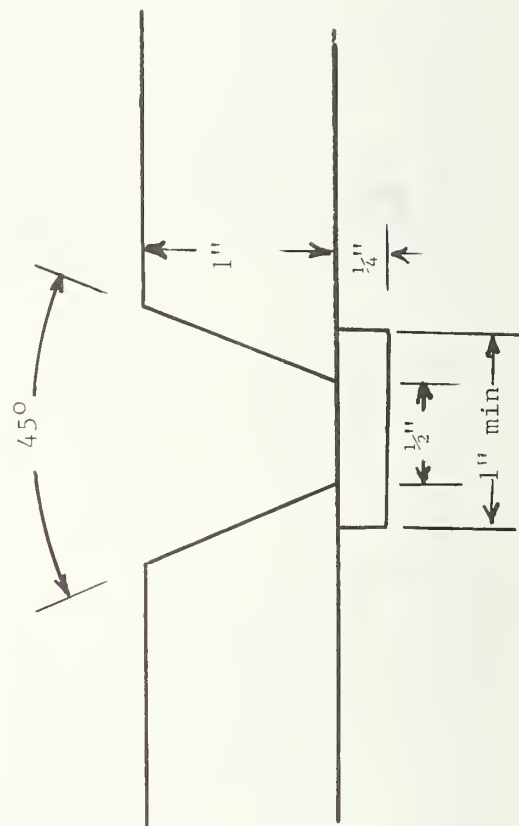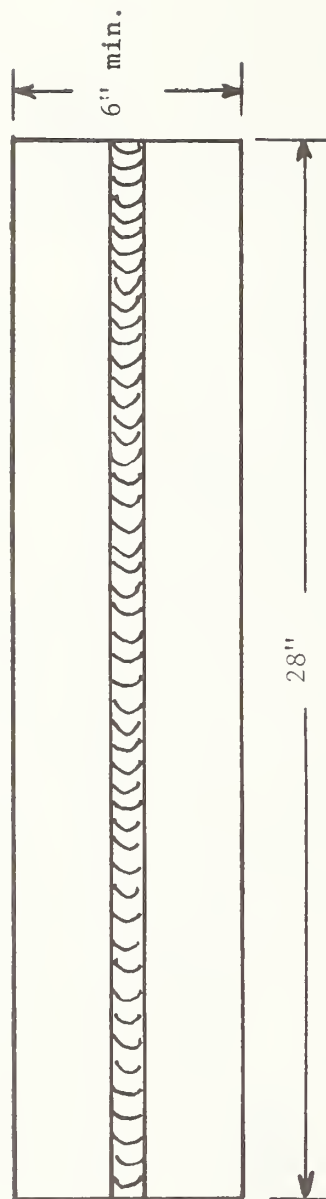
FIGURE 2. Configuration of the test weldments

Weld Energy Input

Current, I in Amps
Voltage, V in Volts
Travel Rate, S in
    inches/min

$$\frac{I \times V \times 60}{S} = \text{Joules per inch}$$

Ambient Temperature

Room
600 F

$$\frac{dT}{dt} = k \frac{(T-To)^2}{J}$$

Weld Bead Shape

Bead-on-Plate

$60°$ $1/16"$ $6"$ $1"$

Bead-in-Groove

$1/8"$ $1/4"$ R
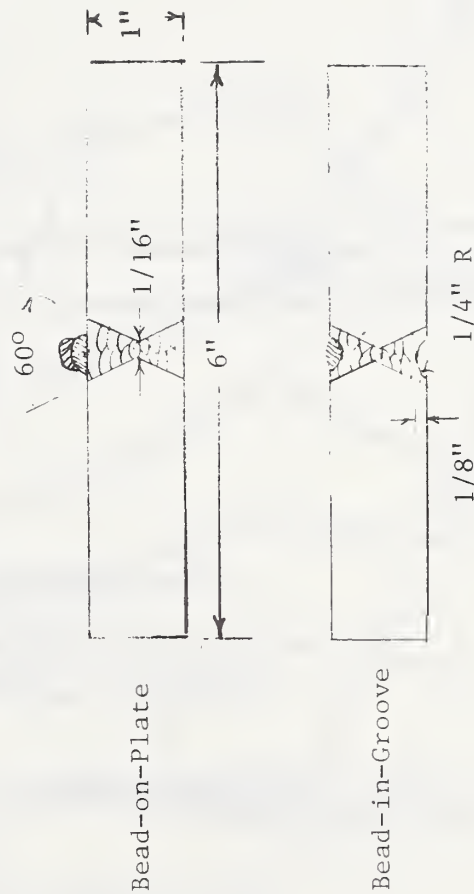
Note: Dilution effects avoided

FIGURE 3. Test plan for Task B—Effect of welding procedure on ferrite values

FIGURE 4. Ferrite content measurements for the Task B welds
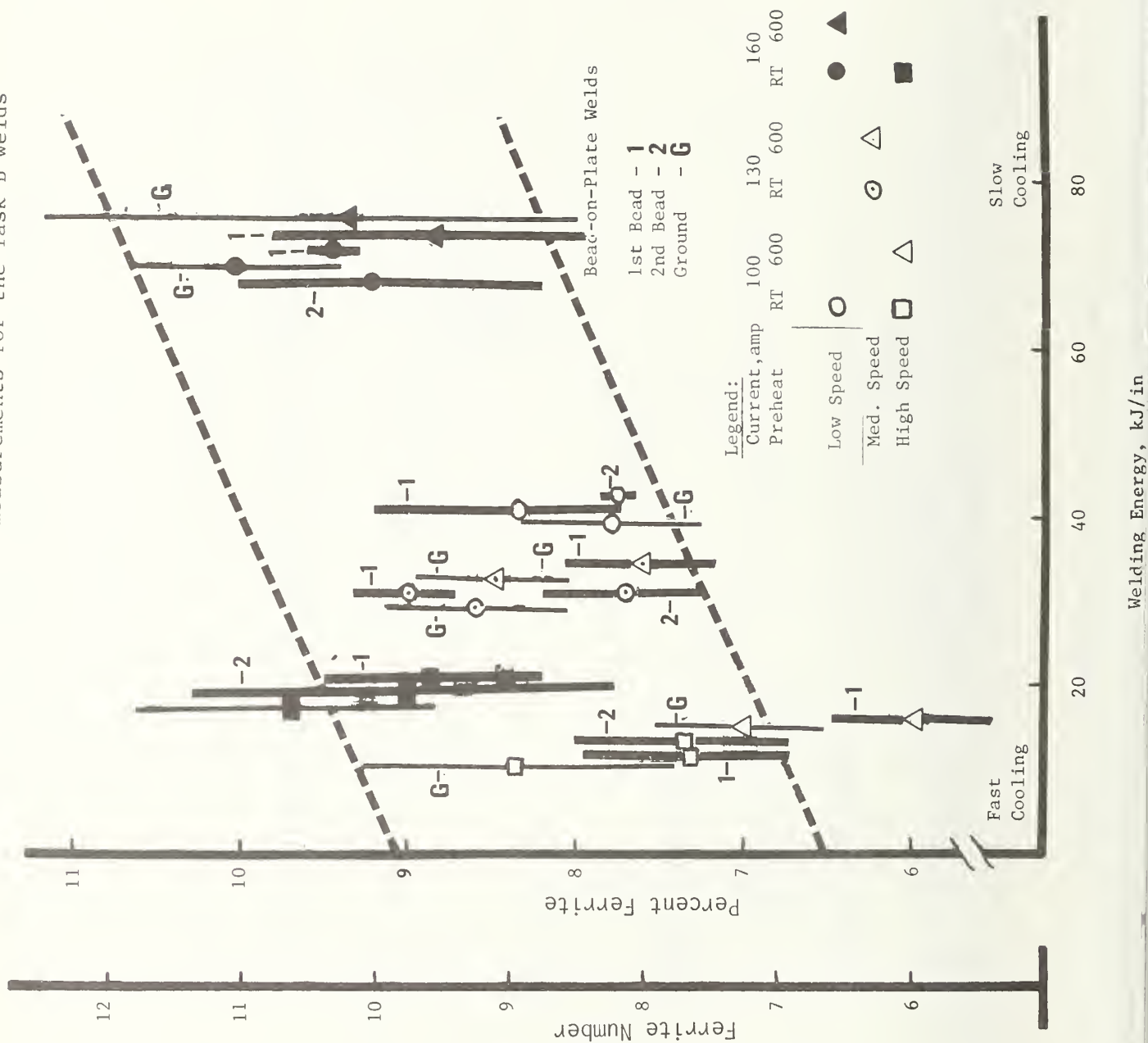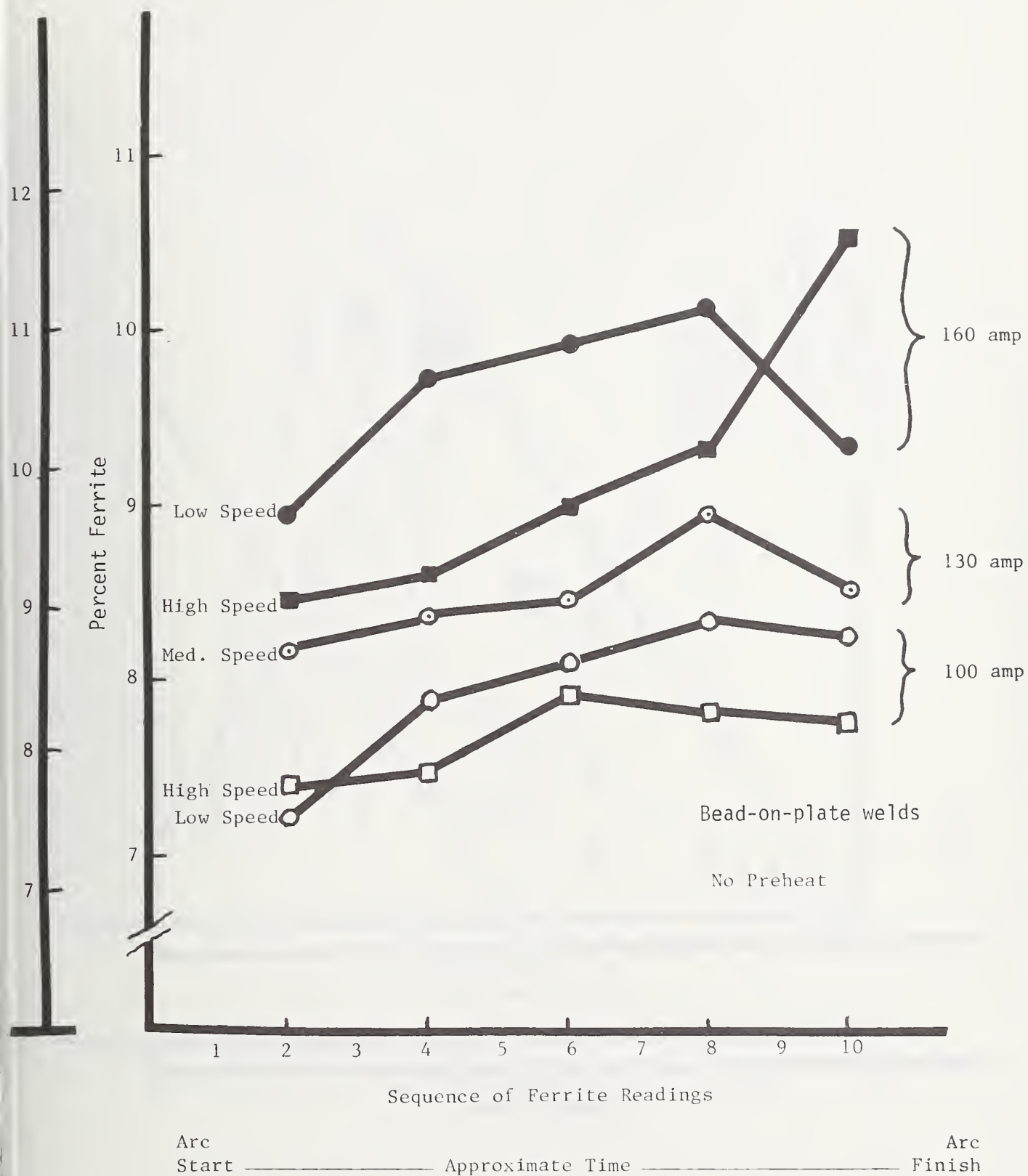
FIGURE 5. Ferrite content as a function of position in the test plate

FIGURE 6. Ferrite content as a function of cooling rate

No Preheat

Data Points are averages
of 4 to 6 figures:

Initial Values
Position #4
Position #6
Position #8

Cooling Rate $\dfrac{(T-T_o)^2}{J}$

Percent Ferrite

Ferrite Number

202
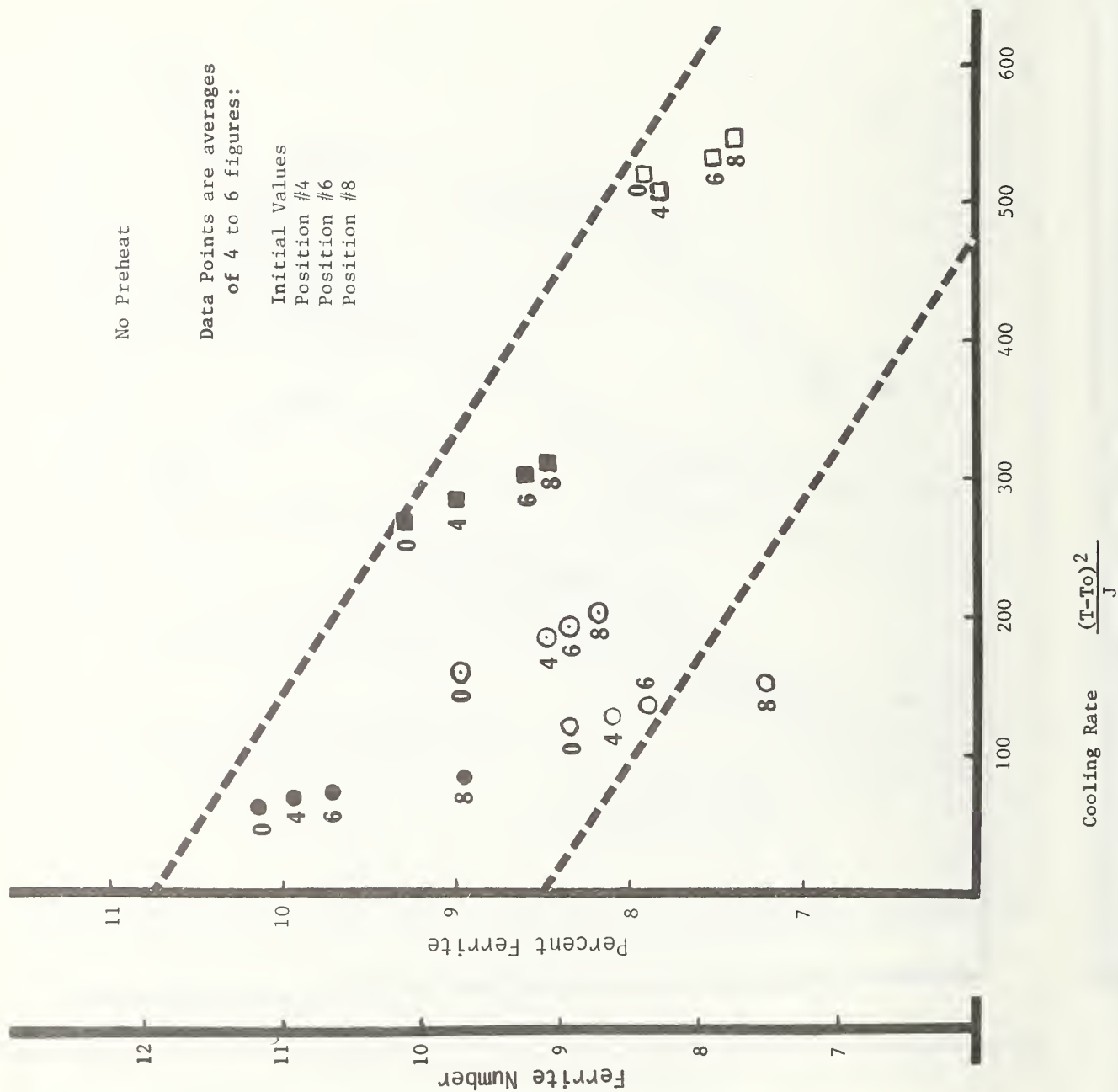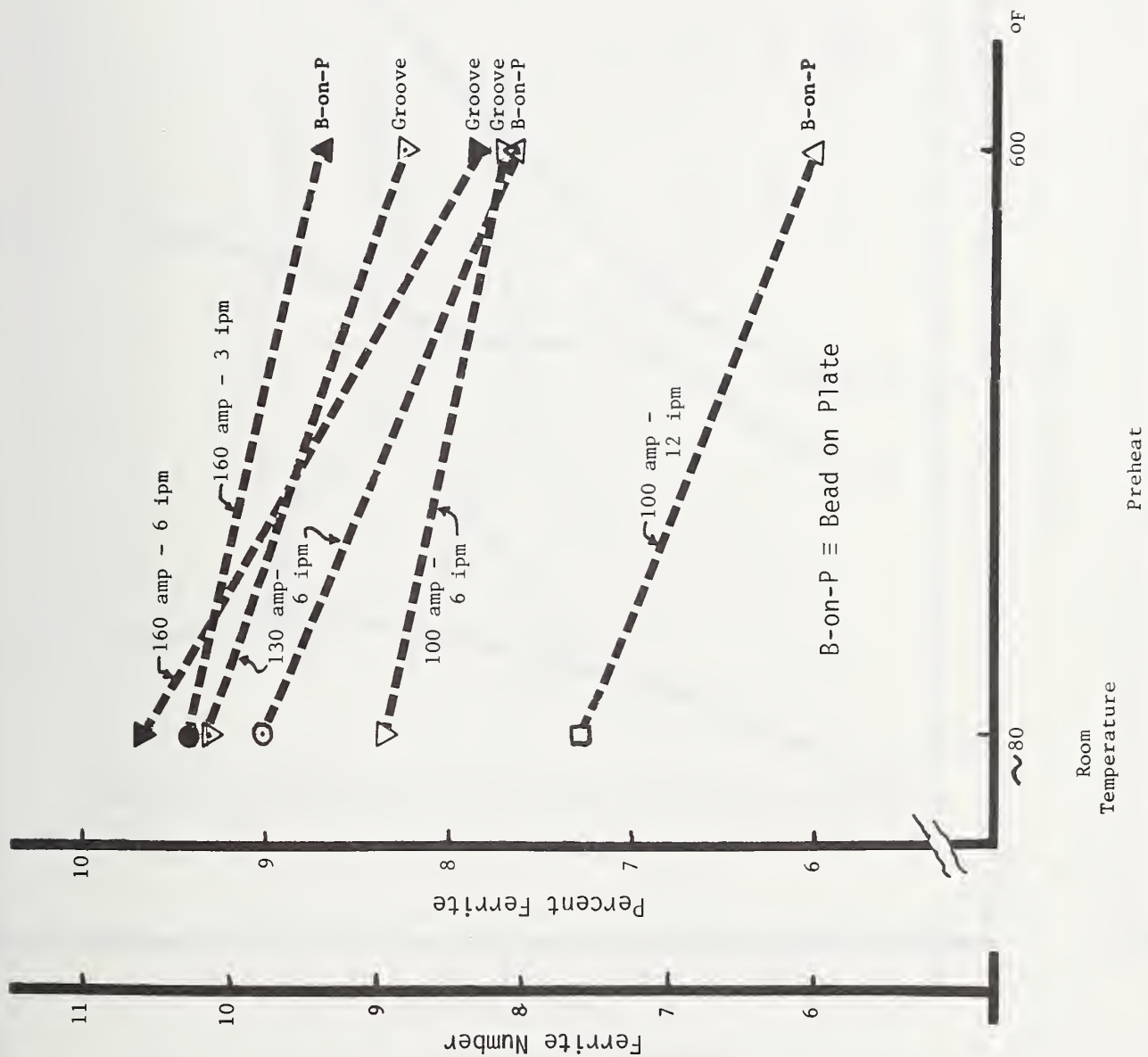
FIGURE 7. Ferrite content as a function of preheat for three heat-input levels

203
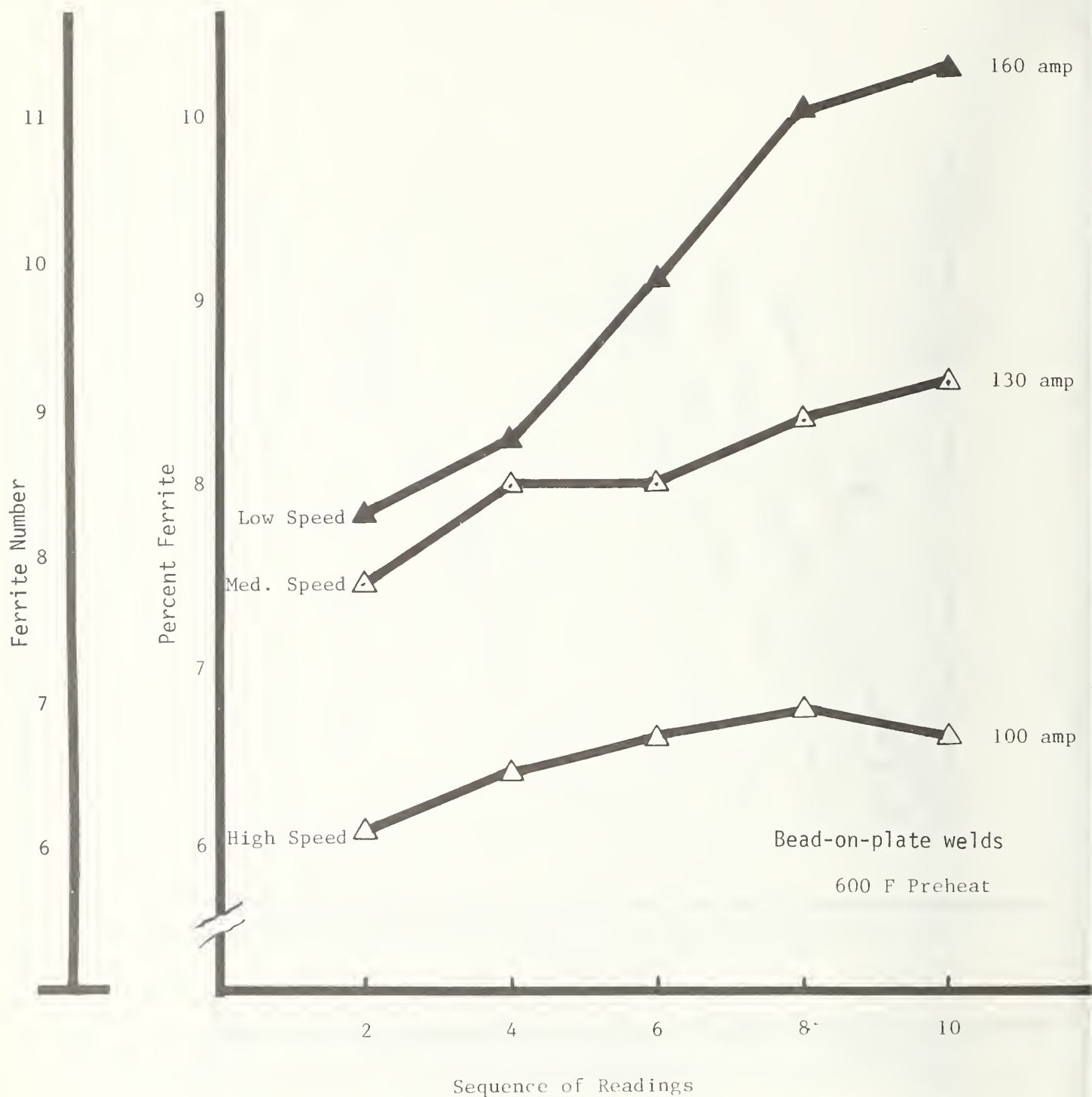
FIGURE 8. Ferrite content as a function of position in the test plate for three heat input levels and 600°F preheat

204
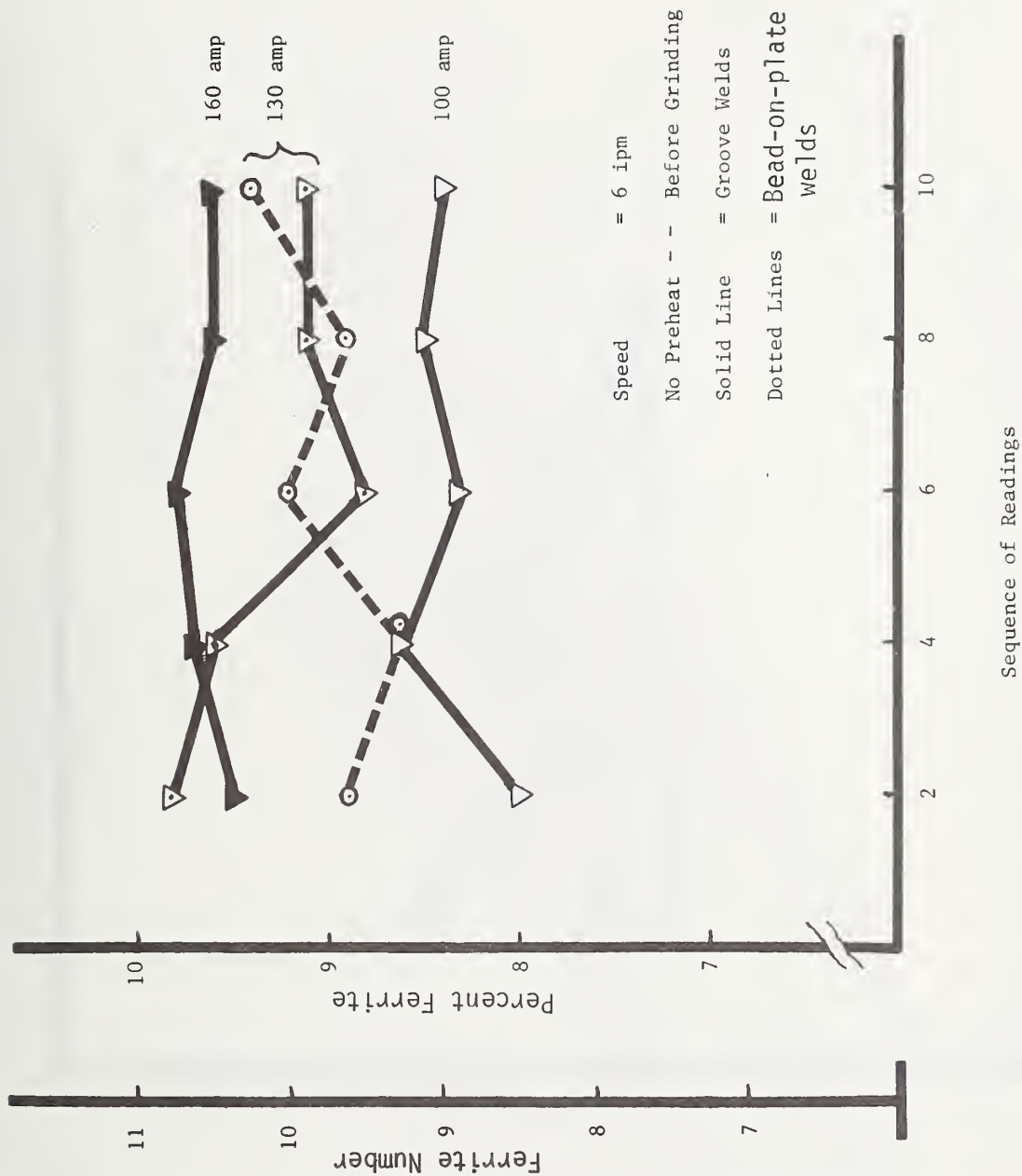
FIGURE 9. Ferrite content as a function of position in the test plate for three current levels

FIGURE 10. Ferrite content as a function of position in the test plate for three current levels and 600°F preheat

130 amp
100 amp
160 amp

Solid Lines = Groove Welds

Dotted Line = Bead-on-plate welds

Medium Speed
600F Preheat (No grinding)

Sequence of Readings

Percent Ferrite

10
9
8
7
6

Ferrite Number

11
10
9
8
7
6

2 4 6 8 10

Liquid

Eutectic Ferrite
and Austenite Growth

Primary
Ferrite Growth

Ferrite
transforms to
Austenite

Austenite
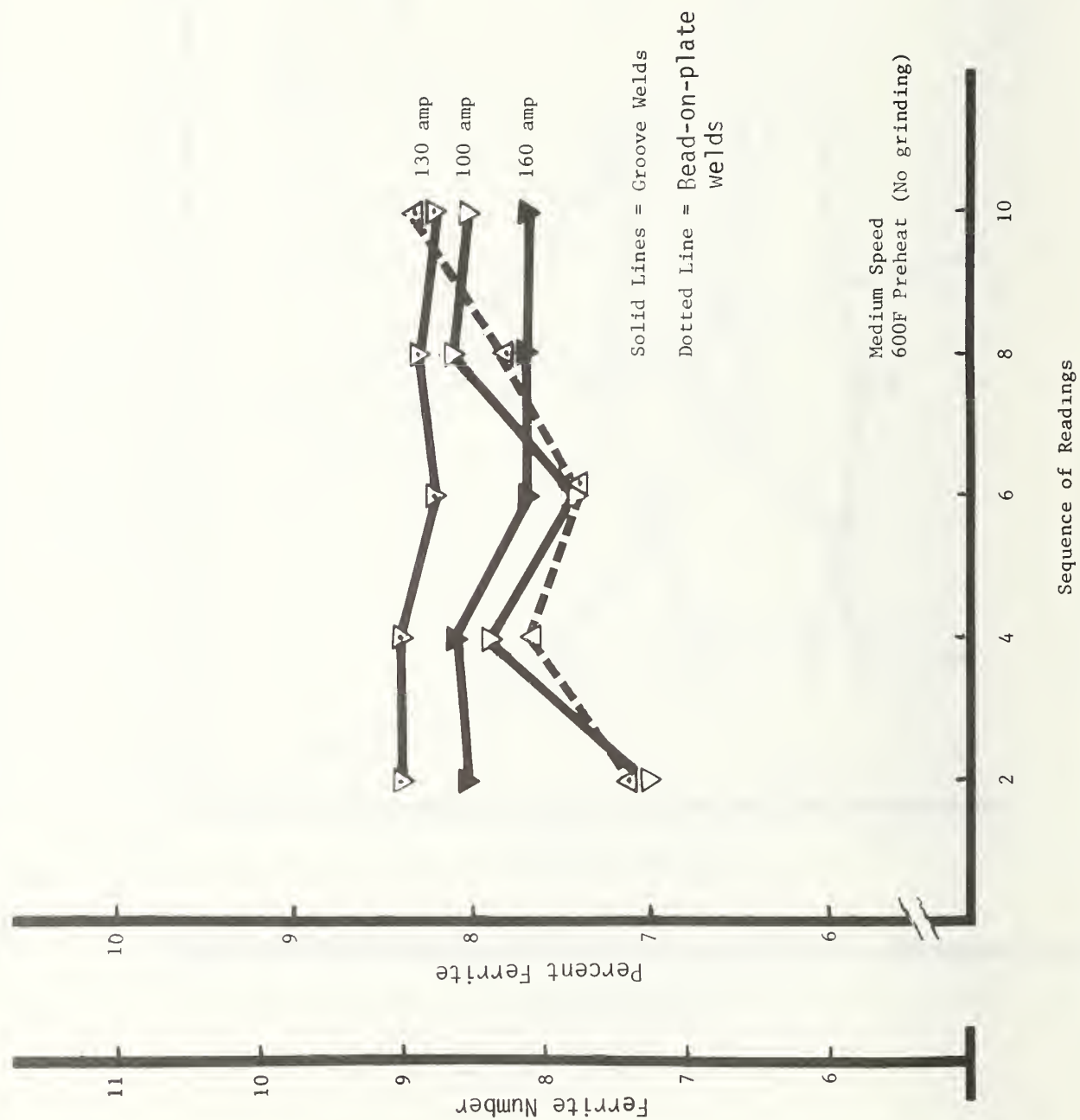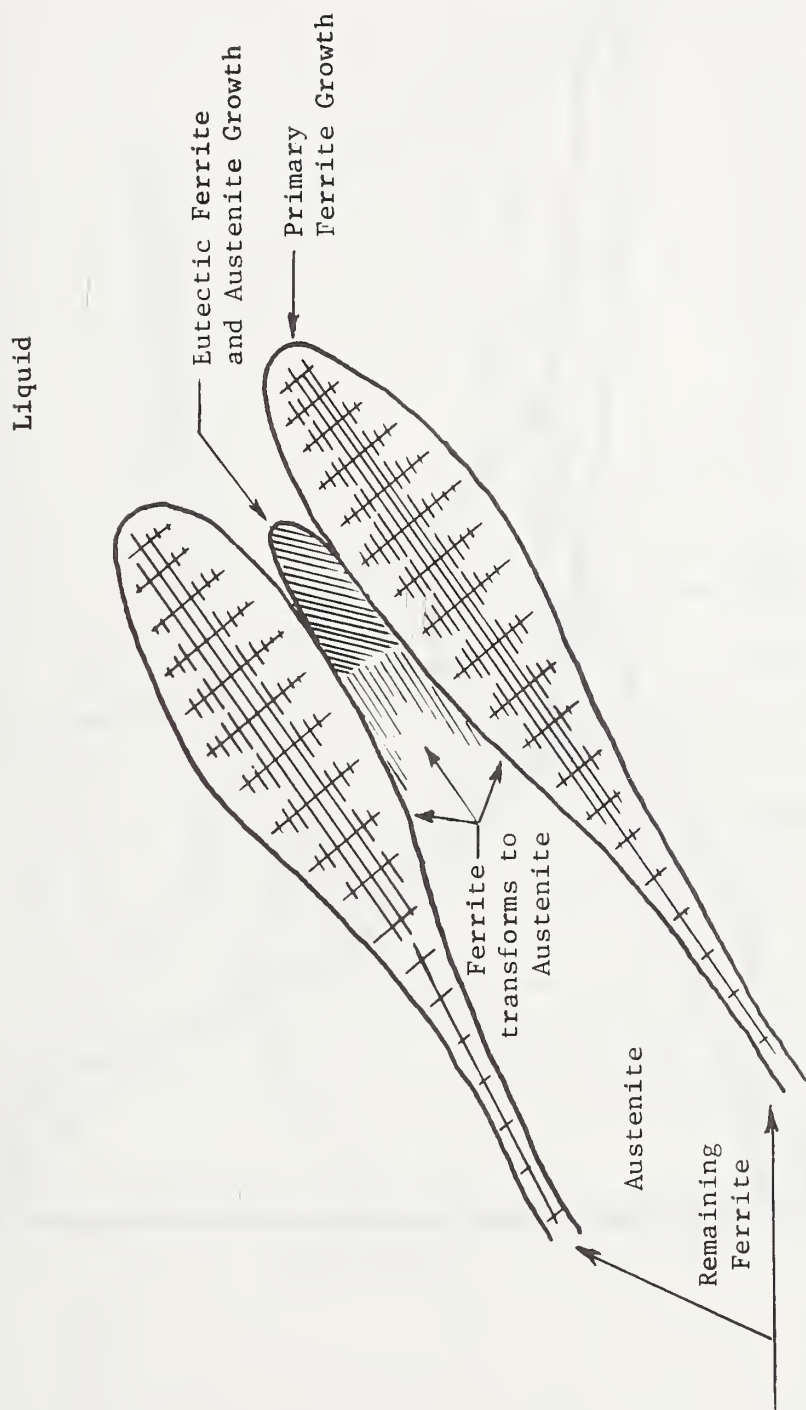
Remaining
Ferrite

FIGURE 11. Schematic representation of ferrite network remaining after
transformation of ferrite to austenite is complete

207

FIGURE 12. Schematic of Fe-Cr-Ni system for 62% Fe

$5(1)$ – Electrode Indentification

Cr (equivalent) = Cr + Mo + 1.5 Si + 0.5 Cb
Ni (equivalent) = Ni + 30 (C+N) + 0.5 Mn
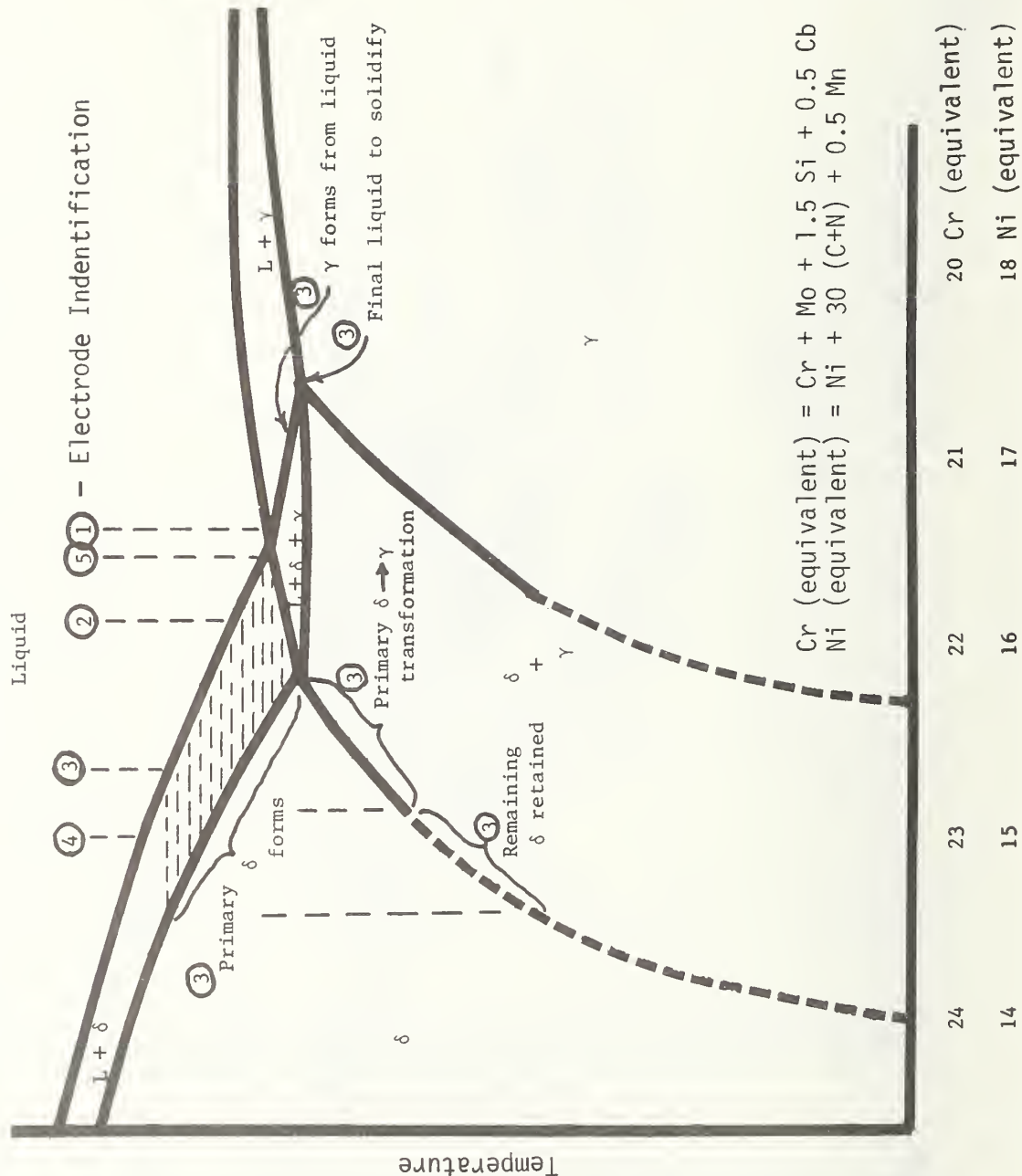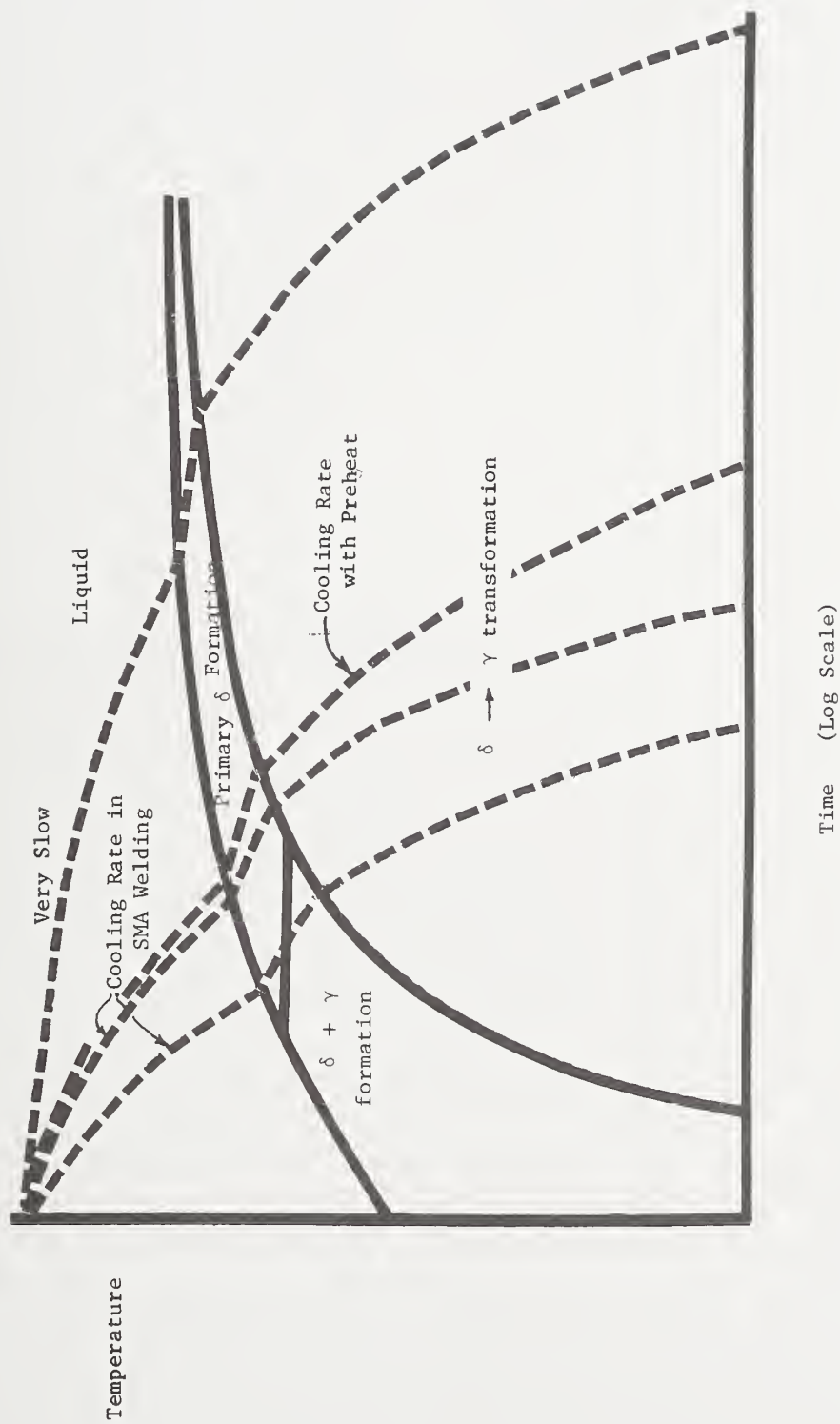
FIGURE 13. Schematic continuous cooling transformation diagram for austenitic-weld metals

PHYSICAL PROPERTIES OF STAINLESS STEELS

LOW-TEMPERATURE ELASTIC PROPERTIES OF 304-TYPE STAINLESS STEELS

H. M. Ledbetter
Cryogenics Division
National Bureau of Standards

Elastic properties of AISI 304-type (304, 304L, 304N) stainless steels are being studied experimentally to determine:

1. elastic-constant changes between room-temperature and liquid-helium temperature.
2. elastic-constant variability due to anisotropy, product form, compositional fluctuations, etc.

Experimentally, longitudinal and transverse sound-wave velocities are measured in several directions in various samples. Four experimental methods are used:

1. pulse-echo (4-10 MHz)
2. pulse-echo superposition for temperature studies (4-10 MHz)
3. continuous-wave resonance with two transducers
4. three-component composite-oscillator resonance (near 60 kHz)

When combined with the mass density, ρ, these velocities, v, are related to the engineering elastic constants by:

Shear modulus = $G = \rho v_t^2$

Longitudinal modulus = $C_\ell = \rho v_\ell^2$

Bulk modulus = $C_\ell - \frac{4}{3} G$

Young's modulus = $\rho v_e^2 = 9GB/(3B + G)$

Poisson's ratio = $(E/2G) - 1$

where subscripts ℓ, t, and e denote longitudinal, transverse, and extensional. The inaccuracy in these methods is typically 1-2%, while the imprecision is about 10^{-4} in the temperature-change measurements.

Elastic constants of a Type 304L stainless steel are given in Table 1 for selected temperatures. Elastic-constant/temperature curves are shown in Figs. 1-3. These constants were measured at near-zero stress and represent the true dynamic elastic constants. For iron at room temperature, dynamic elastic constants exceed static values by about 2% for B, 1% for ν, 0.3% for E, and 0% for G. At zero temperature all these differences vanish, and they remain negligible below about 100 K.

Detailed behavior shown in Figs. 1-3 has not been reported previously. All the elastic constants are regularly behaved between room temperature and about 75 K. G shows the largest change with temperature, and B the smallest.

The reversible anomaly near 45 K is due to a Neel (paramagnetic-antiferromagnetic) transition. All elastic constants are anomalous except perhaps for B where the data are scattered. E and G show nearly parallel behavior. At about 16 K, both C_ℓ and ν data indicate that a second reversible transition may occur in these alloys. This observation is now under study in other specimens.

Besides anomalous temperature behavior, several other observations were made on AISI 304-type stainless steels: (1) elastic constants show very little anisotropy in the bar and plate stock studied so far; (2) no evidence was found for dispersion, sound-velocity variation with frequency, between 2 and 10 MHz; (3) attenuation has not been measured, but it clearly varies strongly from sample to sample, due mainly perhaps to grain-size variations.

Variability effects are still being studied in these alloys, and these results will be reported later.

Table 1. Elastic constants of a Type-304L stainless steel.

T(K)	C_ℓ	G	B	E	ν
		(10^{11} N/m^2)			(dimensionless)
295	2.526	0.763	1.509	1.958	0.284
200	2.587	0.795	1.527	2.031	0.278
100	2.629	0.822	1.533	2.093	0.273
76	2.632	0.826	1.530	2.100	0.271
4	2.611	0.809	1.532	2.065	0.275
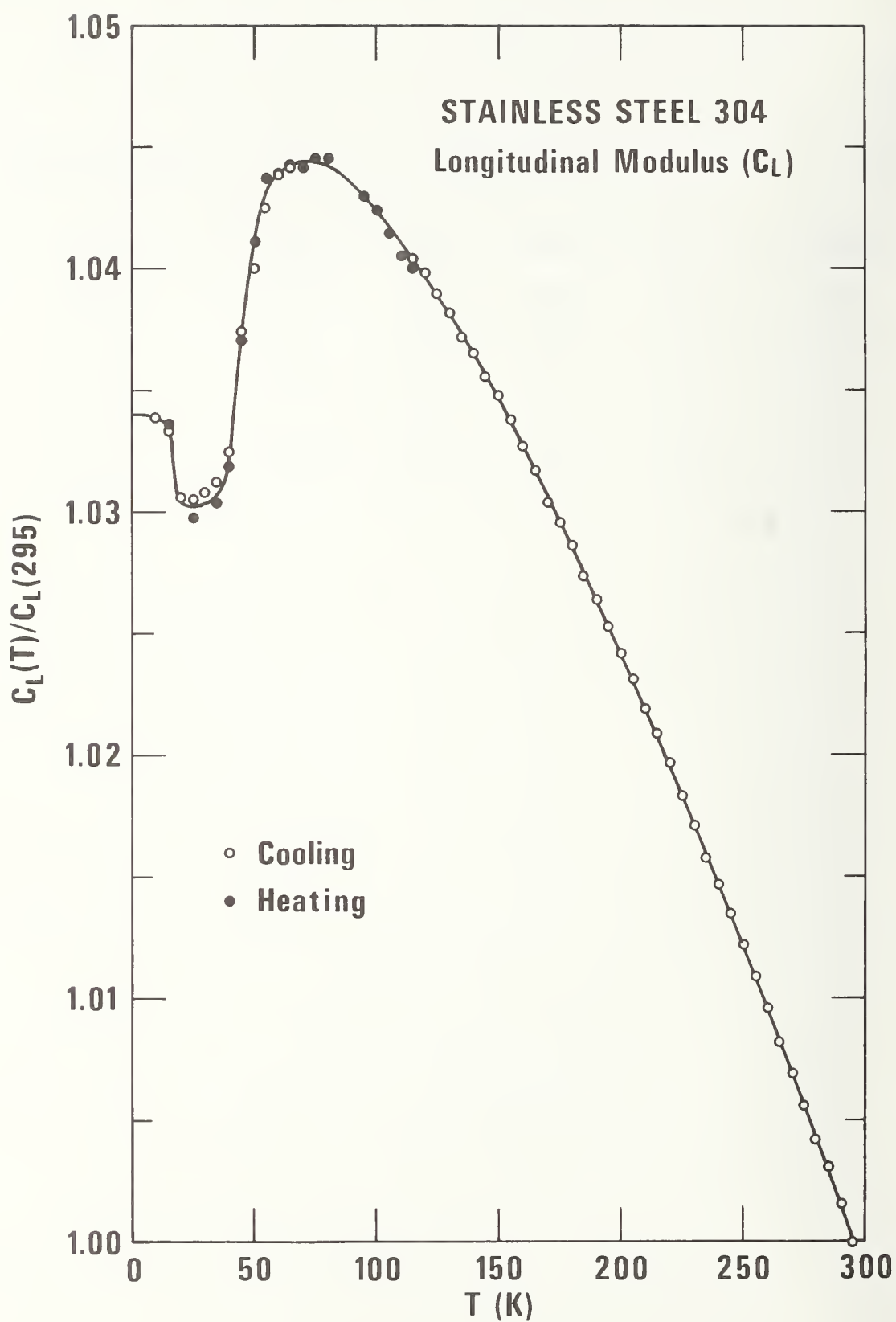
Figure 1. Temperature dependence of the longitudinal modulus.
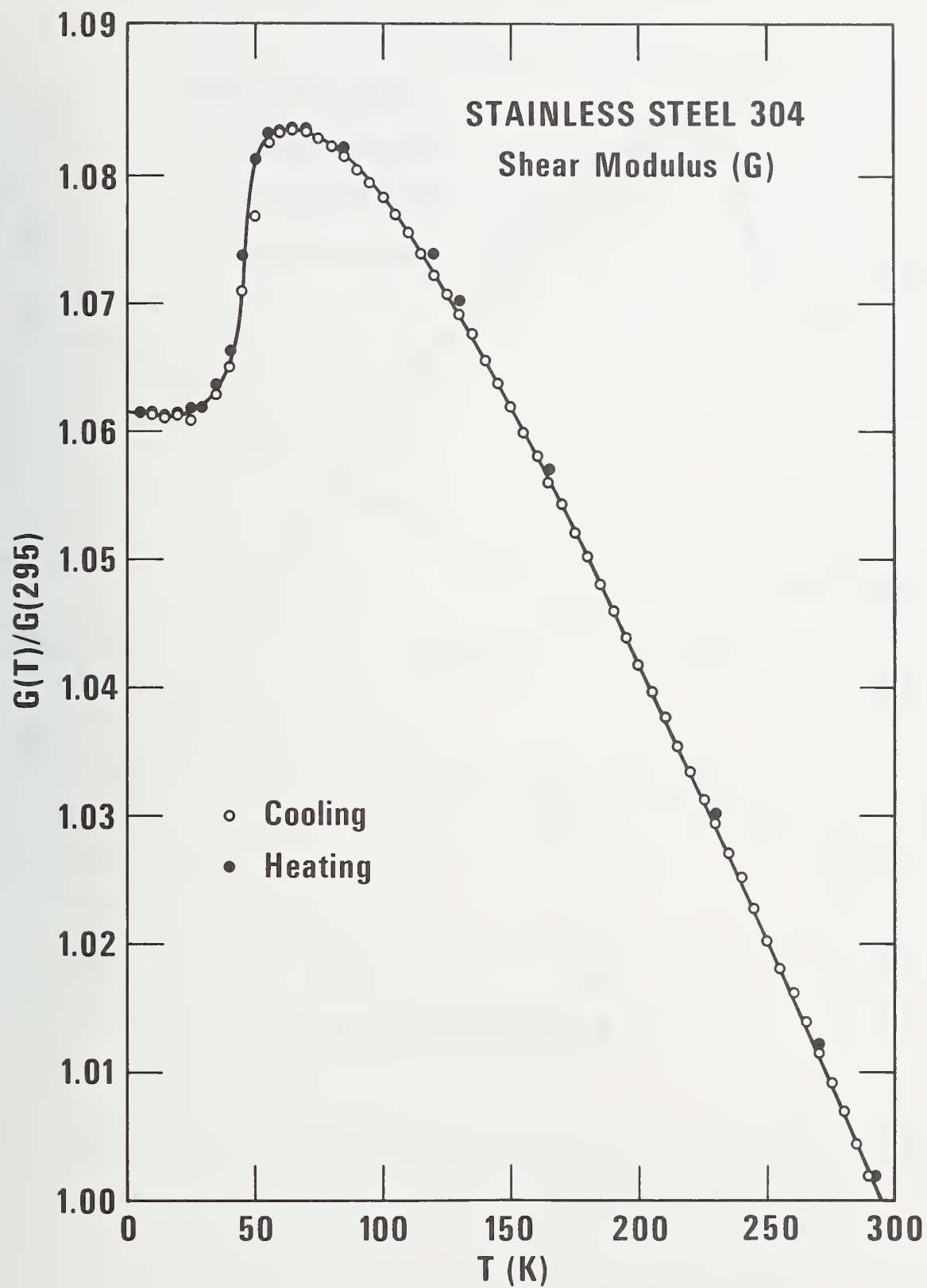
Figure 2. Temperature dependence of the shear modulus.
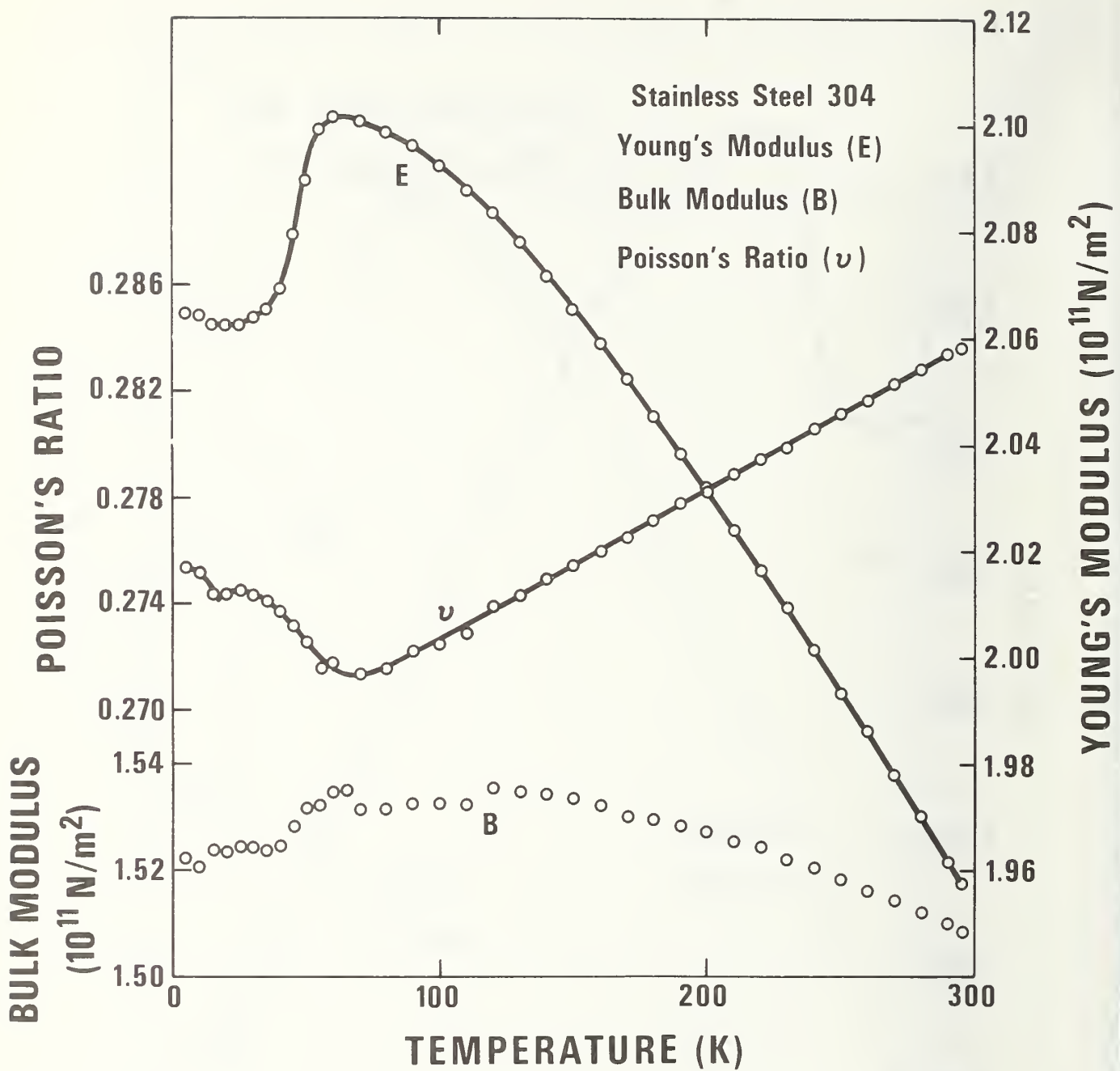
Figure 3. Temperature dependence of Young's modulus, the bulk modulus, and Poisson's ratio.

NONMETALLICS

NONMETALLICS

M. B. Kasen
Cryogenics Division
National Bureau of Standards

Nonmetallics research was not funded during FY 77; however, steps were taken to prepare for work to be undertaken during FY 78. The primary objective is to provide fabricators of superconducting magnets with a dependable, high-pressure industrial laminate system (or systems) for use as electrical or thermal insulation. A major problem in selecting material for such use is the highly proprietary nature of existing NEMA-grade laminates. These materials are presently produced to specified room temperature electrical performance criteria and are not required to meet specific material specifications. Thus, laminates having the same NEMA designation but produced by different laminators have been found to have different mechanical and electrical performance at cryogenic temperatures.

This problem was discussed with the Industrial Laminate Subcommittee of NEMA, with representation by all U.S. laminating firms. The result was a suggestion that NBS work with a single laminating firm to develop specifications for laminate systems that meet MFE needs. The selected laminator would act on behalf of the NEMA organization with product formulations and production methods being made available to all U.S. laminators for competitive production.

The Micarta Division of the Westinghouse Corporation has agreed to work with NBS in this effort. Following discussions with various knowledgeable people in the industry, Westinghouse and NBS have agreed that the following series of laminates would be more appropriate for the initial characterization study:

1. NEMA G-10/MIL-P-18177 Type GEE

    Resin technology to be a published commercial formulation. Fiberglass reinforcement to be Style 7628 fabric with a silane finish. The manufacturing process will be non-proprietary and fully disclosable.

2. NEMA G-11/MIL-P-18177 Type GEB

    As above but a commercial G-11 formulation using an aromatic amine cure agent.

3. NEMA G-11/MIL-P-18177 Type GEB with Boron-Free "E" Glass

    As (2) above but using boron-free glass reinforcement to evaluate potential improvement in radiation resistance.

Westinghouse will produce the laminates in their Durham, NC plant. A sufficient variety of panel thicknesses and sizes will be obtained to permit a thorough characterization of the mechanical, electrical and thermal properties of each product at 4 K. Additionally, sufficient material will be available to facilitate studies of the radiation resistance of the various

products at 4 K. The mechanical, electrical and thermal studies will be undertaken by NBS and by subcontract to industry. It is anticipated that the radiation studies will be undertaken by a National Laboratory having the required facilities and will be incorporated as part of the ongoing work of such a laboratory.

As an independent contribution to the nonmetallics program, the Spaulding Fiber Company of Tonawanda, NY has volunteered to provide a series of published-formulation laminates comparable to (1) and (2) above for characterization along with the Westinghouse material. It is understood that the Spaulding laminates will be representative of current production material.

As laminate systems (1) and (2) proposed by Westinghouse and/or the comparable materials from Spaulding Fiber are credible commercial G-10 and G-11 formulations, fabricators of superconducting magnets who have need to purchase such laminates for immediate use have the option of using these products rather than proprietary, unspecified formulations. It is hoped that fabricators will take advantage of this opportunity, as practical experience with the laminates will contribute to the data base and enhance the credibility of the overall program.

The Westinghouse laminate system (3) remains experimental and should not be used for magnet fabrication until the characterization work is completed.

HANDBOOK PREPARATION

HANDBOOK PREPARATION

F. R. Fickett
Cryogenics Division
National Bureau of Standards

This project started later in the year than the others reported here and, thus, it is still in the formative stages. The handbook is being produced jointly by the Mechanical Properties Data Center (MPDC) of Traverse City, MI and the staff of the NBS Cryogenics Division. The literature searching and document acquisition is done by NBS. MPDC extracts the data and prepares worksheet graphs and characterization tables which are then evaluated by the NBS staff to determine "best value" curves and appropriate error bands. The handbook will present "best value" curves for properties in the two categories listed in Table 1. For the category A properties we will present an error band which will indicate the spread that one might expect due to material variability, experimental error, etc. A typical graph is shown in Figure 1. The published graphs will have SI units primary, but common units will be shown also. Each A category property presentation will also contain a characterization table giving the appropriate information (different for physical and mechanical properties) on each of the original data sources used in constructing the best value curve. The information to be contained in the table is shown in Table 2. Another table will be prepared for the "A" properties providing the data from the best value curve (Table 3). The B category properties will be presented in smaller graphs as shown in Figure 2. Although not shown on the figure, error and variability estimates will also be shown where possible. For all properties a complete bibliography will be included. The materials to be included in the first edition of the handbook are listed in Table 4. Formats, indexing, covers, etc. have all been discussed, but no final form has been decided on yet.

Table 1. Properties to be presented in the handbook.

A	B
Coefficient of Thermal Expansion	Bulk Modulus
Crack Growth Rate	Compression
Fatigue Strength	Creep
Fracture Toughness	Electrical Resistivity
Tensile Strength	Impact Strength
Tensile Yield Strength	Magnetic Permeability
Thermal Conductivity	Poisson's Ratio
Young's Modulus	Shear Modulus
	Specific Heat Capacity
	Stress-Strain
	Tensile Elongation
	Tensile Reduction in Area
	Thermal Diffusivity

Table 2. Sample characterization table.

Author (year)

Grain size

Hardness

Form

Condition

Chemistry

RRR

Test variables

    spec. type

    loading rate

    temperatures of tests

    number of spec. per temp.

Table 3.   Unit conversion table for Figure 1.

Category STRUCTURAL ALLOYS	Class STAINLESS STEELS	Material AISI 316
	ULTIMATE TENSILE STRENGTH	

Tabular Presentation of Data from Graph

T, K ($T,°F$)		σ_u, MPa (σ_u, Ksi)		$T,°F$ (T, K)		σ_u, Ksi (σ_u, MPa)	
4.2	(-452.1)	1431	(207.5)	-452	(4.2)	207.5	(1431)
10	(-441.7)	1409	(204.3)	-440	(10.93)	203.8	(1405)
20	(-423.7)	1391	(201.7)	-420	(22.04)	201.2	(1388)
30	(-405.7)	1362	(197.6)	-400	(33.15)	196.2	(1353)
40	(-387.7)	1348	(195.5)	-380	(44.26)	195.0	(1344)
50	(-369.7)	1327	(192.4)	-360	(55.37)	190.0	(1310)
60	(-351.7)	1298	(188.2)	-340	(66.48)	185.8	(1281)
70	(-333.7)	1266	(183.6)	-320	(77.59)	178.8	(1232)
80	(-315.7)	1227	(177.9)	-300	(88.71)	174.5	(1203)
90	(-297.7)	1200	(174.0)	-280	(99.82)	169.8	(1170)
100	(-279.7)	1170	(169.7)	-260	(110.9)	165.0	(1138)
110	(-261.7)	1140	(165.4)	-240	(122.1)	160.1	(1105)
120	(-243.7)	1110	(161.0)	-220	(133.2)	155.0	(1069)
130	(-225.7)	1079	(156.5)	-200	(144.3)	150.0	(1034)
140	(-207.7)	1047	(151.9)	-180	(155.4)	145.0	(999.7)
150	(-189.7)	1016	(147.4)	-160	(166.5)	139.5	(961.8)
160	(-171.7)	983.9	(142.7)	-140	(177.6)	134.8	(929.1)
170	(-153.7)	951.5	(138.0)	-120	(188.7)	128.8	(887.7)
180	(-135.7)	920.5	(133.5)	-100	(199.8)	124.5	(858.4)
190	(-117.7)	884.6	(128.3)	-80	(210.9)	118.8	(818.8)
200	(-99.67)	857.7	(124.4)	-60	(222.1)	112.5	(775.7)
210	(-81.67)	822.5	(119.3)	-40	(233.2)	107.5	(741.2)
220	(-63.67)	783.9	(113.7)	-20	(244.3)	102.5	(706.7)
230	(-45.67)	750.8	(108.9)	0	(255.4)	96.25	(663.6)
240	(-27.67)	719.8	(104.4)	20	(266.5)	90.75	(625.7)
250	(-9.670)	684.6	(99.29)	40	(277.6)	85.00	(586.1)
260	(8.330)	647.9	(93.97)	60	(288.7)	79.75	(549.9)
270	(26.33)	613.2	(88.94)	80	(299.8)	75.00	(517.1)
280	(44.33)	578.2	(83.86)				
290	(62.33)	546.0	(79.19)				
300	(80.33)						

Table 4.   Materials to be included in the handbook.
(FY 1977, 1978)

Stainless Steels: 316, 304, 21/6/9
(and L and N modifications)

Aluminum Alloys: 5083, 2219, 6061

Category STRUCTURAL ALLOYS	Class STAINLESS STEELS	Material AISI 316

ULTIMATE TENSILE STRENGTH
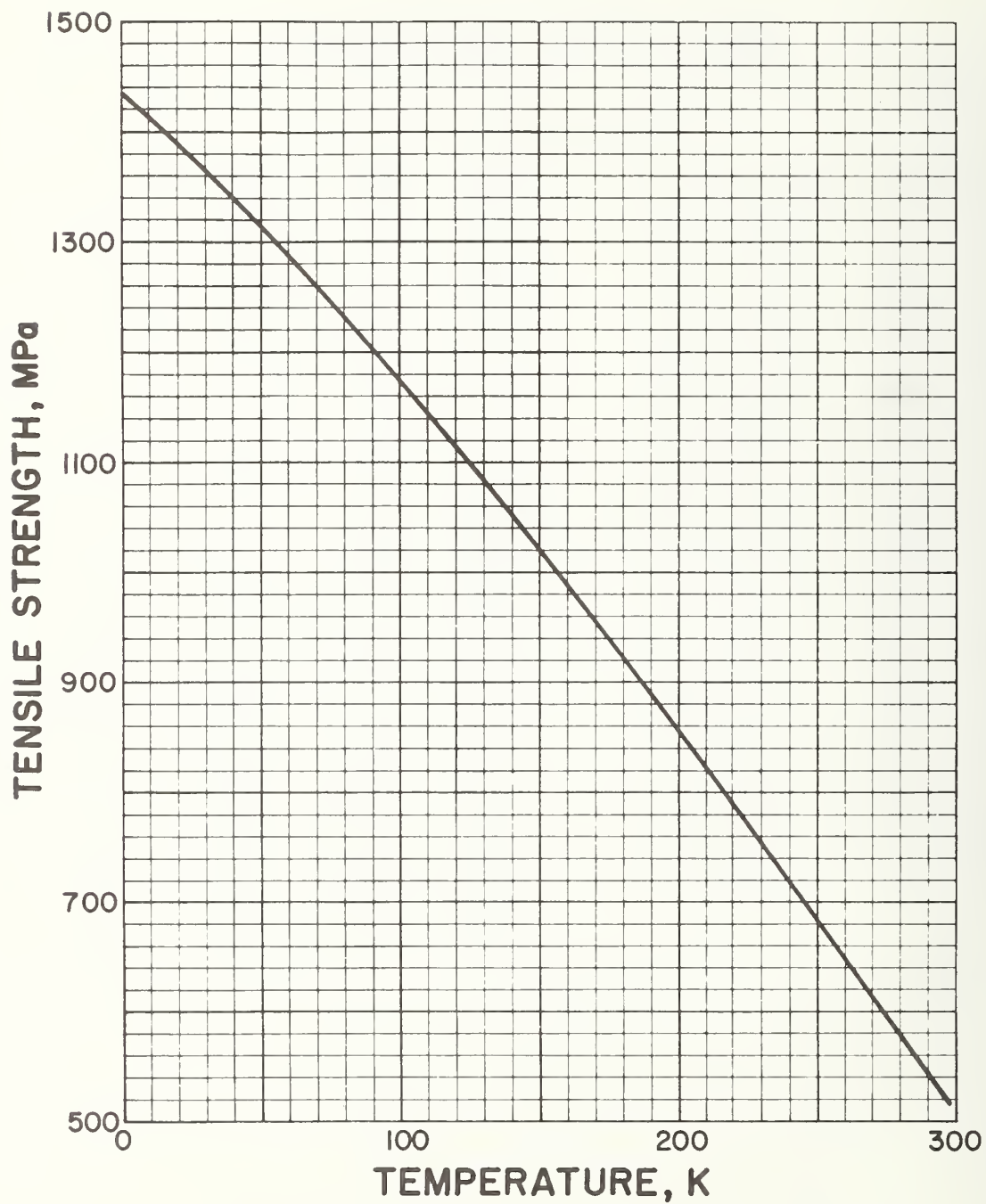
Figure 1.   Tensile strength of AISI 316 stainless steel.

Figure 2. Presentation of type B properties.

Category STRUCTURAL ALLOYS	**Class** STAINLESS STEELS	**Material** AISI 316 LN

THERMAL EXPANSION
ELECTRICAL RESISTIVITY
MAGNETIC PROPERTIES
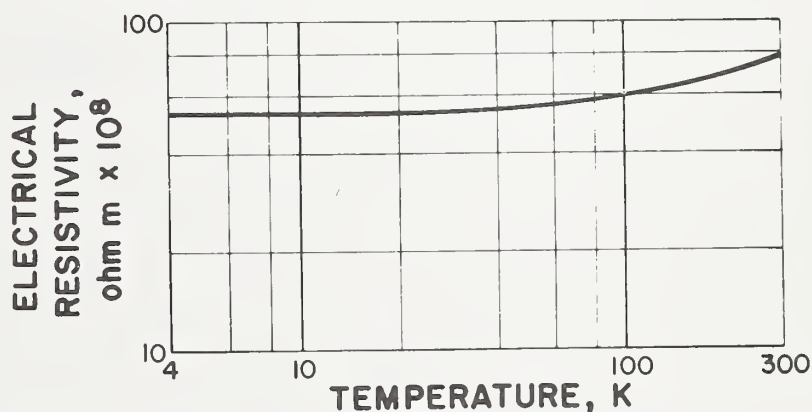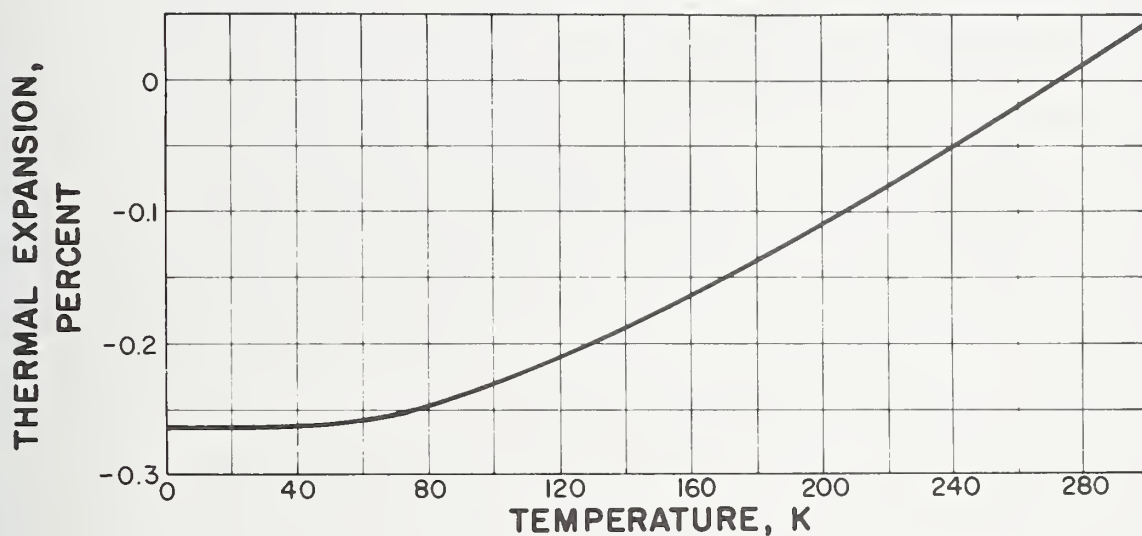
Form: Rods (Low Nitrogen)

Diameter, cm (in.):   0.4 (0.157)

Condition: Annealed (heated at 1348 K (1075 C) for 0.5 hour and
                         water quenched)

Testing Temperature, K (F)	RT	77 (-320)	4.2 (-452)
Magnetic Properties			
Susceptibility, k	25.77×10^{-4}	69.14×10^{-4}	113.38×10^{-4}
Permeability, μ (H = 3 kOe)	12.60×10^{-7}	12.66×10^{-7}	12.71×10^{-7}
Permeability, μ (H = 80 kOe)	—	—	12.683×10^{-7}

231

VAIL WORKSHOP

VAIL WORKSHOP

F. R. Fickett
Cryogenics Division
National Bureau of Standards

A major aspect of the technology transfer part of the program is the workshop. These meetings are to be held each year with the goal of bringing together representatives from all parts of the materials community which are involved with low temperature applications. The attendees at this year's workshop, held at Vail, CO, October 12-14, represented just such a diverse group including: industry, national labs, MFE projects and universities. The following pages give the attendance list, the program for the workshop and a review of the proceedings, which was originally prosented at the 7th Symposium on Engineering Problems of Fusion Research in Knoxville, TN, October 25-28.

J. Benzinger - Spaulding Fiber Co.
P. Bezler - BNL
E. Bobrov - MIT
R. Bourque - General Atomic
R. Braden - Belfour Stulen, Inc.
J. Bronson - LASL
B. Brown - ANL
J. Bywater - ANL
F. Catania - ANL
J. Christian - General Dynamics
T. Collings - Battelle Columbus
E. Dalder - ERDA
R. Espy - Armco
F. Fickett - NBS
R. Foley - LLL
S. Gause - Westinghouse
L. Genens - ANL
R. Gold - Westinghouse
E. Hodge - Battelle Columbus
J. Hust - NBS
H. Johnson - Princeton Plasma Physics Lab.
M. Kasen - NBS
R. Kelsey - Alcoa
V. Kopytoff - LLL
P. Landon - LLL
D. Larbalestier - U. of Wisconsin
H. Ledbetter - NBS
C. Long - ORNL
F. Mazandarany - General Electric
H. McHenry - NBS
H. Mishler - Battelle Columbus
T. Moore - Belfour Stulen, Inc.
J. Morris - Lawrence Berkeley Lab.
R. Nelson - LLL
C. Oberly - AFAPL Wright-Patterson AFB
W. Pelczarski - ANL
D. Read - NBS
R. Reed - NBS
W. Roden - General Dynamics
R. Sampson - Westinghouse
E. Sandersan - Rockwell Int.
P. Sanger - Airco, Inc.
F. Schwartzberg - Martin Marietta
J. Scott - ORNL
J. Shepic - Martin Marietta

T. Siewert - Chemetron
F. Szumachowski - Teledyne-McKay
R. Thomas - Arcos
R. Vandervoort - LLL
W. Vogen - Berkeley
J. Wells - Westinghouse
C. Witherell - U. of California
L. Young - Westinghouse

Wednesday, 10-12-77

I. Introduction (8:30-9:30)

Welcome	R. P. Reed	NBS
	E. N. C. Dalder	ERDA
Presentation of materials survey results	R. P. Reed	NBS
Discussion of data handbook	R. Braden/T. Moore	Belfour-Stulen

II. Current Designs and Materials (9:30-12:30)

Large Coil Project	C. J. Long	ORNL
	J. Christian	General Dynamics
	F. Mazandarany	General Electric
	L. Young	Westinghouse
TNS	R. Bourque	General Atomic
TFTR	H. Johnson	PPPL
MFTF	V. Kopytoff	LLL

III. Applications of Nonmetallics in Magnet Structures (2:00-5:00)

Nonmetallics at low temperatures	M. B. Kasen	NBS
Nonmetallic cryostats	W. Vogen	U. CA, Berkeley
Industrial laminates	S. Gause	Westinghouse
Radiation damage in nonmetallics	C. J. Long	ORNL
Accelerated aging under stress	R. Sampson	Westinghouse

Thursday, 10-13-77

IV. High Strength Stainless Steels for Low Temperature Service (8:30-12:00)

Studies of nitrogen strengthened stainless steels	D. Larbalestier	U. Wisconsin
	D. T. Read	NBS
	R. P. Landon	LLL
	J. Shepic	Martin Marietta

GROUP PHOTOGRAPH (12:00)

V. Thick Section Welding for Low Temperature Applications (2:00-5:00)

Stainless steel welding	H. I. McHenry	NBS
	R. H. Espy	Armco
	R. D. Thomas, Jr.	Arcos
	T. Seiwert	Chemetron
Aluminum welding	R. Kelsey	Alcoa

Friday, 10-14-77

VI. Physical Properties of Magnet Materials (8:30-12:00)

Elastic Properties	H. M. Ledbetter	NBS
Thermal Properties	J. G. Hust	NBS
Radiation Damage	B. S. Brown	ANL
Magnetic Properties	E. W. Collings	Battelle
Electrical Properties	F. R. Fickett	NBS

F.R. Fickett and R.P. Reed
Cryogenics Division
National Bureau of Standards
Boulder, CO 80302

Summary

A workshop treating problems related to low temp-
erature materials applications in superconducting
magnet systems was held at Vail, Colorado October 12-14.
The major topics considered by the participants were:
the recently completed NBS survey of low temperature
materials needs for MFE applications and the produc-
tion of an appropriate data handbook; materials
choices of recent device designs; nonmetallic materials
applications; high strength stainless steels for cryo-
genic service; thick section welding; and physical
properties of magnet materials. A summary of the
presentations and the ensuing discussions is given
along with our assessment of the more pressing of the
many low temperature materials research problems
considered by the workshop participants.

Introduction

The workshop program on materials at low tempera-
tures is designed to bring together all of the diverse
elements of the materials community for discussions
covering problems related to the construction and
operation of large superconducting magnet systems for
fusion energy. There are a number of new problems
with fusion systems which have not been encountered
in a serious way in previous superconducting magnets:
the magnets are very large and must operate at stress
levels near the safe limits for many potential struc-
tural materials; extensive welding and bolting is
essential; significant neutron fluences are found
throughout the magnet structure, a situation which
creates serious problems for nonmetallic insulators
and low resistivity stabilizing metals; pulsed, high
magnetic fields with relatively fast rise times are
likely to exist. One of the goals of the workshop
was to discuss implications of each of these aspects
for materials selection and device design. The only
materials specifically excluded from consideration
were the superconductors (NbTi and Nb_3Sn) themselves,
as we felt they had been adequately treated in a
large number of recent conferences.

A major purpose for the workshop was to provide
input and direction to the ongoing NBS-ERDA program
on low temperature materials research for fusion energy
applications. This program is now entering its second
year and many of the results presented at the workshop
were obtained by the program contractors during the
first year of the project.

The fifty-three attendees represented a wide
range of interests: magnet designers and fabricators;
industrial laminate manufacturers and application
engineers; stainless steel and aluminum producers;
welding specialists; material scientists; and data
handbook specialists.

The six sessions and the topics discussed (in a total
of 28 papers) were:

  I.   Survey Results and Handbook Design
        Materials survey results
        Discussion of data handbook

 II.   Current Designs and Materials
        Large Coil Program (four papers)
        TNS
        TFTR
        MFTF

III.   Applications of Nonmetallics in Magnet
       Structures
        Nonmetallics at low temperatures
        Nonmetallic cryostats
        Industrial laminates
        Radiation damage in nonmetallics
        Accelerated aging under stress

 IV.   High Strength Stainless Steels for Low
       Temperature Service
        Nitrogen strengthened stainless steels
        (three papers)
        Fracture and fatigue of stainless steel

  V.   Thick Section Welding for Low Temperature
       Applications
        Evaluation of weld metal at cryogenic
        temperatures
        Welding nitrogen strengthened stainless
        steels
        Ferrite in austenitic stainless steel
        welds
        Impact properties of stainless steel
        welds
        Aluminum alloy plate for low temperature
        applications

 VI.   Physical Properties of Magnet Materials
        Elastic Properties
        Thermal Properties
        Radiation Damage
        Magnetic Properties
        Electrical Properties

In the following sections we present a brief summary
of the presentations and some of the conclusions and
recommendations reached during the workshop. Further
information regarding specifics can be obtained from
the authors of this paper. No proceedings will be
published.

Survey Results and Handbook Design

The NBS survey[1] considered the detailed materials
choices made in all then-current MFE device designs for
materials to be employed at low temperatures. The
existing data base was investigated, and areas where
more information was needed were determined. The most
critical of these needs were incorporated in a proposal

for a five-year research program. Particular attention
was paid to alternative materials and areas where the
present materials choices may be questionable due to
uncertainties in magnetic field size and pulse time.
The results of the survey have been summarized else-
where[2] in detail, but briefly, for the first year of the
research program we chose to concentrate on the low
temperature properties of structural materials for
very large load-carrying welded or bolted structures,
particularly those using the stainless steels. In the
present year of the program, attention is also being
paid to the nonmetallic components.

The handbook will contain graphical displays of
best value curves for the properties listed in Table 1,
usually as a function of temperature.

Table 1. Properties Covered by Data Handbook

A	B
Coefficient of Thermal Expansion	Bulk Modulus
Crack Growth Rate	Compression
Fatigue Strength	Creep
Fracture Toughness	Electrical Resistivity
Tensile Strength	Impact Strength
Tensile Yield Strength	Magnetic Permeability
Thermal Conductivity	Poisson's Ratio
Young's Modulus	Shear Modulus
	Specific Heat Capacity
	Stress-Strain
	Tensile Elongation
	Tensile Reduction in Area
	Thermal Diffusivity

Category A properties are considered of primary impor-
tance. Those data will also be given in tabular form
and the display will be accompanied by a characteriza-
tion table describing the original data. Only the
graphical display will be used for Category B. In both
categories an attempt will be made to show the extent
to which the general curve displayed represents the
actual data. Materials chosen for inclusion in the
first two years are 316, 304 and 21/6/9 stainless
steels, and 5083, 2219 and 6061 aluminum alloys.

Current Designs and Materials

These devices have been described in some detail
at this and previous conferences. The LCP presenta-
tions indicated that a wide range of structural mater-
ials are being used and that some mechanical properties
data is still needed on the chosen materials, which tend
to be modifications of the conventional austenitic
stainless steels and one aluminum alloy. The TFTR
presentation was particularly interesting in that,
while not a cryogenic system, it is one that is actually
being built and the problems and solutions occur much
more rapidly.

Applications of Nonmetallics in Magnet Structures

The presentations indicated conclusively that
large nonmetallic dewars can be produced. However,
strict attention must be paid to problems of helium
permeability through certain materials and the possi-
bility of severe creep near room temperature. The use
of industrial laminates as load-bearing insulation and
thermal standoffs is an integral part of all magnet
designs. Figure 1, from M. B. Kasen's presentation, com-
pares several composites with welded stainless steel in
terms of the thermal conductivity-to-strength ratio.
All of the NEMA grade laminates meeting the G10 or G11

specifications are highly proprietary formulations at
present. At the workshop we were able to reach agree-
ment with representatives of the industry to provide
three laminates meeting G10 and G11 specifications
with published (i.e. nonproprietary) formulations.
The two G11's will be amine cured and one will contain
boron-free E-glass reinforcement. Both of these
should have relatively good radiation resistance. The
low temperature properties of these laminates, from
industrial production, will be extensively tested in
the NBS program and, hopefully, their radiation
resistance can also be determined.
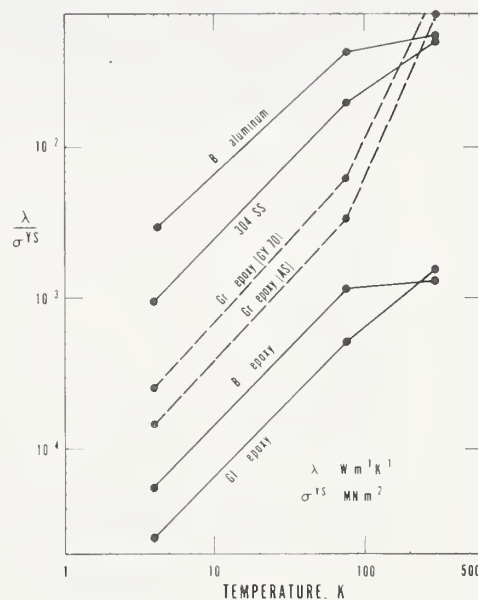
Fig. 1. Thermal conductivity to strength ratio for
several uniaxial composites compared to
welded stainless steel. From M. B. Kasen
NBS.

It seems clear that the radiation resistance of
organic materials of all types must be determined
soon. The very sketchy available data indicate that
these materials may be significantly degraded by the
flux levels presently proposed as operating conditions.
Most available work was not done below room tempera-
ture and has looked at the mechanical properties nearly
exclusively. Degradation of the electrical properties
may well occur at lower fluences. The fact that these
materials are at a temperature of 4 K is a much more
serious change of conditions for organics than
for metals. The only existing research program is very
small when one considers the myriad of questions to be
resolved. We do hope, however, that this program will
be able to determine the seriousness of the situation
in the near future. Perhaps then it will be possible
to pursue a larger scale effort to determine the limits
of existing materials and to start the development of
organic materials more resistant to radiation for
future applications.

High Strength Steels for Low Temperature Service

Nitrogen-strengthened AISI 304N fracture toughness

and tensile tests at 4 K indicate that the yield strength is doubled from its room temperature valve and that the toughness remains high. Use of the nitrogen-strengthened austenitic Cr-Ni steels is very promising, as most current projects do not contemplate using extremely strong alloys, such as the Nitronic series, and the development of intermediate strength, tough austenitic weld filler rods is closer to fruition.

Figure 2, from the presentation by D. T. Read and R. P. Reed shows the interesting relationship between strength and toughness at 4 K for a number of stainless steels. The lines represent a simple calculation of the maximum section size to permit plastic deformation prior to unstable crack growth. The higher the fracture toughness the larger the thickness can be and still achieve elastic-plastic fracture characteristics.
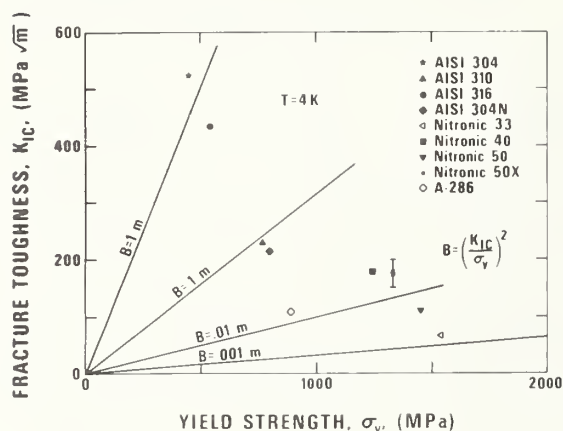
Fig. 2. 4 K fracture toughness versus yield strength for some nitrogen-strengthened and conventional austenitic stainless steels. From D. T. Read and R. P. Reed - NBS.

The next 4 K strength and toughness measurements on this material class will be on AISI 316, in particular AISI 316N and AISI 316LN will be examined. AISI 310S with high nitrogen may be tested also if it becomes available. Those in attendance felt that this program direction, providing preliminary strength data on nitrogen-strengthened Fe-Cr-Ni austenitic steels, could lead to a new higher-strength, tough alloy class for use in superconducting magnet applications.

Thick Section Welding for Low Temperature Applications

Austenitic stainless steels such as AISI types 304 and 316 and the nitrogen strengthened 21Cr-6Ni-9Mn alloy are readily weldable by all common welding processes, providing the appropriate consumables and procedures are used. The service experience with welded assemblies of these alloys has been satisfactory at cryogenic temperatures. A contributing factor to this success has been low design stresses; generally the stresses have been limited to about 140 MPa (20 ksi), the ASME allowable stress for 304 and 316. For large superconducting magnets, the enormous forces that must be contained and the limited space available for structure may necessitate operating at significantly higher stresses, stresses based on the strength of the

alloy at the operating temperature. Many of the unwelded austenitic stainless steels exhibit excellent fracture toughness at temperatures down to 4 K in the base metal, as shown above. However, weld metal fracture toughness has not yet been determined at 4 K. Limited Charpy impact results at 76 and 20 K suggest that the toughness may be marginal for these materials at 4 K, particularly if the stress levels for the magnets become higher than current practice allows. The proposed explanations for this behavior have included weld rod composition, ferrite content and microstructural variations. Welds with varying ferrite content have been prepared from 316 coated electrodes and are now being investigated metallurgically. Some preliminary toughness values of weld materials investigated for this program, and reported by T. A. Seiwert and R. H. Espy, are given in Table 2.

Table 2. CVN Toughness of Welds

Material (nominal composition)	Room Temperature		76 K	
308	58	(43)	35	(26)
310	--	--	42	(31)
330	--	--	90	(66)
13Cr 20Ni 9Mn + Cb	62	(46)	38	(28)
13Cr 20Ni 9Mn + Cb	37	(27)	16	(12)
20Cr 10Ni 9Mn	64	(47)	12	(9)
20Cr 10Ni 9Mn	67	(49)	12	(9)
18Cr 16Ni 9Mn	72	(53)	37	(27)
18Cr 16Ni 9Mn	60	(44)	18	(13)

Heading above table columns: "Toughness in joules (ft.lbs.) at"

No fracture toughness data at 4 K are yet available, but measurements are now being made.

Physical Properties of Magnet Materials

It was shown that measurement of the dynamic moduli of structural alloys provides an easy and inexpensive means of determining the behavior of the elastic properties over a wide range of temperature. Some results are shown in Figure 3, from the presentation of H. M. Ledbetter. Determination by static
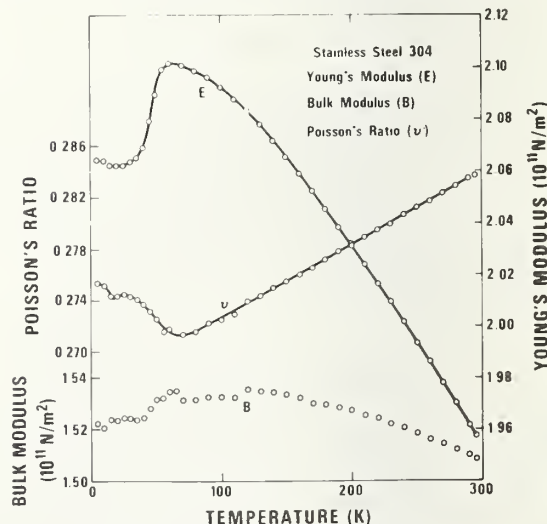
Fig. 3. Young's modulus, the bulk modulus, and Poisson's ratio for 304 stainless steel. From H. M. Ledbetter - NBS.

measurement at these many points would be prohibitively expensive. Agreement with static data is good at all temperatures where comparisons have been made.

The answer to the question "what is the thermal conductivity of copper at low temperatures?" is shown in Figure 4, from J. G. Hust's presentation. Obviously it depends on the specific material at hand. The parameter necessary for determining the conductivities is the residual resistance ratio (RRR). The purity (in "nines" or similar designations) cannot be used!
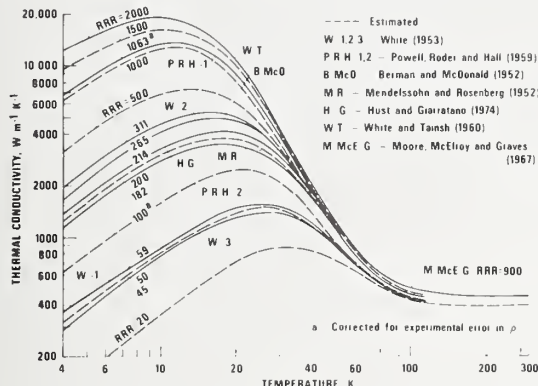
Fig. 4. The thermal conductivity of copper as a function of Residual Resistance Ratio [R(295K)/ R(4K)]. From J. G. Hust - NBS.

The effects of neutron damage on the electrical resistivity of the pure stabilizer metals, copper and aluminum, are reasonably well understood. Some questions remain regarding the effect on the thermal conductivity, the magnetoresistance and the implications of the metals being under stress during irradiation at low temperatures. We feel that the usual prediction schemes, such as the Wiedemann-Franz law relating electrical and thermal resistivity and modifications of Kohler's rule which predicts electrical resistance in a magnetic field, will probably be valid for the case of radiation induced defects. However, these assumptions are of such great importance for the overall magnet design that some attempt should be made to verify them by experiment.

The discussion of the magnetic properties of the stainless steels indicated a complex behavior for these alloys: transitions from room temperature paramagnetism to a low temperature antiferromagnetism occurs in some alloys; other alloys show characteristics of superparamagnetism at low temperatures. Ferromagnetism is associated with the stress induced martensitic transformation and with the presence of the ferrite phase in welds. For the most part, none of these effects appear large enough to have serious consequence for the structural elements. Some questions were raised regarding the source of the often stated requirement that the relative permeability of the structual steels not exceed 1.02, but no answers were provided.

The eddy current losses in both structural elements and pure metals found in the conductor composite and as coating for superinsulation were discussed. The losses can be significant and, coupled with the very low specific heat values at cryogenic temperatures, they

can cause significant temperature excursions. The problem in superinsulations has been solved by etching fine strips of the aluminum coating away so as to produce a grid pattern.

References

1. R. P. Reed, F. R. Fickett, M. B. Kasen, "Magnetic Fusion Energy Low Temperature Materials Program: A Survey," Report to ERDA/DMFE from NBS Cryogenic Division (March 1977).

2. F. R. Fickett, M. B. Kasen, H. I. McHenry and R. P. Reed, "A Low Temperature Materials Research Program For Magnetic Fusion Energy" paper BA 1, International Cryogenic Materials Conference, Boulder, Co, August 1977. To be published in: Advances in Cryogenic Engineering, Vol. 24, Plenum Press, New York (1978).

SURVEY OF LOW TEMPERATURE MATERIALS
FOR MAGNETIC FUSION ENERGY

Magnetic Fusion Energy
Low Temperature Materials Program

A Survey

March 1, 1977

by

R. P. Reed, F. R. Fickett, M. B. Kasen, H. I. McHenry

Cryogenics Division
Institute for Basic Standards
National Bureau of Standards
Boulder, Colorado   80302

to

Division of Magnetic Fusion Energy
Energy Research & Development Administration
Washington, D.C.   20545

TABLE OF CONTENTS

Page

I. INTRODUCTION

The present knowledge concerning magnetic-fusion energy (MFE) devices indicates that economical reactors will require superconducting magnets operating near the temperature of liquid helium. In this temperature region, many materials exhibit properties significantly different from those at room temperature. Sometimes these altered properties work to the advantage of the magnet system designer and sometimes not. In any event, the very high initial cost of the magnets and the difficulty of repair makes it essential that the behavior of magnet construction materials be well understood at the operating temperature and under operating conditions. Our objective is to define the materials problems and to organize a plan of effective materials research and technology transfer that will provide the materials information necessary to insure economical construction and reliable, safe operation of the low temperature components of MFE systems. Both short-term and long-term needs are addressed. The materials considered are structural, thermal and electrical insulation and normal-metal conductors; superconductors while of obvious importance, are not assessed in this survey.

The survey first considers MFE design constraints on material requirements. Materials proposed by the current MFE reference design projects are reviewed by project and material function. The second section presents an overview of the present state of relevant materials technology, discussing candidate materials, experience, property data base, fabrication, availability, costs, inspection and specifications. In these two sections we focus on the low temperature material design requirements and applicable modern materials technology, permitting a rapid appraisal of these two essential concerns and the development of a research program to meet the needs of MFE superconducting magnet technology.

The final major section (blue) presents recommendations for the research program. The entire scope of the work is summarized and the most cost-effective program at a 300-500 K$/year level is itemized. Descriptions of each program element are included.

A complete reference list of the documents used for this survey is provided. Appendices are included that itemize system components and materials of the various major MFE design projects. Also, in the appendices, a number of ongoing research projects that are relevant to this program are described.

We thank the many people engaged in the fusion energy program who contributed to this survey. We solicit their continued interest and request that suggestions be communicated to the authors.

II. MFE MAGNET SYSTEMS

In this section we first describe the extent to which specific operating conditions and design considerations place constraints on materials used in cryogenic components of existing MFE reference designs. We then present an overview of the proposed uses of four classes of materials: alloys, composites, insulators and conductors. Finally, we present a tabular summary of materials suggested for various components of the conductors, the cryostats and the support structures of the various designs.

The designs included in this survey are:
```
        ANL:  EPR-I, -II
        GA:   D-III, EPR-I, -II; TNS (with ANL), DEMO
        MIT:  HDTR
        ORNL: EPR-I, -II; TNS, EBTR, DEMO
        PPPL: TFTR, PLANT
        U. WISC:  UWMAK I, II, III:  TETR
        LLL:  BB-II, MX, FERF
```

Table II-1 gives an outline of the schedule proposed by ERDA for the development of a number of the fusion devices treated here. Table II-2 gives some general parameters of the toroidal system designs.

Table II-1. ERDA Proposed Magnetic Fusion Schedule (1976)*

Project	Start Conceptual Design	Begin Title 1 Funding	Begin Operation	Number Planned	Total 21 yr Cost 76-96** ($M)
Doublet III	Done	Done	1978	1	100
TFTR	Done	1976	1981	1	230
MFTF	1976	1979	1982	1	100
TNS/ITR+	1977	1980	1986	3	400
EPR	1983	1986	1992	2	800
Demo	1983	1986	1999	1	1200

*The schedule actually has many branch points depending on results of experiments completed.

+This is the tokamak version; the mirror version is on the same schedule offset 4 years into the future.

Other Facilities:					
RTNS	Done	Done	1978	1	5
LCP	Done	Done	1980	3-6 coils	37
INS	Done	Done	1981	1	25
Superconducting Magnet Test Facility	1980	1982	1985	1	50
FERF/ETR	1980	1983	1989	1	500

Source: ERDA-76/110/1. **These data are difficult to extract from the available literature.

250

Table II-2. Toroidal Systems Summary

Project	Power output (MWe)	Torus diameter (m)	Toroidal Field Coils			Field on axis/max. (T)	Some poloidal field coils inside TF? n or s?	Pulse Times		Toroidal β %	First Wall Loading (MW/m²)
			Size (m)	#	Normal(n) superconductor(s)			Initiation (s)	Burn (s)		
ANL EPRI		12	9x14 D	16	s	3.34/7.5	no, s (n)	1	37		
ANL EPRII	30	12	9.5x14 D	16	s	4.47/10(3 K)	no, s	2	55	4.8	0.86
GA D III	-										
GA EPRI	180	16	~7x12 D	24	s	4/8	yes, n	~7.5	60		1.03
GA EPRII	124	24	8.1x12.4 D	16	s	3.9/7.9	yes, n	2	105	10	0.85
GA/ANL TNS	-	7.6	6x8 D	12	s	5/10	yes, n	2	30	10	~1.0
GA DEMO	600	30	11x17 D	16	s	3.9/7.5	yes, n		800		0.97
MIT/HDTR		11.2	7.5x12.5 D	24	s	8/14.7	yes, n	~2	400		0.168
ORNL EPRI	300	13.5	8.6x11.4 oval	20	s	4.8/11	yes, n	2	100	3	1
ORNL EPRII		13.5	8.8x11 oval	20	s	5/11	yes, n	2	100		
ORNL/W TNS	~300	10	5x8 D	20	s	4.3/8	yes, n	2	20	14	3.7
ORNL EBTR48	~1600	120	7.2 circ.	48	s	2.5-4.5/7.3	--	--	--	25	1.13
ORNL LCP	--	4.6	2.5x3.5 noncir.	6	s	-/8.0	--	1	--	--	--
PPPL TFTR	--	5.4	3.8 circ.	20	n	5.2/9.5	no, n	4	--		0.15
PPPL Plant	2030	21	14.5x21 D	48	s	6/16	yes, s	~13	6000	4	2
UWMAK I	1500	26	17x24 D	12	s	3.83/8.66	no, s	100	5400	5.2	1.25
UWMAK II	1700	26	21x30 D	24	s	3.67/8.30	yes, s	10	5400	6.5	1.16
UWMAK III	2000	16	15x26 D	18	s	4.05/8.75	yes, s	15	1800	6-8	1.91
TETR	--	6.5	9.5x10.5 D	16	s	4.19/8.5	yes, n	1	60	3.8	1.0

II.A. Operating Conditions
    The following five subsections describe the effects of the MFE designs
on the properties required of the various materials. In general the
magnets are very large, cold structures operating in a relatively severe
radiation environment in the presence of high forces and large magnetic-
fields both of which may change rapidly with time. The aspects of the
environment considered here are: thermal, mechanical, electrical,
magnetic and radiation.

II.A.1. Thermal. Because large MFE magnets must operate at very low
temperatures, thermal effects are a primary consideration. There are
four distinct areas of concern and we will discuss them separately here.

a. Thermal Contraction

    Very large forces can result from differential contraction of the
elements of the magnet structure on cooling to the operating tempera-
ture. For example, the copper in the UWMAK I TF coil, under no stress
at room temperature, acquires a tensile load of 21 MN/m^2 (3000 psi) on
cooldown. In an unrestrained part, the total dimensional change can
be quite significant. A round stainless steel coil form 20 m in
diameter will show a decrease in its circumference of about 20 cm on
cooling to helium temperature. The case of metallic composites, such
as the conductor, with components which contract at different rates
often requires some careful thought. Fortunately, the calculations
involved in predicting the forces are relatively easy to make and, in
most cases, adequate data exist.

b. Heat Transfer

    The removal of thermal energy from the magnet to the coolant is
across an interface whose transfer properties are quite complex. The
various designs assume a heat generation rate of $\sim 0.2-0.4$ W/cm^2 of
copper in contact with a pool boiling system. The permissible value in
force cooled systems, such as proposed by ORNL, is still a topic for
quite a bit of research at present. In the pool boiling case, the
obtainable heat transfer rate depends on a number of variables including
the type and condition of the surface, its physical orientation and tem-
perature distribution.

c. Thermal Transport in Solids

    Probably the most severe demand on materials in a thermal applica-
tion comes when they must provide the mechanical means by which forces
on the cold magnet are transmitted to the room temperature support
structure. Non-metals, usually fiberglass epoxy, are preferred for this
application by all the designs, but, even then, rather clever techniques
must be developed to prevent excessive heat input to the cold region.
One example is that used by UWMAK of insulating rods which contact the
cold surface only in the event of a magnet quench, thereby supporting
the large additional loading caused by the quench. The low temperature
thermal conductivity of homogeneous solids is an area in which a large
amount of data exists. Some specific materials and complex composites
including superconductors and intact coil structures need to be investigated.

The thermal diffusivity, the ratio of the thermal conductivity to the product of the specific heat and density, is an important concept in the magnets. It determines, in effect, how rapidly thermal energy can be moved through the structure. It is a field dependent quantity in metals and, again, its behavior in complex structures needs to be investigated.

d. Dewar Insulation

Nearly all magnet systems in the MFE designs propose evacuated super-insulation, usually aluminized mylar, for this application. In some instances a copper shield cooled to an intermediate temperature is included. There is some indication that radiation damage may make the mylar insulation of questionable value. Even a slight change in reflectivity could represent a serious problem here. Whether or not this is the case must be determined and, if it is, an investigation should be made of the rather wide range of alternate approaches to the insulation problem. ANL suggests that eddy current heating in the aluminum layer could result in unacceptable thermal losses for pulsed coil dewars. The aluminum layer tends to be 0.05-0.1 μm thick. The eddy current calculation requires many assumptions but it seems that this, indeed, may be a general concern. Again, a simple experiment should provide the answers.

II.A.2. Mechanical. The most common mechanical stress, the maximum tensile hoop stress (σ_{max}) of a cylindrical coil can be approximately calculated using the expression:

$$\sigma_{max} \sim KB_m I \left(\frac{r_2^2 + r_1^2}{r_2^2 - r_1^2} \right)$$

where K is a constant proportional to length, B_m is the maximum field; I is the associated coil current, r_2 is the outer coil radius and r_1 is the inner coil radius. Obviously, the higher field magnets, coupled with severe space limitations, results in maximization of the coil hoop stress.

In Tokamak designs the pure-tension TF coils push against the internal support cylinder, with a force (F) equal to:

$$F = \frac{B_{max} I}{2} \quad (\ell)$$

where ℓ is the total length of magnet in contact with the central cylinder. These forces are also quite large, but there is greater bearing area to reduce the radial stress on the cylinder.

Conductor tensile forces from a given current and from a parallel conductor are significant in conductor cable and coil design but are not discussed here.

Table II A-1.

Approximate structural weights and forces

Project, Magnet, Maximum Height	Total Weight 10^3 lbs (10^3 kg)	Selected Approximate Forces 10^6 lbs (MN)
MX, Yin-Yang, 5m	430 (195)	31 (140)[1]
EPR (ANL), TF, 13m	416 (189)	23 (102)[2]
EPR (ANL), Poloidal, 2-20m	--	22 (98)[3]
UWMAK III, Poloidal, 9m	517 (235)	21 (95)[4]
UWMAK, II, TF, 30m	1562 (710)	46 (207)[5] 29 (129)[6]
UWMAK, I, TF, 30m	1980 (900)	71 (315)[7]
EPR (ORNL), TF, 12m	--	20 (91)[8] 79 (350)[9]
LCP (ORNL), TF, 4m	--	22 (100)[10]

[1] Force to open up Yin-Yang coil.
[2] From inadvertent radial coil translation of 2 cm.
[3] Vertical force on poloidal coil.
[4] Maximum coil tension.
[5] Radial from TF coil to central support cylinder.
[6] Radial in TF coil.
[7] TF coil maximum hoop force.
[8] Average tensile force in D-shaped coil.
[9] TF coil centering force in D-shaped coil.
[10] Maximum radial force on central support cylinder.

Forces on shields from rapidly-pulsed coils must be considered.
Shields will probably be required if the pulse-time of some poloidal
coils remains short (probable for TNS-type reactors). Forces from the
toroidal field on the induced eddy currents of the shield will be of the
order of 4.4 MN/m, which will require extensive structural alloy reinforce-
ment or composite construction.

From the design parameters discussed in the recent reports on TNS,
EPR or power reactor studies, approximate structural weights and forces
have been summarized in Table IIA1. These data are extracted from the
project reports as indicated and are, undoubtedly, very approximate.
However, several conclusions are obvious from this table:
   (1) The magnetic field-induced forces are very large. This indi-
cates that care must be taken to carefully choose the proper structural
members.
   (2) The gravitational forces from magnet weight are quite small,
compared to the field-induced forces.
   (3) While radial forces on the central support cylinders from each
D magnet in the tokamak design are the largest, a layer bearing surface
is also assured between the cylinder and the magnet.
   (4) The use of a higher allowable design stress will significantly
reduce the amount of structural material and permit more operating
space. If one assumes pure tensile or compressive forces and an allow-
able design stress of 30 ksi, the minimum cross-sectional areas range
from 700 to 2600 in^2 (4500-15,300 cm^2) to accomodate these forces. It
is obviously advantageous to use materials with larger allowable stresses;
for instance if a system is permitted to use 120 ksi as a 4K design
stress, the structural members are tremendously reduced.
   (5) Yin-Yang coil restraining members are very critical, for there
is a large force which tends to open up the coil.

In the tokamak design inter-coil torque between TF coils is signi-
ficant and arises from the interactions between the poloidal field and
the TF field and from possible malfunctions of a TF coil. Torque shells
or other structures are mandatory to alleviate these loads.

II.A.3. Electrical. The electrical properties of materials which are
of concern in fusion devices can be separated into three groups. Here
we give a brief description of each group and how it relates to the
reactor.

a. Conductors of Magnet Current
Our major interest is with superconductors, although copper and,
occasionally, aluminum are sometimes proposed for cryogenically cooled
magnets. The superconducting material itself has been adequately described
in many reports. Most designs propose to use the ductile NbTi. The Oak
Ridge EPR design does use Nb$_3$Sn in the TF coils.

The stabilizing metal is usually copper, although aluminum is
proposed by the recent University of Wisconsin designs. In general, the
higher the purity of the stabilizer, the better, although there are

practical limits due to problems of fabrication, cost and strength. The designs generally assume minimum resistivity values of $\sim$ 3 nΩ cm for Cu and $\sim$ 1 nΩ cm for Al at 4 K. Magnetoresistance effects are calculated to be large in copper, small in aluminum. Somewhat the inverse is true of radiation damage effects. In some instances, such as in the pulsed coils, it would be desirable to combine the stabilizing and strengthening function in one metal. Cold worked copper has been proposed for this role by ANL and UWMAK. Various dispersion hardened Cu and Al materials are being discussed also, but have not found their way into the designs yet.

A completely demountable superconducting coil joint may be required for access purposes. The problems involved would be immense. In any event, joining materials, principally solders are involved in all real coil systems and surprisingly little is known about them.

b. Eddy Current Losses and Control
The uncertainty in the fast field-rise time in tokamaks makes an assessment of eddy current effects somewhat difficult. It appears that a rise time of 1 sec to fields approaching 7 T is reasonable for near-term devices. The major problem here lies in the possibility of excessive heating of metals operating near liquid helium temperature, such as the conductors, dewar walls and coil forms. Eddy current shields within the superconductor composite used for pulsed coils appears mandatory. Copper-nickel is always the choice. The use of nonconducting composite materials for dewar walls is proposed by GA and may well become desirable or even necessary for the pulsed magnets. The option of shielding the (dc) toroidal field coils with a cryogenically cooled pure metal shield is considered by about half of the designs. One major advantage is that a given refrigerator power can remove a great deal more thermal energy from a 20 K region than from one at 4 K. Eddy current loss calculations are strongly dependent on geometry and quite complex. In general the power dissipation is proportional to the square of the field rate of change and varies inversely with the electrical resistivity. In large reactors, those that produce net power, the suggested field rise times are longer, of the order of 10 sec. This slower time dramatically reduces the concern for eddy-current heating; suggestions of need for non-metallic dewars and supports are replaced by suggestions for using aluminum alloys, which are cheaper and lighter, but have high conductivities.

c. Electrical Insulation
If it were not for the radiation environment, electrical insulation research for these large magnets would be reduced to measurements of the effects of stress and temperature on conventional organics. This is a topic already being studied in connection with superconducting powerline research and is a significant problem in itself. The maximum magnet terminal voltage at quench has been calculated to be as high as 10 kV, while most reasonable (organic) insulation schemes at present can withstand about 1 kV. Unfortunately, most existing information indicates that both the mechanical and electrical properties of the organics will be degraded by the radiation environment in the coils. Nevertheless all extant designs use organic insulators in one form or another and all

indicate concern. There is no question, though, that a radiation resistant, high voltage insulator is needed. It may be that some inorganic, or organic-inorganic, system will be necessary to satisfy these requirements.

II.A.4. Magnetic. In nearly all applications, it has been assumed desirable to avoid highly magnetic materials. As well as the possibility of field distortion and significantly increased forces, there is a hysteretic heating effect in hard ferromagnetic metals. However, some ferritic steels may offer advantages of cost, availability and fabricability and these questions need to be investigated in more detail before ferromagnetic materials are dismissed. In particular, it has been suggested that ferromagnetic materials in the magnet region would not noticeably ($< 0.5\%$) perturb the fields at the plasma. On the subject of hysteretic heating, a cursory look at the literature indicates that very little information exists on the low temperature magnetic properties of materials, such as 400 series stainless steel and conventional steels, whose applications are not directly magnetic. However, what information does exist seems to indicate very narrow hysteresis loops. Since the energy loss is proportional to the area of the loop, one should not expect a problem in general. A calculation for pure iron, a relatively very high loss material in this group, shows a heating of 80×10^{-6} J/cm^3. In a 12 m magnet with a 0.03 m^2 cross section, this represents a loss of less than 1 W over a 100 s burn cycle. Note that the loss per cycle is not dependent on the rate of change of the field and is generated pretty much uniformly over the burn cycle of the reactor. Eddy current losses, on the other hand, depend directly on the the cycle frequency. It, thus, seems that the hysteretic losses are probably not a major concern where long burn times are involved.

A topic which may require special consideration is the matter of ferrite in austenitic stainless steel welds. Typically the welds contain 4-10% ferrite, a ferromagnetic phase, to avoid hot cracking. In nearly all designs such welds may be very close to the conductor. It needs to be determined if magnetic effects from the ferromagnetic phase can cause serious problems in these situations.

II.A.5. Radiation. The prospect of damage to the magnet system by radiation is a concern for all but the largest device designs. Unfortunately, it is difficult to describe a general radiation environment for the cold system with any accuracy. The type and amount of radiation and its energy spectrum are all determined by the exact details of the tritium breeding and blanket and shield systems. It appears, however, that the neutron spectrum seen by the innermost magnet coils will be similar to the fission spectrum. The typical neutron wall loading of 1 MW/m^2, corresponds to a 14 Mev neutron flux at the first wall of 4.5 $\times 10^{13}$ n/cm^2/s. This flux will be attenuated by 10^{-5} -10^{-7} in its trip to the magnets depending on the particular design. In general, the smaller the device, the smaller the attenuation.

The neutrons produce damage by a variety of processes: neutron capture with subsequent γ ray or β emission (n, γ) and recoil of the emitting nucleus, hydrogen production (n, p), helium production (n, α) and damage by secondary charged particle cascades resulting from an elastic interaction between the neutron and atoms of the host material. The cross sections for these interactions are highly dependent on neutron energy and the interaction depends, also, on the presence of particular elements in the system. It is important to realize that the energy deposited in the magnets by some of these interactions may exceed that of the incident neutron flux, perhaps by an order of magnitude in the case of the (n, γ) reaction.

Magnets operating at liquid helium temperatures are very susceptible to thermal input as the heat capacity of copper at 4 K is more than three orders of magnitude below its room temperature value; 1 W of heat input to the helium bath requires about 250 W of room temperature refrigeration capacity. Thus, even if the actual damage due to the radiation is considered acceptable, for example a 5% increase in stabilizer resistivity, the thermal input to the refrigerating system may not be. Furthermore, the possibility of (n, p)-produced hydrogen clogging the liquifier systems must be considered in some instances.

In terms of potential for radiation-induced problems in cold magnets and their surroundings, the materials appear to fall in the following order: superinsulation, organic electrical insulation, stabilizer superconductor structural material. There is little agreement on the exact magnitude of the problem regarding the insulations. It seems most prudent to assume that it is severe, that it is strongly dependent on the type of radiation and that the effects at low temperatures and during annealing cycles will be quite different from those observed at room temperature. Some guidelines exist in the literature regarding polymer susceptibility to energy deposition but direct extrapolation of this information without experimental verification is not wise. Frequent lip service is given to the use of inorganic insulations with all their attendent structural problems, but little hard information exists. It seems imperative to determine quite soon whether or not organics may be used.

The low temperature resistivity of the pure metals used to stabilize the superconductor increases fairly rapidly under neutron irradiation due to the production of vacancy-interstitial pairs. The result is usually expressed in displacements/atom (dpa). The relationship of this parameter to incident neutron energy depends on the metal, but typically 10's of eV are necessary for one displacement. The net effect is quite different for the two common stabilizers, aluminum and copper and there are various complex tradeoffs to be made involving magnetoresistance, strength and radiation effects. It appears that the existing data are barely adequate under a number of assumptions about the neutron spectrum. Furthermore, it seems that room temperature annealing of the magnets about every year is likely to be necessary at the neutron flux levels presently being considered.

Radiation damage of the superconductor itself and the structural
materials does not appear to be a serious concern in the designs. The
materials do provide sources of secondary radiation, and a heat load and
gas load on the refrigerating system. From this point of view, their
impurity element chemistry may be important.

II.B.   Design Considerations
     The MFE project reports to date have dealt with conceptual designs
of superconducting magnet systems. Little consideration is given to the
exact sizing of structural details, fabrication methods and inspection.
In this section, design, fabrication and inspection considerations that
influence material selection are discussed.

II.B.1.   Codes and Specifications. A code is needed for the design,
construction and inspection of magnets for MFE devices. Adherence to
this code should provide assurance that the magnet system provides the
intended field and operates in a safe, reliable and efficient manner.
Establishment of such a code for large magnets must await further develop-
ments in the technology. However, parts of the code should be set forth
as preliminary guidelines to facilitate the orderly development of
magnet systems. In this section, the guidelines and specifications
needed for proper selection, procurement, processing and inspection of
materials are identified.

     Design guidelines needed for selection of materials are definitions
of operating loads and conditions and criteria for establishing allow-
able working stresses for candidate materials. For magnet systems,
description of the operating loads should include the anticipated load
history for normal operation, loads due to credible fault conditions and
procedures for treating combined loads. The operating conditions of
interest are the thermal environment, radiation dosage, magnetic field
profile and design life. Allowable working stresses should account for
the materials strength variability, the fatigue strength for a specified
scatter factor on fatigue cycles, fracture mechanics analysis and a
factor of safety based on uncertainties in the loads and stress analysis.

     Material procurement and processing should be controlled by a set
of specifications which are sufficient to preclude use of materials in
the magnet systems which have properties inferior to those assumed in
design. Material procurement specifications should be prepared for each
material and product form. These documents should specify minimum
acceptable values for tensile properties and, in certain cases, for
fracture toughness and for physical properties such as residual resis-
tance ratio or magnetic permeability. Requirements will be established
for melting and primary processing, heat treatment, chemical composition,
ultrasonic quality and dimensional tolerances. Quality assurance pro-
visions, testing procedures and reporting requirements should be described.
Microstructural requirements should be established as applicable, e.g.
ferrite content, grain size, inclusions, etc. Care should be taken in
the preparation of these specifications to avoid stipulating require-
ments that add cost but do not contribute to magnet performance.

     Processing specifications are needed for processes such as heat
treatment, casting, forging, welding, adhesive bonding, soldering and
composites manufacturing. Requirements are to be established for equip-
ment control, processing procedures, acceptance standards, quality assurance
provisions and workmanship. Where applicable, mechanical properties,

chemical compositions, surface requirements and dimensional tolerances should be defined. Procedures for items such as surface preparation, rework and repair and temperature control should be detailed. Applicable testing procedures, subcontractor provisions and reporting requirements should be covered.

Inspection specifications and standards are needed to provide a high degree of confidence that no defects are present in the raw materials, or introduced during fabrication, which could cause unsatisfactory performance of the magnet system. Receiving inspection should verify that the materials and components meet the requirements of the procurement specifications. Detail part inspection should be conducted in accordance with specific instructions, dimensional tolerances and NDE standards applicable to the part. Final assembly inspection should verify conformance to the material, dimensional and installation requirements specified on the engineering drawing.

II.B.2. Fabrication. The size and complexity of proposed designs cause many problems unique to the construction of MFE devices. Materials considerations related to fabrication of the conductors, coil forms, eddy-current shields, dewars and magnet-support structure are identified in this section. In each case, the problems associated with basic production are not discussed; e.g. it is assumed that the conductor will be supplied, but problems associated with winding the conductor are considered.

a. Conductors

The conductor is a complex assembly consisting of some of the following elements: the superconductor, the stabilizer, a strengthener such as stainless steel and channels or interstices to permit the flow of liquid helium. This assembly must be co-wound into coils with an insulating layer and in some cases a strengthening member. Sufficient winding tension must be used to assure that the relatively stiff assembly conforms to the desired coil shape, maintains that shape during winding and does not move excessively when the coil is energized. The winding tension must be limited to avoid exceeding the strain tolerance, joint strength or crushing strength of the assembly. Fabrication problems may also arise due to the enormous size of the magnets, e.g. perimeters up to 200 m for PF coils.

b. Coil Forms, Central Column and Magnet Support Structure

The structural elements of the magnet systems are large, subjected to large forces and must fit within limited space. The sizes will require build-up by joining many pieces. The forces necessitate use of thick sections; the manufacturing, joining and inspection of thick-section parts require further development, particularly for stainless steels and fiber reinforced plastics. The space limitation may necessitate the use of high strength materials, which are generally more difficult to fabricate.

c. Eddy-Current Shields

Special fabrication procedures may be required to preserve the high RRR of the pure Al or Cu used in eddy-current shields.

d. Dewars

Space limitations and accessability problems may hinder fabrication of dewars. Leak-tight closure of the dewars may require welds with limited inspectability and high restraint. Force transmission from the magnet to the support structure may require close-tolerance assembly to avoid overloading the dewars. Accessability requirements during assembly and service may require fabrication of a removable dewar.

e. Magnet System Assemblies

Cantilever-type loading cranes (we think) have a present capacity of about 300 tons. Giant shipyard gantry loading cranes, fixed on two sides, have capacities up to 900 tons. The magnet systems are extremely large and weigh in excess of 200 tons. The handling of these large assemblies during erection may be prohibitive if the entire magnet system is completely fabricated as a subassembly. It may be necessary to split the coil into segments and assemble the segments into the final configuration on site. This will require development of new coil fabrication concepts and a breakthrough in joining methods. Similarly, dewars may have to be assembled around the coil after installation.

II.B.3. Inspection. A quality assurance system is required for major MFE devises to ensure that the materials, components and final assembly of the devise conforms to the engineering drawings and quality specifications. Procurement controls, inspection standards and process controls will be defined as the detail design and manufacturing plans are developed. The technology to permit specification of reasonable quality standards should either be available or developed for the principal elements of the MFE magnet system. In general, the controls needed to construct large, complex devices are well understood on the basis of military, NASA and nuclear-power-plant experience. However, each new system presents unique needs for quality standards, testing requirements and non-destructive evaluation. The design features of large magnets for MFE devises that may require the development of improved inspection methods and standards are identified in this section.

a. Conductors

The conductors are complex assemblies that will be mass produced and supplied to the magnet fabricator. Procurement quality standards, sampling criteria and receiving inspection tests are needed to assure that consistently satisfactory conductors are used to build the magnets. The standards and tests must ensure that the conductor exhibits the electrical, thermal and mechanical properties needed to function properly in the magnet. During fabrication, controls must be developed to ensure proper fit of the conductor in the winding, complete coverage of the insulation, adequacy of the conductor joints and, where applicable, satisfactory incorporation of the strengthening elements. Upon completion of the magnet assembly, tests may be needed to ensure satisfactory performance of the magnet prior to installation of the magnet into the

MFE devise - a procedure that is nearly irreversible in many of the designs.

The complex nature of the conductors and the diverse requirements for satisfactory performance may eliminate the possibility of routine NDE. Instead, performance tests on representative samples that require removal of the sample from the lot of material may be essential for receiving inspection of conductors. Inspections during magnet winding, e.g. of joints, may be inadequate for complete assurance and thus, there may be a need for stringent fabrication controls that virtually assure satisfactory performance. The current practice of strain gaging the coil form to monitor winding tension is helpful, but further controls may be needed.

b. Coil Forms and Magnet Support Structure

From an inspection standpoint, the choice of structural materials, the thick section requirements, the overall size of the magnets, the need for structural efficiency and the limited accessibility during assembly create inspection difficulties in many MFE conceptual designs. The likely material choices for principal load carrying members are austenitic stainless steel and, where eddy current losses are a consideration, fiber reinforced plastic. These materials are not intrinsically difficult to inspect, however the thick section requirements and the need for joints in stainless steels arising from the large overall size may cause inspection problems. Ultrasonic inspection is not satisfactory for thick section joints and thus reliance is on radiography - a method that does not reliably detect crack-like defects. The need for structural efficiency leads to higher operating stress levels, and consequently, to greater defect sensitivity, more stringent defect acceptance standards and more rigorous inspection. The limited accessibility and other space constraints lead to designs with limited inspectability, e.g. welded corners and blind installations.

c. Dewars

The dewars are likely to be a particularly complex inspection problem because of the variety of materials used to transmit the forces from the magnet to the support structure, to provide the thermal gradient from 4 K to room temperature and to contain the liquid helium without leakage. Proper load transmission and thermal performance requires care in assembly and bonding of many dissimilar materials. The no leakage requirement may require blind closure joints in areas where poor heat-input control may degrade the insulation.

II.C. Materials and Components
      In this section we list the projects reviewed for this study and
present a brief summary of the uses proposed by these projects for four
classes of materials: alloys, composites, insulations and conductors.
Tables summarizing all of the materials choices by project are included
as Appendix A. Detailed discussions of the more important materials
choices for particular applications are given in Appendix B. These
listings include the requirements which must be met by the material.
They also include some assessment as to what research will be required
in order to produce design data for the application.

II.C.1. Material Overview. We present here an overview of the proposed
cryogenic uses for alloys and composites in MFE systems, plus an over-
view of the materials proposed for insulators and conductors.

                        a.   Structural Alloys
      Stainless steel and aluminum alloys are used exclusively for
metallic structural applications in all of the MFE conceptual designs
reviewed. Stainless steels are used for the coil forms (ANL, ORNL, GA)
the Yin-Yang coil case, the central support cylinder of tokamak designs
(UWMAK I and II, ORNL, ANL), the C-clamp structure for FERF, the support
structure (LLL, ORNL/EBT, GA) and dewar walls (ORNL/EBT, GA, UWMAK I and
II). Aluminum alloys are used by ANL for dewar outer-walls, external
support structure and the inner cylinder of the central support, and
by Wisconsin for the coil form, dewar walls, central support and coil-
joint bolts for UWMAK III.

      Generally the specific alloy grades are not designated, however,
most design groups had some preference. For stainless steels, type 316
is preferred by ANL and Wisconsin (for UWMAK I and II); Nitronic 40 is
preferred by LLL; ORNL is considering 304/304L, 310S and Nitronic 40.
For aluminum alloys, ANL prefers 7075-T6 for the external support struc-
ture which is at room temperature; and Wisconsin prefers 2219.

      In an ORNL report, Long (1976) considers superalloys to be one of
the most promising classes of alloys for MFE magnet applications.
Inconels 706, 718, 750 and A286 are mentioned as candidates. No specific
applications for these alloys were included in the conceptual designs
of EPR, Demo and EBT.

                      b.   Structural Composites
      Non-metallic composite materials fill two primary structural func-
tions in current MFE conceptual designs:
      1. Reducing the refrigeration costs by providing supports transi-
tioning from 4.2 K to 300 K.
      2. Reducing eddy current losses (and thus refrigeration costs) due
to interactions between the pulsed magnetic fields of the poloidal mag-
nets and the surrounding metallic structure.

      Thermal Standoffs: All Tokamak designs visualize the entire toroidal
magnet system plus the central support column to be maintained at 4.2 K.
The ORNL EPR reference design cites the need to support the total weight

on insulators having load carrying ability but without specifying the insulator type. ANL proposes to support the central column on a GFRP cylinder, while the TF coils receive additional support from an external G-10 laminate structure loaded in compression and transmitting the load through the vacuum vessel walls. The warm-reinforcement system of BNL supports their TF magnets with an 0.5 m thick thermal barrier of inter-leaved layers of stainless steel and GFRP (1:2 ratio). The barrier modulus is controlled by the stainless, while the overall thermal conduc-tivity is controlled by the GFRP. Thermal shorts are provided at 77 K and 20 K. GA proposes the general principle of supporting the TF coils on long, slender rods of low-thermal conductivity material, providing both gravitational and lateral stability. Stacked ceramic discs and a "bicycle-chain" tension support were considered, however, the GA DEPR design settles for a hollow, non-metallic composite cylinder supporting a stainless steel ball joint which provides some lateral adjustment. No specific material is discussed.

A common problem is transfer of gravitational and fault loads from the TF magnets through the dewars to external supports. PPPL uses G-10 pads inside the dewar which contact the opposite wall only in the presence of fault loads. UWMAK inserts a large number of GFRP struts between the TF magnet dewar walls, 10% of which continuously bear on the opposite wall through conical spring caps to provide a centering force, while the rest contact only under fault loading. The UWMAK diverter coil dewars are similar in design, using Micarta spacers.

ORNL has an EF coil design of concentric stainless steel pipes, the inner of which is the conductor jacket and the outer annulus of which contains LN_2. The coil must be isolated from the surrounding warm struc-ture with load-bearing insulating struts capable of sustaining cyclic stresses.

ANL considers the alternatives of constructing the central support column of their Tokamak from either concrete or a GFRP composite such as G-10. They are concerned, however, that the low modulus of the latter (2×10^6 psi) will result in excessive conductor strain in the TF magnet.

Reduction of Eddy Current Losses: The ORNL, ANL and GA Tokamak designs anticipate unacceptable AC losses due to eddy currents induced in metallic structures near the pulsed poloidal coils. Substitution of non-metallic composites for metal may be mandatory if refrigeration costs are to remain reasonable.

Fiber-reinforced plastic is proposed for use as poloidal coil man-drels (ORNL, GA), for at least the inner wall of the poloidal magnet dewars (ORNL, ANL, GA) and for structural casings surrounding the supercon-ducting bundles in poloidal coils (ONRL, GA). The latter also function as the helium cyrostat, requiring minimum helium permeability.

The ORNL EPR design proposes the GFRP mandrels be divided into 12 coupled groups, each group made up of seven segments, layer wound with enough tension to hold the poloidal coils in place without the need of an outer case. GA proposes that the central OH coil solenoid be wound on a GFRP spool and prestressed with stainless steel bands and inserted into the central bore formed by the mating vertical sections of the TF coil.

ANL proposes non-metallic poloidal coil dewars with a 5-mil metal helium permeability barrier, citing a McDonnell-Douglas automatic glass-filament braiding method as a means of obtaining the desired result. GA proposes a GFRP helium container (inner dewar wall) for their OH-coil cryostat, preventing AC losses at the ends of the coil solenoid where a variable magnetic flux crosses the cryostat wall. Outgassing of the composite is considered a negligible problem due to the low temperature. Good electrical insulation between the OH coil and the outer dewar wall is an added advantage. For the superconducting magnetic energy storage coils in their Scyllac Fusion Reactor, LASL proposes a series of 128 cylindrical GFRP liquid helium dewars, each 1.07 m i.d. by 6.96 m deep, operating at a pressure of 5 atmospheres. S-904 glass filament-winding is proposed using a flexibilized epoxy resin.

ORNL would like to reduce AC losses in their poloidal field coils by surrounding transposed conductor bundles with leak-tight GFRP tubes serving as both a structural member to relieve the stress on the conductor and to contain the supercritical helium used as a coolant. ORNL cites lack of knowledge of the elastic response to load, of failure mechanisms related to load regimes and of response to dynamic fatigue at 4.2 K as major problems facing designers wishing to use GFRP materials for critical applications in superconducting magnets. ANL arrives at a similar solution to eddy current losses in their OH coil, differing from ORNL only in proposing to use a rectangular G-10 tube with a thin-wall stainless liner.

Radiation Effects: The comments under Insulators (see the next section) apply equally well to structural composites.

Alternate Materials: Suggestions for use of industrial laminates reflect familiarity with such materials in normal magnet construction. However, such materials have not been well characterized at cryogenic temperatures, particularly in a radiation environment. Furthermore, industrial laminate tradenames refer to a wide variety of products produced by a given company. The National Electrical Manufacturers Association (NEMA) specifications for industrial laminates are more meaningful; however, the specifications require only functional performance at or slightly above room temperature and can therefore be met by manufacturers products differing significantly in type and weave of the reinforcement or in the matrix resin. Existing NEMA specifications are inadequate for demanding cryogenic laminate performance. It is also highly probable that the less expensive borosilicate glass used in industrial laminates will lead to more rapid degradation of the laminates under neutron irradiation than would be the case with the more expensive (but higher modulus) silica-alumina-magnesia S-type glass used in more specialized composites.

Whenever section stiffness becomes a sufficient problem, higher modulus fibers such as Kevlar, graphite or boron are readily available for substitution for glass at some increase in cost, although hybrid construction can often be used to advantage. Obviously, boron fiber is restricted to areas of low neutron fluence.

These subjects are discussed in more detail in Section III B of this report.

c. Insulators

GA mentions the possibility of using polyethlene, mylar or glass-fiber reinforced plastic (GFRP) for electrical insulation in superconducting coils, while UWMAK suggests Kapton for this purpose. However, the materials most often specified are the NEMA G-10 (glass-epoxy) or the micarta (cellulose-phenolic) industrial laminates.

The possibility of combining electrical insulations with structural support of the superconducting coils is recognized in all designs. However, ORNL believes that the magnet stresses will be too high for adequate strain limitation by low-modulus GFRP restraints, leading to their decision to separate the load-carrying and the insulation function in the coils of their EPR devices.

ANL proposes to spirally wrap the TF coil cables and supporting stainless steel plates with G-10 glass-epoxy, providing nonvapor-locking helium cooling channels. The insulation is given as 1 mm thick, 1 cm wide, with 50% coverage. The 200 V dielectric breakdown required for the application is believed to be well within the capabilities of the insulation. The overall coil form is stainless steel insulated with micarta or G-10, 1 cm thick. ANL notes that the multilayer OH and EF coils require large gaps between layers and proposes to fill them with G-10. Concern is expressed that pinholes and cracks which exist in the material or which form during cooling, or in service, will degrade the dielectric properties of the insulator when the magnet is energized. Such damage is irreversible and, since insulation is almost impossible to replace in a completed magnet, insulations will require much more study. ANL also proposes to "jelly roll" band the 150 basic cables in their poloidal coils with GFRP 2 mm thick, 2 mm wide and with a 3-inch pitch. No stainless steel reinforcement is used, the stresses being transferred through the composite to external support rings. Insertion of 2-cm thick G-10 or Micarta laminates every 10-15 turns is proposed to provide additional resistance to the compressive (repulsive) forces and to relieve stress on the cables. Concerning energy storage and transfer superconducting magnet systems, ANL proposes to separate pancake-type coils by GFRP boards 1.25 cm thick with 50% coverage. The basic conductor support is a U-shaped GRFP channel, 3 cm high, 12 cm wide with an 0.5 x 10 cm slot. A 200-strand, transposed superconducting cable wound around a GFRP board as a coil form is inserted into the slot. Again, ANL expresses concern about dielectric strength and possible arcing problems in use, perhaps accentuated by a radiation environment. In the absence of hard data, ANL tentatively specifies an epoxy set with an aromatic curing agent, reinforced with glass and filled with granular alumina.

The UWMAK design contemplates using GFRP to support and insulate the superconducting windings in the preformed stainless or aluminum discs which form the main structural element in their TF magnets, using Micarta spacers between the discs. Divertor and transformer coils would utilize Kapton between conductors and Micarta spacers between coil pancakes. UWMAK also proposes to spiral wrap the poloidal coil surfaces with B-staged GFRP to 50% coverage.

LLL proposes a polyimide or a polyimide-glass laminate in the form of slotted sheets for interlayer insulation in their FERF (mirror) superconducting magnets. Interturn insulation would be spaced, laminated dots held on a film substrate.

Finally, the DC homopolar energy storage system proposed by LASL would use GFRP struts to insulate and support the superconducting excitation coils in the stator iron and would use a GFRP strut as a double-acting thrust bearing to maintain the axiality of the rotor with respect to the superconducting coils.

Radiation Effects: All designers of MFE systems express concern over the possible adverse effects of neutron and secondary radiation on the integrity of organic materials. ANL believes that the epoxy insulator in the magnet will see 3.5×10^8 rads at a lifetime integrated wall load of 2.5 MW-yr m^{-2}. This is believed to be well below the 10^9-10^{10} rads and 10 MW-yr m^{-2} level at which the properties of epoxy are expected to be significantly damaged. Extrapolation of data from higher temperatures has lead ANL to a choice of the aromatic base epoxies as the organic material most resistant to radiation damage -- perhaps 10-20 times more resistant than mylar. ANL evidence indicates that mylar could only be used up to 1 MW-yr m^{-2} in EPR designs. There are no 4.2 K radiation data. However, ANL believes that the damage to GFRP structures will be primarily manifested in strength reduction rather than in dielectric property changes.

These views are not necessarily shared by LLL who considers that radiation damage might preclude all organic insulators in MFE superconducting magnet systems. LLL states that polyimide is the most radiation resistant polymer presently available and should be used in place of epoxy. Designers of the UWMAK system are somewhat more optimistic about the chances of mylar as an insulator, calculating that the insulation would be exposed to 60×10^6 rads in 30 years in their design, while citing a previous analysis as showing the mylar damage threshold to be at 30×10^6 rads with 1.2×10^8 rads being required for a 25% decrease in tensile strength. UWMAK also assumes a threshold for GFRP damage at 8×10^9 rads, with 5×10^{10} rads required for a 25% strength decrease, suggesting that the problem should be minimal.

A major unknown is the extent to which release of energy stored in polymers during 4.2 K radiation will result in damage when warmup releases the energy (Wigner energy).

Alternate Materials: If radiation damage to unreinforced polymers becomes a significant problem, reinforcing the polymer with S-glass (silica-alumina-magnesia) is expected to double the radiation resistance. The use of the less expensive E-glass may cause a problem, as its lime-alumina-borosilicate composition is sensitive to heating and degradation in a neutron radiation environment.

Should a higher modulus in the plane of the reinforcement be required, fibers such as Kevlar or graphite might be substituted for glass. Graphite-epoxy composites could be substituted for stainless steel support plates

around which the conductor is wound, providing equal or higher stiffness, higher strength and better insulating qualities thus reducing the probability of turn-to-turn shorts. The very low thermal contraction of graphite composites would have to be carefully considered in this and similar applications.

Care should be taken in referring to industrial laminates by company tradename or by NEMA specifications. Neither are sufficiently precise for specifying demanding cryogenic performance. This subject is addressed further in Section III B.

d. Conductors

In nearly all proposed applications in MFE designs, NbTi cryogenically stabilized with copper is the superconductor of choice. In applications which are basically dc and involve the largest forces, such as TF coils in tokamaks, the conductor is strengthened by stainless steel, usually of significant cross section. Allowable strain values tend to be $\sim 0.2\%$, although it seems this constraint is somewhat artificial. It has been suggested that a copper alloy might serve both the stabilizing and strengthening function in some instances. In other designs, such as Yin-Yang magnets and some TF coil constructions, where the load can be transferred to the coil case, the strength of the pure copper stabilizer or a cold worked copper is assumed adequate. When pulsed coils are considered, the coils generally are more complex and contain less stabilizer along with a high resistivity alloy, usually CuNi, which breaks up potential eddy current paths. NbTi is still the superconductor. The conductor structure often is a braid containing a stainless steel wire or strip for strength. Stress levels in general are not as high for these coils as for the dc ones.

Current carrying capacity of the conductors nearly always falls in the 5-20 kA range and most are cooled by pool boiling helium, although forced flow cooled conductors are also under serious consideration as they greatly simplify the overall magnet structure.

Radiation effects expected in the conductor composite depend strongly on the particular design, but it appears that, in all cases, degradation of the low temperature conductivity of the stabilizing metal will require periodic annealing of the magnets at temperatures near room temperature. The effect on the superconductor itself is not expected to be severe.

II.C.2. Component Research Summary. Table II C-1 presents a general summary of the material choices listed by component. Alternate materials are suggested and the required data is summarized in abbreviated form. We have also indicated the project class for which we feel the information will first be necessary and class of data. Detailed listings of the materials selection for the components by each MFE reference design are given in Appendices A and B.

Table II.C-1

Projects Which Need Data: columns **LCP TFTR MX**, **TNS**, **EPR/DEMO**, **Power Plants**

Conductor Components	Materials Suggested	Other Candidate Materials	Data Required	LCP TFTR MX	TNS	EPR/DEMO	Power Plants	Material Screening	Base Material Screening Data	Data for Processing/Joining	Specifications	Design (Codes)
Stabilizer	OFHC Cu	Hi-purity Cu	rad → ρ, ρ(B)	X	X	X	X		X			
	C.W. Cu		σ + rad → ρ, ρ(B)	X	X	X	X		X			
	"Pure" Al	Cu alloy	recovery (4–300K) ρ, ρ(B)	X	X	X	X		X			
			fatigue-strength → ρ, ρ(B)	⊗	⊗	⊗	⊗		X			
			hi-strength stabilizer dev.	X	X	X	X			X		
			processing/purity → RRR	X							X	
Strengthener	S.S. C.W. OFHC Cu	Hi-modulus composites (C,B,W fibers)	dev. of hi-modulus composites (strengthener + insulator)		⊗	⊗	⊗	X				
Electrical insulation	Polymer films Laminates (G-10, G-11, etc.)	Inorganics, polymers	mech., elect., thm. data	X	X	X	X	X				
			compressive σ → ρ,ε,K	X	X	X	X		X			
			rad → mech	X	X	X	X	X				
			rad → ρ, ε, K	⊗	⊗	⊗	⊗		X			
			fat → ρ, ε, K, strength	X	X	X	X		X			
			development of specifications								X	
Adhesive agents	SnPb solder Epoxies		shear strength	X	X	X	X	X	X			
			composition → K, ρ(B)-SnPb	X	X	X	X	X	X			
			rad → shear strength, ρ, K	X	X	X	X	X	X			
			fatigue strength	⊗	⊗	⊗	⊗		X			
Eddy-current shielding	Cu-Ni											
Conduit	SS Al alloy Laminate											
Nb₃Sn conductor components	Cu-Sn		mech		X	X	X		X			
	Ta		rad → mech., elect., thm		X	X	X		X			

List of abbreviations: C.W.-cold worked; S.S.-stainless steel; Mech-mechanical property; Fat-fatigue; ε-dielectric strength; ρ-electrical resistivity; B-magnetic field; →-effects on; K-thermal conductivity; Elect-electrical property; Thm-thermal property; Rad-radiation; ⊗-especially important to poloidal field coils.

Table II.C-1 (continued)

Cryostat	Materials Suggested	Other Candidate Materials	Data Required	Projects Which Need Data — LCP TFTR MX TNS	EPR/ DEMO	Power Plants	Material Screening Data	Base Data	Processing/ Joining	Specifi-cations	Design (Codes)
Coil Form-TF	AISI 316, 2219 Al, 21/6/9 S.S.	AISI 304, A286, ferritic alloy, Al alloy, advanced composites	Aluminum and ferritic alloy, advanced composites development			X	X				x
			Hi-strength weld metal (21/6/9)	X	X	X			X	X	
			Thick-section welding (S.S., Al alloy)	X	X	X			X	X	
			δ ferrite-toughness (S.S.)	X	X	X			X	X	
			Closure welding (S.S., Al alloys)	X	X	X			X	X	
			Weld inspection (S.S., Al alloys)	X	X	X			X	X	
			Hi-strength cast S.S.-mech.	X	X	X			X		
-OH,EF	GFRP S.S.	Advanced composites, concrete, laminates	Chemistry., processing → mech.								
			Mech., thm., elect. (concrete)		⊗	⊗	X				
			Rad., fatigue → strength (GFRP)	⊗		⊗	X	X			
			Rad., fatigue → strength (advanced composites, laminates)			⊗	X	X			
			Rad., fatigue, σ → creep (GFRP)	⊗	⊗	⊗		X			
Dewar Walls (low temp.)	AISI 316, 21/6/9, S.S., Al alloy, GFRP	FRP	Rad. induced outgassing (GFRP)	X	X	X	X				
			He permeability	X	X	X	X				
			Metal-composite joint (GFRP)	X	X	X	X		X		
			Rad. → strength (FRP-Kevlar)	X	X	X		X			
			Also: welding and thick-section research listed under TF coil form (S.S.)	X	X	X			X		x
Dewar Walls (warm)	21/6/9, Al alloy, AISI 316, GFRP	Steel, FRP									
Thermal Insulation	Al-Mylar, multi-layer	Reinforced foams, (20/300K), microspheres	Rad. → K, emissivity	X	X	X	X	X			
			Eddy-current heating in Al film	X	X	X					
Eddy-current shielding	Hi-purity Al/S.S.	Metal-matrix composites, Cu alloys	Development of hi-strength, lo-ρ composite or alloy	X	X	X	X		X		
			Mech. (fat.), elect. (composite, alloy)	⊗	⊗	⊗		X			
			Rad. → elect. (composite, alloy)	X	X	X		X			
			Fat. → bonding (composite)	⊗	⊗	⊗		X			

Table II.C-1 (continued)

Support Structure	Materials Suggested	Other Candidate Materials	Data Required	Projects Which Need Data				Data for				
				LCP TFTR MX	TNS	EPR/ DEMO	Power Plants	Material Screening	Base Data	Processing/ Joining	Specifications (Codes)	Design
Cold-Cold	21/6/9, FRP, AISI 316	Al alloy, A286, AISI 304, advanced composites	*Welding, thick-section, inspection – see TF coil form (S.S., Al alloy)	X	X	X	X	X	X	X	X	X
			Fat.	⊗	⊗	⊗	⊗	X	X			
			Metal-composite joints	X	X	X	X	X		X		
Cold-Warm	21/6/9, S.S., FRP, Ceramics	concrete, advanced composites, AISI 304	Mech., K(FRP, ceramics, concrete adv comp)	X	X	X	X	X	X			
			Rad., compressive $\sigma \to K$ (all)		X	X	X		X			
			Fat.$\to$K (all)	⊗	⊗	⊗	⊗					
Warm	Steel, concrete, 7075, 2219, 21/6/9											
Support Structure or cylinder	concrete, 21/6/9, AISI 316, GFRP, AL alloy, S.S.	Advanced composites	Mech. K (concrete)	X	X	X	X					
			Thick-section research-see TF coil form (S.S., Al)	X	X	X	X	X	X	X	X	X
			Thick-section research (composites)	X	X	X	X	X	X	X	X	X
			Inspection (composites)	X	X	X	X			X		

Other Aspects

Support Structure	Materials Suggested	Other Candidate Materials	Data Required	LCP TFTR MX	TNS	EPR/ DEMO	Power Plants	Material Screening	Base Data	Processing/ Joining	Specifications (Codes)	Design
Normal Magnets	Cu	--	Thick-section processing, inspection	X	X					X	X	
Superconductor Coil Joint	Cu/NbTi, insulators		Exploratory research		X	X	X	X				

272

III. MATERIALS TECHNOLOGY

The previous Section of this report addressed the cryogenic materials problems as reflected in existing MFE design. Only general materials classes were usually suggested for a given component, e.g., stainless steel, Micarta, aluminum, etc. We now consider which specific alloys, composites, etc., are the best current selections based upon contemporary and past experience, on the existing data base, availability and cost. We consider fabrication problems with specific materials and how control over the quality of a material and of components can be established. Finally, specific alternative materials are examined. The Section is divided into four general material classes: alloys; structural composites and bulk insulators; insulating films, coatings and inorganics; and conductors.

III.A. Structural Alloys

Alloys will be used for the main structural members of the super-
conducting magnet systems needed for MFE devices. Designs of tokamak
and mirror machines that require superconducting magnets are currently
in the conceptual stage (except for MX), but many design features that
strongly influence materials selection are reasonably well established.
The principal features governing alloy selection for structural applica-
tions are the enormous size and stored energy of the magnet systems, the
extremely high forces exerted by the magnets, the massive structural
elements needed to restrain these forces, the limited space available
for the structure, and the need for accessability to install and period-
ically remove the blanket and shield systems -- systems that are com-
pletely surrounded by magnets and the support structure. These features
result in the need for alloys with sufficient strength and stiffness to
perform the required structural functions within the space available,
sufficient fatigue and fracture resistance to operate safely, and suf-
ficient fabricability to permit manufacture and assembly of the components.

The choice of materials is further restricted by the adverse operating
environment of the magnet system. The alloys are subjected to temperatures
down to 4 K and must not be susceptible to low temperature embrittlement.
The presence of high magnetic fields cautions against the use of ferro-
magnetic materials in certain application because they would be subjected
to higher forces due to the magnetic field. The rapid magnetic field
changes associated with cyclic operation of the poloidal field coils
cause heat inputs to the structure from eddy current losses. Consequently,
alloys with high electrical resistivity are preferred for use at 4 K.
The radiation environment eliminates use of alloying elements, such as
cobalt, which transmute to long half life products. With this exception,
radiation does not appear to be a significant factor in the selection of
structural alloys because dosage levels sufficient to degrade structural
performance probably cause unacceptable deterioration of other system
materials. Finally, the microstructure of the material must be stable
when exposed to the operating strains, temperature, and radiation; i.e.
the alloy should not transform to either a brittle or a ferromagnetic
state.

The constraints on materials selection caused by size requirements,
space limitations and operating environment significantly reduce the
number of candidate alloys. Further limitations arise due to considera-
tions related to experience, cost and availability. Currently, the
leading candidates are the austenitic stainless steels and aluminum
alloys. The candidate alloys are discussed in detail in the following
sections.

III.A.1. Austenitic Stainless Steels. Austenitic chromium-nickel stain-
less steels are the most widely proposed alloys for structural applica-
tions in MFE magnet systems. These steels have the best combination of
strength, stiffness and toughness at 4 K. The physical properties also
offer advantages over competing materials. Specifically, the modulus is
high, the thermal expansion is close to that of the copper-stabilized
conductor, magnetic permeability is low and the electrical and thermal
conductivites are low. The principal disadvantages are the high cost of
construction and problems arising from microstructural stability and
control.

a. Preferred Grades

For superconducting magnet systems, the preferred stainless steels are AISI grades 304 and 316, and alloy 21/6/9 (Nitronic 40 and Pyromet 538). AISI 304 contains 18-20% Cr and 8-12% Ni; it has a typical yield strength of 413 MPa (60 ksi at 4 K. AISI 316 contains 16-18% Cr, 10-14% Ni and 2-3% Mo; it has a typical yield strength of 551 MPa (80 ksi) at 4 K. Alloy 21/6/9 contains 19-21.5% Cr, 5.5-7.5% Ni, 8-10% Mn and 0.15-0.4% N; it has a typical yield strength greater than 1033 MPa (150 ksi) at 4 K. These three alloys were selected on the basis of strength, toughness, and austenite stability at 4 K, and upon consideration of cost, availability, experience and fabricability. Each of these factors is discussed in detail in the following paragraphs.

Several other 300-series stainless steels have been widely used in cryogenic applications, but are not preferred for magnet system applications for a variety of reasons. Lower nickel grades such as type 301 and 302 have insufficient austenite stability. Type 310 has superior austenite stability but is is expensive (70% more expensive than 304) and not readily weldable in heavy sections. The extra-low-carbon grades (types 304L and 316L; .03 max C) may be used interchangeably with the standard grades (304 and 316, respectively) providing the lower strength (about 20% less) is acceptable. The stabilized grades (321, 347, and 348) are not generally used below 76 K (INCO, 1974); the reason for this is not clear.

For applications requiring higher strengths, several alloys other than Nitronic 40 were considered. Alloy A-286 was eliminated from consideration because heat treatment is required and weldability is poor. Several Ni-Cr-Mn-N stainless steels - alloy 22/13/5 (Nitronic 50), alloy 18/3/12 (Nitronic 33), Cryogenic Tenelon, Kromarc 58, 216 (ASTM 240, Grade XM17) and others -offer great potential for MFE applications, but there is currently insufficient information available on these alloys to permit a reasonable assessment of the potential. Similarly the nitrogen strengthened stainless steels, 304N and 316N, have greater strength and austenite stability than 304 and 316 respectively, but little is known of their properties at 4 K.

b. General Information

Experience: The most widely used stainless steel for cryogenic service are AISI types 304 and 304L. These alloys have been used for structural members in most of the superconducting magnets built for high energy physics devices. NASA used 304 nearly exclusively in ground installations for piping systems and containment vessels for liquid hydrogen at 20 K. The experience has been satisfactory.

Type 316 is a commonly used stainless steel, but experience with this alloy in liquid helium applications is nil. The only known application of type 316 at 4 K is the ANL U-25 superconducting dipole magnet for an MHD device. The heavy section 316 had an abnormally large grain size and exhibited lower strength than expected at 4 K (Reed and Read, 1977).

Alloy 21/6/9 is a relatively new alloy but it has been used by LLL for the Baseball II superconducting magnets. In the Baseball II application, the 21/6/9 is only stressed to 207 MPa (30 ksi) and consequently the successful operating experience is not indicative of this material's performance as a high strength alloy, i.e. in highly stressed applications (Henning, et al., 1969).

Specifications. The ASTM and ASME specifications for various product forms of AISI types 304, 316 and several other 300-series stainless steels are summarized in Table III A-1. The Federal specifications for 300-series stainless steels are QQ-S-766 and QQ-S-763. Alloy 21/6/9 listed as grade XM-11, is covered by ASTM specifications A412 for plate, sheet and strip and A276 for base and shapes.

Many of the ERDA laboratories have specifications for procuring stainless steels for specialized applications. A modified specification for type 304 which requires the Ni content to be at the high end of the allowable range has been used for superconducting magnet applications. Special specifications are also used to purchase high purity stainless steels manufactured by either the vacuum-induction-melt/vacuum-arc-remelt (VIM/VAR) process or by the VIM/electro-slag-remelt (VIM/ESR) process. For procurement of 21/6/9 certain specifications stipulate tighter controls on allowable nitrogen content, e.g. LLL limits the N range from 0.20 to 0.25 instead of 0.15 to 0.40 as specified in the ASTM specifications.

Cost: Cost information for 304, 316, 21/6/9 and several other stainless steels are summarized in Table III A-2. Costs for round bar, flat bar and plates are included to provide information regarding the influence of product form on price. The cost data are applicable to orders over 4500 kg (10,000 lb) delivered in February 1977. The information was obtained from Armco Steel Co. and G. O. Carlson Co.

The cost data of Table III A-2 are applicable to stainless steels purchased to ASTM requirements. These steels are produced in electric furnaces and are not vacuum processed or remelted to improve purity. Many of the ERDA laboratories have more stringent specifications for procuring stainless steels for specialized applications. The processing, chemistry and metallurgical requirements of these specifications can result in significantly higher prices and in some cases limit the number of suppliers and availability.

Availability: The availability of type 304, 316 and 21/6/9 stainless steels is essentially unlimited in standard product forms at the present time. Standard product forms include plate, sheet, strip, bar and forging billets. Each of the alloys can be cast, extruded or welded into pipe or tubing. Since these alloys contain 30 to 40% of Cr, Ni, Mn and Mo, the long term availability may limit applicability in a fusion-power economy. However, there should be no problem for the next twenty years because of the limited number of devices planned.

Table III A-1.

ASTM and ASME specifications for various forms of austenitic stainless steels (including AISI Types 304, 304L, 316 and 316L).

Product Form	ASTM specifications	ASME specifications
Plates	A240	SA-240
Forgings	A473	SA-182
Bars and sections	A479	SA-479
Seamless tubes	A213	SA-213
Welded tubes	A249	SA-249
Seamless and welded tubes	A269	--
Bolts, screws, studs, stud bolts	A320	SA-320
Nuts for bolts	A194	SA-194

Table III A-2.

Cost Data for Stainless Steels
(Dollars per pound)

Grade	Flat Bar[a]	Round Bar[b]	Plate[c]
304	1.29	1.15	.93
304L	1.35	1.21	.99
316	1.60	1.46	1.21
316L	1.66	1.52	1.27
Nitronic 33	1.26	1.12	1.00
Nitronic 40	1.69	1.55	1.32
Nitronic 50	1.94	1.80	1.85

[a] 5 x 10 cm flat, hot rolled, annealed and pickled

[b] 3.8 to 12 cm round, centerless ground

[c] 1.9 to 7.6 cm thick, 122 to 244 cm wide, 305 to 1070 cm long plate; hot rolled, annealed and pickled

c. Properties

Tensile: Typical yield strengths of AISI 304, 316 and Nitronic 40 are 413 MPa (60 ksi), 551 MPa (80 ksi) and 1033 MPa (150 ksi), respectively. In these alloys, the tensile strength and to a lesser degree the yield strength increase with decreasing temperature. This is particularly true for 21/6/9 and other nitrogen-strengthened stainless steels. Although tensile tests have been conducted on many austenitic stainless steels at 4 K, there are insufficient data on any of the alloys to establish an allowable stress based on the minimum credible yield strength.

Compression: The compressive yield strength of AISI 304 has been measured at temperatures to 4 K. The yield strength in compression appears to be significantly higher, 930 MPa (135 ksi) in one investigation (NBS, 1977) and 827 MPa (120 ksi) in another (INCO, 1974), than the tensile yield strength. This is in marked contrast to the behavior of most structural alloys which exhibit approximately equal yield strengths in tension and compression. Tests should be conducted to verify the compressive yield strength in AISI 304 and to determine if similar behavior occurs in AISI 316 and Nitronic 40. An increased allowable stress in compression would significantly reduce some section sizes if either 304 or 316 is selected because of the compressive nature of the centering forces.

Shear and Bearing: The shear ultimate strength and the bearing yield and ultimate strengths have not been determined for any alloys at 4 K.

Fatigue: Smooth and notched (K_t = 3.1) fatigue tests at 4 K have been conducted by Schwartzberg and Kiefer (1976) on 304L, 310, 21/6/9 and A286 stainless steels under fully reversed (R = -1) stress cycling. Strain cycling fatigue tests at 4 K have been conducted by Nachtigall (1974) on 304L and 310 stainless steels. In both investigations, the fatigue life was better at 4 K than at room temperature for endurances greater than 1000 cycles. At low cycle lives (less than 500 cycles), Nachtigall observed a crossover, i.e. less fatigue life at 4 K than at room temperature. Nachtigall compared his experimental data with that predicted by the Manson (1965) method of universal slopes and showed that the fatigue behavior of these materials at 4 K can be predicted within a scatter factor of three from material tensile properties obtained at 4 K.

Fatigue Crack Growth: The fatigue crack growth behavior of several austenitic stainless steels has been determined at 4 K by Tobler and Reed (1976). Alloys tested include 304, 304L, 316, 310, A286 and 21/6/9. Their results indicate that fatigue crack growth rates are generally slower at 4 K than at room temperature. The crack growth rates generally decrease with increasing austenite stability, i.e. AISI 310 and A286 are the best, followed by AISI 304 and 316; alloy 21/6/9 which exhibits faster growth rates at 4 K than at room temperature, is the worst.

Fracture Toughness: Fracture toughness tests at 4 K have been
conducted by Tobler (1976) on 304, 316, 310, A286 and 21/6/9. The
results scale with yield strength. The 300-series alloys have low yield
strength and excellent toughness at room and cryogenic temperatures.
A286 has a relatively high yield strength and low toughness at room
temperature and 4 K. Alloy 21/6/9 exhibits a substantial increase in
yield strength as temperature is reduced to 4 K; the fracture toughness
exhibits a corresponding decrease with decreasing temperature.

Physical Properties: The physical properties of austenitic stain-
less steels are good relative to other alloy systems for MFE-magnet
structural applications. The elastic moduli are relatively high, limit-
ing elastic displacements and improving buckling stability. The thermal
and electrical conductivities are low resulting in reduced thermal
losses. The thermal expansion is close to that of copper thereby mini-
mizing thermal stresses due to cooldown. The magnetic permeability is
low relative to other iron or nickel base alloys resulting in minimal
interactions with the applied magnetic field.

d. Fabrication

The fabricability of austenitic stainless steels is certainly
sufficient for MFE magnet systems as attested by the widespread use of
stainless steels in a variety of industries. Fabrication characteristics
that should receive special consideration for MFE-magnet applications
are briefly reviewed in this section.

Welding: Stainless steel alloys 304, 316 and 21/6/9 are readily
weldable by all common welding processes providing the appropriate
consummables and procedures are used. Filler wires are generally for-
mulated to provide 4 to 10% delta ferrite which tends to reduce the
incidence of hot cracking. For magnet applications, the ferrite phase
is objectionable because it is ferromagnetic and because it may result
in some brittleness at low temperatures. If a wholly - austenitic weld
is desired, the chemistry of the weld deposit must be adjusted - usually
by increasing the Ni or Ni-equivalent as shown by the Schaeffler consti-
tution diagram for stainless steel weldments. Microfissuring can be
minimized by a small increase in carbon, a substantial increase in
manganese and increasing the nitrogen content. Thus, the Mn-N steels,
such as 21/6/9 may be better suited than 300 series steels for obtaining
sound welds with low permeability. Nickel-based filler wires are some-
times used to obtain sound weld deposits with excellent low temperature
toughness under conditions of maximum constraint - such as in the weld-
ing of heavy sections. The main disadvantages of the Ni-base filler
wires are high cost and low yield strength; the latter can be very
important at 4 K where 21/6/9 and to a lesser extent AISI 304 and 316
have substantially higher yield strengths.

An important problem in stainless steel weldments is sensitization -
the grain boundary precipitation of Cr carbides at temperatures between
about 500-800°C which locally depletes the Cr content and therby reduces
corrosion resistance. In MFE magnet applications there is not expected
to be a corrosive environment. Limited impact tests indicate that
sensitization does not significantly reduce fracture resistance at

cryogenic temperatures. However, our recent experience on the U-25 dipole magnet bore tube AISI 316 alloy urges caution: this material exhibited all the characteristics of highly-segregated grain boundaries, having large grain size, intergranular tensile fracture at 4 K, and reduced mechanical properties. Chemistry changes to prevent sensitization, such as specifying stabilized grades (321, 347) and extra-low-carbon grades (304L and 316L) should be avoided for more reasons than simply the added cost. Certain stabilized grades contain Cb and/or Ta which tend to promote microfissuring in wholly-austenitic welds (Linnert, 1967). The extra-low-carbon grades have lower strength, particularly at 4 K, and less austenite stability.

Heat Treatment: The best possible heat treatment is no heat treatment. One of the principal advantages of wrought-annealed-austenitic-stainless-steels is that heat treatment is generally not required. The possible exceptions are annealing at 1000 to 1100°C following severe forming operations and stress relief at 420 to 480°C to reduce peak residual stresses and improve dimensional stability.

Machining: Annealed-austenitic stainless steels are more difficult to machine than carbon steels or aluminum alloys because of their relatively high tensile strength, work hardening rates, and low thermal conductivity. These properties cause poor finishes, heat buildup and excessive tool wear. As a result, it is necessary to use heavier feeds, slower speeds, better quality tool bits, more rigid machines and more power.

Forming: The candidate stainless steels have excellent formability. Alloys with more austenitic stability than types 304 or 316 may be needed if severe forming operations are required. Alloy 21/6/9 is reported to have excellent austenitic stability; even after 60% reduction at room temperature, the permeability is less than 1.02.

Forging: The austenitic stainless steels can be forged into shapes suitable for many MFE-magnet applications, e.g. forged pancake billets for ring rolling coil forms. Stainless steels are more difficult to forge than most common structural alloys because of its high strength at elevated temperatures. Within the family of austenitic stainless steels, the forgeability of types 304 and 316 is rated good (Jensen, 1966).

Casting: The austenitic stainless steels are widely used for manufacturing corrosion resistant casting. The casting alloys equivalent to AISI types 304 and 316 are ACI (Alloy Casting Institute) types CF8 and CF8M respectively. The ferrite content of these alloys may vary from 0 to 40% due to chemistry variations within the allowable ranges. The ferrite content of 21/6/9 casting could reach 20%. Ferrite levels in this range are likely to be unacceptable because of low fracture toughness and high permeability. Ferrite-free castings require use of higher nickel content alloys such as ACI grades CK 20 (corresponding to AISI grade 310) and CN-7M. The CN-7M grade, which has a nominal composition of 28Ni, 18Cr, 3.5Co, 2.5Mo and 0.07C, is widely used for certain corrosion-resistance applications and should be a suitable ferrite free casting alloy for cryogenic applications. The problem with using ferrite-free castings is that the cost benefits of using castings may be lost because of the high alloy content.

e. Inspection

During fabrication of MFE magnet systems, the stainless steel material and components will be inspected using conventional methods. The only problem peculiar to the proposed designs is the wide spread use of heavy-section stainless steel welds. These welds cannot be effectively inspected for the presence of cracks or crack-like defects. Radiography is of limited use because of its inability to reliably detect cracks. Ultrasonic methods don't work effectively because of the high noise levels and large and variable attenuation arising from the large-grain-size welds. Standards are needed to assure that the defect sizes that can be reliably detected do not adversely affect structural integrity.

In-service inspection of magnet-system components will be particularly difficult because of the low temperatures and radiation.

III.A.2. Aluminum Alloys. Aluminum alloys have been proposed for many structural applications in MFE magnet systems. Their principal advantages are: low as-fabricated cost, lightweight, non-magnetic behavior, stable microstructure, and good retention of strength and toughness at cryogenic temperatures. The main disadvantages of aluminum alloys are low strength in weldments, high electrical and thermal conductivity and an unfavorable elastic modulus (too low) and thermal expansion (too high) for many applications.

a. Preferred Alloys

For cryogenic service, the preferred aluminum alloys are 5083, 2219 and 6061. Alloy 5083 is generally used in the annealed condition (5083-0), has a nominal composition of Al-4.5 Mg-0.6 Mn; and has a typical yield strength of 172 MPa (25 ksi) at 4 K. Alloy 2219 is generally used in a heat treated condition (T 851, T 87 etc.), has a nominal composition of Al-6.3 Cu-0.3 Mn, and in the T 851 temper has a typical yield strength of 482 MPa (70 ksi) at 4 K. Alloy 6061 is usually used in the heat treated condition (T 6, T 651, etc), has a nominal composition of Al-1Mg-0.6Si-0.3Cu-0.2Cr, and in the T-6 temper has a typical yield strength of 380 MPa (55 ksi) at 4 K. Although each of these alloys is readily weldable, only 5083 retains full strength in the welded condition and is the best choice for most large welded components. Alloy 2219 has the highest strength of the three alloys and is recommended for bolted construction where space or weight need to be conserved.

Several other aluminum alloys have excellent properties at 4 K and may be used for special applications. Alloy 3003 has been widely used for cryogenic applications and is the best choice when brazing is used for joining. The high strength alloys such as 2024 and 7075 (in an overaged temper such as T 73) may be used for nuts and bolts.

b. General Information

Experience: The most widely used aluminum alloy for cryogenic applications is 5083. Thousands of tons have been used for LNG tanks in plates up to 18 cm thick. Alloy 2219 is used in aerospace applications

including cryogenic tankage for the space shuttle. Alloy 6061 is used primarily for piping systems. Although 2014-T 651 has been successfully used by NASA for propellant tanks (LH$_2$ and LOX), it is not recommended for CTR applications because of its marginal weldability and toughness.

Specifications: The Federal, ASTM and ANSI specifications for aluminum mill products of alloys 5083, 2219 and 6061 are summarized in Table III A-3. For a more complete listing of specifications refer to the Aluminum Standards and Data Book (Aluminum Assn., 1976). Procurement of heavy sections may require additional specification requirements on through-thickness ductility.

Cost: The cost of 2.5 cm-thick aluminum alloy plates are as follows: $1.83/kg for 5083-0, $2.10/kg for 2219-T 851 and $1.90/kg for 6061-T 6. Notice that cost do not significantly vary for the various grades as they do for stainless steels. The costs are applicable to orders over 13,600 kg delivered in February 1977. The information was obtained from Alcoa.

Availability: The availability of 5083, 2219 and 6061 is essentially unlimited in standard product forms at the present time. Standard product forms include plate, sheet, strip, bar and forging billets. Pipe and structural shapes are readily available in alloy 6061. The long term availability of these alloys is excellent because of the abundance of aluminum and the principal alloying elements, Mg and Cu.

c. Properties

Tensile: Typical yield strengths of 5083-0, 2219-T851 and 6061-T6 at 4 K are 172 MPa (25 ksi), 482 MPa (70 ksi) and 380 MPa (55 ksi), respectively. In these alloys, the tensile strength and to a lesser extent the yield strength increases with decreasing temperature. Many tensile tests have been conducted on 5083 to 77 K, but there are insufficient data on any of the alloys to establish an allowable stress at 4 K based on the minimum credible yield strength, particularly for heavy sections.

Compression, Shear and Bearing: Values for these properties have not been determined for any aluminum alloy at 4 K.

Fatigue: Strain cycling fatigue tests have been conducted by Nachtigall (1974) on 2219 and 2014 alloys. The results exhibit the same trends as discussed for stainless steels, i.e. improved life at endurances greater than 1000 cycles and reasonable correlation between Manson's theory and the test results.

Fatigue Crack Growth: The fatigue crack growth behavior of 5083 (Tobler and Read, 1976) and a Al-6Mg alloy (McHenry, et al., 1976) have been determined at 4 K. The results indicate that growth rates are slower at 4 K than at room temperature.

Fracture Toughness: Fracture toughness tests at 4 K have been conducted on 5083 and 2219 (Tobler and Reed, 1976, Read and Reed, 1976). Alloys 5083 and 2219 have greater toughness as measured by the J-integral method at 4 K than at room temperature.

Table III A-3.

Specifications for Aluminum Mill Products

Alloy	Product Form	Federal	ASTM	ANSI
5083	Sheet and plate	QQ-A-250/6	B209	H38.2
	Wire, rod, bar, shapes, tube	QQ-A-200/4	B221	H38.5
	Forgings and forging stork	QQ-A-367	B247	H38.8
2219	Sheet and plate	QQ-A-250/30	B209	H38.2
	Wire, rod, bar; rolled or cold finished	---	B211	H38.4
	Wire, rod, bar; extruded	---	B221	H38.5
	Forgings and forging stork	QQ-A-367	B247	H38.8
6061	Sheet and plate	QQ-A-250/11	B209	H38.2
	Wire, rod, bar; rolled or cold finished	QQ-A-225/8	B211	H38.4
	Wire, rod, bar, shapes, tube	QQ-A-200/8	B221	H38.5
	Structural shapes	QQ-A-200/16	B308	H38.10
	Pipe	---	B241	H38.7
	Forgings and forging stork	QQ-A-367	B247	H38.8
	Structural pipe and tube; extruded	---	B249	H38.16

Physical Properties: With the exception of magnetic permeability, the physical properties of aluminum alloys are not as good as those of stainless steels for structural applications at 4 K. The elastic modulus is relatively low and thus when used for coil case applications, more of the load must be carried by the conductor assembly. The thermal and electrical conductivities are relatively high, resulting in increased thermal loads particularly from eddy current losses.

d. Fabrication

The relative ease of fabricating large aluminum structures is the principal advantage of aluminum over stainless steels. Fabrication characteristics that should receive special consideration for MFE-magnet systems are briefly reviewed in this section.

Welding: Aluminum alloys 5083, 6061 and to a lesser extent 2219 are readily weldable by the gas metal-arc and gas tungsten-arc processes. Alloy 5083 retains full strength in the as-welded condition; 5083 welds have higher strength than either 2219 or 6061 welds unless a post-weld heat treatment is used.

Heat Treatment: Aluminum alloys are generally heat treated by the producer unless fabrication requires heavy forming operations or a post weld heat treatment. Alloy 2219 has exceptionally good response to heat treatment, sections up to 18 inches thick have been produced that develop strengths only about 5% below those of 2 to 3-inch-thick sections (Cryogenic Engr. News, 1966). Post-weld heat-treatment, where feasable, can restore strength levels in 2219 welds to nearly 100% of the base metal values and in 6061 welds to strength levels comparable to 5083.

Machining: Aluminum alloys, particularly the heat treated grades, have excellent machinability. Machined and bolted assemblies of high strength aluminum alloys can frequently replace more costly welded stainless steel assemblies.

Forming: Aluminum alloys have excellent formability in the annealed or the solution treated conditions.

Forging: Aluminum alloys have the best forgeability of all structural alloys because of their very low strength at forging temperatures of 370 to 510°C. The size limit on aluminum forgings is significantly greater than that on stainless steels because of the reduced pressures required.

Casting: Many aluminum casting alloys should be suitable for cryogenic applications. However, limited use of castings is anticipated because wrought products have better properties, can easily be machined into most shapes and limited quantities of a given component are required.

e. Inspection

Aluminum alloys and their weldments are readily inspectable by conventional methods.

III.A.3. Alternative Alloys. Alternative alloy systems do not provide candidate materials for structural applications at 4 K. Consider the following systems:

Nickel Base Superalloys - Ferromagnetic at 4 K, expensive, difficult to fabricate

Nickel Alloys - Ferromagnetic at 4 K, expensive

Titanium Alloys - Brittle at 4 K, expensive, difficult to fabricate

Cobalt Base Superalloys - Transmutes to long half-life reaction products, expensive, difficult to fabricate, generally ferromagnetic at 4 K

Carbon and Alloy Steels - Ferromagnetic, brittle at 4 K

Ferritic and Martensitic Stainless Steels - Ferromagnetic, brittle at 4 K

Copper Alloys - Acceptable, but generally not competitive with austenitic stainless steels

Magnesium Alloys - Low strength, brittle at 4 K

Further consideration of alloys from any of these systems is not warranted at the present time.

III.B. Structural Composites and Bulk Insulators

III.B.1. Overview. Cost, availability and performance of structural composite materials useful in MFE cryogenic systems scale in the general order: industrial laminates (NEMA types or resin-impregnated wood), specialty fiberglass composites and advanced, high-modulus, composites. Industrial laminates are commonly referred to by tradenames (Micarta, Textolite, Phenolite, Permali, etc) which are a general term for a company product line. Specifications established for filamentary-reinforced polymer industrial laminates (NEMA publication Li-1 (1971), ASTM D709-72 Part 40, MIL-P and LP) are room-temperature electrical performance specifications rather than material specifications and are therefore inadequate for cryogenic MFE applications. The industrial laminates on Table IIIB1 are the most likely candidates for cryogenic MFE use.

Improved radiation resistance is expected from specialty fiberglass composites using boron-free S-type glass reinforcement in radiation-resistant polymers such as aromatic-base epoxies or polyimides. The use of impregnated and partially-cured (B-staged) composite tape would likely fall into this category.

Polymer-matrix composites reinforced with the higher-modulus fibers (graphite, boron, Kevlar) can be effectively used at 4 K, offering the possibility of meeting or exceeding strength, fatigue resistance and modulus of stainless steel while providing electrical and thermal insulation plus reduced weight.

III.B.2. Experience. The use of composites as structural materials in superconducting magnets has not been extensive. Existing magnets do not suffer eddy-current losses, and heat leaks through metallic supports has been accepted, although excessive helium consumption is a common problem. Industrial laminates of the NEMA LE or G-10 types are commonly used as bulk electrical insulators in the magnet coils with apparent success, although internal shorts remain a problem. There is no experience operating a coil in a radiation environment.

Glass-reinforced specialty composite straps and cones are presently being used as primary load-carrying thermal standoffs (4.2-300 K) in two designs of a 3000 hp DC superconducting motor, providing substantial savings in refrigeration cost. The only attempt to restrain superconducting coil magnetic forces by composites was in a lightweight MHD magnet for airborne use. This magnet failed because the low-modulus glass-epoxy support permitted excessive superconductor motion. High-modulus fibers should have been used.

Non-conducting composite helium dewars have been hand-made for laboratory use. Results indicate that the concept is feasible, major problems being in construction methods rather than in the fiberglass-epoxy structural material. This technology remains in its infancy.

Table III B-1

Types and Grades of Industrial Laminated Thermosetting Materials
of Primary Interest in Magnetic Fusion Energy Systems

ASTM/NEMA Designation	MIL-P and LP Designation	Description
NEMA/ASTM LE	MIL-P-15035, Type FBE	Cellulose fabric fine-weave, phenolic resin
NEMA/ASTM G-10	MIL-P-18177, Type GEE	Glass cloth, epoxy resin
NEMA/ASTM G-11	MIL-P-18177, Type GEB	Glass cloth, high-temperature epoxy resin
NEMA/ASTM C	MIL-P-15035, Type FBM	Cellulose fabric, medium weave, phenolic resin
NEMA/ASTM G-5	--	Glass cloth, melamine resin
W1, W2 EH	LP 5094	Beechwood veneer, phenolic impregnated

III.B.3. Properties. A fairly extensive mechanical and physical data base exists for industrial laminates, specialty fiberglass composites and advanced composites at room temperature (manufacturers data sheets, NEMA publications, MIL-HBK 17 (a), USAF Advanced Composites Design Guide). However, relatively few efforts have been made to extend these data to cryogenic temperatures. The current state of knowledge of the effect of cryogenic temperatures on the mechanical and physical properties of specialty glass and high-modulus composites has recently been reviewed by Kasen (1975 a-c). Results are encouraging, indicating that cryogenic temperatures are seldom deleterious to strength properties, and usually result in substantial improvement. Unfortunately, most of the available data cannot be generalized; only recently has composite theory permitted predictions of off-axis composite performance to be made from relatively simple uniaxial laminate test data. A conspicuous deficiency is the lack of cryogenic property data on the industrial laminates, hundreds of metric tons of which are proposed for use in current MFE reference designs. The effect of radiation at 4 K has not been studied on any composite materials system.

III.B.4. Specifications, Availability and Cost.

a. Specifications and Quality Assurance
Functional performance specifications for room temperature electrical insulating use of industrial laminates have been established by ASTM, NEMA and by MIL specifications. These are of limited use for cryogenic applications. Material specifications must be established for each constituent of the industrial laminates listed on Table III B-1 unless it can be shown that a general class of constituents is acceptable for MFE cryogenic service. Pre-inpregnated tape commonly used in making specialty fiberglass products require added specifications such as fiber/resin ratio, filament alignment and tape tolerances. The final composite product requires specifications on reinforcement orientation, overall fiber/resin ratio, void content and significant property minimums. Presently, each organization planning to use composite materials prepares its own specifications for internal use. Typical examples are given in Vol. III, USAF Advanced Composite Design Guide (1973).

To insure successful application of composite structures it is necessary to establish a quality assurance program encompassing all aspects of the design and fabrication of parts manufactured from intermediate products such as prepreg tapes. Unlike metals, quality control on the composite material itself is inadequate. Quality assurance procedures are discussed in detail in Vol. III, USAF Advanced Composites Design Guide (1973).

b. Availability and Cost
Neither short-term nor long-term availability of current types of industrial laminates appears to be a problem and the amounts required for MFE applications is well within the capability of the industry. However, if it becomes necessary to impose a tight specification on the constituent components of a given laminate, availability problems may arise should a specific component be taken off the market. Current costs range from about $1.70/lb for NEMA C (cotton-phenolic) to $3.80/lb for NEMA G-11 (glass-epoxy). A tight component specification will increase these costs.

Material shortages are not expected to limit the availability of speciality glass-reinforced composites. However, the tonnage production of these materials is far less than for industrial laminates. Industrial S-glass roving costs about $2.25/lb with the preinpregnated tape form costing $5-6.00/lb. The lime-alumina-borosilicate/type E glass is somewhat less expensive but less radiation resistant.

III.B.5. Fabrication. Industrial laminates are produced in monolithic plate, sheet, block, rod and tube forms. Special channel, tee and zee sections are also available. The material is machined to final shape following the procedures of metals technology.

A large degree of flexibility in fabrication method is available with specialty fiberglass composites depending on the final result desired. Preinpregnated tapes can be used to form complex shapes using relatively simple molds if they can be obtained in widths appropriate for jelly-roll winding of conductors or for tension-wrapping of coil segments. Either cloth or uniaxial fiber orientation is available. Some large parts, such as dewars, might be more efficiently made by hand layup of the woven cloth reinforcement and resin, sacrificing some strength reliability for fewer leaks through joint defects. Large symmetrical cylinders can be automatically braid-wound. The final cure can be at room temperature for uncritical applications or by vacuum-bagging and autoclaving for maximum strength and minimum property variability. Virtually any length of fiberglass angles, beams and channels can be continuously produced by pultrusion in which glass roving is pulled through a resin bath and heated die.

Preimpregnated tapes are used to good advantage in fabricating web or honeycomb type structures in contrast to monolithic structures of metals or industrial laminates. This approach can often reduce weight and produce economies compared to monolithic structures, despite higher base material costs. Fabrication with composites is reviewed in V III, USAF Advanced Composite Design Guide (1973); design with composites is reviewed in V I of that series.

III.B.6. Alternative Matrials. High-modulus graphite-reinforced composites could be effectively substituted for many stainless steel structures in present MFE superconducting magnet designs, the primary obstacle being cost and lack of design experience. The future of these materials is bright because, unlike metals, graphite fiber costs are dropping rapidly and future availability will not be limited due to scarcity of natural resources. While large-scale structural use of such materials remains in the future, certain components can be identified for which graphite-epoxy materials should be presently considered. There are applications where structures fabricated from state-of-the-art, uniaxial, B-staged graphite-epoxy tape can be substituted for stainless steel to obtain an immediate improvement in performance or reduced overall component cost. Existing systems can provide uniaxial ultimate tensile strengths in the range of 69 MPa (100,000 psi) with moduli from 275-324 GPa (40-47 x 10^6 psi) or, alternatively, strengths of about 138 MPa (200 x 10^3 psi) with moduli of about 137 GPa (20 x 10^6 psi) combined with

excellent fatigue properties and negligible thermal contraction on cooling. Candidate components would be coil forms, non-metallic load-carrying helium containers and stiffening filaments interwoven with the conductors in superconducting cables. Current prices for graphite fiber produced from rayon or polyacrilonitrile precursors are $30-40/lb. A reduction to $8-10/lb is considered realistic as production increases and as the less expensive pitch precursor systems become perfected.

The future for boron-reinforced composites is less favorable due to the continuing high cost of the fiber ($\sim$ $200/lb) and increased difficulty in fabrication. The high neutron cross section is also a disadvantage in MFE systems. Nevertheless, the high state of development of this system, its excellent cryogenic performance, particularly its extremely high compressive strength, its insulating qualities and a thermal expansion closely matching that of stainless steel may suggest some special applications.

The aramid fiber Kevlar 49 is a likely replacement for glass in components where the 90% higher fiber tensile modulus and 57% decrease in fiber density is advantageous. This relatively low-cost fiber is already being considered for laboratory helium dewar construction.

High-modulus fiber-reinforced metal composites may have applications where high electrical conductivity must be combined with high strength and stiffness as, for example, in eddy-current shields for poloidal magnets. Boron, graphite, or FP (fire polished) alumina-reinforced aluminum are candidates. Boron-aluminum is commercially available and graphite-aluminum composites are in a late state of development. The FP-aluminum composites are in the initial stages of development but hold promise for a relatively low-cost product having a lower density than aluminum but with equal or higher strength and a modulus higher than that of steel. This product has future potential as a replacement for some of the stainless steel support structures.

III.C. Insulating Films, Coatings and Inorganics

III.C.1. Overview. We consider here the unreinforced polymers, oxides, silicates, etc., used primarily as electrical insulators within magnets but having some uses as thermal standoffs. Polymers may be either applied in the fluid uncured state followed by curing, as films, or as enamel coatings. Oxides can be indigenous to the material to be insulated (anodized aluminum) or bulk oxides, fired or unfired. Coatings can also be sprayed onto the conductor or fired on at elevated temperatures. The particular material and method of application will be conditioned by the design and by the radiation resistance required. Commonly used insulating films, coatings and organics are listed on Table III C-1.

III.C.2. Experience. The organics are favored as they combine strength and flexibility required for ease in fabrication. To accomodate larger radiation fluences the more radiation-resistant polymers (amine-cured epoxy) are impregnated with inorganics (such as Al_2O_3). When these become unsatisfactory (> 109 rads), inorganics without organic binders must be used. Here, the design has to account for the brittleness of the inorganics by providing a rigid supporting structure, either by mechanical clamping or by spraying or firing the inorganic directly onto the conductor. Performance of the inorganic insulators in radiation environments has been generally favorable provided sufficient care was given to subsequent assembly so as not to damage the fragile inorganic material.

III.C.3. Properties. The wide range of properties obtainable by stretching organic films such as PET to obtain differing degrees of crystallinity complicates a discussion of mechanical and physical performance. A recent compilation of published data on PET, PPMI, PPX and PC (Schramm, et al., 1973) contains a large amount of room-temperature data, but comparatively little of cryogenic interest. It is probable that a similar situation exists for the other materials listed on Table III C-1, although the authors have not surveyed the relevant literature. It is evident that studies intended to evaluate the effects of irradiation at 4 K on the properties of polymeric films and coatings must start with well characterized material, carefully selected to meet all obvious design parameters. Subsequent attention must be given to the variability in cryogenic performance created by processing variables.

Experience has thus far indicated that the radiation flux likely to exist at the MFE superconducting magnets will not substantially degrade the properties of the metallic oxides, suggesting that room-temperature data can be used for design purposes. This assumption deserves verification in critical components.

Table III C-1

Commonly Used Insulating Films, Coatings and Inorganics

Generic Name	Common Name
Polyethylene Terephthalate (PET)	Mylar
Polypyromellitimide (PPMI)	Kapton
Polyvinyl Formal	Formvar
Polyamide	Nylon
Polyurethane	
Polyparaxylylene (PPX)	Parylene
Polycarbonate (PC)	Lexan
Aluminum Oxide (Al_2O_3)	Alumina
Magnesium Oxide (MgO)	Magnesia
Porcelain	
Fused Quartz (SiO_2)	
Mineral Silicate	Mica

III.D. Conductors

III.D.1. Overview. As in the proposed designs described earlier, in
existing superconducting magnet technology the material used most often
is one of the niobium-titanium alloys. Most existing magnets tend to be
quite small and are not cryostatically stabilized. This leads to a
quench behavior which would be totally unacceptable in a fusion magnet.

The few very large dc magnets presently in operation use heavily-
stabilized NbTi conductor in very simple configurations and are cooled
by pool boiling. Stainless steel is used for reinforcement. Maximum
magnet current values range from 1.5-2.0 kA. Pulsed superconducting
magnets of a size anywhere near those proposed for MFE do not exist at
present. The few large (by current standards) pulsed magnets have shown
training effects and most have not reached design specifications.

We have purposely ignored the Nb_3Sn superconductor up to this
point. There are a number of programs to procure and evaluate large
conductors ($\sim$ 10 kA) containing this material. A few MFE designs con-
sider it as an option for the future and, in a couple of cases, it may
be essential to the design. However, with the exception of the ORNL/EPR,
it is not proposed for any of the major projects evaluated in this
report. The major difficulties at present appear to be strain sensiti-
vity, which limits the design strain to $\gtrsim$ 0.1%, and the problem of
producing very long wires with uniform characterisitics. The material
is also quite expensive. If tape conductor is acceptable, the objec-
tions are not as serious. However, the tape configuration may lead to
unacceptable losses in pulsed fields. Some basic research is being done
on strain-insensitive A15 composites but it is very limited for a topic
of such potential importance.

In the following subsections we treat each of the components of the
conductor composite in more detail and end with specific comments on the
composite itself.

III.D.2. Superconductor. Niobium titanium alloys are readily available
with 45, 46.5, 48 and 55% Ti by weight. Currently the 46.5% Ti alloy is
the most popular. Other alloy compositions are available if the order
is for $\sim$ 3000 lbs of material. The group at Oak Ridge has worked on
detailed specifications for NbTi. It is available from only two sources
in the U.S., Wah Chang-Teledyne and Kawecki-Berylco. At present the
cost is $\sim$ \$45/lb in rod form. The mechanical properties of a number of
compositions have been measured recently by Read (1976). The supercon-
ducting properties are available for a wide range of alloy compositions
(Roberts 1972, 1974).

The properties of Nb_3Sn and the other A15 compounds are highly
dependent on the precise details of their preparation. Exact stoichio-
metry is not common and rumor has it that the addition of small quantities
of other elements greatly improves the properties. Data are available
on both the mechanical and electrical properties of the compounds, but
they are not of interest to the wire user.

III.D.3. Stabilizer. The choice of stabilizing metal involves a number of concerns. The effect on the electrical and thermal resistivity of the high magnetic fields, strain and radiation all must be considered. The only two serious candidate materials are copper and aluminum. Copper, processed by "oxygen free" techniques, is the most often used material at present. Residual resistance ratio values* of 100-500 are available at a cost of about $0.75/lb. Very pure copper (RRR $\sim$ 2000) is available, but costs about $50/lb. Pure aluminum (RRR $\sim$ 3000) is available at $\sim$ $10/lb. These very high costs could easily drop by an order of magnitude if large quantities were involved.

In the final analysis, of course, the resistivity of the metal in the operating magnet is the parameter of greatest concern. The transverse magnetoresistivity of copper has been measured by several investigators. It appears to obey Kohler's rule which allows prediction of $\rho(H)$ from the RRR value (Fickett, 1972). For oxygen free copper at 4 K this can be written very roughly, as

$$\lambda_{cu}(H) \simeq \rho_0 \left(1 + \frac{H}{2}\right).$$

The situation is not as clear for aluminum, but it certainly has a much smaller magnetoresistance at high fields which, for modest purity materials, saturates at a value 2-3 times that at zero field (Fickett 1971). Surprisingly little information exists on the effect of strain on the electrical resistance of either metal. Aluminum is the most sensitive to strain, but if strain levels $\sim$ 0.1% are maintained it will not degrade significantly.

More work is needed on a variety of prospective materials. Radiation damage causes the resistivity of either Cu or Al to increase quite rapidly due to production of vacancy-interstitial pairs. A graphical representation from the UWMAK III report (1976) is shown in Fig. III.D.1. Again, more work is needed, but it appears that at any reasonable neutron flux design level, magnets will either need to have large amounts of excess stabilizer or must be annealed more often than desirable. Recovery of radiation-induced resistivity on annealing at room temperature appears to be complete for aluminum and about 80% for copper (Thompson, 1969). The times required are quite short, on the order of minutes. The effect of radiation on the magnetoresistive properties must also be considered. In the case of copper it seems that the correlation with RRR still holds, although some recent work by Coltman (1976) at Oak Ridge indicates that the constant may be somewhat higher than given above. Aluminum is not as easy to make predictions about because it does not obey Kohler's rule in general.

Finally there are the thermal properties. Recent work indicates that, at least for commercial copper, the magnetic field effects the thermal resistivity qualitatively the same as it does the electrical

---

*A common measure of purity for low temperature conductors, the RRR value is the ratio of the room temperature resistivity to that measured at T = 4 K. The higher the value, the more pure the metal.
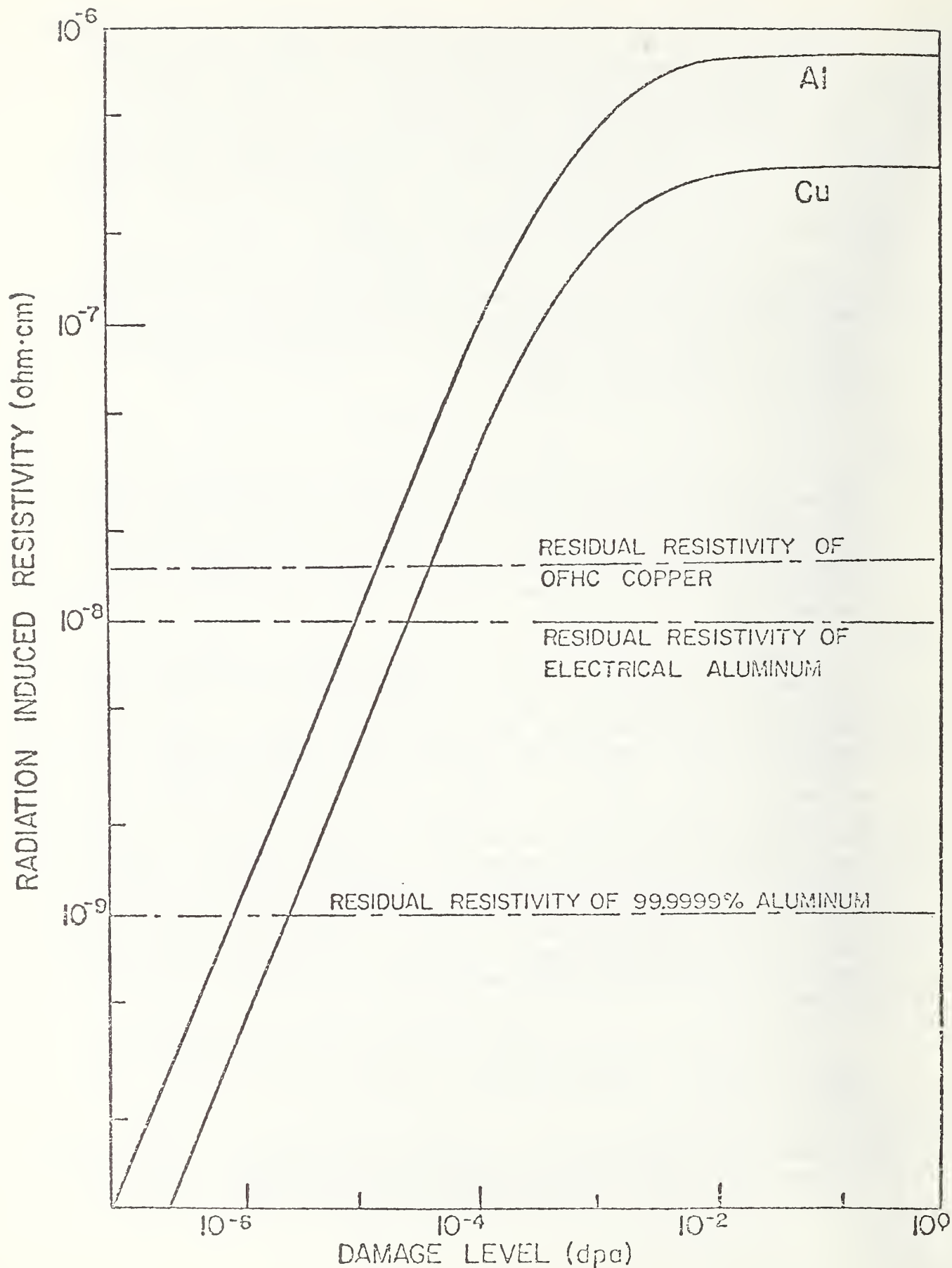
Figure III.D.1. Radiation induced resistivity of copper and aluminum. From UWMAK III.

(Sparks and Fickett 1975). No data exist for aluminum. The bond between the stabilizer and both the superconductor and the strengthener is also a potential problem area for heat transfer, particularly for aluminum.

III.D.4. Strengthener. This component is not always present in the conductor, particularly in the case where the conductor is embedded in a disc or some such structural member. Where it is used, it is nearly always stainless steel strip or wire. The cost probably will be $\sim$ $2/lb when the fabrication is considered. Most of the necessary material properties are available. The possibility of neutron radiation inducing local magnetic regions (Stanley and Garr, 1975), while remote at the anticipated radiation levels, should be considered because of the unknown effect of magnetic field and the proximity to the superconductor. The particular function of the steel is to keep the conductor strain to an acceptable level, usually < 0.1%. To this end, various clever cabling techniques have been described.

The possibility of replacing the steel-stabilizer system with a single component, usually cold worked copper has been proposed (Wilson and Walters, 1976). Such an arrangement might be able to decrease eddy current losses in the magnet considerably.

III.D.5. Other Materials. As long as NbTi is the conductor choice, the only other material involved in the conductor will be the eddy-current shielding barriers which are always proposed to be copper-nickel alloy. In tube form the alloy costs about the same as stainless steel. Its electrical and thermal properties at zero magnetic field have been measured. Magnetoresistive effects have not been studied in any detail, nor has the magnetothermal conductivity. The alloy has already been used successfully in conductors for a number of pulsed magnets (Coupland, 1976).

In Nb_3Sn wire conductors the alloy CuSn is an essential component as it provides tin for the reaction of the niobium filaments to the intermetallic. In existing conductors, alloys containing from 8-13% Sn are used. After reaction, $\sim$ 0.3% Sn remains in the bronze. The bronze is not a good enough conductor to perform a stabilizing function. In order to separate the bronze from the pure copper stabilizer a barrier of tantalum is used. This prevents contamination of the stabilizer with tin from the bronze.

III.D.6. Conductor Composite. The materials described above are combined in the composite conductor. Existing commercial superconductors tend to have critical currents of several hundred to a thousand amperes and to be several millimeters in dimension. It is difficult to state prices with any certainty, but NbTi conductor tends to be $\sim$ $0.10/ft and Nb_3Sn wire $\sim$ $1-2/ft. Superconducting wire and tape is produced by only a few companies in this country. Most processes are highly proprietary and, thus, any properties except those specified by the buyer usually must be determined by measurement.

There have been many successful applications of NbTi superconductor in relatively large magnets. The same is not true of Nb_3Sn, particularly in wire form. Quench initiation and the training phenomenon in medium and small size magnets is still not understood. Much of the problem may lie within the conductor itself.

Detailed specifications for some superconducting wire have been made, but buyers generally specify only critical current at field. NbTi wire is quite readily available, but the industry is small and very large orders could cause delays. Nb_3Sn, while available, is still produced in relatively limited quantities.

Properties data on the composite conductors is being acquired slowly. Work has been done on the effect of stress on critical current (Ekin and Clark, 1976; Easton and Koch, 1977), the effect of fatigue is the subject of the current NBS program. Neutron irradiation experiments (Guess, et al., 1975) have indicated that NbTi critical current is degraded by less than 10% under fluences up to $\sim 10^{18}$ n/cm^2. Annealing at near room temperature repairs the damage. Nb_3Sn shows an improvement in properties to a fluence of $\sim 10^{18}$ n/cm^2. More measurements are needed on all of these topics as the available data are often conflicting. The general area of ac losses in superconducting composites is a complex subject but one which has been investigated in some detail. Brechna (1973) presents a description of the various loss mechanisms and some sample calculations.

Complete fabrication of these materials is nearly always per-formed by the manufacturer. The joining of conductors by the user is often a problem, particularly where very high currents are involved. The inspection or NDE of wire is an area where little is now done and one in which work is needed.

IV. RECOMMENDATIONS

In this Section our recommendations are presented for an effective program of materials research and technology transfer to insure economical construction and reliable, safe operation of low-temperature components of magnetic fusion energy systems. The program objective is stated and the entire scope of required materials research from Section II and the candidate materials from Section III are summarized. Finally the recommended program is discussed. To assemble this, we have performed exhaustive analyses of present designs, visited every principal ERDA-MFE group concerned with superconducting magnets, summarized available materials technology and drawn extensively on our own experience in low temperature materials research.

Our present recommendations are a direct reflection of the materials problems and design constraints defined in the MFE documents referenced in this report. We recognize that progress in understanding the physics of fusion power may result in new MFE designs which will require a shift in emphasis in the materials research program. The present program is designed to be responsive to such changes.

There are some fundamental physics decisions which affect, considerably, the thrust of a low temperature materials research program. For instance, if the smaller prototype reactors continue to use relatively fast rise times for the ramping cycle of the ohmic heating coils, then low conductivity materials will be almost certainly be required to reduce eddy-current heating losses. Cheaper cryostat materials, such as 5083 aluminum, will not be used. Secondly, if the ohmic heating coils are placed immediately adjacent to, or within, the central support cylinder, it may be necessary to use a non-conductor material for the support cylinder, again if the rise times are fast. It is likely that a major influence on shield design and system warm-up will be from two material considerations: (1) the degradation and Wigner storage energy characteristics of the electrical insulators and (2) the radiation-enhanced resistivity and subsequent recovery at room-temperature of the purity-cold work dependent resistivity at 4 K of OFHC copper. Additionally, ultimate reactor design may be directly influenced by the maximum allowable design stress of the structural magnet coil form and casing: higher allowable design stresses will permit less material, thus conserving working space.

We have attempted to consider the impact of ongoing research programs in the formulation of the recommended program. Our compilation of these programs is presented in Appendix C. The potential overlap of these projects is pointed out in the discussion of the individual projects.

IV.A. Program Objective

To assist the design, construction, and safe operation of low-temperature magnetic fusion energy systems, especially superconducting magnets, through effective materials research and materials technology transfer.

IV.B. MFE Research Requirements

A survey of material requirements for all of the proposed MFE magnet systems has been performed. Design analyses, discussions and survey trips regarding all concerned laboratories (ANL, BNL, LASL, LLL, ORNL, GA, U. Wisc., MIT, PPPL) have been summarized. Working data sheets for each major component of each major project are all included in Appendix A and are summarized in Section II.C.2. Table II C-1 provides the information needs to which the research program must be responsive. Since it is convenient to address research programs in terms of material categories, as opposed to system components, it is more descriptive to rearrange these tables into research needs for the major material and material development groups. This is presented in Table IV B-1.

The major material technology categories which have been identified are:
(1) structural alloys
(2) thermal insulators
(3) electrical insulators, films and coatings
(4) structural composites and bulk insulators
(5) conductors (non-superconducting)
(6) adhesives

Some general considerations regarding applications of these material groups are given in the next Section.

Specific materials within each category are listed in subsection, IV D.

Perusal of Table IV B-1 will provide an accurate assessment of the research required for proper design and material selection of superconducting magnets for MFE.

Table IV.B-I

Materials Technology

Subject	Recommended Material Class	Specific	Required Programs General	Specific	Results needed by 1 yr	3 yr	long range
Structural Alloys	Stainless steels	AISI 304, 316, 21/6/9	Welding	δ ferrite control and effects; thick section, hi-strength filler, high restraint welds, heat control, inspection, properties	X	X	X
			Material Variability	Casting, thick-section processing, chemistry - effects on mechanical properties		X	X
			Data Base	Mechanical, electrical, thermal, magnetic properties	X	X	X
	Aluminum alloys	5083, 2219, 6061	Welding	Thick-section inspection, heat control, properties, high restraint welds			X
			Variability	Thick-section processing, chemistry			X
			Data Base	Mechanical, electrical, thermal properties			X
	Ferritic alloy	---	Development	Weldable, low cost, tough Fe-base alloy			X
Thermal Insulators	Superinsulation	Multi-layer (Al-Mylar) microspheres (Al-foam)	Thermal Properties	Effects of radiation, pulsed-fields on thermal conductivity		X	X
Insulating Films, Coatings, and Inorganics	Organics	Industrial films, coatings	Data Base	Mechanical, electrical properties, radiation effects	X	X	
	Inorganics	Oxides, silicates	Data Base	Mechanical, electrical properties, radiation effects		X	
Structural Composites and Bulk Insulators	Low modulus fiber	Industrial laminates specialty GFRP's	Screening	77 K flexure, fatigue	X		
			Characterizing	Mechanical, thermal, electrical at 4 K with and without radiation		X	X
	High modulus fiber	C, B, Kevlar/polymer B, Gr, W, S.S., FP/metal	Data Base	Mechanical, electrical properties, radiation effects			
			Joining	4 K properties of metal-composite joints			X
			Specifications	---			X
	Particulate reinforcement	Concrete	Development	Mechanical, thermal properties at 4 K			X
Conductors	Copper alloys	OFHC, ETP, cold worked Cu-Sn dispersion-strengthened	Electrical Properties	Effects of radiation, fatigue, stress on resistivity, magneto resistivity (OFHC); effects of processing, purity on RRR (OFHC)	X	X	X
	Aluminum	High purity Al (high RRR)	Mechanical&Electrical Properties	Effects of thick-section processing on tensile, creep, and RRR; inspection standards			X
Adhesives	SnPb alloys epoxies	---	Mechanical Properties	Shear, fatigue strength - function of composition		X	X

IV.C. Summary of Materials Considerations

Presented here are some general conclusions which we have reached following our review of the existing MFE designs and the environmental conditions as outlined in the last several sections. Specific materials and recommendations are considered in IV.D and IV.E.

IV.C.1. Structural Alloys. Radiation effects are not serious. Alloy requirements vary depending on the rise time of the pulsed (tokamak) fields. Smaller devices (TNS) will require steels while larger power plants will be able to make use of aluminum alloys. The allowable operating stress is important in determining space available; it is thus desirable to design with 4 K data. Regardless of the material, thick section welding and inspection techniques are an area of prime importance for study. The relatively inexpensive ferritic steels are conceivable as structural materials. The additional magnetic forces must then be considered in the design. In some instances concrete may be an acceptable, economic replacement for steels.

IV.C.2. Thermal Insulators. These materials, primarily aluminized polymers, may be very sensitive to mechanical and thermal degradation by radiation.

IV.C.3. Insulating Films, Coatings and Inorganics. An effort to screen these materials as to radiation resistance, particularly to gamma rays, at low temperatures and on repeated cycling to room temperature is urgently needed. Once this is done, the low temperature physical and mechanical properties of the most resistant materials must be measured. There is little low temperature data on these materials.

IV.C.4. Structural Composites and Bulk Insulators. Again, radiation damage effects are likely to be of prime importance in organic matrix composites and screening measurements to access the severity of the problem are urgently needed as input to this program. For most of these materials there is no low temperature data base. Specifications for industrial laminates (NEMA/ASTM) are generally electrical in nature and mechanical specifications may be necessary additions for low temperature applications. The advanced (high-modulus) composites and speciality fiberglass composites may be needed for low temperature structural applications near pulsed coils. Very few 4 K data exist.

IV.C.5. Conductors. Degradation of the low temperature conductivity of the stabilizing metal by neutron radiation will be a serious problem for economical power systems because of the loss of operating time involved in warming to room temperature to remove the damage. In nearer term systems, the effect of purity, processing and radiation on the stabilizing function of copper and aluminum needs investigation.

IV.C.6. Adhesives. The data base on the electrical, thermal and mechanical properties of solders is surprisingly small. A similar situation exists for epoxies used as adhesives.

IV.C.7. Demountable Coils. Problems of tokamak construction and maintenance would be greatly simplified if demountable joints could be made in large superconducting magnets. We recognize that the task seems nearly impossible, but the possible advantages indicate that the concept needs some investigation.

IV.D. Specific Materials

This section briefly summarizes the specific materials which are recommended for consideration in this program.

Structural Alloys

AISI 304 and 316

stainless steels which are extremely tough at 4 K, relatively easily welded, high modulus, AISI 304 is relatively low cost

21/6/9

nitrogen-strengthened stainless steel having much higher yield strength but less toughness, high modulus

5083, 2219, and 6061

aluminum alloys have greater likelihood of use in slow rise-time reactors, lower cost (5083 is cheapest of all alloys in this list), lower modulus and yield strength, 5083 is easily welded

Possible candidates for high-strength alloys:

18/3/8

nitrogen-strengthened steel that is cheaper than 21/6/9, most properties at 4 K unknown

AISI 304N

nitrogen-strengthened AISI 304, has considerably less yield strength, but greater toughness than 21/6/9

22/13/5

nitrogen-strengthened steel that has comparable strength and more stability compared to 21/6/9, properties at 4 K unknown

Thermal Insulators

Superinsulation

(1) aluminized mylar sheet (2) hollow glass beads, aluminized coating

Reinforced polyurethene foam   (20-300 K)

Insulating Films, Coatings and Inorganics

Polyethylene Terephthalate   (Mylar)
Polypyromellitimide   (Kapton)
Polyvinylformal   (Formvar)
Polyamide   (Nylon)
Polyurethene
Polyparaxylylene   (Parylene)
Polycarbonate   (Lexan)
Aluminum Oxide (Al_2O_3)   Alumina
Magnesium Oxide (MgO)   Magnesia
Porcelain
Fused Quartz (SiO_2)
Mineral Silicate   Mica

Structural Composites and Bulk Insulators

Industrial Laminates

NEMA/ASTM Grade LE	cellulose fabric, fine weave, phenolic resin
NEMA/ASTM Grade G-10	glass cloth, epoxy resin
NEMA/ASTM Grade G-11	glass cloth, high-temperature epoxy resin
NEMA/ASTM Grade C	cellulose fabric, medium weave, phenolic resin
NEMA/ASTM Grade G-5	glass cloth, melamine resin
LP Spec. Grade W1, W2	beechwood veneer, phenolic impregnated

Specialty Fiberglass Composites

S glass/aromatic base epoxy
S glass/polyimide

Advanced (High-Modulus Composites)

Graphite, Boron, Kevlar 49/aromatic-base epoxy, polyimide
Graphite, Boron, FP-alumina, Stainless Steel, tungsten/aluminum, copper

Conductors

OFHC Copper	stabilizing material
Cold worked OFHC Copper	stabilizing material
ETP Copper	room temperature magnet-coil material
CuSn Alloys	partial stabilizing material (Nb_3Sn)
CuNi Alloys	eddy-current shield material
Al	alternate stabilizing and shield material

Adhesives

SnPb solders	common conductor adhesive agent
Epoxies	common potting agent or adhesive agent in magnet winding

IV.E. Program

The recommended program is outlined below. Ongoing research summarized in Appendix C and available research facilities (also in Appendix C) have been considered. The initial three years of the program are devoted to supplying information for TNS-type structural design and construction. The following two years concentrate on TNS follow-up research and on the anticipated needs of future years. Structural alloys, stainless steels are emphasized. Research on structural alloys will insure structural safety and present the opportunity for significant cost and space savings. Aluminum alloy research is delayed for application after TNS; TNS devices presently could better use a low resistivity alloy. This emphasis will be pursued unless there are major changes in the MFE magnet requirements or unless present insulators become unuseable at low levels of radiation, requiring insulator development.

This program has been developed on the premise that radiation research, very important for organic materials, be conducted by the National Laboratories under separate funding. Other projects (12-14) are listed for which funding is recommended, but which fall outside the monetary limitations of the present budget.

PROJECTS	SCHEDULE				
	1/yr	2/yr	3/yr	4/yr	5/yr
1. Screening of Nitrogen-Strengthened Stainless Steels	X	--	--	--	--
2. Base Data of Selected Materials					
Structural alloys	X	X	X	X	X
Thermal insulators	--	--	--	--	--
Electrical insulators, films, and coatings	--	X	X	X	X
Structural composites and bulk insulators	--	X	X	X	X
3. Thick-section Welding	X	X	X	--	--
4. Radiation Effects	*	*	*	*	*
5. Technology Transfer	X	X	X	X	X
6. Project Management	X	X	X	X	X
7. Material Procurement Specifications	--	--	X	--	X
8. Screening, Characterization of Concrete	--	--	--	X	X
9. Applications of Advanced Composites	--	--	--	X	X
10. Inspection Standards	--	--	--	X	X
11. Design Data for Codes	--	--	--	--	X
Other Possible Projects					
12. Heat Product-Form Variability (stainless steels)	X	X	X	--	--
13. Copper Processing and Purity Effects for Stabilizing and Strengthening Material (with INCRA)	X	X	X	--	--
14. Copper Specifications for Copper Magnets (with CDA)	X	X	--	--	--

*Performed by National Laboratories, additional funding will be required for this program.

306

Proposed Complementary Research

Ferritic alloy development (U. Cal-Berkeley). This program, now initiated on Fe-Mn alloy systems by Prof. Morris, is of concern to future MFE systems in that it may result in the development of a less expensive ferromagnetic, ferritic alloy.

High strength/high conductivity composite development (U. Wisc.-Madison). Under the guidance of Prof. Boom, the development of a high strength, high conductivity material could produce long-range material advances. Processing equipment, aluminum experience, and an explosive bonding of aluminum to stainless program indicate that the ingredients are available for significant progress.

Quality requirements for 5083 weldments and thick-section weld development (ALCOA)

The following programs are not funded, but are suggested as possible areas of fundamental research that should, ultimately, impact on materials technology for MFE superconducting systems.

Radiation effects in polymers (fundamental studies - ERDA)

Materials research related to joining (fundamental studies - ERDA)

Effects of magnetic fields on low temperature deformation (fundamental studies - ERDA)

Austenite phase stability as influenced by low temperature, deformation and magnetic fields (fundamental studies - ERDA)

There are projects at the National Laboratories and at NBS which complement this program; these are listed in Appendix C.

Project 1:   Screening of Nitrogen-Strengthened Stainless Steel

Evaluation of available high-strength structural alloys for poten-
tial use in large superconducting-magnet structures has led to the
selection of the stainless steel 21/6/9 (21% Cr, 6% Ni, 9% Mn, Fe
balance) to fill this role.   However, there are other nitrogen-strengthened,
austenitic steels which have some advantages over 21/6/9.   Alloy 18/3/12
(Nitronic 33) is cheaper, while alloys 22/13/5 (Nitronic 50) and AISI
304N are considered to have much better fracture toughness at 4 K and
the alloy 22/13/5 is expected to be completely stable with respect to
the martensite transformation (therefore non-magnetic).   All materials
have higher yield strengths than AISI 304 or 316.

Therefore, the purpose of this screening program is to compare the
4 K mechanical property behavior of these three alloys with alloy 21/6/9.
From this comparison, and accounting for material cost, availability,
and product forms, a program decision will be made to discontinue test-
ing these alloys or to include one of the alloys in the structural alloy
group.

I.   Conduct tensile and J-integral fracture toughness tests at 4 K
on the three alloys 18/3/12, 22/13/5, and AISI 304N.
II.   Evaluate these alloys with respect to the 21/6/9 alloy.

Project 2:   Base Data of Low Temperature Materials

One primary program objective must be to insure that reliable,
relevant data are available for the major construction materials used
in superconducting magnets. This program is designed to supply this
information for a variety of materials. These data will permit effi-
cient design and careful material selection. They will be available
as a standard reference source for RFP preparation and evaluation.

I.   Compile from the recent "Handbook of Materials for Supercon-
ducting Applications," from the ARPA-sponsored materials research at 4
K, and from other recent investigations the relevant properties of the
selected materials for use in MFE superconducting magnets. Some
suggested properties and material categories are presented in the
accompanying Table IV E-1. Prepare, for inclusion in the new MFE-Low
Temperature Handbook, graphs of typical property values versus temper-
ature.

II. Measure, when not available from I, the properties required
as identified in Table IV E-1. The major, significant exclusion from
this program are radiation effects; these are included in Project 4.
To obtain a perspective on structural alloy material variability, the
properties should include several product forms in the annealed condi-
tion and weldments (mechanical and magnetic properties only). For
structural composites data must be available as a function of orienta-
tion. Specifically for composites we recommend determining the mechan-
ical and thermal properties of cellulose-phenolic and glass-epoxy
types of industrial laminates and of S glass-aromatic epoxy and S
glass-polyimide specialty fiberglass composites. No data are presently
available. Data from these measurements should be included in the new
Handbook. Specifically for structural alloys we recommend that
fatigue tests (21/6/9, AISI 304 and 316), multiple product and heat
tensile tests (AISI 304, 316), tensile tests, fracture toughness tests
(21/6/9) be conducted. In alloy 21/6/9 the fracture toughness is
marginal compared to AISI 304 and 316; therefore more tests are
required to reliably describe the fracture behavior.

Table IV. E-1. Test Material Matrix for Base Data Program

PROPERTIES	Structural Alloys	Structural composites & bulk insulators	MATERIALS Thermal insulators	Insulating films coatings & inorganic
Mechanical				
Elastic	X	X		X
Tensile	Ⓧ	X		X
Compression	X	X		X
Shear	X	X		X
Fatigue	X	X		X
Fracture toughness	Ⓧ			
Fatigue crack growth rate	Ⓧ			
Thermal				
Thermal conductivity	X	X	X	
Thermal expansion	X	X		
Specific heat	X	X		
Electrical				
Resistivity	X			
Magneto-resistivity				
Dielectric		X		X
Magnetic				
B-H curves	Ⓧ			
Permeability to He		X		

Ⓧ - includes weldments

X̲ - function of fiber orientation

Project 3: Thick-Section Welding

The construction of large superconducting magnets involves the accomodation of large, field-induced loads; thick-sections of structural alloys are required (Section II.A.2). Significant unknowns are the effect of delta ferrite (which probably must be present to prevent hot cracking in stainless steel thick-section welds) on weld fracture behavior at 4 K, the variability of design properties at 4 K which thick-section processing introduces and the degree to which specifications must be controlled to prevent erratic property behavior at 4 K. This information should be obtained on AISI 304, 316 and the stainless steel 21/6/9; the alloys presently thought useful for TNS type system construction.

I. Conduct fracture toughness tests at 4 K on restrained, thick-section butt welds (1-6 inches thick) of AISI 304, 316 and 21/6/9. The amount of ferrite must be varied, to obtain the dependence of fracture toughness on ferrite concentration. Several weld processes should be evaluated, J-integral fracture toughness procedures will probably be required.

II. Assess tensile property (4 K) variations as a function of thick-section cross-section, in longitudinal and transverse directions, for AISI 304, 316 and 21/6/9 stainless steel.

III. Conduct tensile and/or fracture toughness tests at 4 K as a function of time/temperature of holding in the temperature range 900-1500°F to assess severity of solute grain boundry segregation (sensitization) on low temperature mechanical properties.

IV. Develop a higher strength weld consumable for use with nitrogen-strengthened 21/6/9 stainless steel or similar alloys.

LLL (Witherspoon, Landon) is considering thick-section welding of 21/6/9 for MX construction. HEDL has performed ferrite-related research on AISI 304 and 316. Rennselaer Polytechnic Institute (Nippes, Savage) have a program on ferrite elimination in stainless steel welds. Rockwell Intl. (Rocky Flats Facility, Liby) is planning to evaluate the influence of composition variations on the δ-ferrite content of 21/6/9 welds.

Project 4: Radiation Effects

It is necessary to examine the effects of neutron, beta and gamma radiations at 4 K on material properties at 4 K and on material properties after subsequent warming to room temperature. Little information on material other than the noble metals now is available. Especially it is important to assess very carefully the radiation effects on organic materials which are thought necessary for use in the magnet system, as there is concern regarding their usefulness following radiation at 4 K and warming to room temperature.

This program is best carried out at the National Laboratories (ANL, BNL, ORNL, LLL), where facilities now exist and are available, to produce useful neutron spectra and fluences and to test at cryogenic temperatures prior to recovery. As discussed earlier (Section II.A.5) in this report it is thought that fission spectra are useable, especially for material screening testing. Furthermore, comparison of data with the LLL rotating target 14 Mev neutron source will probably allow the use of a fission spectra (for superconducting-magnet system materials) in the characterization phase of this program.

Phase I - Screening

A. Screen industrial laminates and films, thermal insulators, epoxies, and glass-reinforced plastics by irradiation at 4 K (seeSection IV.C. for complete listing of suggested materials); followed by (1) warming to room temperature and observation of physical condition and (2) flexture (or tensile) strength at 4 K before and after irradiation and after thermal cycling to 300 K. At present there is one program initiated in this area at ORNL (Long), however the candidate lists are long and mechanical property testing at 4 K is desirable, leaving ample research and persisting urgency for another program.

Phase II - Base Data of Selected Materials

A. Measure effect of radiation dosage and thermal cycling to 300 K on thermal conductivity of selected thermal insulator(s).

B. Measure effect of radiation dosage and thermal cycling to 300 K on tensile, compressive and dielectric strength of selected industrial laminates specialty fiberglass composites and films (electrical insulators).

C. Measure effect of radiation dosage and thermal cycling to 300 K on magnetoresistance of selected conductor materials.

D. Confirmation of structural alloy performance by tensile tests at 4 K after irradiation at 4 K of selected alloys in this program.

Project 5: Technology Transfer

I.   A new handbook, MFE Low Temperature Handbook, should be started. It is recommended that the Handbook include both material properties and relevant helium fluid and heat transfer properties. The materials properties will be prepared from six principal sources during the first three years:
  (1) the Handbook on Materials for Superconducting Machinery
  (2) the recent ARPA-sponsored program on 4 K materials research
  (3) the Base Data of Low Temperature Materials Program recom-
       mended in this report
  (4) the Radiation Effects Program recommended in this report
  (5) the Structural Alloy Thick-Section Welding Program recom-
       mended in this report and
  (6) other ongoing research programs at 4 K throughout the world.

There should be the following subdivisions of the materials section of the new Handbook:
  (1) Base Data - figures of significant properties versus temperature
  (2) Specifications - any material procurement specifications developed
       for MFE will be included in a separate section
  (3) Other Specifications and Allowable Stresses - current ASTM, NEMA,
       etc. specifications and current code stress allowables will be
       included in this section
  (4) Design Data - all available data will be presented in this section,
       to establish, eventually, design allowable values.

II.   Once a year a Workshop will be held to accelerate communication between the participants of the program recommended in this report and the National Laboratory MFE project personnel. Proper programming will insure this to be worthwhile to the NL personnel and encouragement of feedback will permit program reevaluation.

III. Twice a year project reports should be assembled, printed and distributed. These reports could include contributions from Project 4 as well as from the complementary programs.

IV.   Consultation, either from individuals or from program teams, must be available to advise or assist RFP writing and evaluation, project material selection, design troubleshooting or failure analysis, and in specification writing and code development.

Project 6: Project Management

The program, although small, involves an inordinate amount of interfacing, limited subcontracting with attendant project monitoring, and semiannual report editing and assembly. A small amount of project management funds is required for these functions.

Project 7: Material Procurement Specifications

Projects 1-4 will result in a considerable amount of information regarding product performance from a material property vantage point. The project must translate this information to specifications and, additionally, conduct more property tests, if needed, to adequately define the material product for purchasing. The objective of this project is to produce material procurement specifications when applicable and significant to insure adequate low temperature performance.

All material classes will be considered and these are some obvious examples:
(1) Weld rod specifications for proper ferrite and hot-cracking control may have to be rigidly controlled. Project 3 results, manufacturer consultation, and, perhaps, additional rod sampling may have to be performed.
(2) NEMA Grade G-10 and G-11 specifications were developed for room temperature insulating performance, and cover a wide variety of glass fiber/epoxy lay-ups. Projects 2 and 4 may indicate that additional control is required to insure adequate 4 K performance. If so, subsequent sampling and testing at 4 K will be required to identify closely the parameters to be controlled (specified).
(3) Thick-section processing and chemistry control of alloy 21/6/9 will probably be identified from Project 3 data. Subsequent control, through material specifications, will then be required. Consultation with suppliers and knowledge of their capabilities, consideration of time, costs and product forms will result in new specifications for purchase.
(4) It is quite possible, if fiberglass/epoxy dewars are constructed, that Project 4 results will imply better performance of specific fiber or epoxy mixes. Additional specimens may be required to compare these component combinations and lay-ups with others. These tests would be followed by material specifications for non-metallic dewars.

LLL (Landon) and Rockwell Intl. (Rocky Flats, Liby) have previously considered 21/6/9 procurement for low temperature use.

314

Project 8: Screening, Characterization of Concrete

For magnet systems following TNS, it is conceivable that one of the better support materials will be reinforced concrete, especially for the tokamak central support cylinder, for Yin-Yang central support (already recommended by Bechtel for this application) and for tokamak support columns for the gravitational weight of the TF coils. Major advantages are low cost and maintenance with good compressive strength, and low thermal conductivity and good radiation resistance. Disadvantages are lack of mobility and the probable requirements of thick cross-sectional areas, using valuable space. Preliminary research on concrete to 76 K has been performed by the University of Wisconsin.

I.   Screen various mixtures (aggregate type, water content) for tensile and compressive properties at 4 K. Assess increase of properties at 4 K with post-tensioned steel.

II. Measure elastic, tensile, compressive and fatigue properties and thermal conductivity of selected concrete composites at 4 K.

Project 9: Application of Advanced Composites

Seven areas may be defined where advanced, high-modulus composites offer the potential of increased performance, comparable cost and reduced consumption of scarce resources:

(1) Poloidal Coil Dewars and Structural Helium Containers. Reduction of ac losses suggest the use of non-metallic composites for at least the inner wall of the OH poloidal coil dewars and for load-bearing helium containers closely surrounding bundles of OH coil poloidal field conductors. Here, stiffness may dictate the use of high-modulus composites.

(2) Coil Forms. Reduction of ac losses promotes the use of non-metallic composites for the OH poloidal magnet coil form. Again, stiffness may require the use of advanced composites.

(3) Nonmetallic Strengthener within Superconducting Cables. Replacement of stainless steel internal conductor reinforcement with an advanced high-modulus composite can provide higher strength, higher modulus, lighter weight and a reduced probability of electrical shorts. This application applies to both solid reinforcement and to filament-reinforcement of braided conductors.

(4) External Reinforcement of Superconducting Coils. Replacing stainless steel tension bands with a high-modulus composite band can provide higher strength, lighter weight, a reduced probability of shorts and facilitate field erection of very large coils, and may act as an electrical insulator-strengthener.

(5) High-Modulus Superconductor Stabilizing Material. Reinforcing high-purity copper or aluminum with high-modulus fibers may substantially stiffen the stabilizing material without significant degradation of its electrical conductivity, thereby reducing strain limitation imposed by the superconductor.

(6) Eddy-Current Shields. Replacing bonded stainless-copper with aluminum or copper reinforced with a high-modulus fiber can substantially increase the strength, stiffness and fatigue resistance of eddy-current shields in poloidal-coil systems where the shield is subjected to pulsating electromagnetic stress.

The data base required for the use of industrial laminates and specialty fiberglass composites in thermal standoffs, poloidal coil dewars and coil forms is encompassed in the recommended base data program. This should be followed by prototype dewar construction to determine the least expensive method of fabricating very large composite-metal dewars.

The use of high-modulus composites as load-carrying helium containers or for internal or external superconductor reinforcement requires a screening program to select the optimum high-modulus composite on the basis of uniaxial fatigue performance under radiation.

Initial studies on fiber-reinforced stabilizing materials and eddy-current shields need only exploit existing state-of-the-art metal-matrix technology to demonstrate feasibility of reinforcing high-purity metals. Favorable results should be followed by prototype testing.

Project 10: Inspection Standards

Subsequent to research primarily directed toward TNS design and material selection and procurement, inspection becomes significant. Weld quality standards, based on ferrite and defect control, will be needed; measurement technique and quantitative standards pertaining to ferrite and defects will be essential to insure reliable weld joint performance. Additionally, multi-pass stainless steel welds may result in some sigma phase formation; requirements may be needed for this phase concentration. Secondly, if non-metallic dewars are constructed, standards and measurement techniques must be stipulated to insure adequate composite properties at 4 K. Composite-to-metal joints will have to be inspected and/or tested. Thirdly, in prototypes extensive strain-gaging is required to compare material performance with design expectations. The magnetoresistance contribution to the strain-induced resistance change of the strain gages must be known. Currently, there is some research on this problem at LLL.

Therefore, the major program thrusts should be:

I.   Weld inspection measurement techniques and standards for ferrite defects, and, possibly, sigma phase for stainless steels.

II.   Inspection measurements and standards for porosity or void content, fiber/resin ratios, fiber orientation, and interlayer debonding in non-metallic composites - if used for dewar construction.

III. Weld inspection measurement techniques and standards for defects in aluminum alloys - if used.

Project 11: Design Data for Codes

At some stage in the development of MFE, codes are inevitable. Perhaps, even at the TNS stage very careful and accurate assessment of 4 K (or 300 K) properties used in design that are critical to structure safety (such as the tensile yield stress) will be required. Furthermore, as is pointed out in the variability discussion, permission for use of 4 K property data in design will surely be contingent on more-than adequate characterization. The structural alloy portion of the program concentrates on the subject of material and property variability, but a complete answer to fully characterize this subject is quite expensive. Heat and product form variability studies, such as performed on the LMFBR program for AISI 316 and 304 at room and elevated temperatures, demands the acquisition of multiple heats, the processing into several product forms, close control and characterization of chemistry, and extensive testing.

Therefore, the purpose of this program is to continue variability studies on structural alloys and/or other materials that are (1) anticipated to fall under regulatory codes or (2) that careful documentation of 4 K properties will permit the use of those properties in design - thus saving material cost, permitting the use of less material, and conserving open space.

Actual program plans must be negotiated with concerned regulatory bodies or with project personnel concerned about decisions pertaining to operating stress levels.

Project 12: Heat, Product Form Variability

Thorough documentation of low temperature properties relevant to
design, especially the tensile yield strength, should provide sufficient
incentive to permit the use of low temperature design allowables. The
use of low temperature property data will be of tremendous assistance in
meeting space requirements. For instance, the permission to have the
design allowable based on a 4 K yield strength of 140,000 psi, as opposed
to the room temperature strength of 55,000 psi, will result in substan-
tial material reduction. Both cost and space will be conserved. There-
fore, there is ample incentive to characterize, reliably, the extent of
the variability of low temperature properties, as influenced by heat,
product form and chemistry.

However, as extensive tests involving a number of material heats
and/or product forms are needed, the program is very expensive. Some of
the needed variability data will accrue from Projects 1-3; however, it is
estimated that for complete examination of these factors, additional
funds will be required.

I.   Tensile tests at 4 K on variations of 12 heat/product forms
per alloy (three alloys, transverse, short transverse and longitudinal
for plate, 4 specimens each).
II.   Compression and shear tests at 4 K on variation of 3 heat/
product forms per alloy (three alloys, longitudinal for sheet and
plate, 2 specimens each).
III. The product performance variability of industrial non-metallic
laminates must be determined whenever such variability impacts on the
laminate application.

ORNL (Brinkman) and HEDL on the LMFBR program have already greatly
assisted this project by their measurement and compilation of room
temperature tensile properties for AISI 304 and AISI 316 stainless
steels.

Project 13: Low Temperature Physical Properties of Copper
and Copper Alloys for Conductor Applications

This program is anticipated as a cooperative effort with the International Copper Research Association (INCRA).

Large amounts of copper and copper alloys are proposed for use in current MFE magnet designs as a stabilizer for the superconductor and as a strengthening element. It is essential that the role of purity of OFHC copper (RRR $\sim$ 200-500) be identified in affecting recovery at room temperature and the final RRR after conductor processing and after irradiation at 4 K. Knowledge of these variables should result in the determination of magnet warmup schedules subsequent to irradiation at 4 K and may result in specification of a minimum purity of OFHC copper.

Secondly, for pulsed magnets the effects of mechanical fatigue on magnetoresistivity, as a function of purity and radiation, must be understood. NBS (Clark, Ekin) is currently conducting a limited fatigue program, but the results are likely to apply only to small conductors and to Cu/NbTi composites.

Project 14: Copper Specifications for Copper Magnets

This program is anticipated as a cooperative program with the Copper Development Association (CDA).

Recent experience of several manufacturers of large copper magnets indicates that existing product specifications accepted by the copper industry are not adequate when the product is to be used in high current magnet applications such as those required by the controlled thermonuclear research devices now under construction. As normal-metal copper magnets will continue to contribute to the MFE program, it is expected that this demand for copper will increase in the near future. Significant economy could be achieved if available large copper plate products were compatible with magnet design requirements.

This program would rely on a strong cooperative effort between the industry, the magnet designers and builders and appropriate research laboratories to arrive at a mutually-acceptable solution to the problem. Its objective would be to set specifications for thick-section copper plate for MFE magnets that were compatible with both MFE requirements and producer capabilities. Inspection procedures would also be formulated.

V. REFERENCES

The references listed here are, for the most part, those used in this materials review in one way or another. The first group consists of the laboratory design reports and closely related documents. These are listed under the appropriate laboratory. Next we have included a list of general references on fusion. Specific materials references are listed next with a separate listing of those specifically treating radiation effects. In Section III of the report specific references are given in the format (Jones, 1976). These refer to the two materials sections in this listing.

Argonne National Laboratory (ANL)

"Tokamak Engineering Technology Facility Scoping Study," ANL/CTR-76 (1976) W. M. Stacey, Jr., et al.

"A Tokamak Experimental Power Reactor," ANL/CTR/TM-47 (1975) W. M. Stacey, Jr., et al.

"Tokamak Experimental Power Reactor Conceptual Design," ANL/CTR-76-3, Vol. 1 and 2 (1976) W. M. Stacey, Jr., et al.

"Tokamak Experimental Power Reactor Studies," ANL/CTR-75-2 (1975) W. M. Stacey, Jr., et al.

Brookhaven National Laboratory (BNL)

"Fusion Magnet Safety Studies Program; Superconducting Magnet Protection System and Failure," BNL 20787 (1975) J. Allinger, et al.

"Program Plan for CTR Magnet Safety Studies," BNL 19620 (1975) G. Danby, et al.

"Warm Reinforcement and Cold Reinforcement Magnet Systems for Tokamak Fusion Power Reactors: A Comparison," BNL 17434 (1972) Engineering Division/Department of Applied Science.

"Summary of Existing Superconducting Magnet Experience and Its Relevance to the Safety of Fusion Magnet," IEEE 75 CH 1097-5-NPS (1975) S. Y. Hsieh, et al.

"BNL Cryogenic Data Handbook," (1966) J. Jensen, R. Stewart, W. Tuttle.

"Workshop on Structural Analysis Needs for Magnetic Fusion Energy (MFE) Superconducting Magnets," BNL (1976) proceedings to be published.

Energy Research and Development Administration (ERDA)

"Fusion Power Research and Development Summary Report on Magnetic Confinement Experiments," ERDA 76-34 (1976) Confinement Systems Program.

"Neutral Beam Energy and Power Requirements for the New Generation of Tokamaks," ERDA 76-77 (1976) Division of Controlled Thermonuclear Research.

"The 1974 Review of the Research Program," ERDA 39-75 (1975) Division of Controlled Thermonuclear Research.

"Programs of the Materials and Radiation Effects Branch," ERDA 76-83 (1976) Division of Magnetic Fusion Energy.

"Materials Sciences Programs," ERDA-76/123 (1976) Division of Physical Research.

"Physical Research Program: Research Contracts and Statistical Summary," ERDA 63-75/UC-2 (1976) Division of Physical Research.

"An Assessment of the Role of Magnetic Mirror Devices in Fusion Power Development," ERDA 76-74 (1976) ERDA.

"Report of the Ad Hoc Panel on RF Heating in Tokamaks," ERDA 76/115 (1976) ERDA.

"Fusion Power by Magnetic Confinement," ERDA 110/0-4, Vol. 0-4 (1976) ERDA.

"Fusion Power Research and Development Program C5-Year Program Budget and Milstone Summaries," ERDA, Vol. 1-3 (1976) ERDA.

"New Directions in Fusion Magnet Development," Proc. Appl. Super-conducting Conf. (1976) C. D. Henning, to be published.

"Applications of Superconductivity in the Controlled Thermonuclear Research Program," Proceedings of 1974 Applied Superconductivity Conf. (1975) G. Hess, et al.

Los Alamos National Laboratory (LASL)

A 100-MJ Superconducting Magnetic Energy Storage System," LA 5882-MS (1975) W. V. Hassenzahl.

"Superconducting Magnetic Energy Storage," LA 5935-PR, Vol. 1 and 2 (1975) W. V. Hassenzahl.

"An Engineering Design Study of a Reference Theta-Pinch Reactor (RTPR): Environmental Impact Study," LA 5336, Vol. 1 and 2 (1975) LASL.

"Proposed METS-FTR Coupled Superconducting Prototype System," LA 5918 (1975) J. D. Rogers, et al.

"Conceptual Engineering Design of a 1-GJ Fast Discharging Homopolar Machine for the Reference Theta-Pinch Fusion Reactor," EPRl ER-246 (1976) K. Thomassen.

"Conceptual Design Study of a Scyllac Fusion Test Reactor," LA 6024 (1976) K. Thomassen.

Lawrence Livermore Laboratories (LLL)

"Conceptual Design of a Mirror Reactor for a Fusion Engineering Research Facility (FERF)," UCRL-51617 (1974) T. Batzer, et al.

"The MX Major Project Proposal," LLL-Prop-142 (1976) F. W. Coensgen.

"The MX Magnet System," UCRL-78335 (1976) R. H. Bulmer, et al.

"The Field Reversed Mirror and Power Reactor," Presented at Richland ANS Meeting (1976) W. Condit, et al.

"High Field Test Facility Major Project Proposal," LLL-Prop 130 (1975) D. N. Cornish, et al.

"2X11B Mirror Machine," UCRL-52000-75-11 (1975) LLL.

"An Evaluation of the Technical and Economic Feasibility of Mirror Fusion Devices," UCRL 13695 (1976) LLL.

"Magnetic Fusion Energy Program," UCRL-52000-76-6 (1976) LLL.

"Program for Development of High-Field Superconducting Magnets for Fusion Research," MISC-2007 (1975) LLL.

"Conceptual Design of a Mirror Hybrid Fusion-Fission Reactor," UCRL-76515 (1975) R. Moir, et al.

Massachusett Institute of Technology (MIT)

"A High Density, High Field Tokamak Demonstration Power Reactor," Proceedings of the Meeting on the Technology of Controlled Nuclear Fusion, Richland, WA (1976) D. R. Cohn, et al.

"Annual Report," (1976) Francis Bitter National Magnet Laboratory.

"The Elmo Bumpy Torus Reactor," Proceedings of the Meeting on the Technology of Controlled Nuclear Fusion, Richland, WA (1976) D. G. McAlees, et al.

"Promising New Results from Alcator," Physics Today 18 (Jan 1976).

"A Magnet Field System for a High Density Tokamak Reactor," Paper (1976) J. Williams.

Oak Ridge National Laboratory (ORNL)

"High Beta Flux-Conserving Tokamaks," ORNL/TM-5429 (1976) J. F. Clarke.

"Conceptual Design of the Blanket and Shield Region and Related Systems for a Full Scale Toroidal Fusion Reactor," ORNL/TM-3096 (1973) A. Fraas.

"Mechanical Engineering Design Considerations for a Tokamak Scientific Feasibility Experiment and Plasma Test Reactor," ORNL/TM-4371 (1973) A. Fraas, et al.

"Program for Development of Toroidal Superconducting Magnets for Fusion Research," Paper (1975) H. Long, et al.

"Oak Ridge Tokamak Experimental Power Reactor Study - 1976 Part 3 Magnet Systems," ORNL/TM-5574 (1976) J. W. Lue, et al.

"The Elmo Bumpy Torus Reactor (EBTR) Reference Design," ORNL/TM-5669 (1976) D. McAlees.

"ORNL-EPR Study - Results and Implications," 76-WA/NE-10 (1976) D. McAlees.

"Annual Progress Report - Solid State Division," ORNL-5135 (1975) ORNL.

"Annual Progress Report - Thermonuclear Division," ORNL-5154 (1975) ORNL.

"OR Tokamak Experimental Power Reactor Study Reference Design," ORNL/TM-5042 (1975) ORNL.

"Superconducting Magnet Development Program Annual Report," ORNL/TM-5019 (1975) ORNL.

"Research, Development and Demonstration Needs," ORNL/TM-5577 (1977) M. Roberts, et al.

"The Effect of High Magnetic Fields on Metal Foil Strain Gauges at 4.2 K," Cryogenics (May 1975) P. Walstrom.

"A Summary of Tritium Handling Problems in Fusion Reactors," ORNL/TM-4022 (1972) J. Watson.

"ORNL Fusion Power Demonstration Study: Arguments for a Vacuum Building in which to Enclose a Fusion Reactor," ORNL/TM-5664 (1976) R. Werner.

Princeton Plasma Physics Laboratory (PPPL)

"Analytic Solutions for Constant-Tension Coil Shapes," Journal of Applied Physics, Vol. 47, 2710 (1976) S. L. Gralnick, et al.

"Princeton Lab Starts Largest U.S. Tokamak," Industrial Research (May 1976).

"Neutral-Beam-Injected Tokamak Fusion Reactors: A Review," PPPL-1280 (1976) D. L. Jassby.

"A Fusion Power Plant," MATT-1050 (1974) R. Mills.

"Poloidal Diverter Experiment," Physics Today (April 1976) Physics Today - FCB.

"A Plan to Demonstrate the Scientific Feasibility of Controlled Fusion," Special Report 71/3 (1971) Princeton U. Plasma Physics Lab.

"Reactor Applications of Two-Component Tokamak Plasmas," MATT-1161 (1976) F. H. Tenney.

"A Review of the Fusion-Fission Hybrid Reactor," Proceedings of the Meeting on the Technology of Controlled Nuclear Fusion, Richland, WA (1976) F. H. Tenney.

"A Tokamak Hybrid Study," PPPL-1284 (1976) F. H. Tenney.

General Atomic

"Fusion Reactor Studies: Doublet III Design," EPRI 115-2 (1975).

"Conceptual Design Study of a Noncircular Tokamak Demonstration Fusion Power Reactor," GA-A13992/UC20 (1976) Fusion Engineering Staff.

"Doublet III Design," GA-A13318 (1975) Fusion Engineering Staff.

"Doublet III - Schedule and Cost Report," GA-C13711 (1976) Fusion Engineering Staff.

"Experimental Fusion Power Reactor Conceptual Design Study," GA-A14000, Vol. I-III (1976) Fusion Engineering Staff.

"Experimental Power Reactor Conceptual Design Study," GA-A13534 (1975) Fusion Engineering Staff.

"Magnetic Field System Design - Part I," Design News (1975) R. F. Stengel.

University of Wisconsin

"Engineering Feasibility of a Fusion Reactor," FDM-43 (1973) R. Boom, et al.

"Thermal and Mechanical Design Considerations for Lithium-Cooled Tokamak Reactor Blankets," FDM-41 (1973) Dai-kai Sze, et al.

"Optimization Considerations in the Design of a Tokamak Reactor," FDM-44 (1973) D. Klein, et al.

"Major Technological Problems for Fusion Reactor Power Stations," FDM-33 (1972) G. L. Kulcinski.

"A Possible Scenario to Commercial Tokamak Power Reactors Based on the Results of the UWMAK-I and II Conceptual Design Models," UWFDM-130 (1975) G. Kulcinski, et al.

"University of Wisconsin Tokamak Reactor Design," FDM-46 (1973) C. Maynard, et al.

"UWMAK-I A Conceptual Tokamak Reactor Design," (1974) U. of Wisconsin

"UWMAK-II A conceptual Tokamak Power Reactor Design," UWFDM-112 (1975) University of Wisconsin.

"UWMAK-III A Noncircular Tokamak Power Reactor," UWFDM-150 (1976) University of Wisconsin.

"Wisconsin Superconductive Energy Storage Project," (1976) U. of Wisconsin.

"Materials and Cost Analysis of Constant-Tension Magnet Windings for Tokamak Reactors," FDM-27 (1972) W. Young, et al.

General

F. R. Fickett, "Controlled Thermonuclear Reactors," Report to International Copper Research Association (Aug. 1976).

W. Gough, "Prospect of Fusion Power," Sci. American 224, 50 (1971).

R. Hirsch, "Status and Future Directions of the World Program in Fusion Research and Development," Annual Rev. Nuclear Sci. 25, 79 (1975).

M. O. Hoenig, et al., "Cryostabilized Single-Phase Helium Cooled Bundled Conductors for Large High Field Superconducting Magnets," Paper (1976).

IEEE, "5th Symposium of Engineering Problems of Fusion Research," IEEE Pub. No. 73CHO843-3-NPS (1973).

IEEE, "6th Symposium of Engineering Problems of Fusion Research," IEEE Pub. No. 75CH1097-5-NPS (1975).

Inter. Atomic Energy Agency, "World Survey of Major Facilities in Controlled Fusion Research," (1973).

T. Kammash, Fusion Reactor Physics, (Ann Arbor Science, Ann Arbor, MI, 1975).

P. Komarek, "Superconducting Magnets in the World of Energy Especially Fusion Power," Cryogenics 16, 131 (1976).

M. Kristiansen, et al., "Proceedings of the Symposium on Thermonuclear Fusion Reactor Design, June 2-5, 1970," ORO-1171-1 (1970).

C. Laverick, "Review of Superconductivity and Magnets for Fusion," Annals New York Academy of Science (1975) p 494.

W. D. Metz, "Fusion Research (I)", Science 192, 1320 (1976).

W. D. Metz, "Fusion Research (II)," Science 193, 38 (1976).

W. D. Metz, "Fusion Research (III)," Science 193, 307 (1976).

R. G. Mills, "Problems and Promises of Controlled Fusion Power," Mechanical Engineering 97, 20 (1975).

R. Mills, "The Promise of Controlled Fusion," IEEE Spectrum (Nov 1971) p 24.

R. F. Post, "Nuclear Fusion," Annu. Rev. Energy 1, 213 (1976).

R. Post, "Prospects for Fusion Power," Physics Today (April 1973) p 30.

F. L. Ribe, "Fusion Reactor Systems," Reviews of Modern Physics 47, 7 (1975).

D. J. Rose, "The Prospect for Fusion," Technology Review (Dec 1976) p 21.

D. Steiner, "The Technological Requirements for Power by Fusion," Nuclear Sci. and Engineering 58, 107 (1975).

AEC Symposium Series 31, "(Texas Symposium on the) Technology of CTR Experiments and the Engineering Aspects of Fusion Reactors," Proceedings (1972).

K. F. Alexander, "Prospects and Problems in Nuclear Fusion, " Energietechnik 26, 189 (1976).

Materials

Air Force Flight Dynamics Laboratory, "Advanced Composites Design Guide," Five Volumes (1975).

Alcoa Aluminum, "The Cryogenic Metal."

The Aluminum Association, "Aluminum Standards and Data," (1976).

ANL, "Selected Properties of Materials with Application to CTR Design," ANL/CTR-72-01 (1972).

Anon., "Aluminums for Cryogenic Environments," Cryogenic Engineering News (Mar. 1966).

ARMCO, "ARMCO Nitronic 40 Stainless Steel Sheet and Strip," Product Data Sheet, S-26e (1976).

ARMCO, "ARMCO Nitronic Stainless Steels," Product Data Sheet, S-55a (1976).

Battelle Pacific N.W. Laboratory, "Pacific Northwest Laboratory Report on Controlled Thermonuclear Reactor Technology," BNWL-19393 (1976).

A. Bauer and L. Bates, "An Evaluation of Electrical Insulators for Fusion Reactors," RMI-1930 (1974). (Battelle Columbus Laboratories)

H. Brechna, Superconducting Magnet Systems, Springer-Verlag, New York (1973).

S. H. Bush, "Structural Materials for Nuclear Power Plants," Journal of Testing and Evaluation, 2, 435 (1975).

D. A. Cononico, "Materials and Their Application in the Nuclear Industry," Metallography, 9, 459 (1976).

J. L. Christian, et al., "Evaluation of Superconducting Materials and Joint Properties," CASD-ERR-76-014 (Dec 1976). (General Atomic Co.)

R. Coltman, ORNL (Private Communication, 1976).

S. H. Coupland, "The Pulsed Superconducting Magnet AC5," Proceedings of the 5th International Conf. on Magnet Technology (1975).

W. Delong, "Calibration Procedure for Instruments to Measure the Delta Ferrite Content of Austenitic SS Weld Metal," Welding Journal, 1222 (1976).

D. W. DeMichele and J. B. Darby, Jr., "An Analysis of the Material Constraints on Superconducting Thermonuclear Reactors," Proceedings of the Symposium on Technology of CTR Experiments and Engineering Aspects of Fusion Reactors. AEC Symposium Series 31 (1972) p 384.

D. S. Easton and C. C. Koch, "Mechanical Properties of Superconducting NbTi Composites," Advances in Cryo. Engineering, 22, p 453 (1977).

Effects Technology, Inc., "Fracture Toughness Data for Ferritic Nuclear Pressure Vessel Materials," NTIS No. PB-252-210 (1976).

J. W. Ekin and A. F. Clark, "Effect of Strain on the Critical Current of Nb_3Sn and NbTi Multifilimentary Composite Wires," AIP Conference Proceedings 34, 84 (1976).

F. R. Fickett, "Magnetoresistance of Very Pure Polycrystalline Aluminum," Phys. Rev. B, 3, 1941 (1971).

F. R. Fickett, "A Preliminary Investigation of the Behavior of High Purity Copper in High Magnetic Fields," Annual Report to International Copper Research Association, Project 186 (1972).

K. J. Froelich, "Lap Shear Strength of Selected Adhesives (Epoxy, Varnish, B-Stage Glass Cloth) in Liquid Nitrogen and at Room Temperature," ORNL/TM-5658 (1976).

R. Hay, et al., "A Review of Electrical Insulation in Superconducting Magnets for Fusion Reactors," (1976). (Magnetic Engineering Associates)

HEDL, "Controlled Thermonuclear Research Progress Report," HEDL-TME-76-7 (1975).

C. D. Henning, et al., "Large Superconducting Baseball Magnet," Advances in Cryogenic Engineering, 14, 98 (1969)

C. Henning, et al., "Material Selection for Baseball II Coil Form," ENRP68-1 (1968).

I. Ishii, et al., "Electrical Insulating Materials at Cryogenic Temperatures," 5 and 10 (1975).

J. E. Jenson, Ed., Forging Industry Handbook, Forging Industry Association, Cleveland, OH (1966).

M. B. Kasen, "Mechanical and Thermal Properties of Filamentary-Reinforced Structural Composites at Cryogenic Temperatures, " Cryogenics 15, 327 and 701 (1975).

M. B. Kasen, "Properties of Filamentary-Reinforced Composites at Cryogenic Temperatures," ASTM STP580 (1975) p 586.

V. I. Kononenko and V. V. Pustovalov, "Effect of a Constant Magnetic Field on the Yield Stress of Nickel at 4.2° K," Soviet Journal of Low Temperature Physics, 2, 132 (1976).

C. A. M. vander Klein, "The Organic Insulation in Fusion Reactor Magnet Systems," Reactor Centrum Nederland, Report No. 240 (1975).

V. I. Kozlovskaya, "Weldability and Mechanical Properties of Joints in Martensitic Steel 03Kh12N10MT at Low Temperatures," Science and Technology (1975).

G. Kulcinski, "Materials Problems and Possible Solutions for Near Term Tokamak Fusion Reactors," EDM-186 (1976). (Univ. of Wisconsin)

G. L. Kulcinski and N. M. Burleigh, Eds., "Proceedings of the Second Topical Meeting on the Technology of Controlled Nuclear Fusion," ERDA/CONF-760935-P1, Four Volumes (1976).

D. Larbalestier, et al., "High Strength Austenitic Stainless Steels for Cryogenic Use," RL-76-048 (1976).

G. E. Linnert, "Welding Characteristics of Stainless Steels," Joining of Stainless Steels, American Society for Metals, Metals Park, OH (1967).

C. J. Long, "Structural Materials for Large Superconducting Magnets for Tokamaks," ORNL/TM-5632 (1976).

S. S. Manson, "Fatigue: A Complex Subject - Some Simple Approximations," Experimental Mechanics, 5, 193 (1965).

H. I. McHenry, S. E. Naranjo, D. T. Read and R. P. Reed, "Low Temperature Fracture Properties of a USSR Aluminum-6% Magnesium Alloy," Proceedings of the Applied Problems of Low-Temperature Materials and Welding Cryogenic Structures, Kiev, USSR (1976).

A. J. Nachtigall, "Strain Cycling Fatigue Behavior of Ten Structural Metals Tested in Liquid Helium (4 K), in Liquid Nitrogen (78 K), and in Ambient Air (300 K)," NASA TN D-7532, (1974).

L. E. Morgan, et al., "Material Fabrication Study for Fusion Power Reactors," CASD-ERR-76-019 (1976). (General Dynamics, Convair Division)

NASA, "The Stress Corrosion Resistance and the Cryogenic Temperature Mechanical Behavior of 18-3 MN (Nitronic 33) Stainless Steel Parent and Welded Material," NASA TM X-73309 (1976).

NBS/ARPA, "Handbook on Materials for Superconducting Machinery," (1976).

NBS/ARPA, "Materials Research for Superconducting Machinery," Six Volumes (1974-1976).

NBS Cryogenic Data Center, "Bibliography of References - Mechanical Properties of Chromium-Nickel-Manganese Steels at Cryogenic Temperatures," (1975).

ORNL, "Controlled Thermonuclear Materials Technology Program Annual Progress Report," ORNL-5082 (1975).

ORNL, "Magnetic Fusion Energy Materials Technology Program Annual Progress Report," ORNL-5189 (1976).

D. T. Read, "Summary of Metallurgical Effects in Bulk NbTi," ASM Conf. on the Manufacture of Superconducting Materials (1976).

R. P. Reed and D. T. Read, "Summary of NBS-Boulder Test Results for U-25 Bore Tube Material," (1977) (Test Report from NBS to ANL).

B. W. Roberts, "Properties of Selected Superconductive Materials," NBS Tech. Note 724 (1972).

B. W. Roberts, "Properties of Selected Superconductive Materials - 1974 Supplement," NBS Tech. Note 825 (1974).

L. H. Rovner and G. R. Hopkins, "Ceramic Materials for Fusing," Nuclear Tech. $\underline{29}$, 274 (1976).

SAE/ASTM, "Unified Numbering System for Metals and Alloys," J1086/ASTM DS-56 (1974).

R. E. Schramm, et al., "A Compilation and Evaluation of Mechanical, Thermal and Electrical Properties of Selected Polymers," NBS Monograph 132 (1973).

F. R. Schartzberg and T. Kiefer, "Study of Fracture Behavior of Metals for Superconducting Applications," NBS/ARPA Materials Research for Superconducting Machinery, $\underline{4}$ (1975).

L. L. Sparks and F. R. Fickett, "Magnetothermal Conductivity," NBSIR 74-393 (1974).

R. L. Tobler, "Fracture of Structural Alloys at Temperatures Approaching Absolute Zero," NBS/ARPA Materials Research for Superconducting Machinery, $\underline{6}$, 279 (1976).

R. L. Tobler and R. P. Reed, "Fatigue Crack Growth Resistance of Structural Alloys at Cryogenic Temperatures," NBS/ARPA Materials Research for Superconducting Machinery, $\underline{6}$, 256 (1976).

R. L. Tobler and R. P. Reed, "Fracture Mechanics Parameters for 5083-0 Aluminum Alloy at Low Temperatures," NBS/ARPA Materials Research for Superconducting Machinery, $\underline{6}$, 135 (1976).

L. A. A. Warnes and H. W. King, "The Low Temperature Magnetic Properties of Austenitic Fe-Cr-Ni Alloys," Cryogenics $\underline{16}$, 659 (1976).

J. Wells, "Evaluation of Nitronic 33 SS for TFTR Device Applications," (1975).

J. M. Wells and M. W. Hagadorn, "Evaluation of Nitronic 33 Stainless Steel for TFTR Device Applications," 75-8C3-WETWO-R1 (1975) (Westinghouse Research Labs).

M. Wilson and C. R. Walters, "Development of Superconductors for Fusion Technology," RL-76-038 (1976). (Rutherford Laboratory).

W. Witzke, et al., "Effect of Minor Reactive Metal Additions on Reactive Toughness of Iron-12% Nickel Alloy at -196°C and 25°C," NASA TN D-8232 (1976).

H. Yoshimura, et al., "Microstructures, Low Temperature Toughness and Thermal Expansion Coefficients of High Manganese-Chromium Austenitic Steels," Transaction ISU, Vol. 16 No. 2 (1976).

Radiation Effects

H. Brechna and W. Maurer, "Irradiation Effects in Superconducting Synchrotron Magnets," KFK-1468 (1971). (Kernforschungstentrum Karlsruhe).

B. S. Brown, et al., "Critical Current Changes in Nb_3Sn Irradiated with Fast Neutrons at 6 K," Journal of Applied Physics, 46 (1975).

B. S. Brown, et al., "Radiation Effects on Superconductivity," ASM Seminar (1975).

R. Bullough, "A Systematic Approach to the Radiation Damage Problem in Fission and Fusion Reactor Structural Alloys," FDM-184 (1976). (University of Wisconsin).

M. Couach, et al., "Effects of Fast Neutron Irradiation at Low Temperature on the Properties of Nb-Ti Superconducting Wires," IEEE Trans. on Magnetics 11, 170 (1975).

J. F. Guess, et al., "A Survey of Radiation Damage Effects in Superconducting Magnet Components and Systems," ORNL-TM-5187 (1975).

J. F. Kircher and R. E. Bowman, Eds. Effects of Radiation on Materials and Components, (Reinhold Publishers Co., New York, 1964).

Lockheed Nuclear, "Effect of Nuclear Radiation on Materials at Cryogenic Temperatures," NASA CR-54881 (1965), NASA CR-72056 (1966), and NASA CR-72332 (1967).

R. McDaniel, et al., "Combined Effects of Reactor Radiation and Cryogenic Temperatures on Nerva Structural Materials," FZK394-1 (1973). (General Dynamics, Convair Aerospace Division).

P. L. Merz, "Interim Report on Evaluation of Dielectric Materials Under Irradiation," (1976) (General Atomic Co.)

ORNL, "Summary of U.S. LMFBR Programs on High Temperature Structural Design and Associated Materials Testing," ERDA-76/146 (1976).

D. M. Parkin, et al., "Neutron Irradiation of Nb_3Sn and NbTi Multi-filamentary Composites," IEEE Trans. on Magnetics 11, 166 (1975).

N. L. Peterson and S. D. Harkness, Eds., Radiation Damage in Metals, (ASM, Metals Park, OH, 1976).

W. Weleff, et al., "GTR-16 Radiation Effects Test on Structural Materials at -423°F," NO. RN-S-0290 (1966). (NERVA Program, Aerojet General Corp.).

C. Restat, et al., "The Effect of Radiation on Superconducting Coils," CERN ISR-MA/75-20 (1975).

L. W. Ricketts, Fundamentals of Nuclear Hardening of Electronic Equipment, (Wiley-Interscience, New York, 1972).

H. Schonbacker, et al., "Radiation and Fire Resistance of Cable-Insulating Materials Used in Accelerator Engineering," CERN 75-3 (1975).

E. Seibt, "Irradiation and Annealing Effects of Neutron Irradiated NbTi and V_3Ga Multilfilamentary Composite Wires at Low Temperatures," IEEE Trans. on Magnetics 11, 174 (1975).

M. Soell, et al., "The Influence of Low Temperature Neutron Irradiation on Superconducting Magnet Systems for Fusion Reactors," IEEE Trans. on Magnetics 11, 178 (1975).

J. T. Stanley and K. R. Garr, "Ferrite Formation in Neutron Irradiated Type 316 Stainless Steel," Metallurgical Transactions 6A, 531 (1975).

A. R. Sweedler, et al., "Neutron Induced Disorder in Superconducting A-15 Compounds," IEEE Trans. on Magnetics 11, 163 (1975).

M. W. Thompson, "Defects and Radiation Damage in Metals," (Cambridge Press, 1969).

F. L. Vook, "Effects of Radiation on Materials," Physics Today, 28, 34 (1975).

F. L. Vook, et al., "Radiation Effects on Materials," Reviews of Modern Physics, 47, 51 (1975).

M. Van de Voorde, et al., "Selection Guide to Organic Materials for Nuclear Engineering," CERN 72-7 (1972).

J. M. Williams, et al., "A Method of Transferring Irradiated Samples in Liquid Helium," ORNL 76-22 (Jan. 1976).

Appendix A. Summary of Project Materials and Components

    The tables presented here summarize the materials choices made by the various MFE projects evaluated for this report. We have attempted to achieve a uniform format for the tables and, as a result, it is probably not perfect for any project. The major component material choices are described in more detail in the next section.

ANL (EPR)

I. Magnet Coils	TF	OH (EF)
A. Conductor Components		
1. Normal magnets...............		
Conductor......................	--	--
Eddy current barrier............	--	--
2. Superconducting magnets.........		
Superconductor..................	NbTi	NbTi
Pure metal stabilizer...........	OFHC Cu	OFHC Cu
Alloy for diffusion process......	--	--
Diffusion barrier...............	--	--
Eddy current barrier............	--	--
Strengthening material...........	316 SS	SS wire or CW Cu wire
Joining material	PbSn solder	PbSn solder
Metallic potting (cables)	--	Soft solder
B. Electrical Insulation		
1. Turn to turn	Formvar	Formvar
2. Coil to confining structure	FEP	FEP
C. Bonding Agents		
1. Insulation to coil	--	--
2. Insulation to confining structure	--	--

A-2

D.	Current leads	--	--
E.	Spacers, Shims and Coolant Channels	Micarta G 10	--
F.	Coil Form and Confinement		
	1. Structural material................	316 SS	SS
	2. Joining materials (bolts, etc.)...	--	--
II. Eddy Current Shields		Al/SS panels	--
III. Magnet Dewars			
A.	Inner Wall	--	--
B.	Insulation	Superinsulation	Superinsulation
C.	Outer Wall	Al alloy	Al alloy
D.	Thermal Shields		
	1. Within insulation space...........		
	2. Nitrogen jacket...................		
IV. Support Structure			
A.	Magnet to Dewar Inner Wall	FEP	FRP
B.	Dewar Inner Wall to Outer Wall	FEP	FEP
C.	TF Coil Central Support	SS(Shield to OH coil) Al(Inside cylinder) FRP(Cylinder to floor)	--
D.	External Support Structure (warm)	FRP	7075 Al

Coil Type	Component	MX Materials and Form (FER in parens when distinct
Yin-Yang	Conductor Components	
	Conductor	NbTi filaments
	Stabilizer	OFHC Cu wire, sheet
	Potting	Soft solder
	Electrical Insulation	
	-layers	NEMA Grade G-11 sheet (poly-imide or polyimide-glass laminate)
	-turns	NEMA Grade G-11 buttons
	-corners	Mylar sheet
Yin-Yang	Cryostat	
	Coil Form	21/6/9 stainless steel plate and rings
	Insulation	Vacuum and multi-layer
	Thermal Sink	(LN_2 cooled Cu sheet (FERF))
Yin-Yang	Outside Structural Supports	
	Minor Axis Reinforcement	21/6/9 stainless steel plate
	Interconnecting Core (C-clamps, FERF)	21/6/9 stainless steel plate
	Magnets to Floor	21/6/9 stainless steel columns
	Magnet-to-Magnet and Floor	Post-tensioned concrete

ORNL (EPR)

I. Magnet Coils	TF		OH (EF)
A. Conductor Components			
1. Normal magnets..................	--		--
Conductor......................	--		--
Eddy current barrier............	--		--
2. Superconducting magnets.........	Hi-field	Lo-field	
Superconductor..................	Nb$_3$Sn	NbTi	NbTi
Pure metal stabilizer...........	Cu	Cu	Cu
Alloy for diffusion process......	Cu-Sn	--	--
Diffusion barrier...............	Ta	--	
Eddy current barrier............	--	--	CuNi
Strengthening material...........	Stainless steel		
Joining material	Solder		Solder
Metallic potting (cables)	Al-Alloy conduit		SS tube conduit (FRP potentially)
B. Electrical Insulation			
1. Turn to turn	"Insulation"		"Insulating matrix"
2. Coil to confining structure			
C. Bonding Agents			
1. Insulation to coil			
2. Insulation to confining structure			

D. Current leads	Vapor cooled	Vapor cooled
E. Spacers, Shims and Coolant Channels		
F. Coil Form and Confinement 1. Structural material...............	Stainless steel	FRP
2. Joining materials (bolts, etc.)...		
II. Eddy Current Shields		
III. Magnet Dewars		
A. Inner Wall		
B. Insulation		
C. Outer Wall		
D. Thermal Shields 1. Within insulation space...........		
2. Nitrogen jacket..................		
IV. Support Structure		
A. Magnet to Dewar Inner Wall		
B. Dewar Inner Wall to Outer Wall		
C. TF Coil Central Support	Stainless steel	FRP
D. External Support Structure (warm)		

ORNL - LCP (data from RFP)

	TF	OH (EF)
I. Magnet Coils		
A. Conductor Components		
1. Normal magnets...................	--	
Conductor......................	--	
Eddy current barrier............	--	
2. Superconducting magnets.........		
Superconductor..................	NbTi or Nb3Sn, a 7 T strain > .05% in a 7 T field region.	
Pure metal stabilizer...........	Calculate effect of 0.5×10^{17} n/cm^2 (E > 0.1 Mev)	
Alloy for diffusion process......		
Diffusion barrier...............		
Eddy current barrier............	Pulsed to $\sim$ 0.15 T field normal to conductor in 1 sec.	
Strengthening material..........		
Joining material		
Metallic potting (cables)........		
B. Electrical Insulation	Max dose 1.0×10^{7} rad	
1. Turn to turn	100 kr at .8 x max voltage	
2. Coil to confining structure	100 kr at 4.2 x max voltage	
C. Bonding Agents		
1. Insulation to coil		
2. Insulation to confining structure		

D. Current leads		
E. Spacers, Shims and Coolant Channels		
F. Coil Form and Confinement 1. Structural material..............	Materials with known properties	
2. Joining materials (bolts, etc.)...		
II. Eddy Current Shields		
III. Magnet Dewars		
A. Inner Wall		
B. Insulation		
C. Outer Wall		
D. Thermal Shields 1. Within insulation space..........	ORNL provides vacuum enclosure at $p < 10^{-5}$ torr with 80 K cold wall	
2. Nitrogen jacket.................		
IV. Support Structure		
A. Magnet to Dewar Inner Wall		
B. Dewar Inner Wall to Outer Wall		
C. TF Coil Central Support	Provided by (ORNL)	
D. External Support Structure (warm)	Torque rings (provided by ORNL)	

General Atomics EPR - I, II

I. Magnet Coils	TF	OH (EF)
A. Conductor Components		
1. Normal magnets.....................		ETP Cu (EF)
Conductor........................		
Eddy current barrier.............		
2. Superconducting magnets..........		
Superconductor...................	Monolithic NbTi	Braided NbTi
Pure metal stabilizer............	OFHC Cu	OFHC Cu
Alloy for diffusion process......		
Diffusion barrier................		
Eddy current barrier.............		
Strengthening material...........	Stainless	Stainless
Joining material		
Metallic potting (cables)		
B. Electrical Insulation		
1. Turn to turn	Micarta	
Layer to Layer	GFRP	
2. Coil to confining structure	Epoxy	
C. Bonding Agents		
1. Insulation to coil		
2. Insulation to confining structure		

D. Current leads		
E. Spacers, Shims and Coolant Channels	Micarta, GFRP	
F. Coil Form and Confinement		
1. Structural material...............		GFRP
2. Joining materials (bolts, etc.)...		
II. Eddy Current Shields		
III. Magnet Dewars		
A. Inner Wall	Stainless	GFRP
B. Insulation		
C. Outer Wall	Stainless	Stainless
D. Thermal Shields		
1. Within insulation space..........		
2. Nitrogen jacket..................		
IV. Support Structure		
A. Magnet to Dewar Inner Wall	Stainless, GFRP ceramics, epoxy	
B. Dewar Inner Wall to Outer Wall		
C. TF Coil Central Support		
D. External Support Structure (warm)	Stainless	

General Atomics DEMO (DFPR)

	TF	OH (EF)
I. Magnet Coils		
A. Conductor Components		
1. Normal magnets..................		
Conductor......................		Cu (EF)
Eddy current barrier...........		
2. Superconducting magnets.........		
Superconductor.................	NbTi	NbTi
Pure metal stabilizer..........	Cu	Cu-CuNi
Alloy for diffusion process......		
Diffusion barrier..............		
Eddy current barrier...........		
Strengthening material..........	Stainless	Stainless
Joining material..............		
Metallic potting (cables)........		
B. Electrical Insulation		
1. Turn to turn...................		
2. Coil to confining structure......		
C. Bonding Agents		
1. Insulation to coil.............		
2. Insulation to confining structure		

D. Current leads		
E. Spacers, Shims and Coolant Channels		
F. Coil Form and Confinement 1. Structural material...............	Stainless	`
2. Joining materials (bolts, etc.)...		
II. Eddy Current Shields	Aluminum	
III. Magnet Dewars		
A. Inner Wall		
B. Insulation		
C. Outer Wall		
D. Thermal Shields 1. Within insulation space..........		
2. Nitrogen jacket..................		
IV. Support Structure		
A. Magnet to Dewar Inner Wall		
B. Dewar Inner Wall to Outer Wall		
C. TF Coil Central Support	GFRP	
D. External Support Structure (warm)		

UWMAK I, II, III

		TF	OH (EF)
I.	**Magnet Coils**		
A.	Conductor Components		
	1. Normal magnets.....................	--	--
	Conductor........................	--	--
	Eddy current barrier.............	--	--
	2. Superconducting magnets..........		
	Superconductor...................	TiNb	TiNb
	Pure metal stabilizer............	Cu (I, II) Cu + pure Al (III)	Cu (I, II) Cu, work hardened (III)
	Alloy for diffusion process......	--	--
	Diffusion barrier................	--	--
	Eddy current barrier.............	--	CuNi sheath on sc filaments
	Strengthening material...........	--	316 SS in some cases
	Joining material.................	Solder	Solder
	Metallic potting (cables)........	--	--
B.	Electrical Insulation		
	1. Turn to turn....................	No turns in contact	Kapton
	2. Coil to confining structure......	FEP	FEP
C.	Bonding Agents		
	1. Insulation to coil..............	Epoxy	Not given
	2. Insulation to confining structure	Epoxy	Not given

D.	Current leads	Vapor cooled	Vapor cooled
E.	Spacers, Shims and Coolant Channels	Micarta	Micarta
F.	Coil Form and Confinement		
	1. Structural material...............	316 SS (I, II) 2219 Al (III)	None
	2. Joining materials (bolts, etc.)...	Al alloy bolts	Al alloy bolts
II. Eddy Current Shields			
III. Magnet Dewars			
A.	Inner Wall	SS	SS
B.	Insulation	Aluminized Mylar	Aluminized Mylar
C.	Outer Wall	SS (I, II) Al alloy (III)	SS (I, II) Al alloy (III)
D.	Thermal Shields		
	1. Within insulation space...........	--	--
	2. Nitrogen jacket...................	--	--
IV. Support Structure			
A.	Magnet to Dewar Inner Wall	Micarta	Micarta
B.	Dewar Inner Wall to Outer Wall	GFRP struts	Probably GFRP str
C.	TF Coil Central Support	SS (I, II) Al alloy (III)	--
D.	External Support Structure (warm)	Cylinder-piston elements. Secondary vacuum wall (II, III)	"Some vertical structure"

ELMO Bumpy Torus

I. Magnet Coils	TF	OH (EF)
A. Conductor Components		
1. Normal magnets.....................	--	--
Conductor......................	--	--
Eddy current barrier.............	--	--
2. Superconducting magnets...........		
Superconductor...................	NbTi	NbTi
Pure metal stabilizer............	Copper	Copper
Alloy for diffusion process......	--	--
Diffusion barrier................	--	--
Eddy current barrier.............	--	--
Strengthening material...........	--	--
Joining material	Solder	Solder
Metallic potting (cables)	--	--
B. Electrical Insulation		
1. Turn to turn	Kapton	Kapton
2. Coil to confining structure	"Insulation"	"Insulation"
C. Bonding Agents		
1. Insulation to coil	--	--
2. Insulation to confining structure	--	--

D. Current leads	--	--
E. Spacers, Shims and Coolant Channels	GFRP	GFRP
F. Coil Form and Confinement		
1. Structural material...............	SS	SS
2. Joining materials (bolts, etc.)...	--	--
II. Eddy Current Shields	--	--
III. Magnet Dewars		
A. Inner Wall	Austenitic SS	Austenitic SS
B. Insulation	Aluminized Mylar	Aluminized Mylar
C. Outer Wall	Austenitic SS	Austenitic SS
D. Thermal Shields		
1. Within insulation space...........	Copper W/LN piping	Copper W/LN pipin
2. Nitrogen jacket..................	--	--
IV. Support Structure		
A. Magnet to Dewar Inner Wall	SS tendons 304L	SS tendons 304L
B. Dewar Inner Wall to Outer Wall		
C. TF Coil Central Support	--	--
D. External Support Structure (warm)	Concrete	Concrete

Appendix B. Project Information Sheets

The sheets in this appendix are summaries of the work sheets which we used in our project evaluations. They are included here by laboratory. The units used are those listed by the original report. The sheets cover each major component of the cold magnet system and give a description of the material chosen as well as information on the component environment. In many instances a listing of the data which we feel is required for the material in this application is given. In a lesser number of cases possible alternate materials are described.

ARGONNE NATIONAL LABORATORY

Component: TF Conductor Composite - Conductor
Project: ANL - EPR (1976)
Function: Carry current
Description: NbTi filaments
Requirements:
 Critical current = 0.70-2.5×10^5 A/cm^2 @ 10 - 3 T field @ 3 K
 Operational current = 60 kA/turn
 Total conductor length/coil = 151×10^6 A·m
 Smallest radius of curvature = 2 m @ 10 T field
 Ave. hoop force/turn = 133×10^3 lbs
 Ave. turn cross-section = 40.6 cm^2
 NbTi cross-section = 1.2 - 0.3 cm^2/turn
 NbTi volume/coil = 0.267/m^3
 Radiation: large doses of 10^{18} n/cm^2 reduce I_c by 10-15%
 Forces: gravitational (bottom) - 208 tons weight
                 D straight section - 8 ksi compression

Component: TF Conductor Composite - Stabilizer
Project: ANL - EPR (1976)
Function: Carry full current if conductor goes normal
Description: Copper wire and copper sheet
Requirements:
 Cryostatic stabilization
 Average stress = 14.5 ksi in wire
 Radiation-induced resistivity saturates at 3×10^{-7} Ω cm
 Radiation-induced resistivity of 6×10^{-4} Ω cm with 1 MW-yr integral
   wall loading
 Using safety factor of 2.5, designed to 1.5×10^{-8} Ω cm
 If 0.5 MW/m^2 wall loading and 50% capacity factor, 4 yrs to reach
   1.5×10^{-8} Ω cm, radiation removed if warmed to 300 K
 Copper thickness/turn = $0.46 \rightarrow 0.23$ cm/turn
 Copper volume/coil = 6.82 m^3
 Sheet $\simeq$ 30 to 50 cm wide and 0.43 cm thick
 Other forces: gravitational (bottom) - 208 tons weight
                 D straight section - 8 ksi
Data Required: Magnetoresistivity as a function of radiation, purity, stress and cold work.

Component: TF Conductor Composite - Strengthener
Project: ANL - EPR (1976)
Function: Carry conductor load
Description: Stainless steel strip
Requirements: Average stress = 26 ksi, stainless steel/copper ratio = 1.5,
smallest radius of curvature $\sim$ 2 m, thickness varies from 0.31 cm/turn
at 10 T field to 0.54 cm/turn at 3 T field, width varies between 30 to 50 cm.
    Forces: gravitational (bottom) - 208 tons weight
             D straight section - 8 ksi compression

Component: TF Conductor Composite - Potting
Project: ANL - EPR (1976)
Function: To grip conductor to copper sheet stabilizer
Description: SnPb soft solder
Requirements: Cu/NbTi conductor is pretinned, then soft-soldered to
copper sheet.
    Forces: gravitational (bottom) - 208 tons weight
             D straight section - 8 ksi compression

Component: TF Conductor Composite - Electrical Insulators
Project: ANL - EPR (1976)
Function: To electrically insulate conductors, turn to turn
Description: Wetted fiberglass-epoxy strip
Requirements: Thickness of 1 mm, width of 1 cm, covers 50% of conductor
area, electrical insulation, turn to turn, for 1 mm thick is $\sim$ 200 V.
Cure of 150-200° F needed for prepreg, aromatic-type curing agent.
    Radiation: thought to degrade at 10^9-10^{10} rads designed to receive
                3.5×10^8 rads at 2.5 MW-yr/m^2.
Data Required: Influence of radiation; compressive strength (4 K), thermal
conductivity, specific heat, thermal expansion, electrical properties
(300-4 K).

Component: TF Conductor Composite - Electrical Insulators
Project: ANL - EPR (1976)
Function: Reduce ac losses, insure magnet charging
Description: Formvar coating on conductor
Requirements: Not discussed
Data Required: Influence of irradiation

Component: TF Cryostat - Coil Form
Project: ANL - EPR (1976)
Function: Support conductor
Description: Stainless steel containment case
Requirements:
    AISI 316 plate
    Thickness of 1.25 cm
    Width of 68-104 cm, height of 68 cm, length in D shape about 36 m
    Strengthening rib to divide case allows use of 1.25 cm thick stain-
less, instead of 2.5 cm thick plate.
Data Required: Weld specifications

Component: TF Cryostat - Coil Form Electrical Insulation
Project: ANL - EPR (1976)
Function: Electrically insulate coil form from radiation assembly
Description: NEMA Grade G-10 or micarta sheet
Requirements:
      Sheet thickness = 1 cm
      Grooved sheets for LN_2 channels for venting
Data Required: Tensile, compression (4 K), electrical and thermal (4 K),
irradiation effects, purchase specifications, joining to stainless steel.

Component: TF Cryostat - Eddy-current Shield
Project: ANL - EPR (1976)
Function: Shield conductor components from pulsed magnet fields
Description: Aluminum-stainless composite panels
Requirements:
      RRR aluminum $\sim$ 5000 (2 x 10^{-11} Ω-cm at 4 K in 4 T field, 5 x 10^{-11} Ω-cm
at 18 K in 4 T field.
      Operating temperatures vertical D-coil section = 3, 4.2 K, 3-10 T
and peak fields: outside D-coil section = 12.5-23.5 K; 1.5-5.0 T with
0.5 T ac field
      Thickness of aluminum at vertical D-coil section = 4 cm, stainless
= 0.25 cm
      Thickness of aluminum at outside D-coil section = 5 cm, stainless
= 1.0, 0.25 cm
      Aluminum explosively joined to stainless (estimated stainless stress
= 60 ksi, aluminum strain = 0.17)
Data Required:
      Joining techniques
      Irradiation effect on electrical resistivity
      Composite, aluminum-base exploritation
      ac losses = 18 K portion = 8.5 KW/coil
                   3 K portion = 0.3 KW/coil

Component: TF Cryostat (Outer section) - Insulation: Shield to
outside wall
Project: ANL - EPR (1976)
Function: Thermal insulation of aluminum shield
Description: Superinsulation in vacuum
Requirements:
      Radiation loss 300 K wall to 18 K shield = 64.5 W/coil
      Multiple layer superinsulation
      Thickness = 3.5 cm
Data Required: Effect of radiation on superinsulation

Component: TF Cryostat (Outside section) - Outside wall
Project: ANL - EPR (1976)
Function: Enclose coil and provide support
Description: Aluminum alloy plate casing
Requirements: Aluminum alloy plate, 3.5 cm thick

Component: TF Coil Cryostat (Vertical section) - Support: Shield to OH coil
Project: ANL - EPR (1976)
Function: To absorb compressive stresses from D coils
Description: Stainless steel cylinder
Requirements: Approximate 4 m diameter stainless steel/cylinder with thickness of 22 cm.
     Load on cylinder = 8.6×10^5 lbs.
     Circumferential stress $\simeq$ 60 ksi
     Compressive stress $\simeq$ 7.7 ksi
Data Required: Thick-section processing and welding of stainless steel mechanical properties of welds (4 K)

Component: TF Coil Cryostat (Vertical section) - Insulation: Support to OH coil
Project: ANL - EPR (1976)
Function: Electrically insulate OH coil from support cylinder
Description: Cylinder
Requirements: Probable NEMA G-10 sheet, thickness = 5 cm.
Data Required: Compressive strength at 4 K, effects of irradiation, electrical and thermal properties under load.

Component: TF Coil Cryostat (Vertical section) - Insulation: OH coil to LN_2 shield
Project: ANL - EPR (1976)
Function: Thermally insulate OH coil from LN_2
Description: Vacuum and superinsulation layer
Requirements: Superinsulation thickness $\simeq$ 0.5 cm, vacuum spacing = 2.5 cm.
Data Required: Effects of irradiation

Component: TF Coil Cryostat (Vertical section) - Inside cylinder
Project: ANL - EPR (1976)
Function: Structural support on inside for double-walled dewar
Description: Aluminum alloy inner dewar wall cylinder
Requirements: Aluminum alloy vacuum wall thickness = 3.5 cm at 300 K
Data Required: Thick-section welding procedures

Component: TF Outside Support Structure - Coil to Coil
Project: ANL - EPR (1976)
Function: Provide support for coil-to-coil torque loads
Description: Composite support panels
Requirements:
     Operate within TF cryostat at 4 K
     Positioned along outside perimeter of D-coils
Data Required: Compressive and fatigue properties at 4 K of fiberglass-epoxy composites, thermal expansion and specific heat (4-300 K).

Component: TF Outside Support Structure - Support Cylinder to Floor
Project: ANL - EPR (1976)
Function: Carry gravitational forces through temperature gradient
(4-300 K)
Description: Composite cylinder
Requirements:
      Temperature gradient (4-300 K)
      Load of 8.5 x 10^5 lbs (assuming 1/2 of total TF coil load)
      Glass-reinforced epoxy material
Data Required:
      Compressive properties (4-300 K)
      Thermal conductivity (4-300 K) under load of FRP
      Creep, fatigue properties (4-300 K) of FRP
      Thermal expansion, specific heat (4-300 K) of FRP

Component: OH/EF Conductor Components - Conductor
Project: ANL - EPR (1976)
Function: Carry current to produce magnetic field
Description: NbTi filaments
Requirements:
      Wire diameter $\simeq$ 0.3 mm
      Basic strand Cu/NbTi ratio = 2 to 1
      Overall Cu/NbTi ratio = 11 to 1
      NbTi cross-sectional area = 2.3 x 10^4 cm^2
      Operate at 4.2 K, pool boiling
      $I_c \simeq$ 117 KA/cm^2, basic strand carry 27 A
      Basic strand 1171 filaments, 5 μ filament diameter

Component: OH/EF Conductor Components - Stabilizer
Project: ANL - EPR (1976)
Function: To carry current if superconductor locally goes normal
Description: Cu wire and CuNbTi strands
Requirements: Cu wires of 0.3 mm diameter interwoven with Cu/NbTi (2 to
1 strands to produce Cu/NbTi ratio of 11 to 1. Operate at 4.2 K, cryo-
static stabilization.
Data Required: Magnetoresistance and magnetothermal conductivity of oxygen
free Cu under stress. Effect of purity on final RRR of oxygen free Cu
fatigue strength.

Component: OH/EF Conductor Components - Strengthener
Project: ANL - EPR (1976)
Function: Provide strength to conductor composite
Description: Stainless steel or cold-drawn Cu wire
Requirements:
      For large hoop stress: 1.2 mm diameter stainless steel wire
      For small hoop stress: 1.2 mm diameter cold drawn Cu wire
      Cu and Cu/NbTi strands woven on strengthener; this cable will carry
270 A at 5 T.
Data Required: Fatigue strength of stainless and cold drawn Cu at 4 K.

Component: OH/EF Conductor Components - Potting
Project: ANL - EPR (1976)
Function: Provide structural stability to Cu and Cu/NbTi strands
Description: Soft solder
Requirements: Soft solder, high resistivity, will be used to join strands with structural-reinforcing wire.
Data Required: Shear strength at 4 K.

Component: OH/EF Conductor Components - Electrical Insulator
Project: ANL - EPR (1976)
Function: Provide strand to strand electrical insulator
Description: Coating on Cu/NbTi strands
Requirements: Not discussed
Data Required: None

Component: OH/EF Conductor Components - Electrical Insulation
Project: ANL - EPR (1976)
Function: Provide turn-to-turn electrical insulation
Description: NEMA Grade G-10 wetted strip
Requirements:
      Strip - 2 mm thick, 2 cm wide, covering 2/3 area of cables
      Wetted, must be heated to 150-200° F for setting
Data Required: Electrical and mechanical properties at 4 K

Component: OH/EF Cryostat - Supports
Project: ANL - EPR (1976)
Function: Provide internal support about coil form
Description: Inner and outer internal FRP supports, separated by permeation barrier.
Requirements: Must have high electrical resistivity to reduce ac losses and good strength. Stainless steel permeation barrier to reduce helium permeability.
Data Required: Tensile and fatigue strength at 4 K, joint behavior at 4 K, need for permeability barrier.

Component: OH/EF Cryostat - Insulation
Project: ANL - EPR (1976)
Function: Thermal insulation between 300 and 76 K
Description: Multi-layer insulation
Requirements: Reflective coatings must be segmented, designed to minimize eddy-current heating. Used in vacuum.
Data Required: Proper design of multi-layer insulation to minimize eddy-current losses.

Component: External Support Structure
Project: ANL - EPR (1976)
Function: To support magnets and forces between beam-panel structure
magnets
Description: 7075 aluminum alloy
Requirements:
     Use 7075-T6 aluminum alloy, bolted together.
     McDonnel-Douglas study selected this alloy - comparing many, but
excluding normal plate steel.
     Design with allowable stress level either 0.6 tensile yield, 0.4
tensile strength (shear), and 0.6 tensile yield for buckling.
     Fatigue allowable for 7075 at 10^6 cycles is about 0.6 tensile yield.
Data Required: None

Component: Conductor Components - Conductor
Project: LLL - MX (1976)
Function: Carry current to produce magnetic field.
Description: NbTi filaments
Requirements:
      Current density - 3400 Al cm^2
      Maximum field = 7 - 5 T
      Conductor design current = 6.8 kA
      Conductor mass, both coils = 60 x 10^3 kg
      Cu/NbTi conductor $\simeq$ 6 x 6 mm square cross-section
      Operate at 4.2 K, cryostatic stability

Component: Conductor Component - Stabilizer
Project: LLL - MX (1976)
Function: Carry current in event superconductor goes normal
Description: Cu wire and sheet
Requirements:
      Superconductor element has Cu/NbTi ratio of 1-1.5 to 1.
      Other 3 quadrants of conductor are OFHC Cu, therefore, the
         overall ratio of Cu/NbTi $\simeq$ 8 to 1.
      Conductor I^2R loss = 1.9 W/cm
      Cooling surface = 5.3 cm^2/cm
      Required heat transfer rate = 0.36 W/cm^2
      Total conductor mass is 30,300 Kg
Data Required: Cu magneto-electric and thermal properties.

Component: Conductor Component - Potting
Project: LLL - MX (1976)
Function: To hold 4-segments of conductor together
Description: Soft solder
Requirements:
Data Required: Shear strength at 4 K

Component: Conductor Component - Electrical Insulation
Project: LLL - MX (1976)
Function: Electrically insulate between turns.
Description: Discs of NEMA Grade G-11
Requirements: Discs - 1 mm thick, about 1 cm diameter to be joined together
to prevent migration. NEMA Grade G-11 will probably be used. Maximum
compressive stress = 6 ksi. Voltage about 1 KV.
Data Required: Compressive and dielectric properties at 4 K.

Component: Conductor Component - Electrical Insulation
Project: LLL - MX (1976)
Function: To electrically insulate between layers
Description: NEMA Grade G-11 sheet
Requirements: NEMA Grade G-11 sheet - 2 mm thick. Sheets separated to
provide cooling channels. Maximum compressive stress = 6 ksi. Voltage
about 1 KV.
Data Required: Compressive strength at 4 K. Dielectric breakdown under
stress.

Component: Yin-Yang Cryostat
Project: LLL - MX (1976)
Function: Structural support
Description: Casing for magnet windings
Requirements: Casing thickness about 3 inches thick of 21/6/9 stainless steel. Reinforced in some areas. Forces on casing are between -1.25 to 27.7 x 10^6 lbs. Maximum design stress, combined, = 50 ksi. 300,000 lbs needed for magnets. (Baseball operates at combined design stress of about 15 ksi.)
Data Required: Properties of thick-section welds at 4 K. Thick-section processing and welding specifications.

Component: Conductor and Coil Form for Poloidal Field Coils
Project: ORNL - EPR
Function: Provide the primary flux swing that establishes the plasma current; the vertical fields that stabilize the plasma position in the TF coils and the magnetic fields that determine the shape of the plasma cross-section.
Description: The PF coil systems consists of the shield-vertical field (S-VF) and decoupling coils (resistive-coils), the trim vertical field (T-VF) coils and the ohmic heat (OH) coils. The conductor for the T-VF and OH coils is a round bundle of 37 strands of NbTi superconductor in a Cu stabilizer with CuNi eddy current barrier. The strands are transposed, enclosed in a stainless steel tube, and surrounded by an insulating matrix. The conductor has a rectangular cross-section measuring 4 x 4.44 cm and is wound on a fiberglass coil form.
Requirements: The OH coils in the central solenoid sustain the highest fields (7 T), the largest rate of field change (7 T/s) and the largest field swing (-7 T to + 7 T). The principal requirements for these coils are to minimize eddy-current losses and to remove the heat produced by these losses. The conductor bundle must be sufficiently flexible to permit wrapping the central solenoid and strong enough to sustain an average hoop stress of 12,500 psi. The rectangular cross-section insulating matrix must be able to tolerate the radiation environment.
Data Required: The mechanical, thermal and electrical properties of the insulating matrix and GFRP coil forms should be characterized along with the effects of radiation and fatigue on these properties.

Component: Conductor and Coil Form for TF coils
Project: ORNL - EPR
Function: Produces plasma confining field
Description: Four conductors are simultaneously wound in parallel, insulated and enclosed in L-shaped stainless steel segments that are welded to each other and to the coil case. Each conductor consists of 93 triplex strands (2 superconductor composite wires and 1 Cu or Al wire all soldered together) encased in an Al alloy conduit. Nb_3Sn and NbTi are used for high field and low field regions of the magnets, respectively.
Requirements: The 93 strands within the conduit must permit cooling by the forced-flow of supercritical helium. The conductor/conduit assembly must be sufficiently flexible to permit winding into a coil that is tight enough to resist movement when the coil is energized. The insulation surrounding the four parallel conductors must survive the welding operation used to enclose the conductors in stainless steel. The stainless steel is stressed to 45 ksi. The maximum field at the winding is 11 T at a current density of 6200 A/cm^2.
Data Required: Properties of the welds (laser welding suggested by ORNL) used to join the L-shaped stainless reinforcement without damaging the insulation should be determined.

      The thermal and mechanical properties of the solder, the Al alloy for the conduit and the stainless steel structural elements and weldments need to be characterized.

      Mechanical properties of the thick-section stainless steel weldments used for the coil form must be determined.

Component: Normal EF Coils
Project: GA - EPR
Function: Plasma field shaping
Description: Electrical tough-pitch copper, water-cooled. Each conductor
5 x 5 cm, insulated either with fiberglass-epoxy or with oxides or sili-
cates (mica) if radiation is a problem. Located inside TF coils. Total
of 22 coils of 155 turns each, segmented into 6 sections each, bolted
together. Welded steel casing on each coil. Aluminum also considered
but rejected for EPR because of larger volume required. May be used on
larger reactors. Specifications require 2 KV turn-to-turn and 100 KV
layer-to-layer insulating capability.
     Superconducting coils are likely to be used in commercial plants.
Dynamically-stabilized Nb_3Sn would be required along with improved shield-
ing by the blanket.
Alternate Materials: None
Data Required: Properties of thick-sections of Al and Cu as affected by
irradiation.

Component: Superconducting TF Coil Composite
Project: GA - EPR
Function: Plasma driving
Description: NbTi in copper matrix. Stainless steel strip interleaved
with conductor.
Requirements: Maximum magnetic field in TF coils is 8 tesla, 4 tesla
at plasma major radius. May use either Nb-45% Ti or Nb-55% Ti, (over
atomic fraction Ti for higher fields. Either copper or aluminum could
serve as stabilizing materials; the lesser magnetoresistivity of aluminum
being an advantage. Nb_3Sn is rejected due to inferior state of develop-
ment and necessity to restrain larger forces at higher fields. Con-
ductor is monolithic with about 1060 200 µm diameter NbTi filaments.
Conductor is jacketed by copper stabilizer and bonded to S.S. strength-
ener. Of 17 radial conductor layers, 3 nearest plasma are of 8.0-T
grade, next three are 7.1-T grade and remaining 11 are 5.7-T grade.
Alternate Materials: None
Data Required: Radiation effects on NbTi and Nb_3Sn conductors.

Component: Superconducting OH Coil Composite
Project: GA - EPR
Function: Ohmic heating of plasma
Description: NbTi interwoven with stainless steel to form a braid.
The central solenoid would be wound on a glass-epoxy spool and prestressed
by 2.5 mm thick stainless steel bands on the outside of the cable. The
coil would be prestressed vertically and radially. AC losses sustained
at solenoid ends are reduced by subdividing the stainless reinforcing
bands into ribbons. Internal pressure from the radial magnetic load
would be about 13.2 MPa (1900 psi) along most of the OH SC solenoid,
increasing 30% at the ends. Magnetic loading reduces the compressive coil
stress to 3.6 MPa (530 psi) and increases the tensile load on the stain-
less bands by 109 MPa (15.8 ksi) to a maximum overall stress or 226
MPa (32.8 ksi).

They originally considered normal water-cooled coils of semi-hard ETP copper each conductor 5 x 5 cm square. Each turn typically 20 x 40 cm reinforced with adjacent prestressing belt of high-strength steel. Insulation to withstand 500 V conductor to conductor, 2 KV turn to turn and 100 KV layer to layer. Insulation not stated - probably same as EF coil, glass-epoxy or mica. Most of the OH turns are inside the central bore with several at outer periphery of the torus. Aluminum could replace copper in large reactors.

Alternate Materials: None

Data Required: Properties of thick sections of Cu and Al for normal coils.

Component: Superconductor Stabilizer
Project: GA - EPR
Function: Superconductor stabilization
Description: OFHC copper is specified for EPR due to availability; however, aluminum is an acceptable alternative, superior to copper at cryogenic temperatures due to lower magnetoresistivity. Copper stabilizer must withstand total fluence of 10" n/cm^2-sec at inside of TF coil (year operation) and integrated fluence of 2×10^{18} n/cm^2 without excessive resistivity increase. Radiation-induced resistivity changes in stabilizer will most likely dictate acceptable radiation levels. Limited data indicate this fluence will reduce the critical current density by 10%, recoverable 70% by 300 K annealing. May be a problem in a commercial reactor, but not in EPR due to frequent warm-ups. Stresses on the copper stabilizer are 76.4 MPa (11 ksi) compared to the 85 MPa (12 ksi) at which increased resistivity is noted.

Alternate Materials: Filamentary or dispersion strengthened copper or aluminum to increase the strength without increasing the resistivity.

Data Required: Effect of 4.2 K neutron irradiation and of strain on the resistivity of copper and aluminum of purities suitable for stabilization. Exploratory work on reinforced high-conductivity Cu and Al.

Component: Strengthening Material - Superconducting Coils
Project: GA - EPR
Function: Resisting static and cyclic forces on superconductor
Description: A stainless steel support structure encloses the superconductors in the TF coils to resist the Lorentz conductor force resulting from the TF coil current and torrodial magnetic field. Calculated 134.9 MPa (21.6 ksi) stress carried by the stainless steel to reduce the stress in the copper stabilizer to values below that causing resistivity increases (85 MPa, 12.3 ksi). Also, an austenitic stainless steel strip is interleaved with the NbTi conductor in the TF coils. The operating stress in the reinforcement is calculated to be 198 MPa (28.7 ksi). Associated stress in the stabilizer is given at 112 MPa (16.2 ksi) - at variance with the maximum value given above but perhaps reflecting preliminary thinking.

Conceptual design of a superconducting OH coil postulates NbTi interwoven with stainless steel to form a braid. The central OH solenoid is prestressed to 117 MPa (17 ksi) by 2.5 mm thick stainless bands on the outside of the cable. The bands are subdivided into ribbons at the solenoid ends where higher AC losses are sustained. Magnetic loading increases the stainless stress to 226 MPa (32.8 ksi).

Alternate Material: Graphite or boron-reinforced composites might be used for banding, for interleaving with the conductor or for a structural form on which the conductor is wound.

Data Required: Fatigue of stainless steel at 4.2 K. Fatigue of graphite and boron-reinforced composites under irradiation at 4.2 K. Effect of Wigner energy release on the mechanical and thermal properties of composites.

Component: Electrical Insulation
Project: GA - EPR
Function: High-voltage breakdown barrier
Description: Polyethylene, mylar, reinforced epoxies and inorganic insulators mentioned as possible alternatives for the TF coil insulation. More specifically, the NbTi conductor is helix wound with 0.05 cm micarta spacers between adjacent turns and 0.10 cm thick glass-epoxy strips between radial layers covering half the surface area to form helium cooling passages. Space between the end TF coil windings and cryostat wall is filled with epoxy. Epoxy also used to insulate and to smooth the irregular exposed surface of the final layer which bears against the inner cryostat wall. No details on OH coil insulation in the superconducting variant.

Alternate Materials: Polyimide-matrix composites for probable superior radiation resistance.

Data Required: Mechanical and physical properties of organic insulators under neutron irradiation.

Effect of Wigner energy release on insulating properties of polymers and composites.

Component: Coolant Channel
Project: GA - EPR
Function: Superconductor cooling
Description: TF coils - coolant channel formed by 0.05 cm micarta spacers between adjacent turns and by 0.10 cm thick epoxy-fiberglass strips between radial layers covering half the surface of the helically-wound conductors.

OH coils - coolant flows through small radial grooves carved in the turn-to-turn spacers (material not given).

Alternate Materials: None

Data Required: Electrical properties of micarta, fiberglass epoxy, etc., at 4 K under fatigue and radiation.

Effect of release of Wigner energy on the probability of coolant channel blockage by composite breakup.

Component: Coil Form - OH Magnet
Project: GA - EPR
Function: Support of ohmic heating coil
Description: 15.3 m high, 2.75 m o.d., 1.95 m i.d. epoxy-fiberglass
spool inserted into central bore formed by mating of straight sections
of TF coil cryostats. Subjected to prestress both vertically and radially
by stainless straps pressing on NbTi conductors. Maximum radial com-
pressive stress 22 MPa (3,200 psi) reducing to 3.6 MPa (530 psi) when
coil is operated. Spool sees axial torque producing shear stress of
about 1 MPa (140 psi) with 1° angular deflection. Will see fatigue, but
analysis for 500,000 cycles at 4 K indicates no problem. Prestressing
expected to compensate for differential thermal expansion coefficients
during cooldown. Vertical prestressing by steel bolts through a top
fiberglass cap and penetrating the fiberglass core. Axial compressive
stress 376 MPa (40,000 psi), coil form (and coil) shrinks 2 mm. Energizing
coil reduces axial stress to 2.9 MPa (420 psi). Epoxy-fiberglass coil
form is selected to minimize ac losses.
Aternate Materials: Kevlar or graphite-reinforced polymer composites.
Data Required: Mechanical, thermal, electrical properties of thick section
fiberglass at 4 K including fatigue, thermal cycling effects and radiation.
        Feasibility of replacing solid composite section with web of a higher
modulus composite. All above data required.

Component: Inner Wall - Magnet Dewars
Project: GA - EPR
Function: Vacuum containment, helium containment
Description: OH coil helium pressure vessel made of glass-epoxy to
prevent ac losses from occurring at 4.2 K at the ends of the OH solenoid
where variable magnetic flux crosses the dewar (cryostat) wall. Negligi-
ble outgassing expected due to low temperatures. Inner dewar wall of TF
coil is austenitic stainless steel.
Alternate Materials: Glass-polyimide, Kevlar- or graphite-epoxy or polyimide.
Data Required: Permeability of composites to helium at 4.2 K. Effect of
irradiation on permeability at 4.2 K. Composite-metal joints at 4.2 K.
Possible permeability barrier development.

Component: Magnet Dewar Insulation
Project: GA - EPR
Function: Reduce thermal losses.
Description: OH dewar uses superinsulation (multilayers). Laminar
insulation in TF coil dewar.
Alternate Materials: 3-D reinforced form if thermal short is used in
the dewar.
Data Required: Radiation effects on thermal and mechanical properties.

Component: Magnet Dewar Thermal Shields
Project: GA - EPR
Function: Minimize radiation losses.
Description: OH coil: liquid nitrogen cooled shield located in vacuum
region between outer wall and helium container, no material stated.
        TF coil: 0.5 cm copper thermal radiation shield cooled by gaseous
helium at 77 K.

Alternate Materials: None
Data Required: Effect of radiation at 77 K on thermal conductivity of shield materials.

Component: Outer Wall - Magnet Dewar
Project: GA - EPR
Function: Vacuum containment, warm structure
Description: Stainless steel in all dewars. The TF dewars see an average bearing stress of 28.6 MPa (3,900 psi) from the centering forces on the straight sections of the coils.
Alternate Materials: Aluminum, FRP
Data Required: Outgassing of FRP candidates under irradiation.

Component: Support Structure - Cold-to-Cold
Project: GA - EPR
Function: Contain electromagnetic forces, dewar supports.
Description: Magnet to dewar inner wall: fiberglass-epoxy or ceramic standoffs covering less than 1% of dewar surface area support the inner dewar walls from the TF coil cryostat. The space between the TF coil and the cryostat wall is to be filled with epoxy to assure a uniform bearing surface for transferring large conductor forces to the cryostat.
     Magnet-to-magnet: out of plane loads on TF coils due to pulsed poloidal fields are resisted by tie rods between the coils and contained in the TF coil dewar. Four or five rods between adjacent magnets. Referred to as hollow cylinders 50 cm o.d. and 40 cm i.d., no material specified. Maximum cyclic stress is less than 140 MPa (20 ksi) so stainless, aluminum or composites are candidates.
Alternate Materials: Advanced composites if design requires excellent fatigue life under high compressive stress at 4.2 K.
Data Required: Cyclic fatigue at 4.2 K under irradiation - all materials composite-metal joints and fatigue performance at 4.2 K.

Component: Support Structure - Cold-to-Warm
Project: GA - EPR
Function: Thermal standoff structural support transitioning from 300 K through the magnet dewars to the magnet coils.
Description: Primarily gravity support for TF coil. Alternatives are ceramic wafers in compression, a long hollow cylinder loaded in tension or a long "bicycle chain" loaded in tension. Example given of two stainless steel pipes, 18 cm i.d., 20 cm o.d., 100 cm long.
Alternate Materials: Industrial laminates, GPRP or advanced composites.
Data Required: Radiation effects on creep of metal supports. Radiation effects on long term strength (aging effects) of composites.

Component: TF Coil Central Support
Project: GA - EPR
Function: Support of OH solenoid
Description: Central bore formed by butting together tapered sections
of the TF coil cryostats. OH coil and dewar placed inside bore,
apparently supported by a warm structure in contact with the OH dewar
walls. No distinct, load-bearing cold central support column is used.
Alternate Materials: None
Data Required: None

Component: EF Coils
Project: GA - DFPR
Function: Plasma field shaping
Description: Normal EH coils were selected for the initial conceptual
design but consideration was also given to superconducting coils.
     Normal coils: similar to the EPR design, copper, water or oil cooled.
Anticipate radiation damage will require annealing at about 300°C at regular
intervals. Expect 10% increase in resistivity for neutron dose of 6 x
10^{20} n/cm^2 at 80°F. 20 MPa (2900 psi) maximum stress on conductor. 32
coils, 150 turns of 5 x 5 cm conductors. Total copper weight 3576 metric tons.
     Superconducting coil: Also 32 coils, NbTi superconductor with 2-
component Cu/CuNi stabilizer. Superconducting composite 0.5 mm diameter,
braided. Current density maintained less than 90% of NbTi critical current
at 5.2 K based on radiation damage and combined toroidal and poloidal field
strengths at the coil. Stress on superconducting composite kept below
83 MPa (12 ksi) so added reinforcement is not needed. Low ac loss construc-
tion. Conductor is force-cooled inside thin 0.05 cm stainless steel casing.
Alternate Materials: Nb_3Sn
Data Required: None

Component: TF Coil Conductor Composite
Project: GA - DFPR
Function: Plasma driving magnet coil
Description: Monolithic NbTi/Cu composite, 100 kA conductor current,
cryostatic stabilization. Conductor spirally wrapped around thin 120 cm
wide, 0.275 cm thick OFHC copper strip which provides added stabilization.
14,000 NbTi filaments, 0.0175 cm diameter required for 100 kA and 30
kA/cm^2.
Alternate Materials: Nb_3Sn conductor, aluminum stabilizer.
Data Required: None

Component: OH Coil Conductor
Project: GA - DFPR
Function: Plasma ohmic heating
Description: NbTi with Cu/CuNi stabilizer braided into cable with stain-
less steel wire reinforcement. Average stress on the OH solenoid is
92.7 MPa (13.4 ksi). Design concept same as in EPR.
Alternate Materials: Nb_3Sn conductor, graphite-epoxy filaments replacing
stainless steel for higher modulus, higher strength and reduction of
electrical shorting problems.
Data Required: Feasibility study of braiding conductor with graphite
epoxy reinforcement.

Component: Superconductor stabilizer
Project: GA - DFPR
Function: Cryogenic stabilization or conductor
Description: Two component Cu/CuNi stabilizing matrices are used in the
OH coils and in the EF coil if the latter is superconducting. Both use
braided cables. The monolithic conductor for the TF coil apparently uses
only copper for stabilization. The monolithic conductor is inset into a
copper stabilizing element and the resulting conductor is spiral wrapped
around an OFHC copper strip 120 cm wide, 0.275 cm thick which adds addi-
tional stabilization. Apparently, this layer stabilization is required
for the 100,000 amp conductor rating.
Alternate Materials: Aluminum; fiber or dispersion-strengthened copper
or aluminum.
Data Required: Feasibility study on strengthening copper and aluminum
while maintaining conductivity.

Component: Strengthener for Superconducting Composite
Project: GA - DFPR
Function: Relieve stress on the superconductor
Description: OH Coil: Stainless steel wires intermixed with supercon-
ductor wires in the braided cables. Some indication of additional sup-
port in form of tube surrounding conductor bundle.
     TF Coil: Stainless steel interleaved between layers of the 100,000 A
conductor elements. Entire coil inside stainless steel helium vessel.
Alternate Materials: Graphite-epoxy strands replacing stainless wire for
improved strength, modulus and to reduce shorting problems. Interleaved
stainless in TF coil could be replaced by a high-modulus graphite-polymer
composite to achieve similar benefits.
Data Required: Combined effect of radiation and cyclic loading at 4.2 K
on the mechanical and electrical properties of graphite-polymer composites.

Component: Electrical Insulation
Project: GA - DFPR
Function: Electrical standoffs turn-to-turn, layer-to-layer, coil-support
Description: Conventional EF Coil: mica, data indicate little degrada-
tion of mechanical properties at doses to 10^{20} n/cm^2.
     Superconducting EF Coil: combination of mica and dry fiberglass
cloth for turn-to-turn insulation.
     Superconducting OH Coil: no information.
     Superconducting TF Coil: no information
Alternate Materials: Glass or linen-reinforced industrial laminates.
Data Required: Effect of release of Wigner energy during warmup on the
electrical properties of insulators.

Component: Coil Forms
Project: GA - DFPR
Function: Support of windings, perhaps electrical insulation function
Description: Superconducting TF Coil: stainless steel helium vessel
also serves as coil form.
     Superconducting EF, OH Coils: no information, probably same as EPR.
Alternate Materials: Composite materials for coil form of OH coil.
Data Required: Effect of irradiation, cyclic loading and release of
Wigner energy on structural and electrical integrity of composites.

Component: Eddy Current Shields
Project: GA - DFPR
Function: Reduction of ac losses due to pulsed coils.
Description: Aluminum at 15 K proposed as magnetic flux shield sur-
rounding TF coils. Time constant of shield must be long compared to
poloidal field flux swing and long compared to shield hysteretic losses.
Alternate Materials: Copper, fiber-reinforced aluminum or copper to
resist electromagnetic stresses.
Data Required: Effect of 4.2 K radiation on electrical properties of
reinforced and unreinforced copper and aluminum.

Component: Magnet Dewars and Cyostats
Project: GA - DFPR
Function: Thermal insulation of superconducting coils
Description: TF coil dewar must be remotely opened for reactor mainte-
nance. No material discussion, selection would be similar to the EPR
(stainless steel plus a non-metallic inner dewar wall for superconducting
OH coils).
Alternate Materials: Aluminum
Data Required: Helium permeability of non-metallic composites as a func-
tion of temperature from 4.2 K and as affected by irradiation including
release of Wigner energy on warmup.

Component: Support Structures
Project: GA - DFPR
Function: Resistance to electromagnetic and gravitational loads.
Description: TF coil gravity support: Fiberglass cylinder with length
greater than its cross-sectional area. A stainless steel ball joint on
cold side provides limited radial coil movement.
    Central support cylinder: In contrast to EPR, DEMO uses a 25 cm
thick support cylinder which also provides partial gravity support for
the TF coils. Material not stated, but cross-sectional drawings imply
glass-reinforced epoxy. Centering force on cylinder given as 36,800
MT per coil.
    Out-of-plane loads: Resisted by circular tie rods between adjacent
TF coils enclosed in common TF coil dewars. Structural fatigue is a major
concern. No material stated.
Alternate Materials: Stainless steel, high-modulus composites
Data Required: Properties of thick-wall glass-epoxy including irradiation
effects and aging effects under sustained loading (creep). Fatigue
behavior of stainless steel and composites under irradiation at 4 K
including Wigner energy release damage to composites.

UNIVERSITY OF WISCONSIN

<u>Component:</u>   Superconductor composite for TF coils
<u>Project:</u>   UWMAK I, II and III and TETR
<u>Function:</u>   Produces toroidal field
<u>Description:</u>   NbTi with copper stabilizer (I and II).
NbTi in copper surrounded by pure aluminum to stabilize (III and TETR).
<u>Requirements:</u> Mostly described in (I). Conductor is wound into a groove
in a disc. Maximum strain level allowed for the conductor is 0.002. It
occurs where the conductor crosses the disc and where it leaves the wind-
ing, both are low field regions. This system puts the copper into yield
but the resulting resistivity is acceptable. Prestress of the conductor
is not necessary; it happens when the magnet is activated. Maximum stress
levels in the copper of the conductor and the stainless steel of the coil
form were calculated for (I). They are:

<u>Magnet Condition</u>	Copper		S. S.	
	$N/m^2 \times 10^{-6}$	psi	$N/m^2 \times 10^{-6}$	psi
After assembly	0	0	0	0
After cool down	20.7	3,000	-20.7	-3,000
After magnetic loading	103.4	15,000	413.7	60,000
Cold after removing magnetic loading @ 3.83 T central field	-68.9	-10,000	68.9	10,000
After warm up to room temperature	-75.8	-11,000	75.8	11,000

The amount of superconductor is chosen so as to carry full magnet current
at 5.2 K. This maximum temperature is that which the magnet will reach
with all current in the stabilizer, in liquid helium with a heat transfer
coefficient of 0.4 W/cm^2 and edge cooling of windings. A large number
(34) of 10 kA superconductor joints are required in each coil. The
plan calls for lapping and clamping of conductor for 20 cm with a result-
ing maximum current path length in the copper of 0.5 cm. Joints are
located in low field regions and have a predicted resistance of 10^{-8} Ω
for a total heat loss of 376 W. There is no description of the solder
to be used.
    Neutron damage is expected to be negligible in the TF coils for all
designs except I and TETR. Damage levels in II and III are predicted
$\sim 10^{-8}$ dpa/yr. They indicate that 10^{-3} dpa is necessary to degrade I_c
by 10% in NbTi and 5×10^{-5} dpa is necessary to cause a 10% increase in
the resistivity of OFHC copper at 4 K. Radiation levels of this latter
order may occur in TETR. In I additional copper was provided as was a
regular schedule of annealing to handle the predicted 3×10^{-4} dpa/yr.
<u>Data Required:</u>
    Strain vs I_c characteristics of the conductors.
    The combined effect of stress and neutron damage on the resistivity
and magnetoresistivity of copper and aluminum.
    An estimate of the pulsed loads due to the poloidal fields is
needed followed by fatigue studies on the superconducting properties
of the composite.
    Thermal diffusivity of the conductor composite.
    Magnetic diffusivity of the conductor composite.
    Heat transfer coefficients.
    Stress and resistivity characteristics of joints.

Component: Superconductor composite for OH and EF coils
Project: UWMAK I, II and III and TETR
Function: Produces the plasma driving field, the stability and
director fields.
Description: NbTi/Cu/CuNi composite strengthened with either cold
worked copper or stainless steel in I, II and III. Cryogenically cooled
(20 K w helium) pure Al on a stainless steel backing for some TETR magnets.
Requirements: Stress effects are not as important as in TF coil design.
Effects due to the rapidly changing fields predominate. Details of the
separate designs are:
    (I) EF coils are outside TF coils. Depending on the particular
location of the coil, it uses Al or Cu or Cu-SS to provide strength and
stability. Yield strengths assumed are 4000 psi for aluminum and 12000
psi for copper. The coils are layer wound, edge cooled, pancakes. Struc-
ture of superconductor to eliminate ec effects pretty much ignored except
to say CuNi will be used along with fine, twisted and transposed filaments.
Rise time is 100 sec, dB/dt = .076 T/sec.
    (II) EF coils are inside TF coils. Eddy current shielding treated
in detail requires CuNi clad filaments to be transposed inside a copper
matrix! Very little stainless steel used in the coils. Rise time is
10 sec, dB/dt = .57 T/sec. Design stress levels depend on type of winding
but are well within reasonable limits. No specific neutron damage cal-
culations for these coils but the TF coil treatment indicates that they
do not expect a problem.
    (III) EF coils are inside TF coils. Three conductor types con-
sidered. A design much like LLL four components conductor. The conductor
component has the CuNi shielded superconductor in work hardened OFHC
copper for all designs. The other components are either work hardened
copper or 3/6 stainless steel depending on which conductor type is used.
Design stress at 4.2 K:

$$10\% \text{ cold reduced OFHC} = 1.24 \times 10^8 \text{ N/m}^2 \text{ (18 ksi)}$$

$$316 \text{ ss} = 2.11 \times 10^8 \text{ N/m}^2 \text{ (30 ksi)}$$

One conductor type allows 2.07×10^8 N/m^2 (30 ksi) in the copper and
3.5×10^8 N/m^2 (51 ksi) in the steel. The parts of the conductor are
soldered together on 50% of their adjoining surfaces. The use of the
higher resistivity, worked copper greatly reduces eddy current losses
(ρ = 1.86 x 10^{-10} Ω m @ 300 K, RRR = 110 at H = 0 and 30 at H = 9 T.
They point out that if one designs to 60% of yield stress for a Cu/SS
composite, the copper can be in yield. Rise time is 15 sec, dB/dt =
0.57 T/sec.
Data Required:
    All data listed for the TF coil conductor.
    Eddy current and hysterisis effects in the conductor.
    Electrical resistivity and thermal conductivity as a function of
stress for the various coppers and aluminum which have been proposed.

Component: Coil bond to TF coil form
Project: UWMAK I, II and III
Function: Hold coil in groove in stainless steel coil form.
Description: Epoxy, filled around B-stage FEP-wrapped conductor.
Requirements: Bonding failure will permit conductor motion during field
changes leading to frictional heating. Quality control is essential here.
Micarta spacers must provide a clamping action to stop the spread of a
crack.
      Compressive stress < 8000 psi but not stated.
      Threshold for observable radiation damage is 8000 M rads and 25%
degradation occurs at 50000 M rads thus they forsee no problem with
radiation effects on the mechanical properties. Because the coil is
wound into the form, each turn sees the maximum voltage to ground and
this can be as high as 10 kV (III-IV-A-9). The effect of radiation
is less certain here.
Data Required:
      Tensile and shear strength.
      Thermal contraction of metal to epoxy bond.
      Effect of radiation on electrical properties.
      Crack initiation and propagation.

Component: Spacers
Project: UWMAK I, II and III, all coils.
Function: To transfer loads between windings and to provide
cooling channels.
Description: Micarta spacers (linen phenolic)
Requirements:
      TF: Need to provide a clamping action to keep conductor epoxy
bond to the stainless steel form in good shape. Prevent cracks from
spreading through the epoxy.
      OH & EF: Micarta block spacers between pancakes. Whole structure
bolted together with Al bolts.
Data Required:
      Micarta is used in almost all low temperature magnet structures and
very little information has been gathered on its properties. All mechanical
and thermal tests are needed.

Component: Coil form
Project: UWMAK I, II and III and TETR
Function: Winding form for TF coil
Description: A series of pancakes grooved to accept the conductor.
Requirements: The TF conductor description sheet gives a complete
stress cycle. The solid pancake design is used because: electrical
connections can be easily made on the outside; internal heating due to
relative motion of conductor and coil form is minimized; stresses on
the insulation are low; coolant channels are stable; bolting is easy.
Forging, machining, heat treating and winding techniques are unknowns.
(I and II) To limit design strain to 0.2% in the copper stabilizer
requires the use of AISI 316 with a design stress of 4.14×10^8 N/m^2 (60000
psi). (III and TETR) allow 0.38% strain in the Al stabilizer and use Al
2219-T8T for the form. The design stress in the aluminum form is 3.11
$\times 10^8$ N/m^2 (45000 psi).

Data Required:
      Fabrication data appear to be most critical here
      Eddy current heating of the aluminum alloy could be significant
      Low temperature mechanical properties

Component: Insulation for dewars
Project: UWMAK I, II and III. Most detailed treatment is in II.
Function: Thermal insulation, not load-bearing
Description: Aluminized mylar (superinsulation)
Requirements: Will be subject to both neutron and gamma radiation.
(II) predicts a λ energy of 0.137 ev/DT neutron and 0.884 ev from the
neutron. The maximum exposure is 0.9 Rad/sec or 690 M Rad in 30 yrs.
They feel that actual levels may only be 10% of this (II-IV-H-57). The
threshold for damage is given as 30 M rads and a 25% decrease in tensile
strength occurs at 120 M rad.
Data Required: This is one of the most serious materials problems. Imme-
diate work is needed to determine the changes in thermal properties under
irradiation. There are indications that it may be much less radiation
tolerant than this design assumes.

Component: Magnet to outer dewar wall support
Project: UWMAK I, II and III, TF coils.
Function: Transfers lateral loads, i.e. those in the toroidal direc-
tion, from the magnet coil to the outer shell of the dewar when necessary.
Description: FEP struts
Requirements: If one magnet fails (I) those on either side would experience
a force > 8×10^7 kg tending to push them away from the failed magnet.
Smaller forces can occur in a normally operating system if exact symmetry
is not achieved.
      Cold supports are not practical - too many are needed to prevent shear
at micarta spacer - as stainless steel coil form interface.
      FEP struts are connected to outer dewar wall. 9 of 10 clear magnet
by 1 cm, the 10th makes contact. When magnet failure is detected (?),
external pistons drive all struts to full contact (see external support
structure IVD writeup). Wall at long strut is designed to deflect 1 cm
elastically. This involves use of a nonlinear conical spring cap which
must be lubricated to slide against outer dewar wall in a vacuum!
(II-III-A-21).
Data Required:
      Compressive stress of composites
      Spring material
      Thermal conductivity

Component: External support structure
Project: UWMAK, I, II and III, TF coils
Function: Keeps TF coils from moving laterally.
Description: A cylinder piston element, driven by gas or fluid, which
pushes the outer case of the dewar against the linear (reversibly) in the
case of loss of one coil. (II and III) use a continuous wall between the
TF magnets which serves as a secondary vacuum barrier as well as a support
for the coil system.
Requirements: A complex mechanical system
Data Required: No cryogenic parts

Component: Central support for TF coils
Project: UWMAK I, II and III, TF coils
Function: Supports weight of coils and radially inward force due to magnetic field interaction.
Description: A massive stainless steel or aluminum alloy cylinder to which TF coils attach.
Requirements: Supports TF coils by their straight sections.

Is cold, $\sim$ 4 K, and thus, must be isolated by a thermal barrier - not discussed in UWMAK design. The column also supports some of the OH and VF coils.

TF coils hang on with a shear beam-shear pin attachment. Shear stress is kept to < 1000 kg/cm^2 in pins. Also stress on welds attaching shear beam to magnet discs will be kept < 1000 kg/cm^2. Bottom shear beam does not have pins - used only for alignment.

When magnets are energized, the compressive force of magnets against the central support exceeds the outward radial tensile force on the upper shear beam. When unenergized, though, the total force will be $\sim$ 615 M tons.

More massive structure in (II) because D's are not constant tension and forces are larger and are often out-of-plane. Also there are radial outward forces now. Limits for II: 414×10^6 N/m^2 (60 ksi) in tension 207×10^6 N/m^2 (30 ksi) in shear. Shear pins ("high strength alloy") 345×10^6 N/m^2 (50 ksi), shear stress, will se 3.1×10^8 in shear and 3.9×10^8 in tension.

Forces on the central cylinder: effective internal pressure 1.24×10^8 producing a tangential stress of 2.9×10^8 and a radial stress of 1.24×10^8. There is also an axial force of 20.8×10^6 kg/magnet to be transferred to straight leg of magnet by the support beam resulting in a shear stress of 1.9×10^8 N/m^2.

(III) central cylinder is aluminum alloy and coils, which are smaller and lighter than the other two designs, are attached by a key system.

Data Required:
Mechanical and fatigue properties of welds and shear pin materials at low temperatures.

Eddy current heating in the cylinder.

The general problem of transfering forces from the TF magnets to the central column is one that needs a good deal of investigation.

Appendix C.   Research Capabilities

In the course of this survey a number of on-going, relevant low-temperature materials research programs have come to our attention. In addition a number of research laboratories which are interested in this program have been identified. This section lists these and briefly explains the type of research. We realize that we have probably missed some projects at the national laboratories and have not done justice to the many fine low temperature facilities at universities across the country with whom we have not come in contact - regarding this program. We urge any interested reader to call these deficiencies to our attention.

National Laboratories

Argonne National Laboratory (ANL)

Superconductor joining techniques: (J. Hafstrom)	ultrasonic welding - MHD magnets, NDE procedures for joints, acceptance criteria
Tensile, fatigue at 4 K: (E. Fisher)	effects of high cycle fatigue on critical current of Cu, Nb-Ti, and Nb_3Sn
Radiation of superconductors: (B. Brown)	studies (fission, CP-5 reactor) on Nb3Sn, intiated international conference on subject in 6/77

Brookhaven National Laboratory (BNL)

Dielectric tape development: (A. Muller)	hi-modulus polyethylene tapes for sc cable; electrical, thermal, mechanical property measurements on insulators for screening
Strain-insensitive sc conductors: (M. Suenaga, B. Sampson)	development of composite (Nb3Sn) permitting more strain
Thick epoxy castings: (A. McNerny)	large (10 ft x 1 ft-dia) castings, insensitive to thermal shock, to be used as insulators, matching thermal expansion of Al
Radiation of materials: L. Snead, A. Sweedler)	proton irradiation (30 Gev) of superconductors, glass-epoxies, and insulators

Los Alamos National Laboratory (LASL)

Electrical insulation: (P. Chowdhuri)	dc power transmission, consideration of cellulose paper and plastics -dielectric breakdown

Composite dewars: very large composite dewar per-
    (C. King)   formance and specifications for
                                                 energy storage program

Conductor testing: Nb_3Sn critical current testing,
    (R. Bartlett, D. Carlson)   effects of prestrain, acoustic-
                                                 emission monitoring

Lawrence Livermore Laboratories (LLL)

Superconductor development and testing: Nb_3Sn development, critical cur-
    (D. Cornish)   rent, stress measurements -
                                                 3000 A capacity

Welding, processing, specifications: research on 5083 Al and 21/6/9
    (P. Landon)   stainless steel for specifications
                                                 for use at low temperatures

Radiation: rotating target (14 Mev neutron)
    (D. Vandervoort, R. Scanlon)   irradiation of Nb-Ti, Cu, Nb_3Sn
                                                 and AISI 316 (300 K only)

Welding: weld rods and processes for
    (C. Witherall)   thick-section 21/6/9 stainless steel

Oak Ridge National Laboratory ORNL)

Solders: shear tests of variety of solders
    (A. Morehead)   for superconductor bonding, also
                                                 NDE-related research

Stress-effects in superconductors: critical current measurements as
    (D. Easton)   a function of stress, field, and
                                                 conductor

Radiation effects in insulators: assess gamma and neutron damage,
    (J. Long)   using fission spectrum, BSR reactor,
                                                 of electrical insulators and
                                                 potting compounds

Radiation effects in conductors: irradiated Cu at 300 K and low
    (R. Coltman)   temperatures, using BSR reactor,
                                                 measured low temperature magneto-
                                                 resistance

Conductor characterization: studies of conductor variability,
    (W. Fietz)   including critical current,
                                                 dimensions

| Stainless steel variability:
(A. Morehead, C. Brinkman) | variations of mechanical properties of multiple heats of AISI 304 and 316 for LMFBR (no low temperature measurements) |

Low Temperature Research at Other Laboratories Closely-Associated with ERDA-MFE

Rocky Flats (Golden, CO)

| Welding:
(A. Liby) | chemistry, weld process, and base-metal effects on welding of 21/6/9 stainless steel |

University of Wisconsin

| Fatigue, electrical:
(H. Segal) | effect of plastic deformation on electrical resistivity of Al |

| Thermal conductivity:
(T. Stone) | thermal conductivity of fiber-glass/epoxy and selected non-metals |

| Dispersion strengthening:
(T. Hartwig) | hi-strength, lo-resistivity Al development using precipitation |

| Al stabilization:
(R. Boom) | conductor design and processing varying NbTi-Cu/hi-purity Al/Al alloy ratios and geometries - for energy storage program |

University of California - Berkeley

| Alloy development:
(B. Morris) | development of ferritic, low-temperature alloy, mechanical properties |

NBS Program

| Structural materials for superconducting machinery
(R. Reed, A. Clark, M. Kasen, R. Tobler, et al.) | large program (involving subcontracts) designed to screen structural alloys, provide base data (mechanical, electrical, thermal) of structural alloys and composites, developed test procedures at 4 K, published handbook, held workshops |

| Welding of structural alloys:
(H. McHenry, R. Tobler) | five separate programs on weld properties at cryogenic temperatures, including Ti alloys, Al alloys, steels and Fe-Ni alloys |

Properties of superconducting magnet:
  materials, conductors and coils
    (A. Clark, J. Ekin)

program for NSRDC superconduct-
ing machinery project; measured
critical current as function of
stress, field and temperature; now
measuring fatigue properties of
conductor composites and critical
current, temperature and field

Superconductor standards:
    (A. Clark, D. Read)

establishing definitions and stan-
dard measurement procedures

Cu-Nb$_3$Sn processing:
    (F. Fickett)

research to assess thermal-mechanical
processing effects on Nb$_3$Sn precipi-
tation in Cu, CuSn matrices

Composite development:
    (M. Kasen)

mechanical properties, develop-
ment of graphite/epoxy struc-
tural dewars

Other Low Temperature (4 K) Test Facilities

ALCOA Center:
    (R. Kelsey, G. Barthold, E. Spuhler)

mechanical properties, thick-
section welding, composite develop-
ment, processing, alloy development

Battelle Memorial Institute:
    (T. Collings, F. Jelinek)

thermal expansion, specific heat,
thermal conductivity, magnetic
properties, stress-fatigue, super-
conductor processing

Boeing Aerospace Corporation:
    (J. Boysen)

mechanical properties, composite-
fracture experience

General Dynamics:
    (J. Christian, M. Campbell)

thermal expansion, thermal conduc-
tivity, specific heat, mechanical
properties, insulation-composite-
joining-processing experience

Martin-Marietta Corporation:
    (F. Schwarzberg)

mechanical properties; composite-
fracture experience

Westinghouse Electric Corporation:
    (J. Wells)

mechanical, magnetic properties;
processing-joining-fracture
experience

U.S. DEPT. OF COMM. BIBLIOGRAPHIC DATA SHEET	1. PUBLICATION OR REPORT NO. NBSIR 78-884	2. Gov't Accession No.	3. Recipient's Accession No.

4. TITLE AND SUBTITLE Technical Reports on Materials Studies for Magnetic Fusion Energy Applications at Low Temperatures - I	5. Publication Date April 1978
	6. Performing Organization Code

7. AUTHOR(S) F. R. Fickett and R. P. Reed	8. Performing Organ. Report No.

9. PERFORMING ORGANIZATION NAME AND ADDRESS NATIONAL BUREAU OF STANDARDS DEPARTMENT OF COMMERCE WASHINGTON, D.C. 20234	10. Project/Task/Work Unit No. 7360531
	11. Contract/Grant No.

12. Sponsoring Organization Name and Complete Address (Street, City, State, ZIP) Department of Energy Division of Magnetic Fusion Energy Washington, D.C. 20545	13. Type of Report & Period Covered
	14. Sponsoring Agency Code

15. SUPPLEMENTARY NOTES

16. ABSTRACT *(A 200-word or less factual summary of most significant information. If document includes a significant bibliography or literature survey, mention it here.)*

   The reports presented here summarize the work of the low temperature materials research project for the first year of the program. The various projects are outlined and the research results are presented. The major thrust of the measurements has been the evaluation of the low temperature properties of stainless steel base metal and welds, with particular emphasis on the nitrogen strengthened stainless steels. Some initial work has also been done on the production and properties of nonmetallics, primarily industrial laminates, for low temperature applications. A handbook of material properties is also planned. A survey of low temperature materials needs and problems related to magnetic fusion energy, performed by NBS as groundwork for the program, is included as is a brief description of the first workshop held in October 1977.

17. KEY WORDS *(six to twelve entries; alphabetical order; capitalize only the first letter of the first key word unless a proper name; separated by semicolons)*
   Data compilation; low temperatures; mechanical properties; physical properties; stainless steel; welding.

18. AVAILABILITY [X] Unlimited	19. SECURITY CLASS (THIS REPORT) UNCLASSIFIED	21. NO. OF PAGES 364
[ ] For Official Distribution. Do Not Release to NTIS		
[ ] Order From Sup. of Doc., U.S. Government Printing Office Washington, D.C. 20402, <u>SD Cat. No. C13</u>	20. SECURITY CLASS (THIS PAGE) UNCLASSIFIED	22. Price $12.50
[X] Order From National Technical Information Service (NTIS) Springfield, Virginia 22151		